Methane emissions from petroleum-bearing basins: a modeling and mass balance approach

vorgelegt von
Diplom-Geochemiker
Luiyin Alejandro Berbesi
geb. in Mérida, Venezuela

von der Fakultät VI – Planen Bauen Umwelt
der Technischen Universität Berlin
zur Erlangung des akademischen Grades

Doktor der Naturwissenschaften
- Dr. rer. nat. -

genehmigte Dissertation

Promotionsausschuss:

Vorsitzender: Prof. Dr. Wilhelm Dominik
Gutachter: Prof. Dr. Brian Horsfield
Gutachter: Prof. Dr. Ralf Littke

Tag der wissenschaftlichen Aussprache: 24. März 2015

Berlin 2015

Authorship statement

I, Luiyin Alejandro Berbesi, hereby state that the work contained in this thesis and any parts thereof have not previously been submitted to the Fakultät VI - Planen, Bauen, Umwelt at the Technical University of Berlin, or any other institution except where explicitly stated.

To the best of my knowledge and belief, the thesis does not contain any previously published material or any material written by another person except in those cases where the reference has been made. This study counts with the approval to use data from previous research carried out at the Helmholtz Centre Potsdam-GFZ German Research Centre for Geosciences, and the sources of the data have been clearly acknowledged across the manuscript.

Hiermit erkläre ich, Luiyin Alejandro Berbesi, dass weder die vorliegende Arbeit noch ein Teil von ihr bereits an der Fakultät IV – Planen Bauen Umwelt an der Technischen Universität Berlin oder anderen Institutionen eingereicht wurde, außer da, wo ausdrücklich darauf hingewiesen ist.

Ich habe die Arbeit nach bestem Wissen und Gewissen verfasst. Sie beinhaltet kein bereits publiziertes Material oder von anderen Personen verfasstes Material, außer in den Fällen, wo dies durch Verweise kenntlich gemacht wurde. Diese Arbeit ist mit Erlaubnis zur Verwendung von Daten aus vorangegangenen Studien des Helmholtz Centre Potsdam-GFZ Deutsches Geoforschungszentrum verfasst worden. Die Quellen dieser Daten sind im Manuskript deutlich angegeben.

Luiyin Alejandro Berbesi
Date: 24.03.2015

Acknowledgements

On a technical and professional level, I would like to thank:

- Prof. Dr. Rolando di Primio, Prof. Dr. Brian Horsfield and Dr. Zahie Anka for the opportunity of developing this project under your supervision.
- Prof. Dr. Brian Horsfield and Prof. Dr. Ralf Littke for acting as reviewers of this work, and Prof. Dr. Wilhelm Dominik for acting as dissertation chairman.
- Dr. Debra K. Higley (U.S. Geological Survey) and Dr. Judith Sippel (GFZ Potsdam), for the data provided to this project and for the productive feedback offered during the redaction of the publications. Thanks to Dr. Karsten Kroeger and Dr. Volkmar Neumann because their scientific contributions served as basis and input for this research work.
- Prof. Dr. Heinz Wilkes for the interesting conversations about the oil biodegradation process and for your suggestions to the mass balance calculations performed in Chapter 4.
- Prof. Dr. Steve Larter, Prof. Dr. Kenneth E. Peters, Prof. Dr. Giuseppe Etiope, and Dr. Stuart D. Harker for acting as reviewers of the scientific articles here presented. The quality of this scientific work has certainly profited from your advice and opportune comments.
- Dr. Christian Zwach and Dr. Arild Buland (Statoil ASA) for the cooperation and support offered during the final phase of the thesis writing process.
- All the colleagues and fellow students from the Organic Geochemistry section at the GFZ Potsdam; in particular Enmanuel Rodrigues Duran , Ilya Ostanin, Alexander Hartwig, Nikolaus Baristeas, Victoria Sachse, Jingqiang Tan and Gabriela Marcano for the time we shared.
- Frau Claudia Engelhardt for the help in all types of administrative issues during my stay at GFZ Potsdam.

On a more personal level, I would like to thank:

- My mother and brother for giving me your help when I decided to move abroad in order to pursue this goal. Also thank you for all your words of encouragements during the last 5 years.
- Rolando di Primio for all the help provided during the first months of my stay in Germany. I hold in esteem all your efforts and I owe you not one, but a lot.
- Zahie Anka for the advice and support you gave me, not only on a professional but also on a personal level.
- Prof. Dr. Manuel Martínez Santana because you guided my first steps in the world of organic geochemistry and encouraged me to pursue this endeavor.
- Robert G. Radu for your patience and for helping me to keep positive, no matter the size of the challenge faced.
- Enmanuel Rodrigues Duran for being a loyal friend, colleague, and classmate during the last 11 years.
- Dr. Maria Mendez Casaal and Dr. Gabriela Marcano for the long conversations about geology that very often deviated into more philosophical topics, and for extending me your hand in times of adversity.
- Mariela, Mailyng, Kris, Maren, Francisca, Virginia, and Naledi, because from a few meters or from thousands of kilometers distance, you gave me moral support when I needed it.

I could go on for pages but I would like to close saying thanks to all the people I met during my stay in Berlin/Potsdam, for being part of a very special and learning-full phase of my life.

Preface

This scientific work was carried at the Helmholtz Centre Potsdam-GFZ German Research Centre for Geosciences as part of the Methane on the Move (MOM) research program. The main goal of MOM was to estimate past and present methane seepage from petroleum systems in sedimentary basins, addressing this way their link with the Earth's climate evolution.

The results contained in this manuscript were obtained between July 2009 and August 2012. The two initially planned study areas were both Canadian basins: these are the Western Canada Sedimentary Basin (WCSB) and the Beaufort-Mackenzie Basin (BMB). Initial WCSB input data were provided by the U.S Geological Survey and Debra K. Higley. These included a base 3D model consisting of 22 isopach maps and preliminary lithofacies assignment, temperatures (DST and corrected bottom-hole temperatures) and measured vitrinite reflectance ($\%R_0$) from 33 wells. In the case of the Mackenzie Basin, input and output data from previous 3D models developed at the GFZ Potsdam (Kroeger et al., 2008; 2009) were available.

The first year of work consisted of compiling an extensive literature and data base in order to get up to date with the state of the art on the selected topics and study areas. This year also included acquiring expertise on the applied modelling software and obtaining the first set of results. The final phase of this year consisted on planning and training for a field trip related to the MOM program. The field trip aimed at measuring the atmospheric methane concentrations in the Richards and Herschel Islands of the Beaufort-Mackenzie Basin, applying the boreal laser technique. It took place in July 2010 and had duration of 3 weeks, including one week of logistics at the Aurora Research Institute in Inuvik (Canada). Necessary training and pre-field work comprised literature revision about the area and methodology, a "safety and weapon handling in polar bear environments" course, plus calibration and testing of the boreal laser at GFZ and Potsdam surroundings. To the best of my knowledge, no

conclusive results have been derived from the field trip data, which belong to another project (Dr. Torsten Sachs, Inorganic and Isotope Geochemistry Department, GFZ Potsdam) and are therefore not shown in this manuscript.

The second year saw the planning and startup of paper writing plus the participation in several meetings and conferences. Initially, WCSB source rock samples were available for the determination of compositional kinetic models (e.g. di Primio and Horsfield, 2006). Consequently, laboratory work including Microscale Sealed Vessel (MSSV) Pyrolysis and Pyrolysis Gas Chromatography-Flame Ionization Detector (PyGC) was performed during approximately a month and half, under the supervision of the laboratory staff from the section 4.3 (Organic Geochemistry) at the GFZ Potsdam. However, data from this work was not converted into compositional kinetic models due to time limitations, the existence (and availability) of kinetic models for the source rocks of interest (Higley et al., 2009), and the need of consistence in certain parameters with respect to previous studies, as explained in Berbesi et al. (2012). The output from PyGC determinations is provided in the CD accompanying this Thesis.

During the analysis of potential emissions from the WCSB and comparison against seepage rates measured at several basins around the globe, it became obvious that a publication clearly and systematically integrating petroleum system modeling (subsurface) and methane seepage measurements (surface) was needed. Results from the WCSB modelling alone would have been insufficient for such a goal, but the incorporation of an initially non-considered study area, the Central Graben of the North Sea, was considered key for the endeavor. From this sedimentary basin, both in-house developed petroleum system models (Neumann, 2007; di Primio and Neumann, 2008), and published indirect surface methane leakage estimates (Judd et al., 1997) were available. In this manner, basin modelling (Berbesi et al., 2012) and biodegradation mass balance on the WCSB were combined with basin modeling and surface methane appraisal on the Central Graben, resulting in a publication (Berbesi et al., 2014) that, although considerably time consuming and challenging, answered questions of a scale beyond the initial objectives of this project.

By the third year of the PhD, heat flow, isopach maps, and calibration data derived from thermal studies on the Beaufort-Mackenzie Basin (Dr. Judith Sippel, Basin Anlysis Department, GFZ Potsdam) were kindly provided for this study. The later isopach maps covered a much larger portion of the BMB than those initially at hand (Kroeger et al., 2008; 2009), and the heat flow map was the product of extensive thermal modelling in the area (Sippel et al., 2013). Besides, a new version of the modelling software (PetroMod) was available. Therefore, it was decided to build an entirely new petroleum system model instead of working on top of the previous model by Kroeger et al. (2008, 2009).

In October 2012, I joined Statoil ASA Norway as Geologist/Petroleum Systems Analyst and I have since then used part of my spare time on finishing this manuscript and in the peer-review process of the papers it contains. It is important to mention that the papers are presented in a logical rather than a chronological order. Basin modeling on the WCSB and BMB pursue basin-wide goals and are therefore presented as paper 1 and 2 (chapters 2 and 3), whereas the paper combining WCSB and the Central Graben is placed as paper 3 (chapter 4) because of its larger scope and impact. Chapters 5 of this manuscript, and in particular section 5.4 “geological methane emissions from petroleum systems and their potential for climate feedback”, can be seen as an integration of the knowledge generated during the entire PhD work in order to answer the basic questions that gave origin to it.

List of Publications

In the scope of this dissertation the following articles, conferences contributions and internal seminars were published and/or presented:

Publications included in this manuscript

Paper 1. Berbesi, L. A., R. di. Primio, Z. Anka, B. Horsfield, and D. K. Higley, 2012, Source rock contributions to the Lower Cretaceous heavy oil accumulations in Alberta: a basin modeling study: AAPG Bulletin, v. 96, p. 1211-1234.

Paper 2. Berbesi L.A., R. di Primio, Z. Anka, J. Sippel, B. Horsfield., 2014, Inferences of gas hydrate deposits in the Beaufort/Mackenzie Basin based on petroleum system analysis. Submitted to Marine and Petroleum Geology.

Paper 3. Berbesi, L.A., R. di Primio., Z. Anka., B. Horsfield., H. Wilkes.,2014, Methane leakage from evolving petroleum systems: masses, rates and inferences for climate feedback. Earth and Planetary Science Letters, v. 387, p. 219–228.

Published abstracts not included in this manuscript

Berbesi, L. A.; di Primio, R.; Anka, Z.; Horsfield (2012). Methane leakage during the evolution of petroleum systems in the Western Canada Sedimentary Basin and the Central Graben area of the North Sea. European Geosciences Union General Assembly (EGU). 22.-27. Apr. 2012, Vienna, Austria.

Berbesi, L. A.; di Primio, R.; Anka, Z.; Horsfield, B.; Wilkes, H. (2011). Addressing thermogenic and biogenic gas emissions during the formation of the oil sands deposits of the Western Canada Basin. International Meeting on Organic Geochemistry (IMOG). 18.-23. Sept. 2011, Interlaken, Switzerland.

Berbesi, L. A.; di Primio, R.; Horsfield, B.; Anka, Z.; Higley-Feldman, D.; Dallimore, S. (2010). Beyond conventional petroleum systems modelling: thermogenic and biogenic hydrocarbon emissions through geologic time. AAPG International Conference and Exhibition.12.-15. Sept. 2010, Calgary, Canada.

Presentations without published abstracts not included in this manuscript

Berbesi, L. A.; di Primio, R.; Anka, Z.; Horsfield, B., 2012, Quantifying geologic methane emissions from sedimentary basins: examples from the Western Canada Sedimentary Basin and the Central Graben area of the North Sea. Internal seminar. Department 4.3 Organic Geochemistry. Helmholtz Centre Potsdam-GFZ German Research Centre for Geosciences.

Berbesi, L. A.; di Primio, R.; Anka, Z.; Horsfield, B., 2011, Adressing thermogenic and biogenic gas emissions during the formation of the oil sands deposits of the Western Canada Basin. Internal seminar. Department 4.3 Organic Geochemistry. Helmholtz Centre Potsdam-GFZ German Research Centre for Geosciences.

Berbesi, L. A.; di Primio, R.; Horsfield, B.; Anka, Z.; Higley-Feldman, D., 2010, Thermogenic and biogenic hydrocarbon emissions from petroleum systems. The Western Canada Basin as a case study. Poster presentation. Helmholtz Centre Potsdam-GFZ German Research Centre for Geosciences.

Abstract

The main objectives of this study are to model the evolution of petroleum systems in different sedimentary basins and to quantify their associated methane leakage through geologic time. In this way, the study aims to contribute to the understanding of any link between petroleum-bearing basins and the Earth's climate evolution, and the main processes involved. The analyzed study areas are two Canadian basins: the Western Canada Sedimentary Basin (WCSB) and the Beaufort/Mackenzie Basin (BMB); and the Central Graben of the North Sea province.

The methodology involves petroleum system modeling and analysis, mass balance approaches and comparison of results from the selected study areas against world-wide published data. Although the main focus is on thermogenic gas generation, migration, and leakage; other relevant processes taking place in the selected geological settings are addressed. In the case of the WCSB, a quantification of the microbial methane generation during the biodegradation of the original oils in Athabasca is carried out. In the case of the BMB, petroleum system modeling and analysis allows to assess the methane gas hydrate potential of the region.

Maximum predicted thermogenic gas generation rates are in the order of 10^{-2} (WCSB) to 10^{-3} (BMB and Central Graben) Teragrams (1 Tg=10^{12} g) per year. Biogenic methane could have been produced in the WCSB at rates of up to 10^{-3} – 10^{-2} Tg/yr, depending on assumption regarding the degradable oil mass. Modeling results suggest that gas leakage spread out over a large area, not concentrated or focused, and driven by generation in kitchen areas cannot take place at rates as those reported in the literature, regardless of the sedimentary basin size and carbon pool. Only the reservoir part of the petroleum systems is able to interact with the atmosphere at significant speed, and the mechanisms driving leakage are, by far, more relevant than the carbon inventory of sedimentary basins.

It is proposed that future studies on the topic should concentrate in basins where large gas accumulations and focused release mechanisms are present (e.g., highly fractured settings and arctic basins), and that surface measurements should be combined with petroleum systems modeling in order to reasonably perform aerial extrapolations of measurements, and address paleo-seepage.

Zusammenfassung

Das Hauptanliegen der Studie ist es, die Entwicklung von Erdölsystemen in verschiedenen Sedimentationsbecken zu modellieren und den mit ihnen verbundenen Methanaustritt über geologische Zeiträume zu quantifizieren. Dadurch will die Studie einen Beitrag zum Verständnis der Verbindungen zwischen erdölführenden Becken und der Entwicklung des Weltklimas sowie den damit verbundenen Prozessen leisten. Die analysierten Gebiete waren zwei kanadische Becken: das Western Canada Sedimentary Basin (WCSB) und das Beaufort/Meckenzie Basin (BMB); sowie der Zentralgraben der Nordsee.

Die Methodologie beinhaltet die Modellierung und Analyse von Erdölsystemen, Massenbilanzansätze und einen Vergleich der Ergebnisse mit weltweit publizierten Daten. Obwohl der Hauptfokus auf der Bildung, Migration und dem Austritt von thermogenem Gas liegt, werden auch andere relevante Prozesse, die in den ausgewählten geologischen Gebieten auftreten, angesprochen. Im WCSB wird eine Quantifizierung der biologischen Methanbildung während der Biodegradation des ursprünglichen Öls in Athabasca durchgeführt. Im BMB erlaubt es die Erdölsystemmodellierung und –analyse, das Methangashydrat Potential der Region zu bewerten.

Das Maximum der berechneten thermogenen Gasbildungsraten liegt in der Größenordnung von 10^{-2} (WCSB) bis 10^{-3} (BMB und Zentralgraben) Teragramm (1 Tg=10^{12} g) pro Jahr. Biogenes Methan könnte im WCSB in Raten bis zu 10^{-3} – 10^{-2} Tg/Jahr produziert worden sein; dies hängt von Annahmen hinsichtlich der abbaubaren Masse an Öl ab. Die modellierten Ergebnisse legen nahe, dass sich der Gasaustritt über eine große Fläche, nicht konzentriert oder fokussiert, ausbreitete und, gesteuert durch die Bildung im Muttergestein, nicht in dem Maß stattfinden kann, wie es in der Literatur berichtet wird, ungeachtet der Größe des Sedimentationsbeckens und Karbonpools. Allein das Reservoir als Teil des Erdölsystems kann mit der Atmosphäre in signifikanter Geschwindigkeit

interagieren, und die den Austritt fördernden Mechanismen sind weitaus relevanter als der Karbonbestand von Sedimentationsbecken.

Künftige Studien zu diesem Thema sollten sich auf Becken konzentrieren, in denen große Gasansammlungen und bekannte Freisetzungsmechanismen vorhanden sind (z. B. hoch zerklüftete Bereiche und arktische Becken). Oberflächenmessungen sollten mit Erdölsystemmodellierungen kombiniert werden, um Extrapolationen der Messungen in die Atmosphäre sinnvoll ausführen zu können, und sich mit Paleo-Leckage befassen.

Contents

List of figures

List of tables

Chapter 1

Introduction

1.1 Scientific topic and objectives

Petroleum systems represent a priority topic for the modern society largely due to one reason: they provide the majority of the energy consumed by the Earth's population every year. However, this might not be the main reason why a deep understanding of this topic is needed. Recent studies have proposed that petroleum systems might play an important role in the carbon exchange between sedimentary systems and the atmosphere (Etiope, 2012; Kroeger et al., 2011), which is relevant considering that the former contains around 22 000 times the C mass of the latter. Some other works have even proposed that petroleum systems might represent the missing carbon source in previous climate calibrations (e.g Etiope et al., 2008; Kvenvolden and Rogers, 2005; Judd et al., 2002; Etiope, 2004). In other words, petroleum systems might also represent a key factor for understanding climate evolution.

Carbon emissions during the geological evolution of petroleum systems occur mainly in the form of methane, through a wide range of mechanisms related to tectonic processes, pockmark and mud vulcanoes formation, permafrost retreat and gas hydrate destabilization among others (Etiope, 2012; Judd, 2004). These petroleum system-related emissions (PSE), together with those related to geothermal and volcanic processes, constitute the so-called Geologic Emissions of Methane (GEM) (Etiope and Klusman, 2002). GEMs have been mostly quantified by direct measurements performed at the Earth's surface. From these data, global GEM have been estimated around 30-80 $Tgyr^{-1}$ (Etiope, 2012; Judd, 2004; Etiope and Klusman,

2002). Unfortunately, many studies of this type attribute the leaking gas to petroleum systems without doing mention to the timing of gas generation, migration and accumulation, as well as the estimated reserves in the basin. These details are important and should be addressed because the possible leakage is finite, i.e., it will be conditioned by the mass of hydrocarbon generated and accumulated during specific time frames. In this regard, basin and petroleum system modeling (BPSM) could be a key complementary technique. By providing knowledge about the sub-surface gas feeder system, BPSM could help to seize the meaning and limitations of the measured present-day leakage, and it also would allow assessing paleo-leakage (Kuhlmann et al., 2011; Naeth et al., 2005).

At this point, any reader would agree that an appropriate assessment of the PSE during the Earth's geologic history should consist of the combination of a worldwide seepage survey, in cooperation with a global BPSM initiative. However this idea becomes extremely challenging when considering the existence of around 576 sedimentary basins in Planet Earth, and the minimum requirements for such a task. Direct measurements imply high-tech equipment and access to in many cases remote areas. BPSM requires large datasets including geologic formation depths and thicknesses, deposition ages, paleo facies distribution, paleo and present heat flow, erosional events, source rock type and quality, hydrocarbon generation kinetics, fault development and properties, among others (Hantschel and Kauerauf, 2009). Clearly, the assessment of methane leakage during the formation of global petroleum systems would require simplification, which is not possible without knowing:

- Main mechanisms acting in sedimentary basin where significant methane seepage is known to take place.
- Relevance of the carbon inventory of a basin (i.e organic matter pool) against leakage mechanism.
- Whether all sedimentary basins or only a particular group of them need to be addressed. In the second case, which ones.

This study, divided into 3 scientific articles, applied BPSM in different geological settings in order to better understand their petroleum systems and estimate their individual methane contribution to the atmosphere through geologic time. The goals of this study can be sub-divided according to the aerial scale of their implications.

On a basin-wide scale, the objectives are to:

- Model, analyze, and understand oil and gas generation, migration and accumulation.
- Quantify methane leakage through geologic time.

On a global scale, the study aims to:

- Compare geological methane generation rates against seepage measured at present day.
- Weight the relevance of carbon availability in a basin versus leakage promoting mechanisms, in terms of climate feedback potential.
- Suggest priority geological settings and scientific approaches for future studies in this field.

The objectives of this study are systematically addressed through 3 scientific publications, here presented as manuscript chapters. The basin-wide scale objectives are covered in chapter 2 (Western Canada Sedimentary Basin) and 3 (Beaufort-Mackenzie Basin). The global scale objectives are covered in chapter 4, which combines data derived from this study with information from previous 3D modeling on the Central Graben (performed at GFZ Potsdam), as well as published data. Chapter 5 summarizes the work performed on each basin, but also integrates and discusses the main results in the scope of the general objectives of the dissertation.

A brief introduction to the 3 publications supporting this thesis is presented in the following:

Paper 1:

Berbesi, L. A., R. di. Primio, Z. Anka, B. Horsfield, and D. K. Higley, 2012, Source rock contributions to the Lower Cretaceous heavy oil accumulations in Alberta: a basin modeling study: AAPG Bulletin, v. 96, p. 1211-1234.

The objective of this work was to contribute to the understanding of the origin of the immense oil sand deposits in Lower Cretaceous reservoirs of the Western Canada Sedimentary Basin though petroleum system modeling. In particular, the work focused on reproducing the initial accumulated oil masses and quantifying the petroleum contributions from the main source rocks in the basin. A sensitivity analysis of source rock definition was performed in the case of the two main contributors, which are the Lower Jurassic Gordondale Member of the Fernie Group and the Upper Devonian to Lower Mississippian Exshaw Formation. This sensitivity analysis included variations of assigned TOC and HI for both source intervals, and in the case of the Exshaw Formation, also variations of thickness in areas beneath the Rocky Mountains were considered.

Paper 2:

Berbesi L.A., R. di Primio, Z. Anka, J. Sippel, B. Horsfield., 2013, Inferences of gas hydrate deposits in the Beaufort/Mackenzie Basin based on petroleum system analysis. Submitted.

The purpose of this work was to better constrain petroleum generation and migration, as well as the gas hydrate resources in the Beaufort-Mackenzie Basin (BMB). The applied methodology consisted of numerical modeling and analysis of the petroleum system in the subsurface. The 3D petroleum system model developed in this work represents a further step on previous contributions (Kroeger et al., 2009; Kroeger et al., 2008; Sippel et al, 2012). The model considers not only the lateral and vertical lithological variations, but also the main faults influencing the petroleum system in the basin, as well uncertainties related to source rock properties. Additionally, an estimate of the total geologic gas leakage during the evolution of petroleum systems in the region is provided.

Paper 3:

Berbesi, L.A., R. di Primio., Z. Anka., B. Horsfield., H. Wilkes .,2013, Methane leakage from evolving petroleum systems: masses, rates and inferences for climate feedback. Earth and Planetary Science Letters, v. 387, p. 219–228.

The purpose of this work was to investigate the climate feedback potential of naturally-occurring gas leakage controlled by petroleum generation and degradation as a forcing mechanism for climate at geologic time scales. The potential methane contributions to the atmosphere during the evolution of petroleum systems of the Western Canada Sedimentary Basin (WCSB) and the Central Graben area of the North Sea were addressed. Besides 3D numerical simulation, different types of mass balance and theoretical approaches were applied depending on the data available and the processes taking place in each basin. Finally, the results derived from the study are placed in a global context and compared against data from previous works in order to discuss the potential of global petroleum systems to drive climate, and the main mechanisms involved.

1.2 Theoretical background

1.2.1 Methane, Carbon Dioxide and their role on climate change

Carbon is an element of supreme importance, not only for being the main constituent life is made of, but also because of the influence of its geochemical cycle on the evolution of terrestrial ecosystems. From about 10^{23} g of carbon contained in the Earth, around 1.56 x10^{22} g are contained in organic compounds (Figure 1.1) finely dispersed in sedimentary systems (Des Marais et al., 1992). Carbonates are another big carbon reservoir, holding around 6.5 x 10^{22}g C (Li, 1972). Other carbon deposits include the oceans (3.8 x 10^{19} g, Schimel, 1995), extractable fuels (4 x 10^{18} g, Schlesinger, 1997), soils (2 x 10^{18} g including peat, Schimel, 1995), as well as the atmosphere and biota, estimated to posses 7.5 x 10^{17} g C and 5.6 x 10^{17} g C, respectively (Schimel, 1995).

Two particular compounds participating on the carbon cycle are of special relevance, given their relation with development of the human society and their role on the Earth's climate evolution. These compounds are carbon dioxide (CO_2) and methane (CH_4), whose increased atmospheric concentrations from preindustrial times to present days have been suggested as the main cause for the current climate warming trend. In the following, you will find some information about the atmospheric sources and masses of these gases, as well as their role with respect to climate evolution.

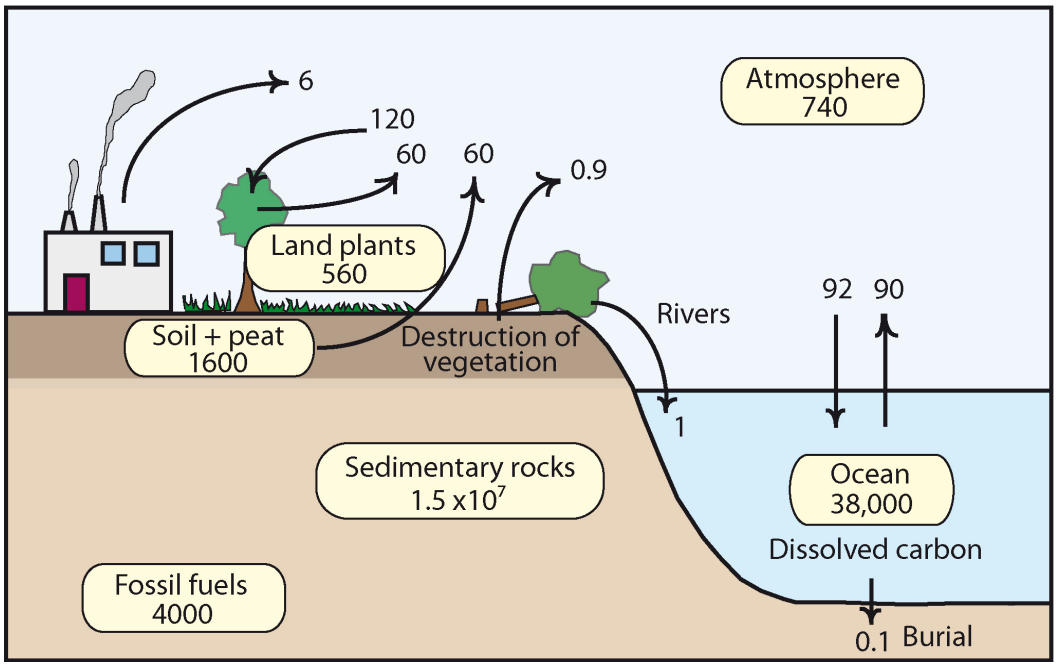

Figure 1.1 Global carbon cycle. The numbers accompanied by arrows correspond to annual fluxes. The main reservoirs of carbon are shown in boxes. All masses are expressed in units of 10^{15} g of carbon (Modified from Schlesinger, 1997).

Carbon dioxide

Carbon dioxide represents a trace component of the Earth's atmosphere, with a concentration around 360 ppm (parts per million), and a total atmospheric mass of 2.8 $x10^{18}$ g (Trenberth and Guillemot, 1994). Since the largest fluxes of the carbon cycle are those where CO_2 is involved, this compound plays a decisive role on the carbon exchange between the subsurface geosphere and the surface biosphere, hydrosphere and atmosphere which comprise the Earth system (Figure 1.1). Atmospheric sources of CO_2 can be divided in two categories, namely natural and

anthropogenic. Natural sources include volcanic eruptions, degradation of organic matter during plant and animal decay, natural forest fires, as well as the respiration process of living aerobic organisms. Anthropogenic contributions are those related to human activity. Burning fossil fuels represent the highest portion of this group, followed by other inputs such as deforestation, as well as the burning of solid waste and wood (Environmental Literacy Council, 2008). The most important of the fluxes within the carbon cycle are those linking atmospheric CO_2 to land vegetation and to the sea. CO_2 dissolution in seawater is considered to be the main sink process of atmospheric CO_2, involving the transfer of more than 100 $x10^{15}$ g of CO_2 form the atmosphere to the oceans every year (Schlesinger 1997).

Methane

The total atmospheric methane burden has been estimated to be around $4.8x10^{15}$ g, which is almost 600 times lower than the CO_2 burden. While sources and fluxes of CO_2 are in the order of 10^{15} g yr^{-1} to 10^{17} g yr^{-1}, the annual contributions of methane to the atmosphere range from 10^{12} gyr^{-1} to 10^{14} gyr^{-1} (Schlesinger, 1997). However, the relevance of atmospheric methane contributions lies on the strong greenhouse potential of this gas, which is 23 times higher than that of CO_2 on a 100 year time horizon (Forster et al., 2007).

Around 500-600 Tg of methane enter the atmosphere every year, mainly as the result of microbial processes (Bousquet et al., 2006). Among these processes are methanogenesis in wetlands, ruminant and termite digestive systems, rice fields and microbial oxidation under anoxic and oxic conditions (Conrad, 2009). The last group contributes around 69 % of the methane entering the atmosphere annually. A 25 % of the annual input is linked to mining and combustion of fossil fuels or burning biomass, and the other 6 % is related to chemical CH_4 production from plant material (Conrad, 2009). A particular group has not yet been taken into account by the Intergovernmental Panel on Climate Change (IPCC). This group consists on the geologic emissions of methane (Etiope and Klusman, 2002; Etiope, 2004), which will be described in more detail later in this chapter.

The main sink for atmospheric methane is the reaction with hydroxyl radicals, which removes around 445 x 10^{12} g from the troposphere every year (Schlesinger, 1997). Some other sinks include oxidation by methanotrophic bacteria during diffusion through soils and utilization as substrate by nitrifying bacteria (King, 1992; Bédard and Knowles, 1989). Since the annual CH_4 input is generally higher than the sum of sinks, the atmospheric concentration of methane has been increasing more than 1 % per year during the last 200 years, except for some specific intervals, like the early 1990s, when the rate of increase slowed significantly (Steele et al, 1992; Dlugokencky et al., 1994; Frankenberg et al., 2011).

Carbon dioxide and methane as greenhouse gases

When the solar radiation reaches the Earth, it is absorbed on the surface and by the atmosphere. In equilibrium conditions, the amount of radiation absorbed should be equivalent to the amount of outgoing thermal radiation; otherwise, a variation on the surface temperature is expected. This variation due to non-equilibrium conditions can be exemplified by the present day global warming trend, best known as the greenhouse effect. This process is characterized by the partial trapping of thermal radiation by particles or molecules in the first 10 - 15 Km of the atmosphere, making the surface temperatures higher than they would be in the absence of this perturbation (Dickinson and Cicerone, 1986). From the main gases composing the atmosphere, water vapor is by far the strongest absorber. Some other gases with atmospheric concentrations less than 1 part per billion (trace gases), can also play an important role on the trapping of thermal radiation. Among these are carbon dioxide and methane, and some others like ozone, nitrous oxide and certain chlorocarbons (Dickinson and Cicerone, 1986).

The thermal radiation emitted by the Earth's surface has a wavelength from 4 to 100 µm (Prabhakara, 1976), limiting the role of atmospheric gases to the range of wavelengths at which they can absorb the thermal radiation. The interval for water vapor corresponds to wavelengths lower than 8 µm and higher than 18 µm, which is most of the spectrum of the Earth's thermal emission. The strong absorption from CO_2 takes place for radiation between 12 and 18 µm, and the rest of the trace gases

previously mentioned (including methane) play an important role on trapping radiation with a wavelength from 8 to 12 μm. The atmospheric concentrations of CH_4 and CO_2 are very susceptible to the influence of anthropogenic and natural perturbations on the carbon cycle. Therefore, a fundamental understanding of the human and natural processes that can contribute these gases to the atmosphere, as well as the masses involved, is essential for the understanding of past and present Earth's climate evolution, and for the future development of our civilization. This contribution focuses on methane emissions during the geologic evolution of petroleum systems.

1.2.2 Petroleum systems

By definition, a petroleum system (PS) includes an active source rock, the generated oil and gas, and all the other geological elements (reservoir interval, seal layer, and overburden units) and processes (generation, migration and accumulation and preservation) required for the existence of oil and/or gas accumulations (Magoon, 1987; Perrodon, 1992; Magoon and Dow, 1995).

The first element, the source rock, can be defined as a fine grained, clay-rich siliclastic rock (mudstones, shales) or dark coloured carbonate rock (limestones, marlstones) which has generated or has the potential to generate significant quantities of hydrocarbons (Demaison and Moore, 1980; Tissot and Welte, 1984; McCarthy et al., 2011). The formation of a source rock begins in aqueous environments where organic matter (dominantly phytoplankton, algal and woody material) is deposited along with sediment particles. This process will result in a suitable proportion of organic matter compared to sediment if biological activities produce large quantities of organic matter, depositional conditions concentrate this matter and post-depositional condition allow its preservation (Durand and Espitalié, 1976; Dow, 1977; Durand, 1980; killops and killops, 1993). Oxygen in the water column stimulates the production of organic matter but also promotes its biodegradation and oxidation, leaving only relatively resistant materials to be incorporated into the sediment (Hunt, 1996; Al-Hajeri et al., 2009). Anaerobic environments are the most

favorable for the preservation of organic matter because of the lack of benthic organisms which can digest it, and due to the extremely little concentration of oxygen, sheltering the organic material from oxidation processes (Demaison and Moore, 1980). In marine and freshwater systems, the organic material is mostly linked to algal and bacterial biomass, which is rich in hydrogen. However, these systems can also receive organic material derived from higher land plants and transported by rivers, glaciers or wind-blow. This material is generally rich in oxygen (ENI, 2005, and references therein). Following deposition of organic rich sediments, the transformation and maturation of the organic matter takes places in three stages: diagenesis, catagenesis and metagenesis (Tissot and Welte, 1984).

During diagenesis, most of the organic particles in the sediments are transformed by microbiological processes into kerogen, accompanied by release of volatiles such as CH_4, NH_3 and CO_2 (Hantschel and Kauerauf, 2009). Heat normally plays a minor role in this process, which normally takes place at temperatures lower than 50°C (Peters et al., 2005). The type of organic matter giving origin to kerogen will determine its composition, which at the same time will determine the type of products (i.e., oil or gas) generated when this kerogen is exposed to burial and high temperatures (Horsfield, 1989; Vandenbroucke and Largeau, 2007). Type I kerogen generates mostly in lacustrine environments and, to a lesser extent, marine environments. Its elevated hydrogen content and low oxygen content makes it oil prone, although it can produce gas at some thermal maturities (Tissot, 1987). Type II kerogen is related to marine settings, and it is mostly oil prone due to its high hydrogen and low oxygen contents. Type IIS are sulphur-rich kerogens which generate oil at anomalous low temperatures and hence levels of maturity compared with standard kerogens (Baskin and Peters, 1992; Tissot, 1987). Type III kerogen derives mostly from terrigenous plant debris deposited in shallow to deep or nonmarine environments. This type of kerogen has low hydrogen content and high oxygen content compared to types I and II, and therefore tends to generate dry gas. Finally, type IV kerogen orginates from reworked organic material, and has almost no oil or gas potential (Tissot and Welte, 1984).

Petroleum is mostly generated during catagenesis (Vassoyevich et al., 1970), when kerogen is buried and transformed into heavier and lighter hydrocarbons and NSO (nitrogen, sulfur, oxygen) compounds (Tissot and Welte, 1984). Based on results from laboratory experiments, catagenesis is considered to be mostly controlled by temperature with a minor influence from pressure (e.g., Behar and Vandenbroucke, 1987; Pepper and Corvi, 1995; Hill et al., 1996; Carr et al., 2009). Heavier compounds are generated first and later these are cracked into lighter components when higher temperatures are reached. This is termed as the "oil window", and takes place within times in the order of 10^6 years, at depth depths from 2 to 4 Km, where temperatures range from 80 to 150 °C, depending on the geothermal gradient. By the end of this stage, secondary cracking of oil molecules results in wet gas generation (Behar and Vandenbroucke, 1987; Hunt, 1996; Schenk et al., 1997; McCarthy et al., 2011). If the burial depth continues to increase and temperatures prior to green schist metamorphism (150-200 °C) are reached, kerogen will enter the metagenesis stage (Peters et al., 2005). From this point on, cracking of all petroleum compounds will derive in dry gas (methane) and a carbon residue (Killops and Killops, 1993; Tissot and Welte, 1984; Behar and Vandenbroucke, 1987; McCarthy et al., 2011).

Once generated, petroleum may experience primary migration, i.e., it can be expelled from the source rock into adjacent permeable carrier beds. Primary migration is considered as driven by capillary forces, diffusion and petroleum potential gradients (England et al., 1987; Kuo, 1997; Stainforth and Reinders, 1990). The proportion of oil expelled from the source rock as a percentage of the total oil generated is called the expulsion efficiency (McKenzie et al., 1987). The more oil is generated in a source rock, the more oil can be expelled from it. In this way, the expulsion efficiency directly correlates with the source rock maturity. Expulsion efficiency values of 60 to 80% are common in source rocks within the main oil window. The other 20 to 40 % remains in the source rock, whether adsorbed on pore walls or on kerogen particules (McKenzie et al., 1987). If burial continues, the oil remaining in the source rock can be cracked to gas, in a process known as secondary cracking (killops and killops, 1993). The primary migration of natural gas components occurs mostly when they are dissolved in oil, as the pressures during the oil window are

normally above the critical point of the petroleum phase diagrams (ENI, 2005, and references therein).

The process of secondary migration takes place when petroleum has abandoned the source rock and has entered a carrier bed, then migrating through it (Tissot and Welte, 1984). In a carrier bed, the porosity, permeability, and pore sizes are considerably higher, and therefore migration is controlled by different mechanisms to those involved in primary migration. Buoyancy, fluid potential gradients and to a minor extent by capillary forces are considered to be the main drivers of secondary migration (Hantschel and Kauerauf, 2009). In general, short migration distances occur in sedimentary basins with strong alternation of sandstones and shales, and in systems were fractures and faults are abundant (Demaison, 1984), such as the Central Graben and the Mackenzie Basin. In contrast, migration distances can also be of kilometers or tens of kilometers in other types of settings such as Foreland Basins. For example, migration from the kitchen areas in the Western Canada Sedimentary Basin to the area where the tar sands are located has been suggested to be in the order of 1000 Km (Larter et al., 1996; Higley et al., 2009; Berbesi et al., 2012).

In ideal petroleum system, petroleum will continue migrating through the carrier bed until reaching trap; that is, a geological feature enabling petroleum to accumulate and be preserved for a certain time interval (Tissot and Welte, 1984). This trap can be either structural, i.e., generated by tectonic activity such as faulting, or it can be stratigraphic, owing its origin to sedimentary depositional patterns (Tissot and Welte, 1984). The existence of adequate reservoir rock and seal rocks are basic for the existence of a hydrocarbon trap. A reservoir is defined as a rock having sufficient porosity and permeability to store and transmit fluids (Biddle and Wielchowsky, 1994). Porosity and permeability are mainly a consequence of both depositional pore-geometries of the reservoir sediment and post-depositional diagenetic changes (Biddle and Wielchowsky, 1994; Allen and Allen, 2005). While the porosity affects the reserves of a hydrocarbon field, permeability affects the rate at which petroleum fluids may be extracted from the reservoir during its production (Allen and Allen, 2005). A seal is an impermeable rock such as shale, anhydrite or salt, which forms a

barrier above and around the reservoir avoiding the fluids migration beyond it (Biddle and Wielchowsky, 1994).

The previously described sequence of generation, migration, accumulation and preservation is basic for the existence of present-day oil and gas fields. However, there is another process taking place during the evolution of petroleum systems which is of major relevance for this study; this process is leakage. Leakage from petroleum systems can take place thorough different mechanisms. Tectonic processes can negatively affect the sealing capacity of oil and gas accumulations, resulting in escape of the previously accumulated hydrocarbon (Ostanin et al., 2013; Etiope and Martinelli, 2002). Also, leakage can be related to portions of the oil and gas expelled from the source rock that never reached an effective trap and continued migrating, eventually reaching the Earth surface. In arctic environments, large amounts of gas (mostly methane) can accumulate under permafrost and within gas hydrates and be released later when hydrate/permafrost stability conditions no longer occur (Chapter 4, Berbesi et al., 2014).

1.2.3 Basin types and their link to petroleum occurrence and distribution

Classification schemes of sedimentary basins

Several attempts to classify sedimentary basins have been made during the last 60 years (e.g Weeks, 1952; Knebel and Rodriguez-Eraso, 1956; Uspenskaya, 1967; Halbouty et al., 1970; Perrodon, 1971; Klemme, 1971, 1975; Bally, 1975; Dickinson, 1974; Huff, 1978; Bally and Snelson, 1980; Bois et al; 1982; Kingston et al., 1983; Ingersoll, 1988; Ingersoll and Busby, 1995). The main goal behind those efforts has been to create a system whereby basins can be compared with each other, facilitating the recognition of similarities and differences among them, which can have implications for oil exploration (Kingston et al., 1983). Plate tectonic has played a significant role on the establishment of basin types, in the sense that the tectonic elements of divergence, convergence and transform movements are common criteria behind any basin classification attempt. Many of the ideas presented in the following

are from Allen and Allen (2005), who offer a discussion about the main recent classification schemes of sedimentary basins.

The first classification schemes were more general, as they grouped sedimentary systems according to the main tectonic regime giving origin to them. For example, Dickinson (1974) proposed a system were a basin would be classified according to its type of lithospheric substratum, the distance between the basin and a plate margin, and the type of boundary (divergent, convergent, transform) nearest to the basin. This system did not consider strike slip or transform related basins, a fact that was acknowledged and corrected by Reading (1982). Other classification schemes (Bally, 1975; Bally and Snelson, 1980) paid special attention to the location of sedimentary basins in relation to megasutures, which are areas where different terrains or tectonic units have been joined together, due to predominantly compressional deformation (Allen and Allen, 2005). In this way, Bally (1975) and Bally and Snelson (1980) differentiated three different families of sedimentary basins which are described in detail in Table 1.1:

- Basins located on rigid, relatively undeformed lithosphere unassociated with the formation of megasutures.
- Basins associated with but outside of megasutures on rigid, relatively undeformed lithosphere (perisutural).
- Basins located upon and mostly contained within megasutures (episutural).

Ingersoll (1988) proposed a classification system mostly based on the work by Dickinson (1974), which was later updated in 1995 and 2012 (Table 1.2). Ingersoll and Busby (1995) propose 26 different basin types, distributed in five major groups which are divergent settings, intraplate settings, convergent settings, transform settings, and hybrid settings. Ingersoll (2012) added new basin types to the scheme by Ingersoll and Busby (1995), although applying the same classification criteria and the same five major basin groups.

Table 1.1 Basin classification of Bally and Snelson (1980) (modified from Allen and Allen, 2005).

1 Basins located on the rigid lithosphere, not associated with the formation of megasutures
- 1.1 Related to the formation of oceanic crust
  - 1.1.1 Rifts
  - 1.1.2 Oceanic transform faults associated basins
  - 1.1.3 Oceanic abyssal plains
  - 1.1.4 Atlantic-type passive margins (shelf, slope and rise) which straddle continental and oceanic crust
    - 1.1.4.1 Overlying earlier rift systems
    - 1.1.4.2 Overlying earlier transform systems
    - 1.1.4.3 Overlying earlier backarc basins of (321) and (322) type
- 1.2 Located on pre-Mesozoic continental lithosphere
  - 1.2.1 Cratonic basins
    - 1.2.1.1 Located on earlier rift grabens
    - 1.2.1.2 Located on former backarc basins of (321) type

---

2 Perisutural basins on rigid lithosphere associated with formation of compressional megasuture
- 2.1 Deep sea trench or moat on oceanic crust adjacent to B-subduction margin
- 2.2 Foredeep and underlying platform sediments, or moat on continental crust adjacent to A-subdiction margin
  - 2.2.1 Ramp with buried grabens, but with little or no block faulting
  - 2.2.2 Dominated by block faulting
- 2.3 Chineese-type basins associated with distal block faulting related to compressional megasuture and without associated A-subduction margin

---

3 Episutural basins located and mostly contained in compressional megasuture
- 3.1 Associated with B subduction zone
  - 3.1.1 Forearc basins
  - 3.1.2 Circum Pacific backarc basins
    - 3.1.2.1 Backarc basins floored by oceanic and associated with B-subduction (marginal sea sensu stricto)
    - 3.1.2.2 Backarc basins floored by continental or intermediate crust, associated with B-subduction
- 3.2 Backarc basins, associated with continental collision and on concave side of A-subduction arc
  - 3.2.1 On continental crust or Pannonian-type basins
  - 3.2.2 On transitional and oceanic crust or W. Mediterranean-type basins
- 3.3 Basins related to episutural megashear systems
  - 3.3.1 Great basin-type basins
  - 3.3.2 California-type basins

---

4 Folded belt
- 4.1 Related to A-subduction
- 4.2 Related to B-subduction

5 Plateau basalts

Table 1.2 Basin classification from Ingersoll (2012) including modern examples.

Setting	Basin type	Definition	Modern example
Divergent	Continental rifts	Rifts within continental crust, commonly associated with bimodal magmatism	Rio Grande rift
	Nascent ocean basins and continental margins	Incipient ocean basins floored by new oceanic crust and flanked by young rifted continental margins	Red Sea
Intraplate	Intraplate continental margins		
	Shelf-slope-rise configuration	Mature rifted intraplate continental margins with shelf edge near boundary between continental and oceanic crust	East Coast of USA
	Transform configuration	Intraplate continental margins that originate along transform plate boundaries	South Coast of West Africa
	Embankment configuration	Progradational intraplate continental margins with shelf edge above oceanic crust	Mississippi River Gulf Coast
	Intracratonic basins	Broad cratonic basins underlain by fossil rifts	Chad basin
	Continental platforms	Stable cratons with thin and laterally extensive sedimentary strata	Barents Sea
	Active ocean basins	Basins floored by oceanic crust formed at active divergent plate boundaries unrelated to arc-trench systems	Pacific Ocean
	Oceanic islands, seamounts, aseismic ridges, and plateaus	Sedimentary aprons and platforms formed in intraoceanic settings other than arc-trench systems	Emperor-Hawaii seamounts
	Dormant ocean basins	Basins floored by oceanic crust, which is neither spreading nor subducting	Gulf of Mexico
Convergent	Trenches	Deep troughs formed at oceanic subduction zones	Chile Trench
	Trench-slope basins	Local structural depressions on subduction complexes	Central American Trench
	Forearc basins	Basins within arc-trench gaps	Offshore Sumatra
	Intraarc basins		
	Oceanic intraarc basins	Basins along intraoceanic arc platforms, which include superposed and overlapping volcanoes	Izu Bonin arc
	Continental intraarc basins	Basins along continentalmargin arc platforms, which include superposed and overlapping volcanoes	Lago de Nicaragua
	Backarc basins		
	Oceanic backarc basins	Oceanic basins behind intraoceanic magmatic arcs (including interarc basins between active and remnant arcs)	Marianas backarc
	Continental backarc basins	Continental basins behind continental margin arcs without foreland foldthrust belts	Sunda Shelf

Continued on next page

Table 1.2 - Continued

Setting	Basin type	Definition	Modern example
Convergent	Retroforeland basins		
	Retroarc foreland basins	Foreland basins on continental sides of continental-margin arc-trench systems	Andes foothills
	Collisional retroforeland basins	Foreland basins formed on overriding plates during continental collisions (may have retroarc precursors)	Western Tarim basin (China)
	Broken-retroforeland basins	Basins formed among basement-cored uplifts in retroforeland setting	Sierras Pampeanas basins (Argentina)
	Remnant ocean basins	Shrinking ocean basins between colliding continental margins and/or arc-trench systems, and ultimately subducted or deformed within suture belts	Bay of Bengal
	Proforeland basins	Foreland basins formed on continental crust that is part of the subducting plate during continental and/or arc collision	Persian Gulf
	Wedgetop basins	Basins formed and carried on moving thrust sheets	Peshawar basin (Pakistan)
	Hinterland basins	Basins formed on thickened continental crust behind foreland foldthrust belts	Altiplano Plateau (Bolivia)
Transform	Transtensional basins	Basins formed by extension along strike-slip releasing bends and steps	Dead Sea
	Transpressional basins	Basins formed by shortening along strike-slip constraining bends and steps	Santa Barbara Basin (foreland type) (California)
	Transrotational basins	Basins formed by rotation of crustal blocks about vertical axes within strike-slip fault systems	Western Aleutian forearc (?)
Miscellaneous and hybrid	Aulacogens	Reactivated fossil rifts at high angles to orogenic belts	Mississippi embayment
	Impactogens	Newly formed continental rifts at high angles to orogenic belts, without preorogenic history (in contrast to aulacogens)	Baikal rift (distal) (Siberia)
	Collisional broken foreland	Diverse basins formed on deformed continental crust due to distant collisions	Qaidam basin (China)
	Halokinetic basins	Basins formed due to deformation of salt, most commonly in continental embankments and proforelands	Mini-basins of deep Gulf of Mexico
	Bolide basins	Depressions in Earth's surface resulting from extraterrestrial impacts	Meteor Crater (Arizona)
	Successor basins	Basins formed in intermontane settings following cessation of local taphrogenic or orogenic activity	Southern Basin and Range (Arizona)

Some other schemes (e.g., Klemme, 1975, 1980; Fischer, 1975; Halbouty et al., 1980; Huff, 1978; Kingston et al., 1983) were mostly developed by- and for petroleum geologists, with the main objective of being able to assist in forecasting the occurrence and magnitude of petroleum resources (Miller, 1987, and references therein) .

Halbouty et al. (1980) considered not only tectonic but also spatial and geometrical features of sedimentary basins. Klemme (1975, 1980) proposed eight main types of sedimentary basins based on architectural characteristics such as linearity, asymmetry, and cross-sectional geometry (Allen and Allen, 2005, and references therein). Kingston et al. (1983) classification system is based on the "cycle" concept, which consists of the sediments deposited during one tectonic episode (Figure 1.2). The latter work emphasized the idea that, while some basins have only one tectonic cycle (simple basins), many others contain more than one cycle (polyhistory basins). These cycles were classified attending to basin-forming tectonics, depositional sequences, and basin-modifying tectonics, resulting in eight simple cycle types covering continental, continental-margin and oceanic areas. Something relevant about Kingston and collaborators' classification is the fact that the basic cycle types, their depositional fills and tectonic modifiers were assigned letters and numbers so that the specific geologic history of each basin could be written as a formula. These formulas could then be compared in order to find similarities and differences between basins.

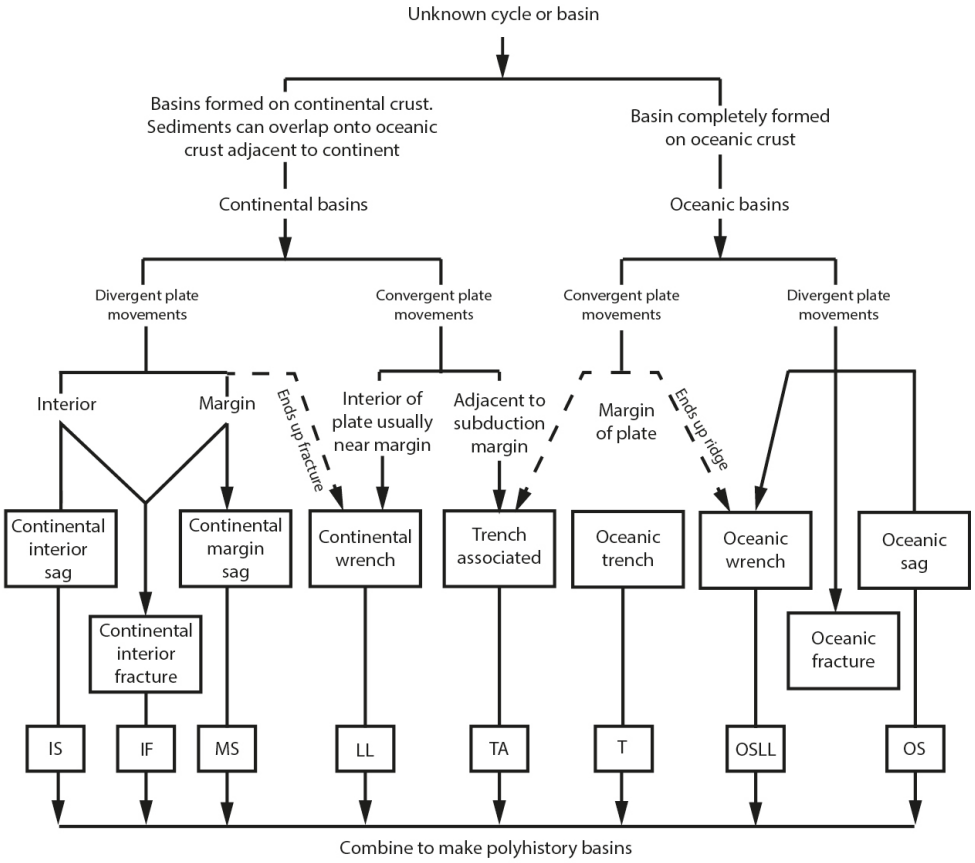

Figure 1.2 Basin classification of Kingston (1983) (modified from Allen and Allen, 2005).

Basin types and distribution of petroleum provinces

Perrodon (1978) defined a petroleum province as a unit composed of one or several sedimentary basins having common geological features and a comparable history, and generally including several petroleum zones. Several studies have shown that the world's petroleum provinces are not evenly distributed, and that the likelihood of finding oil and gas is higher in certain types of geological settings and within strata of particular ages than in others. Nehring (1978) and Perrodon (1978) indicated that some 20 giant petroleum provinces contained 85% of the total known oil reserves at the time, although those provinces cover only 20% of the surface of sedimentary basins. The latter observations have served as motivation to several attempts to create predictive methods that can be applied in petroleum exploration, for example the use of basin analogues (Beglinger et al., 2012; Doust, 2003; Doust and Sumner, 2007). In the following, the main factors linked to this uneven distribution of worldwide

hydrocarbon resources, and some key concepts developed by relevant studies in the field are provided.

Demaison (1984) emphasized that a reduction of the exploration risks requires not only paying attention to the geotectonic style of a basin, but it also requires an evaluation of whether a trap has had access to hydrocarbon migration from mature petroleum source beds. The same work introduced the "generative basin" concept, which describes a sedimentary basin containing one or more petroleum generating depressions. This petroleum generative depression, or hydrocarbon kitchen, is an area underlain by generative source rocks (Demaison, 1984). After reviewing a set of 12 basins including rift basins, intracratonic downwarps, passive margins, multicycle basins and foreland basins, Demaison (1984) identified the following regularities: (1) regardless of basin type and other factors, petroleum occurrence was always linked to generative depressions (2) the largest petroleum accumulations tend to be close to the center of the generative depression (3) in most of the cases, migration distances are in the range of tens of miles. Larger migration distances correlate with some foreland and peri-Andean basins, due to a favorable combination of stratigraphic and structural factors.

Klemme and Ulmishek (1991) related the worldwide recoverable oil and gas reserves to the age of the source rocks giving origin to those reserves. They did not consider unconventional resources of extra heavy oil and bitumen because of difficulties to estimate their initial (i.e., before secondary alteration) recoverable reserves, and because the latter were considered as not significant at the time. The study concluded that more than 90 % of the recoverable oil and gas reserves of the world have been generated by source rocks within six stratigraphic intervals; namely the Silurian (9%), Upper Devonian-Tournaisian (8%), Pennsylvanian-Lower Permian (8%), Upper Jurassic (25%), middle Cretaceous (29%), and Oligocene-Miocene (12,5%). Silurian, Upper Devonian-Tournaisian, Upper Jurassic and middle Cretaceous source rocks were deposited during generally transgressive stages, while Pennsylvanian-Lower Permian and Oligocene-Miocene source rocks were deposited during marine regressions. No cyclicity on the appearance of effective source rocks was identified.

On the contrary, the favorable combination of different types of factors (i.e., tectonic, climatic, hydrologic, biologic) was considered as the responsible for the uneven distribution of effective source rocks within the stratigraphic record. Likewise, the maturation timing of source rocks is uneven in geologic time. The Hercynian orogeny and widespread deposition of thick molasses played a relevant role on the maturation of Paleozoic source rocks. Two other important maturation events taking place during the Late Cretaceous and Tertiary are linked to the Alpine orogeny and deposition of thick clastic wedges during this time. From the petroleum reserves in the six principal stratigraphic intervals, two-thirds were suggested as deposited between the paleoequator and 45° paleolatitudes, in Tethyan basins. These were located within the Tethyan realm, a Silurian-Holocene latitudinal seaway between Gondwana and the northern group of continents. Besides, 78 % were proposed as deposited in platforms, circular sags and linear sags.

Considering the uneven distribution of worldwide hydrocarbon reserves, Brooks (1990) anticipated that the world's petroleum production through the 21st century would be focused on the "classic" or mature petroleum provinces, with a minor contribution from "frontier areas of exploration" such as deep water, jungles, mountain terrains, ice-covered lands or remote continental interiors. The same work compared the basin type following the Bally and Snelson classification (1980) with the percentage of success in finding hydrocarbon (Figure 1.3), which showed that the most successful exploration is in Atlantic-type passive margins overlying earlier back arc basins. In this type of settings, 85% success in finding hydrocarbons was proposed.

Carmalt and St John (1986) also applied the Bally and Snelson basin classification (1980) in order to analyze the relationship between basin type and occurrence of giant oil fields. The study pointed out that the largest group of giant fields is found in the "Foredeep and underlying platform sediments"; a group that includes most of the Middle East and Venezuela hydrocarbon provinces, the North Slope of Alaska and Alberta provinces, and several mega-provinces in the former USSR. Another important group were in "Cratonic Basins in the Pre-Mesozoic continental crust",

including petroleum discoveries in Western Siberia and the North Sea. "Atlantic margin" type basins were indicated by Carmalt and John (1986) to contain about 78 giant oil fields, including the Niger Delta, the US Gulf Coast and the Campeche province in Mexico.

Finally, Brooks (1990) indicated that, while there are between 20 000 to 30 000 fields smaller than $100x10^6$ bbl, those fields only contained about 10% of the known reserves at the time. The major petroleum provinces were suggested to contain about 920 fields larger than $100x10^6$ barrels, which was enough to account to a 90% of the known oil reserves. Brooks (1990) also stressed out that only 35 mega-fields within the classic petroleum provinces contain 50% of the world's reserves (Figure 1.3).

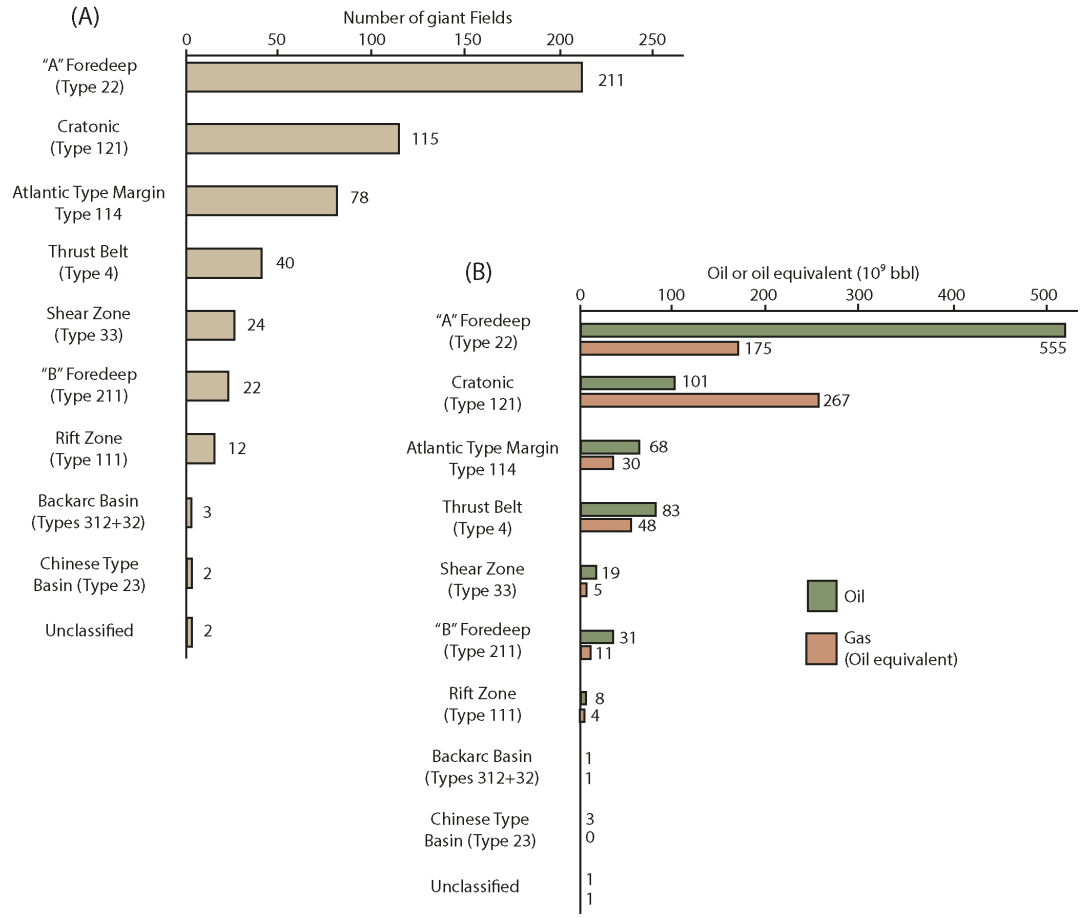

Figure 1.3 (A, upper left) number of giant fields in different types of basins (B, lower right) oil and gas reserves in giant fields. Basin types follow the Bally and Snelson (1980) classification (modified from Brooks, 1990).

Based on the previous information, it can be said that the set of petroliferous basins chosen for this study are optimal for the achievement of the proposed goals. Firstly; it emcompases basins that evolved under different structural settings: a platform stage followed by compressional tectonics (foreland basin) in the WCSB, extensional tectonics and failed rifting in the Central Graben, and a combination of extensional-compressional phases in the BMB (see section 1.3). Secondly; the chosen petroleum systems are known to have generated, and potentially leaked significant petroleum (oil and gas). The WCSB holds the world's largest known accumulations of petroleum classified as crude bitumen (Canada, 2010). The Central Graben ranks, according to the USGS, number 8 among the 76 world priority provinces in terms of volumes of discovered oil and gas. The Beaufort/Mackenzie Basin (BMB), not only contains significant reserves of conventional oil and gas, but it also might hold immense natural gas reserves in the form of gas hydrate (Dixon, 1996; Chen et al., 2007; Osadetz and Chen, 2005). Besides, source rocks deposited at different times (between Devonian and Tertiary) and containing different kerogen types (I, II, IIS, and III) but also coals are being considered. Finally, the mechanisms promoting methane generation and leakage in each basin are different, which allows to cover different processes such as thermal generation, oil biodegradation, gas hydrate and permafrost formation and decay, as well as gas seepage through fractured rock. Sections 1.2.4 to 1.2.7 offer background information needed for the understanding of these processes were addressed in this study.

1.2.4 Methane emissions from sedimentary basins

The term Geologic Emissions of Methane, or GEM (Etiope and Klusman, 2002) refers to a large group of naturally occurring methane exhalations observed or measured in the Earth's surface, which owe their existence to geological processes. The two main groups within the GEM are those related to hydrocarbon-bearing basins and those linked to geothermal areas (Figure 1.4). The present study focusses on the former, which could also be termed petroleum system-related methane emissions (PSME) in order to differentiate it from the larger GEM group.

Surface gas leakage during the evolution of petroleum systems takes place mainly in the form of methane (CH_4), which is the main constituent of natural gas. The mechanisms involved are several; among them tectonic processes, pockmark and mud vulcanoe formation, permafrost retreat and gas hydrate destabilization (Berbesi et al., 2014; Etiope, 2012; Judd, 2004). Depending on the presence of a morphological expression at the Earth surface or the lack of it, seepage can be defined as macro-seepage or as micro-seepage. Macro-seepage is linked to visible manifestations perturbing soil conditions and surface morphology (Etiope et al., 2008; Etiope and Martinelli, 2002). Micro-seepage is an invisible but pervasive, diffuse exhalation of light hydrocarbons from soil, that can be detected by standard analytical procedures (Brown, 2000; Etiope and Klusman, 2010; Etiope et al., 2008).

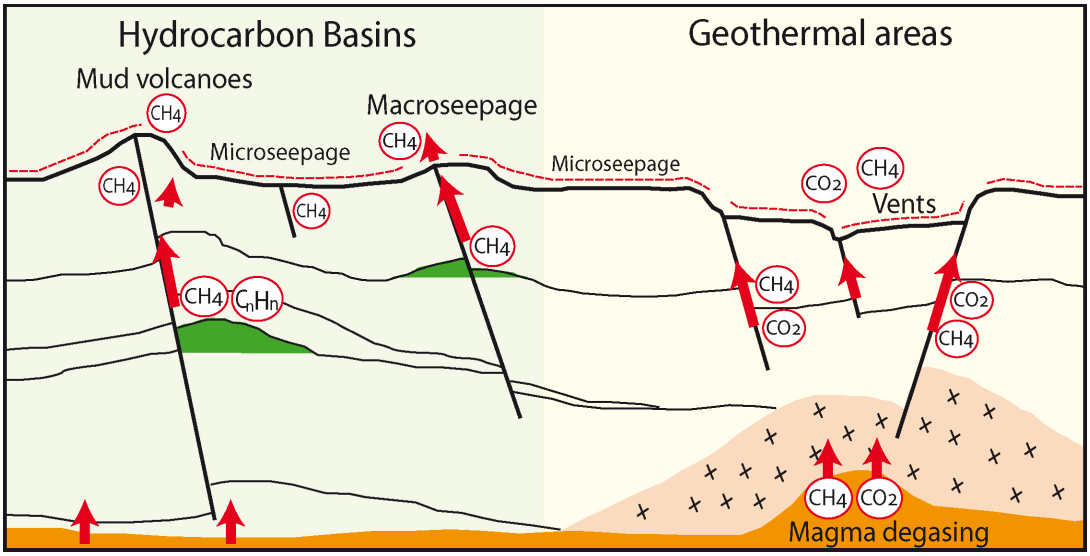

Figure 1.4 Geologic emissions of methane (modified from Etiope and Klusman, 2002).

Most of the available knowledge about GEM, PSME and their relevance with respect to the total annual methane burden derives from direct measurements at actively leaking locations, as well as indirect appraisals based on surface data (Etiope, 2004; Etiope, 2012; Etiope et al., 2008; Dimitrov, 2002; Hornafius et al., 1999; Judd, 2004). Among the PSME, seeps related to gas hydrate destabilization and those occurring from submarine petroliferous basins are of special relevance. The size of the contribution from gas hydrates has been estimated between 5 Tg of CH_4 y^{-1} (Crutzen, 1991) and 100 Tg of CH_4 y^{-1} (Cicerone and Oremland, 1988), but these

amounts, as well as the amount of carbon stored within hydrate deposits, remains uncertain and under discussion (Milkov, 2004). Conversely, a consensus exists on the importance of the contribution from submarine petroleum-related seeps. Some of the areas where this process has been documented are Coal Oil Point California (Hornafius et al., 1999) the Bulgarian Black Sea (Dimitrov, 2002), the Black Sea Continental shelf (Dimitrov, 2002) and the UK continental shelf (Judd et al., 1997). The annual submarine CH_4 seeps from individual basins can range from less than a thousandth $Tgyr^{-1}$ to around 1 $Tgyr^{-1}$ (Judd., 2004). When data derived from these and other marine areas is extrapolated to a global scale, a total of 18-48 Tg of CH_4 yr^{-1} is suggested to leak from seabed gas seeps (Etiope, 2012; Judd, 2004; Hornafius et al., 1999).

Although the link between petroleum systems and global climate evolution is not clear, it has been previously suggested. Etiope (2004) indicated the existence of an unbalance in previous atmospheric methane budget estimates by the IPCC (Intergovernmental Panel on Climate Change) and proposed that GEM not only constitute the "missing source" of methane in those estimates, but also have the same relevance as other sources such as biomass burning (40 $Tgyr^{-1}$) and termites (20 $Tgyr^{-1}$). Etiope et al. (2008) proposed that GEM may constitute around 50 % of the fossil methane entering the atmosphere every year. This work indicated the strong correlation between macro-seeps and active tectonics (presence of faults and fractures), therefore suggesting a link between the Earth's greenhouse budget and geophysical processes. Judd et al. (2002) suggested that geological methane is one of the influences on global climate, and that methane seepage from coastal and continental shelf sediments should be studied in depth. This work also suggested the climate feedback potential of arctic regions. Assuming an annual methane flux similar to that existing in the UK continental shelf at present day, that study suggested that those continental shelves covered by ice or permafrost during the last glacial maximum could have accumulated around 2-56 Tg of methane per year. Microseepage, a large part of which occurs above hydrocarbon-prone sedimentary basins, could contribute 10-25 Tg of methane per year, thus being one of the largest sources of geological methane (Etiope and Klusman, 2010).

It is important to mention that extractable fuels are estimated to contain around $4x10^{18}$ g (4 million Tg) of carbon (Schlesinger, 1997). This mass is significant compared to the 10^{17} g of carbon contained in the Atmosphere (Schimel et al., 1995) but it is more than 3500 times smaller than the total sedimentary carbon pool. It has been estimated that sedimentary systems contain around $15x10^{21}$ g (15000 million Tg) of dispersed carbon (Berner, 1989; Hedges and Keil, 1995), constituting a gigantic carbon reservoir which, as discussed by Kroeger et al. (2011), could be more dynamic than commonly realized. The state of knowledge on the burial and remobilization process of organic matter in sedimentary basins, as well as a discussion of potential influence on climate are provided by Kroeger et al. (2011).

Remobilization of only 1% from the carbon in sedimentary systems would amount to $15x10^{19}$ g of this element, which could have a large impact on the surficial carbon cycle (Kroeger et al., 2011); however, carbon interactions between sedimentary basins and the atmosphere are difficult to study and analyze because of the different time scales of the processes involved, and because of the multiple feedback mechanisms taking place (Berbesi et al., 2014; Kroeger et al., 2011). If carbon burial and remobilization in sedimentary basins are considered as a closed system were all the buried organic carbon reaches the surface again through generation of petroleum and CO_2 (and ultimately exhumation), then the rate of carbon burial can be used as criteria for the study of remobilization and leakage rates (Kroeger et al., 2011). Applying a rate of global carbon burial of $1.6x10^{13}$ g/yr (Hedges and Keil., 1995), a remobilization of 1.6 $x10^{19}$ g/Myr (16 Tg/yr) is obtained. This mass could represent an important contribution over geologic time intervals, but the release rates could be too slow to drive short-term climate change (Kroeger et al., 2011). Although several evidence demonstrate that significant interactions between the sedimentary carbon pool and the atmosphere occur in the present (e.g Hovland and Judd, 1988; Milkov, 2000; Dimitrov, 2002; Etiope and Klusman, 2002, 2010; Judd, 2004; Naeth et al., 2005), the existence of a link between sedimentary carbon remobilization and previous known climate events remains an enigma.

1.2.5 Petroleum systems modeling

A petroleum systems model is, as its name suggests, a digital representation of a petroleum system in which all its elements and processes are simulated, in order to better understand and predict them (Hantschel and Kuerauf., 2009). The scale of these models ranges from tens to hundreds of kilometers, and the periods covered may reach hundreds of millions of years (Al-Hajeri et al., 2009). These models are dynamic; not only regarding their geometry, which often changes during the simulation, but also regarding the simulated processes, including sediment deposition, faulting, burial, kerogen maturation kinetics and multiphase fluid flow (Al-Hajeri et al., 2009). In this way, petroleum system models can provide information regarding generation, migration, accumulation and loss of oil and gas in a sedimentary basin through geologic time (Hantschel and Kauerauf, 2009).

Petroleum system models generally perform deterministic computations in which the layers are subdivided into grid cells within which properties are uniform (Al-Hajeri et al., 2009). The building of a model requires large sets of geologic, geophysical and geochemical data (Peters et al., 2009). In a first place, the aerial distribution, depth, lithology and age of all formation intervals are needed (Schlumberger, 2010, 2011). The timing and magnitude of relevant erosion and hiatus events, as well as faults and their migration properties (open or closed to fluid migration) should be implemented (Schlumberger, 2010). The source rock quality and thermal behavior are defined trough the assignment of total organic carbon (TOC), hydrogen index (HI) and hydrocarbon generation kinetics (Dieckmann, 2005; di Primio and Horsfield, 2006). The calculation of surface and sub-surface temperature through time requires the assignment of heat flow values for the different stages of basin evolution (Welte et al., 1996; Schlumberger, 2010; Hantschel and Kuerauf, 2009). Model outputs such as vitrinite reflectance, temperature, pressure, porosity, accumulation volume or fluid composition can be compared against measured data, and, if needed, the model can be later adjusted to improve the match (Peters et al., 2009).

Modeling can be one-dimensional (1-D), two dimensional (2-D) and three dimensional (3-D), depending on the purpose of the study and data available. 1-D burial history models are point locations, mainly wells. 2-D models can be either maps or cross-section based; while as 3-D models incorporate both lateral and vertical elements and processes simultaneously (Higley et al., 2006). The requirements, advantages and limitations of each modeling technique have been previously discussed in the literature (e.g., Higley et al., 2006; Hantschel and Kuerauf, 2009). Some of the main advantages of 3-D modeling are the possibility to simulate 3-D heat propagation, vertical and lateral pressure changes, and phase behavior (Higley et al., 2006; Schlumberger, 2010). Nonetheless, the main advantage is the capacity to simulate petroleum migration using different fluid flow algorithms such as Darcy (vertical), flow-path (Lateral) or hybrid (vertical and lateral) or invasion percolation (Higley et al., 2006).

The most accurate formulation of fluid flow in porous media is given by the Darcy flow algorithm, which considers all the forces acting on the migrating fluid. These forces include capillary pressure, friction, buoyancy, and additional external forces such as aquifer flow (Hantschel and Kauerauf, 2009). However, the large computing time and low grid resolutions needed in order to perform Darcy migration simulations are the main disadvantages of this method (Hantschel et al., 2000). In contrast, flowpath algorithms allow performing migration analysis within shorter times. This method assumes that hydrocarbons entering a carrier move straight upwards until they reach a seal and then follow the steepest direction upwards below the seal, ultimately accumulating once a trap is reached (Hantschel and Kauerauf, 2009). This method is a good approach describing petroleum migration through efficient carriers but it might be too simplistic for heterogeneous reservoirs and complex geological settings. Another method, which is the hybrid Darcy/flowpath, enables fast calculations without losing any of the dynamic framework provided by the full physics calculations (Welte et al., 2000). This method alternates between Darcy and flowpath modeling depending on the permeability of the layer though which the fluid migrates. In this way, it applies Darcy flow for migration trough low permeability lithologies such as shales and siltstones, and flowpath for migration

though more permeable carrier lithologies (Hantschel et al., 2000; Welte et al., 2000). Another alternative migration method is invasion percolation, which assumes migration as a movement of separated stringers (Hantschel et al., 2000; Carruthers and Wijngaarden, 2000), under the effects of capillary forces and buoyancy, and neglecting viscous effects (Meakin et al., 2000; Carruthers, 1998). This method is mostly advantageous in complicated geometries and in cases where the effects of lamitated, crossbedded, and pervasively faulted strata are of crucial relevance for migration (Hantschel and Kauerauf, 2009). In this work, both hybrid and invasion percolation methods have been applied.

1.2.6 Oil biodegradation and biogenic methane generation

Biodegradation of crude oil is a selective metabolization of certain types of hydrocarbons by microorganisms (Tissot and Welte, 1984). Biodegradation decreases the oil quality by lowering the API gravity while increasing oil density, sulphur content, viscosity and metal content, which negatively affects the recovery factor of the reservoir and the oil value (Head et al., 2003). Moreover, biodegradation leads to the formation of naphthenic acid compounds, which increase the acidity of the oil, or Total Acid Number (TAN). The consequence is a further reduction of the oil value and production problems such as corrosion and formation of emulsions (Wenger et al., 2002).

The occurrence of biodegradation has long been recognized (Winters and Williams, 1969; Milner et al., 1977; Connan, 1984), and its effects on the molecular composition and physical properties of crude oil and natural gases are empirically well known (Hunt, 1979; Connan, 1984). Although the mechanisms and processes behind biodegradation of crude oil in reservoirs deeper than a few hundred meters remain a matter of discussion and research (Larter et al., 2006), connections between oil quality, microbes and reservoir properties are known to be key for the understanding of the process, as discussed in this section (Figure 1.5).

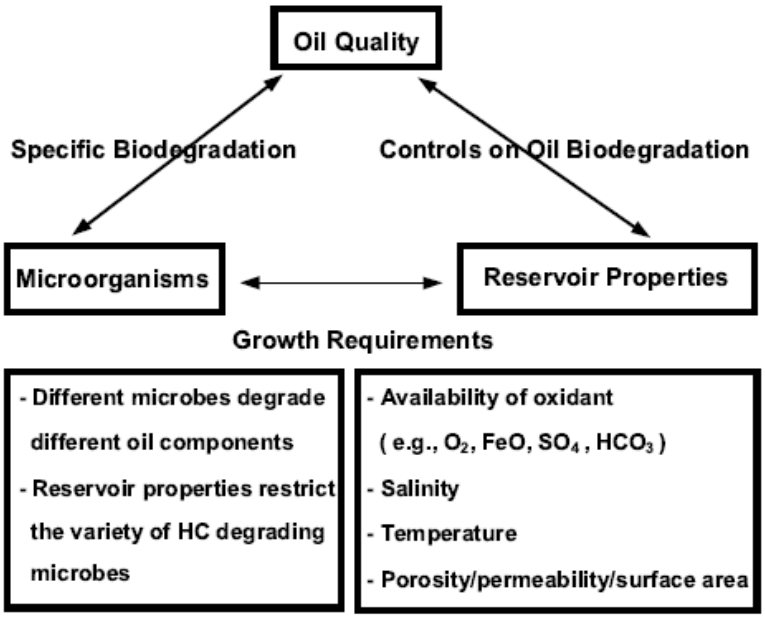

Figure 1.5 Connections between oil quality, microbes, and reservoir properties (from Wenger et al., 2001).

Many of the early studies acknowledging the effects of biodegradation on oil quality were from shallow, onshore reservoirs such as the tar sand deposits in Western Canada, where meteoric water influx was suspected (Milner et al., 1977). This observation pointed towards the idea that biodegradation was carried out by aerobic bacteria only, and that it required oxygen influx (i.e., fresh meteoric water influx) towards the reservoir (Wenger et al., 2002, and references therein). This hypothesis lost strength once the drilling activities moved towards deep waters, were biodegradation in shallow reservoirs was still being observed. In this type of system, it was difficult to explain where fresh and oxygenated waters would come from. Besides, mass balance studies by Horstad et al. (1992) suggested that the amount of water required to transport sufficient oxygen to a volume of trapped oil are unrealistically large in most cases. One observation contradicting the aerobic biodegradation hypothesis is the presence of saline water in deep biodegraded oilfields, which indicates minimal flushing of deep aquifers with fresh water (Head et al., 2003). It has been pointed out that, even if meteoric waters reach the basin, it is unlikely that oxygenated waters will reach the deep reservoir because all oxygen will be removed by reactive organic matter and pyrite in shallow reservoirs (Head et al., 2003).

The currently accepted explanation to the biodegradation process relies on the fact that anaerobic bacteria, such as sulfate reducing bacteria, are capable of degrading petroleum (Wenger et al., 2002, and references therein). Jobson et al. (1979) acknowledged the possibility of anaerobic degradation though sulfate reduction and simulated the processes of aerobic and anaerobic biodegradation in the laboratory. Although hydrocarbon degradation under anoxic conditions takes places at much lower speeds than under oxic conditions (Bailey et al., 1973), early studies (e.g., Shmonova and Shaks, 1971) suggested that the low speed of anaerobic degradation could be compensated by the long, geological residence times of petroleum in reservoirs. The relevance of anaerobic biodegradation is supported by the widespread presence of anaerobic bacteria and archea in subsurface petroleum systems (Röling et al., 2003) and by several studies (e.g., Stetter, 1993; Rueter et al., 1994; Zengler, 1999; Wilkes et al., 2000, 2002; Rabus et al., 2001; Grasby et al., 2009) showing that different types of bacteria such as sulfate-reducing bacteria, iron oxide-reducing bacteria, and bicarbonate-reducing bacteria are able to biodegrade oil in the absence of dissolved oxygen. The finding of reduced sulfur species (e.g., Holba et al., 1996), reduced iron species (e.g., Holba et al., 2004) and methane biologically generated by methanogens (e.g., Larter and di Primio., 2005; Milkov and Dzou, 2007) suggests that anaerobic biodegradation of oil constituents may occur via utilization of a range of different electron acceptors (Skaare et al., 2007, and references therein).

Formerly, the selective removal of hydrocarbon by bacteria was interpreted to occur in the following sequence: n-alkanes (below nC25), isoprenoid alkanes, low-ring cycloalkanes and finally, aromatics (Peters and Moldovan, 1993). This quasi-stepwise concept of biodegradation is the fundament for some of the most widely applied scale systems of the biodegradation extent (Peters and Moldovan, 1993; Wenger et al., 2001; Wenger and Isaksen, 2002). However, recent studies point towards the idea that the quasi-stepwise models of biodegradation might be too simple (Skaare et al., 2007). There are reported cases of incipiently biodegraded oil fields in which long chain alkyl aromatics (LCAA) have been affected (Blanc and Connan, 1994), and even cases in which LCAA's are affected before n-alkane degradation (Holba et al., 2004). Although a depletion in benzene and toluene is

commonly attributed to water washing, cultures of anaerobic bacteria able to degrade toluene and benzene in anoxic conditions have been reported (Widdel et al., 2006). Studying a suite of genetically related oils that had experienced varying degrees of biodegradation, Kim et al. (2005) observed removal of NSO compounds associated with long alkyl side chains, regardless of the NSO core or the degree of biodegradation. Analysis of biodegraded oils from the Troll field in the North Sea suggests the occurrence of simultaneous biodegradation of n-alkanes, branched alkanes, cycloalkanes, alkyl naphthalenes and methyl phenanthrenes (Skaare et al., 2007). The plausible explanations for these observations have been: (a) the presence of various types of bacteria breaking down the various substrates at different rates, or (b) spatial heterogeneity within the reservoir, with various bacteria inhabiting and growing with different substrates in different regions (Skaare et al., 2007). Both possibilities are in agreement with the substrate specificity observed in cultivated anaerobic hydrocarbon-degrading bacteria (Widdel et al., 2006, 2010). Larter et al. (2006) proposed that all compound classes are biodegraded simultaneously but at different rates. According to this view, the relative concentration of more resistant compounds increases as the relative concentration of the more labile ones decreases, giving the impression of a sequential alteration of compound groups (Larter et al., 2003). Also, a revised version of the Peters and Moldovan scale (1993) replaces the term “quasi-stepwise” for “quasi-sequential” (Peters et al., 2005).

Biodegradation takes place at the oil-water contact (OWC) under anaerobic conditions (Heat et al., 2003) and proceeds on a similar scale to oil charging (Larter et al., 2003; Larter et al., 2012). Temperature is the major parameter controlling biodegradation (Head et al., 2003). In general, biodegradation is expected for shallow reservoirs which have not exceeded the temperature threshold for biodegradation (around 80°C) during their geological history (Head et al., 2003). Wilhelms et al. (2001) explain the existence of shallow but non-degraded oil fields with a “paleo-pasteurization” theory which suggests that these petroleum reservoirs were sterilized by heating to temperatures around 80-90 °C during deep burial, inactivating hydrocarbon degrading organisms living in the deep biosphere.

Previous biodegradation modeling (Larter et al., 2006; Larter et al., 2003) has shown that average degradation fluxes for fresh petroleum in clastic reservoirs are in the range of 10^{-4} Kg of petroleum destroyed per m^{-2} oil-water contact (OWC) per year, but diminish at very low reservoir temperatures and as the oil becomes degraded, as in the Athabasca case (Larter et al., 2006; Adams, 2008; Adams et al., 2012).

Methane is the main ultimate product of petroleum biodegradation, accompanied by Carbon Dioxide (Jones et al., 2008; Zengler et al., 1999). The existent knowledge about the mechanism of methane formation from alkanes in anaerobic conditions (methanogenesis) derives mostly from laboratory experiments (e.g., Ferry, 1993; Schink, 1997; Zengler et al., 1999; Jones et al., 2007) in which the hydrocarbon and isotopic compositions of degraded oils and the generated gases are monitored as biodegradation under controlled conditions takes place. Zengler et al. (1999) considered hexadecane ($C_{16}H_{34}$) as a representative compound of the alkane family and suggested that the conversion of this compound to CH_4 and CO_2 involves at least three groups of microorganisms including: acetogenic (syntrophic) bacteria decomposing hexadecane to acetate and H_2 (equation 1), a group of archaea cleaving acetate into CH_4 and CO_2 (eaquation 2) and another group of archaea converting CO_2 and H_2 to CH_4 (equation 3).

$$4\ C_{16}H_{34} + 64\ H_2O \rightarrow 32\ CH_3COO^- + 32\ H^+ + 68\ H_2 \quad (1)$$

$$32\ CH_3COO^- + 32\ H^+ \rightarrow 32\ CH_4 + 32\ CO_2 \quad (2)$$

$$68\ H_2 + 17\ CO_2 \rightarrow 17\ CH_4 + 34\ H_2O \quad (3)$$

Net reaction

$$\mathbf{4\ C_{16}H_{34} + 30\ H_2O \rightarrow 49\ CH_4 + 15\ CO_2}$$

The isotopic composition ($\delta^{13}C$) of methane associated with subsurface oil biodegradation conditions is normally in the range of -45 ‰ to -55 ‰, but the carbon dioxide associated with biodegraded oils shows a wide range and is isotopically heavy ($\delta^{13}C$ up to +15 ‰), which is indicative of almost complete closed-system reduction of carbon dioxide to methane (Head et al., 2003, and references therein). However, in the experiments by Zengler et al. (1999), significantly less than one

third of the total methane was assumed to be formed by CO_2 reduction (equation 3) mainly because of the presence of sulphate-reducing bacteria that would partly deplete the hydrogen generated in equation 1. Jones et al. (2007) proposed a model in which all the hydrogen required to promote significant methanogenic CO_2 reduction, and therefore match the observed isotope compositions, derives from syntrophic alkane oxidation (equation A) and coupled syntrophic acetate oxidation (equation B). Although the model by Jones et al. (2007) proposes different intermediate steps for the methanogenic hydrocarbon degradation, the net equation is the same as that by Zengler et al. (1999).

Syntrophic alkane oxidation

$$4\ C_{16}H_{34} + 64\ H_2O \rightarrow 32\ CH_3COO^- + 32\ H^+ + 68\ H_2 \quad (A)$$

Syntrophic acetate oxidation

$$32\ CH3COO^- + 32\ H^+ + 64\ H_2O \rightarrow 128\ H_2 + 64\ CO_2 \quad (B)$$

Acetoclastic methanogenesis

$$32\ CH3COO^- + 32\ H^+ \rightarrow 32\ CH_4 + 32\ CO_2 \quad (C)$$

Hydrogenotrophic methanogenis

$$196\ H_2 + 64\ CO_2 \rightarrow 49\ CH_4 + 15\ CO_2 + 98\ H_2O \quad (D)$$

Net reaction

$$\mathbf{4\ C_{16}H_{34} + 30\ H_2O \rightarrow 49\ CH_4 + 15\ CO_2}$$

Milkov (2011) estimated that around 65 500 trillion cubic feet (~1.9×10^{15} m^3, or 1.3×10^{18} g) of secondary microbial methane could have been generated in existing worldwide accumulations of oil and bitumen through their geologic history. This is more than 250 times the present-day atmospheric methane burden (~4.8×10^{15} g). The same work proposed that measurements of methane fluxes above shallow reservoirs with biodegraded oil (especially in the WCSB and eastern Venezuela) are needed in order to clarify if reservoirs with methanogenic biodegradation are quantitatively important geological sources on methane emissions into the atmosphere. The latter question is addressed in Chapter 4 of this manuscript (Berbesi et al., 2014), through the implementation of petroleum system modeling and biodegradation mass balance.

1.2.7 Arctic petroleum systems and their role on climate

The dynamics of methane leakage from petroleum systems differs from the simple scenarios previously described in areas where permafrost and gas hydrates are present. Gas hydrates are naturally occurring ice-like solids consisting of water molecules forming a cage in which other molecules (mostly methane) are contained (Sloan, 1998; Taylor et al., 2004). The gas can be either biogenic, derived from the microbial alteration of organic matter, or thermogenic, resulting from thermal cracking of organic matter contained within deeply buried strata (Kvenvolden, 1995). The fact that one cubic meter of methane clathrate can contain 164 m^3 of methane gas at standard conditions (Hyndman and Dallimore, 2001), has motivated the study of gas hydrates as a possible energy resource. Some estimates suggest that methane hydrates contain more organic carbon reserves than all other types of fossil fuels combined (Collett et al., 2009; Booth et al., 1996; Kvenvolden, 1993).

Extensive natural gas hydrates can be found on land and shallow seas in arctic permafrost areas (Figure 1.6) but also beneath some continental slopes at all latitudes (Hyndman and Dallimore, 2001; Milkov and Sassen, 2002). Hyndman and Dallimore (2001) suggested that the former are probably more sensitive to climate change; however gas hydrate and permafrost modelling (Majorowicz et al., 2008) propose that the presence of thick permafrost provides terrestrial gas hydrates of a higher thermal inertia and makes them more resistant to interglacial periods.

It is known that the Earth has experienced several periods of glaciations alternating with periods of warm climate (Gornitz, 2009, and references therein). Gas hydrates can store methane during those cold weather periods and later release the gas when the temperature conditions for gas hydrate occurrence are no longer met (MacDonald, 1990; Kvenvolden, 1993). This combination of factors has suggested a link between gas hydrate dynamics and catastrophic warming events. A relevant example is the Paleocene-Eocene Thermal Maximum (PETM), which took place 55.5 Myr ago. During this period, the temperatures at high-latitude locations and in the deep ocean increased more than 4 °C over less than 10^4 yr (Kenneth and Stott,

1991; Zachos et al., 1993). In high-resolution open-ocean benthic foraminifera records, the section corresponding to the PETM shows a rapid decrease of $\delta^{13}C$ of around 2.5 ‰, returning to near initial values over approximately $2x10^5$ yr. Climate models within the framework of the present-day carbon cycle indicate that release of $1.12\ x10^6$ Tg of CH_4 with a $\delta^{13}C$ of -60 ‰ from a geologic source such as oceanic hydrates would explain this $\delta^{13}C$ excursion (Dickens et al., 1997). However, it is appropriate to mention that the role of gas hydrates as a main driver of previous warming events is still a matter of discussion. In the case of the PETM, Milkov (2003) suggested a maximum methane contribution from gas hydrates around $6x10^5$ Tg, which would have been mostly limited by the gas yield per volume of hydrate-bearing sediments.

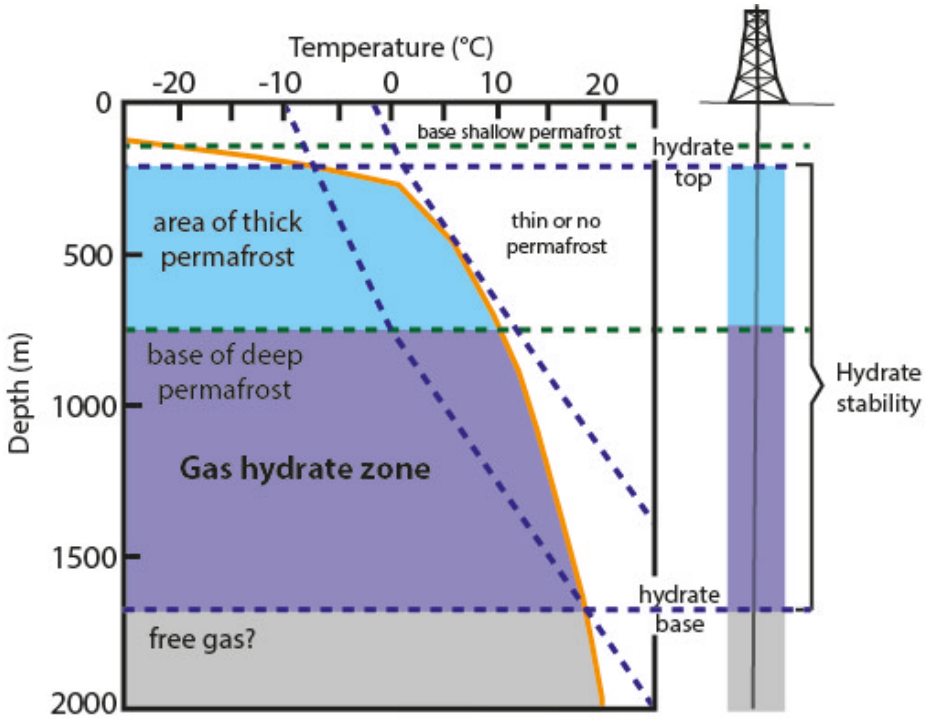

Figure 1.6 Temperature and depth conditions related to the occurrence of gas hydrates in areas of thick permafrost and areas of thin or no permafrost (Modified from Hyndman and Dallimore, 2001).

The way petroleum systems modeling and analysis can be combined with glacial history interpretations in order to perform gas hydrate resource assessment is illustrated in Chapter 3. The latter could have economic implications but also provides relevant data for the understanding and prediction of past and future methane seepage from the underlying petroleum systems into the atmosphere.

The relevance of the concentration-sudden release mechanism exerted by permafrost and gas hydrates is acknowledged and weighted against the relevance of other factors such as the carbon pool of sedimentary basins in Chapter 5.

1.3 Study areas

1.3.1 Western Canada Sedimentary Basin

Geological background

The WCSB (Figure 1.7) holds the world's largest known accumulations of petroleum classified as crude bitumen (Canada, 2010). Total oil sand in-place reserves are estimated around 260 billion m^3 (1635 billion bbl), the main accumulations being Athabasca (189 billion m^3), Cold Lake (32 billion m^3) and Peace River (21 billion m^3).

Deposition and erosion of the sedimentary sequence in the Western Canada Sedimentary Basin took place during two main tectonic phases: a platform (Paleozoic to Jurassic) and a foreland basin stage (Late-Jurassic to Paleocene) (Mossop and Shetsen, 1994; Wright et al., 1994). The most prolific source rocks (Duvernay, Exshaw, Doig, Gordondale, and Poker Chip formations) were deposited during the platform stage. Upper Jurassic strata constitutes a transitional phase from a stable continental shelf to a subsiding foredeep trough (Wright et al., 1994), as a consequence of the collision of allochthonous terranes in the eastern Pacific with the westerly drifting North American Continent (Poulton et al., 1990).

The sea level dropped during Early Cretaceous time, resulting in erosion across the foreland trough (pre-Mannville unconformity). During the Barremian, loading with thrust sheets related to allochthonous terrane accretion brought a new subsidence phase, in which the interval holding today's Athabasca oil sand deposts, the Lower Cretaceous Mannville Group, was deposited (Cant and Stockmal, 1989). This period was followed by another sea level drop and erosion (post-Mannville unconformity). During the Late Albian, a major sea level rise resulted in flooding of most of the

basin and deposition of the main seal for the oil accumulations in Cretaceous reservoirs, the Joli Fou Shale (Smith, 2008; Creaney and Allan, 1990). The Lower to Upper Cretaceous is represented by multiple periods of sea level rise and drop, evidenced by the offshore to shoreface facies of the Colorado Group (Mack and Jerzykiewicz, 1989). The Paleocene Paskapoo Formation in Alberta, named Ravenscrag Formation in Saskatchewan, was deposited during the thrusting in the Cordillera, and is characterized by fluvial channel facies. The phase of foreland basin deposition finishes with the onset of the Laramide Orogeny, around (58 Ma), when intense uplift and erosion takes place (Flowers et al., 2006).

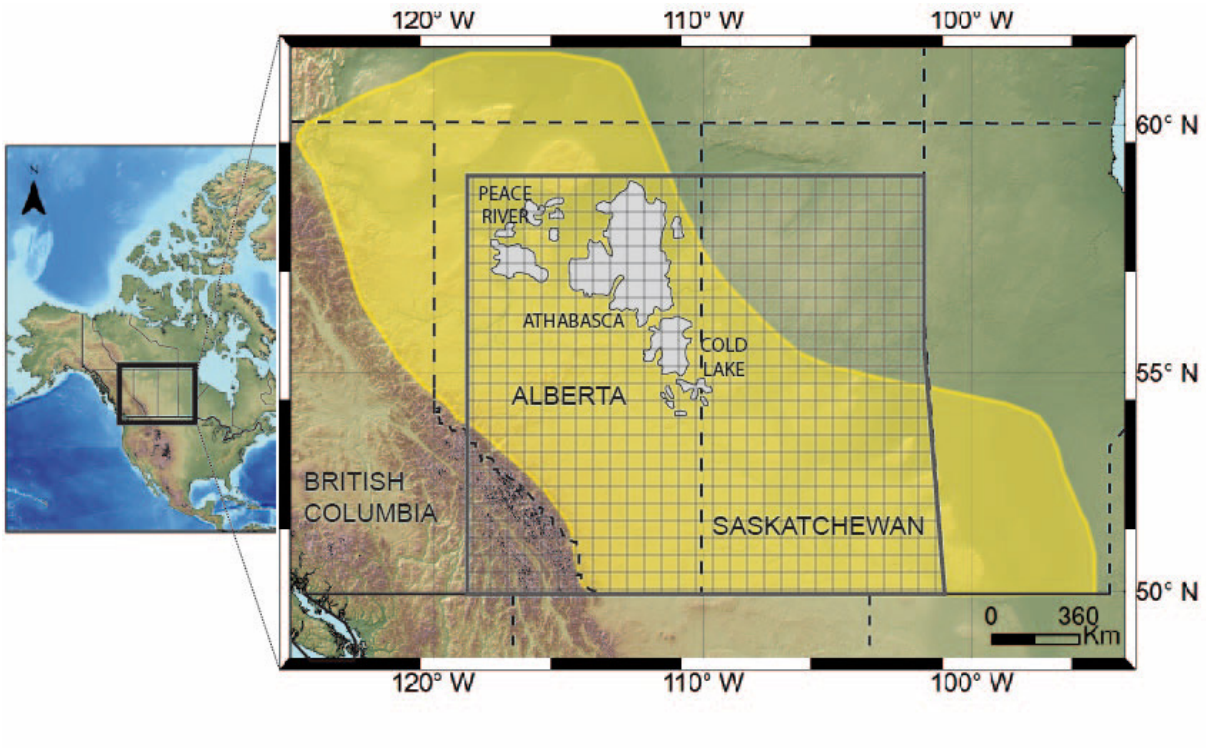

Figure 1.7 Location of the Western Canada Sedimentary Basin (WCSB). The meshed polygon indicates the area modelled in this study (modified from Berbesi et al., 2012).

Petroleum system elements

The typical foreland wedge geometry of the WCSB is basic for the understanding of the interrelation among its different petroleum system elements and events. While the main oil sand accumulations are located in the low-angle dipping eastern margin, the kitchen areas are located in the deeper portions, towards the west. Source rock intervals range from Type II marine, oil prone (Duvernay, Exshaw, Doig, Poker

Chip), to sulfur-rich, type I/II S marine (Gordondale) as well as the gas-prone, type III shales and coals (Ostracode Zone).

More than 70% of the oil found in the main deposits in Alberta (Athabasca, Cold Lake and Peace River), is contained within the Lower Cretaceous Mannville Group (Hayes et al., 1994), a sequence of interbedded sandstone and shale that truncates Jurassic and older strata (Gingras and Rokosh, 2004). The Athabasca and Cold Lake oil sands occur mainly within the McMurray and Clearwater Formations and equivalent strata (Vigrass, 1968), while the accumulations at Peace River are mainly in the Bluesky and Gething Formations (Gingras and Rokosh, 2004; Vigrass, 1968). The Joli Fou Formation of the Middle Cretaceous Colorado Group represents the regional seal for petroleum within Mannville strata. This formation was deposited during a major sea level rise (Leckie et al., 2008), and consists of fine-to medium-grained sandstone (Leckie et al., 2008; Wickenden, 1949).

Although the trapping mechanism at Cold Lake and Peace River has been attributed to pinchouts and structural highs (Vigrass, 1968), controversy exists regarding the Athabasca trapping mechanism (Ranger, 2006). Vigrass (1968) proposed that most Athabasca oil accumulated in an initially subtle domal structure that increased in amplitude around Early Cretaceous time, and another portion occurs in the trough and northeastern limb of a syncline that resulted from salt dissolution of Devonian evaporites. Ranger (2006) proposed that the effect of salt dissolution was important in the southeastern part of Athabasca, while the main control to the northeast should be stratigraphic. Evidence of the last idea has not been found, because it might have been destroyed during Pleistocene erosion (Ranger, 2006).

Current understanding of petroleum generation and migration in the basin

The source of the hydrocarbon accumulations in Alberta has been a topic of discussion for many years. Based on biomarkers, Brooks et al. (1988) proposed that Cretaceous reservoirs were filled with oil generated by one or many similar sources rocks, and via long distance migration. Literature published from the 90s on is divided in two main schools or interpretations, one of them suggesting the dominant

contribution from Jurassic source rocks (Fernie Grroup) and the other suggesting a major contribution from Devonian-Mississippian source rocks (Exshaw Formation). The first school or interpretation is based on mass balance approaches such as by Creaney and Allan (1990) and numerical modeling as performed by Higley et al (2009). The second interpretation is mostly supported by organic geochemical analysis (Riediger 1990a, Riediger 1994, Fowler et al., 2001; Leenheer, 1984; Riediger et al., 2001). Adams et al. (2010) used biodegradation-resistant parameters to conclude that the Peace River reservoirs received an important contribution from the Gordondale Member, but that the Athabasca and Cold Lake deposits originated mainly from the Exshaw Formation.

The time when the Athabasca oil sands were charged with originally lighter, undegraded oil is another topic of discussion. Based on PSM, Higley et al. (2009) suggest that oil accumulations in the Lower Cretaceous Mannville Group should have been filled at around 75 Ma, although no details are given when it comes to the filling of individual accumulations. Adams et al. (2012) used biodegradation modeling and could only reproduce the API gravity observed in Athabasca oils when the reservoirs were considered to be charged from 100 to 60 Ma; that means, during the 40 Myr previous to the timing of maximum burial. Some discussions about the petroleum generation timing in Alberta can be found in Creaney et al. (1994), Creaney and Allan (1990), and Selby et al. (2011). Combining all available data, the onset of filling of Athabasca reservoirs can be placed between Albian and Maastrichtian, and its culmination before the Eocene.

Chapter 2 addresses several knowledge gaps regarding the origin of the oil sands in Alberta, including contributing source rocks, trapping mechanism and reservoir filling time. Moreover, a quantification of the methane mass released to the atmosphere during the evolution of the analyzed petroleum system is presented in Chapter 5.

1.3.2 Beaufort/Mackenzie Basin

Geological background

The Beaufort/Mackenzie Basin (BMB) represents a promising petroliferous region (Figure 1.8), not only because of its significant reserves of conventional oil and gas, but also because it might hold immense natural gas reserves in the form of gas hydrate (Dixon, 1996; Chen et al., 2007; Osadetz and Chen, 2005). Conventional recoverable reserves are around 1.5-3 billion barrels of oil, and around 12 trillion cubic feet of natural gas (Dixon et al., 1994). Gas hydrates are estimated to contain between $2.4x10^{12}$ and $87x10^{12}$ m^3 of natural gas (Chen et al., 2012; Davidson, 1978; Dixon, 1994; Majorowicz and Osadetz, 2001).

Two main tectonic phases are of interest regarding the petroleum system evolution in this basin: a Mesozoic extensional phase and a Maastrichtian to late Miocene orogenic phase (Lane, 2002). The Jurassic to Aptian was dominated by extensional faulting and is represented by shoreface to marine shelf deposits with some fan-delta, deltaic and non-marine deposits (Dixon, 1992a). A shift in the sedimentological regime occurred during the Albian, as a consequence of the Cordilleran Orogeny. The Upper Cretaceous to Tertiary section consists of delta facies corresponding to three main tectono-stratigraphic phases, separated from each other by major unconformities (Dixon, 1996, 1992a). The first phase started with the deposition of the Fish River sequence and ended with the development of an unconformity between Taglu and Richards sequences (Dixon, 1996, 1992a). The second tectono-stratigraphic phase is represented by the deposition of Richards, Kugmallit, Mackenzie Bay, and Akpak sequences. Initially, sedimentation was focused on the south-central part of the basin, but it later shifted towards the basin. This tectono-stratigraphic phase finished by the end of the Miocene, as indicated by another erosional unconformity (Dixon, 1992a). The Pliocene phase, consisting of basinward deposition with minimal deformation, is represented by the Iperk sequence (Dixon, 1992a).

Glaciation processes are of particular relevance in the Mackenzie Region because of their role controlling gas hydrate resources and their distribution (Chen and Osadetz, 2010), as well as for modeling the present-day landscape (Ehlers, 1996). Geological records suggest that significant glacial activity in the region started around the Late Pliocene (Rodkin and Lemmen, 2000). One-dimensional (1D) numerical modeling of permafrost and gas hydrate formation suggest that the latter could have started forming at some time between 6 and 0.9 Myr ago. At least five episodes of continental ice advance are considered to have taken place in Northwest Canada (Barendregt and Irving, 1998), although geomorphic and stratigraphic records propose that only the Laurentide Ice Sheet (Late Wisconsian, around 30 Ka BP) reached the Richardson and Mackenzie Mountains.

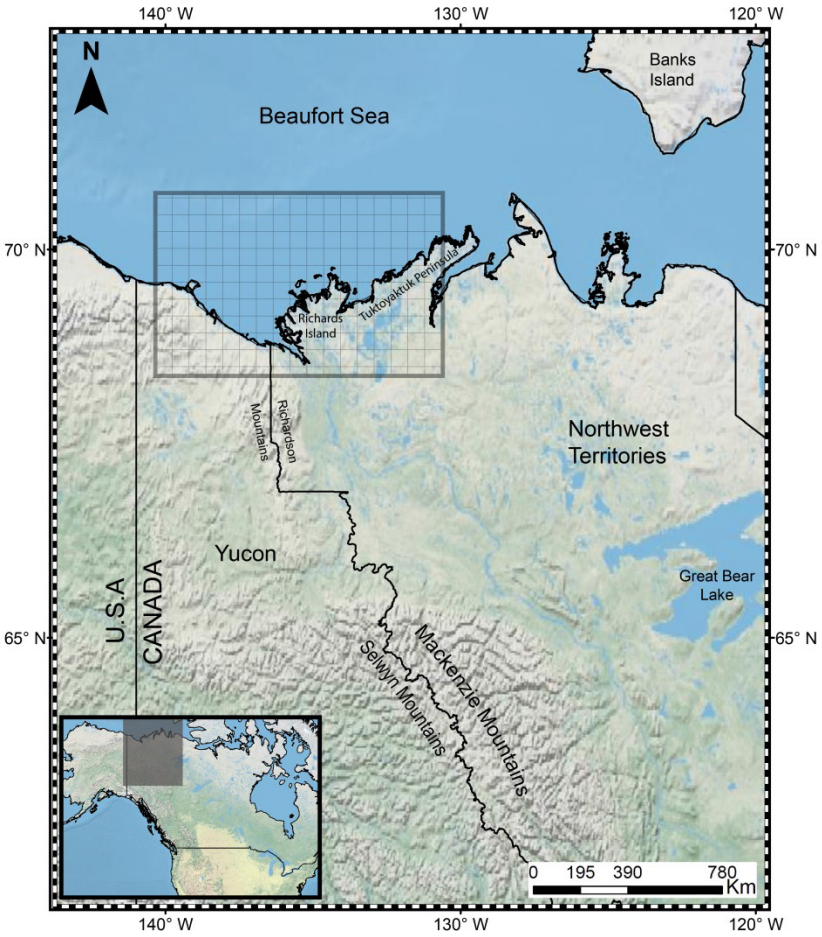

Figure 1.8 Location of the Beaufort/Mackenzie Basin (BMB). The meshed rectangle indicates the modelled portion of the basin (From Berbesi et al., 2014, submitted).

Petroleum system elements

Source rocks in the Baufort/Mackenzie Basin can be divided in two main groups: Upper Cretaceous source rocks and Tertiary source rocks (Dixon, 1992b). Cretaceous sources (Boundary Creek and Smoking Hills Formations) are marine-dominated, while the Tertiary ones (Aklak and Taglu Formations) are mostly terrestrial (Saison, 2010; Snowdon, 1990). The main reservoirs are Eocene to Oligocene sandstones, those belonging to the Kugmallit and Taglu sequences being of particular relevance (Dixon, 1992b). In average, these sandstones have porosity of 20-25 %, although even values of 30% can be found at some wells (Dixon, 1992b). Sandstones in the Taglu sequence tend to be (on average) less porous than those of the Kugmallit sequence (Dixon et al., 2008). The lateral distribution and vertical stacking of individual deltaic reservoirs is a result of basin configuration, syndepositional tectonics and auto-cyclic deltaic processes (James and Baxter, 1988).

Most of the discovered hydrocarbons are contained within three main types of structural traps (Dixon et al., 2008): (1) structures associated with the rifted margins where reservoirs are usually in Lower Crataceous sandstones or fractured Paleozoic carbonates, (2) rotated fault blocks associated with listric faults and (3) faulted anticlines of the Beaufort Foldbelt (Dixon et al., 2008).

Gas hydrate reserves

In addition to holding significant conventional oil and gas reserves, the BMB might contain considerable gas hydrate resources (Hyndman and Dallimore, 2001; Osadetz and Chen, 2010; Osadetz et al., 2003). Gas hydrates are known to exist both onshore and offshore, within the Kugmalit, Mackenzie Bay, and Iperk sequences (Dallimore et al., 1999). Although previous attempts have been carried out in order to constrain those resources, there is, up to date, no consensus regarding what proportion of the natural gas hydrate is recoverable, either technologically or economically (Osadetz et al., 2003).

Chen and Osadetz (2010) indicated that the occurrence of gas hydrates in the BMB, particularly onshore, directly correlates with the thickness of terrestrial permafrost.

This permafrost is a relic from the Laurentide Ice sheet, which covered the entire Mackenzie region around 30 000 years ago (Rodkin and Lemmen, 2000). The natural gas (mainly methane) contained within the gas hydrates is sourced by underlying petroleum systems (Osadetz and Chen, 2010). Faults and fractures constitute the basic permeable migration network through which gas expelled from deeper kitchen moves towards reservoirs in the gas hydrate stability zone. In areas where these migration pathways are absent, gas hydrates are less common (Osadetz and Chen, 2010).

Osadetz and Chen (2010) estimated the gas hydrate resources in the Beaufort/Mackenzie Basin between $2.4x10^{12}$ and $87x10^{12}$ m^3 , based on GH stability zone volume, reservoir porosity, hydrate saturation and a gas volume expansion factor (Majorowicz and Osadetz, 2001). These values are higher than the previous estimate of $88x10^9$ m^3 by Davidson et al. (1978), but of a similar range to the $1.6x10^{13}m^3$ estimated by Smith and Judge (1995). A wide discussion about previous conventional and non-conventional petroleum reserves estimates in the BMB, as well as their limitations, can be found in Osadetz et al. (2003). In Chapter 3, petroleum system modeling is performed in order to estimate the methane mass generated by petroleum systems feeding gas hydrates in the basin. In this way, an upper limit to previous gas hydrate resource estimates solely based on reservoir properties can be set. Methane leakage during the geological evolution of petroleum systems in the Beaufort/Mackenzie Basin is also appraised in Chapter 3.

1.3.3 Central Graben of the North Sea Petroleum province

Geological setting

The North Sea Graben Province (Figure 1.9) represents a highly explored petroliferous region (Brennand et al., 1998) which, according to the USGS, ranks number 8 among the 76 world priority provinces in terms of volumes of discovered oil and gas. It is located in territorial waters of Denmark, Germany, the Netherlands, Norway, and the United Kingdom, and is estimated to contain up to 3200 Tg (4 billion m3) of undiscovered oil and up to 1800 Tg (2000 billion m3) of undiscovered

associated and non-associated natural gas (Gautier et al., 2005). It is divided into three sub-basins which are the Viking Graben, the Central Graben and the Moray Firth/Witch Ground.

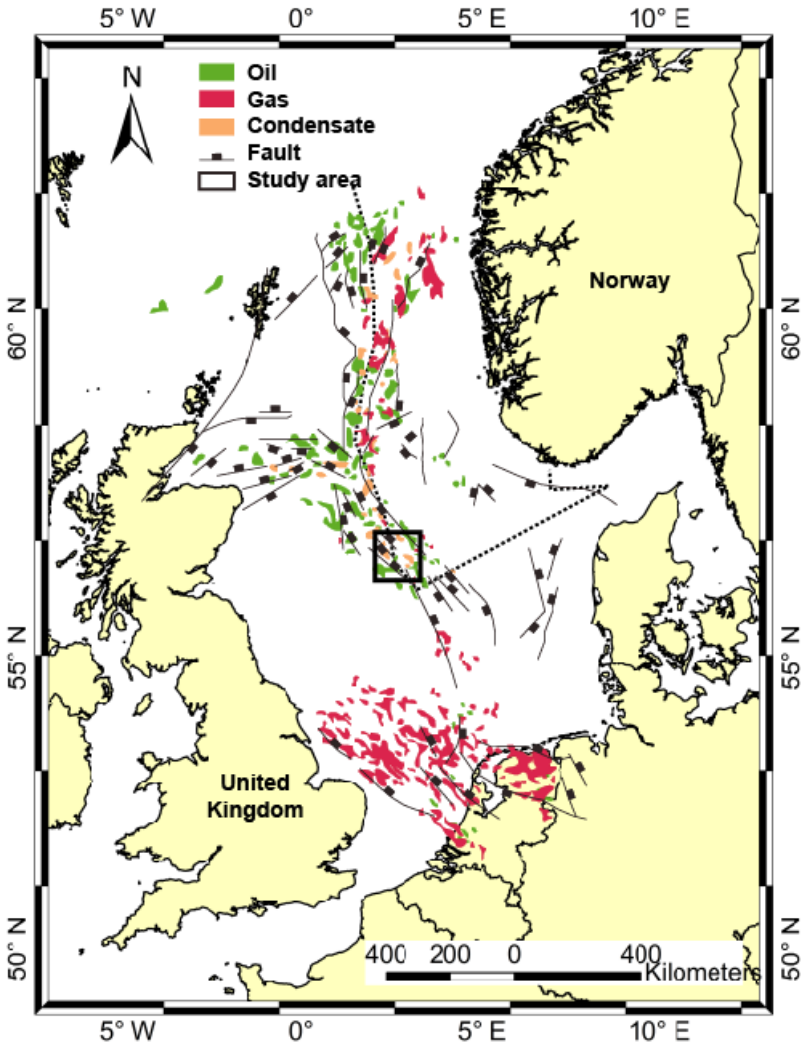

Figure 1.9 Location map of the North Sea Graben Province. The 3D model developed by Neumann (2007) and di Primio and Neumann (2008) is located in the Norwegian side of the zoomed square (from Berbesi et al., 2014).

Petroleum occurrence in the North Sea is, to a great extent, consequence of extensional tectonics and failed rifting taking place from Late Jurassic to Early Cretaceous (Brooks and Glenie, 1987). Therefore, the play analysis in this region is usually performed attending to three stages of basin evolution with respect to the main rifting episode (e.g., Gautier et al., 2005; Johnson and Fisher, 2009): these are the pre-, syn- and post-rift phases. Main events during the pre-rift phase include the Caledonian and Variscan plate cycles, Permo-Triassic rifting and thermal subsidence,

and domal uplift during the Middle Jurassic (Glennie and Underhill, 1998). The last event lead to widespread erosion of the Central North Sea area, volcanism and the subsequent development of the triple rift system we know today (Viking, Central, and the Moray Firth/Witch Ground Grabens). The onset of the syn-rift phase during the Late Jurassic is characterized by accelerating extension and subsidence, accompanied by marine transgression. During this time, subsidence took place in all three rift arms. Marine sediments were deposited along the entire graben, including the site of the North Sea Dome (Gautier et al., 2005). In addition to syn-rift sedimentation, this phase of extension resulted in development of major faults, dissection and tilting of earlier sedimentary sequences (Glennie and Underhill, 1998). At the same time the organic-rich shale was being deposited, uplift and erosion of several structural blocks promoted deposition of coarse sandstones and conglomerates near the fault blocks (Cornford and Brooks, 1989). Extension in the North Sea started to cease by the end of the Jurassic, and ceased completely by the end of the Early Cretaceous (Glennie and Underhill, 1998). In general, the post-rift phase saw a time of tectonic quiescence, with thermal cooling and subsidence in most of the North Sea (Glennie and Underhill, 1998). Late Cretaceous to early Paleocene sediments are dominated by fine-grain, pelagic carbonates (Gautier, 1995). The Tertiary sedimentary section consists of mainly mudstones, with some local fan sedimentation, the latter being particularly relevant during the Paleocene and Eocene (Reynolds, 1994).

Petroleum system elements

The USGS adopted a total petroleum system approach (Gautier et al., 2005) for the North Sea Graben province, mostly based on the previous work by Cornford (1994) and his collaborators. Main ideas from Gautier et al. (2005) of relevance for this manuscript are presented in this section.

Source rocks range in age from Late Jurassic to earliest Cretaceous (Cornford, 1994) and mostly contain type II kerogen, with TOC values ranging from 2 to 15 %wt. These source rocks are called Kimmeridge Clay in the Moray Firth/Witch Ground,

Mandal Formation in the Central Graben, the Draupne Formation in the Viking Graben, and the Tau Formation in the Norwegian-Danish Basin.

North Sea reservoirs are non-uniformly distributed both in time and space (Gautier et al., 2005). Pre-rift reservoirs of pre-Jurassic age hold only a small portion of the reserves and consist of both sandstones and carbonates. Conversely, the majority of the Pre-rift reservoirs of Early and Middle Jurassic age are high porosity sandstones which contain a significant portion of the hydrocarbon resources. Syn-rift reservoirs are restricted to those reservoir rocks actually deposited during maximum rifting, and present high variability regarding thickness, lithology and reservoir quality (Gautier et al., 2005). Post-rift reservoirs range in age from Early Cretaceous to Eocene and consist of both sandstones and chalk.

The trapping mechanisms are variable, ranging from conventional four-way closures to rotated fault blocks and reservoir pinch outs against sealing layers. In the southern North Sea, the Zechstein evaporates act as a regional seal for all types of petroleum accumulations (Gautier et al., 2005).

Previous North Sea gas seepage estimates

The occurrence of gas seepage from the Central Graben of the North Sea has been reported since the early 90's (Salisbury, 1990). However, Judd et al. (1997) report the first and only contribution in which these seepage rates were systematically estimated and extrapolated. This work took into consideration (a) the distribution of possible sources of methane, i.e, the distribution of strata with source rock potential for thermogenic methane, and sediments in which biogenic methane is likely to be generated (b) available evidence (mainly shallow seismic profiles) of gas seepage points (c) possible flux rates based on previous estimates in the United Kingdom Continental Shelf (UKCS) and elsewhere, and (4) theoretical considerations regarding the survival of methane bubbles as they ascend through the sea-water column. Based on this approach, Judd et al. (1997) estimated an average methane flux of 0.2-5.6 $x10^{-6}$ teragrams of methane per square kilometer per year (Tg Km^{-2}

yr^{-1}) that they later extrapolated to the 602 000 Km^2 of the UKCS, resulting in an estimate of 0.12 and 3.5 Tg of methane seeping from the UKCS every year.

In Chapter 5, these surface methane seepage estimates are compared against published data from other basins around the world and also compared against methane generation rates predicted by numerical modeling. By doing this, this contribution discusses the main mechanisms resulting in significant methane surface leakage from petroleum bearing basins, and weights the relevance of carbon availability versus leakage mechanism in terms of the potential of petroleum systems to naturally influence climate change.

1.4 Data and methods

1.4.1 Petroleum system model building workflow

Petroleum system modeling represents the main technique applied in the three papers constituting this manuscript. Different versions of Schlumberger's PetroMod software were the modeling tool applied in this work. Although values assigned to different parameters depend on each basin's geological history, the general workflow followed during the building these models is the same. The workflow applied for the building of 3-D models in this manuscript includes the following basic steps:

Model start-up. In this step, formation top depth maps (for example *.GRID, *DAT files) are imported into the modeling software. The quality of the maps is checked, and several cross sections are extracted in order to make sure that different formation tops do not overlap. Afterwards, layers are created between consecutive formation tops. If available, relevant culture data such as exploration blocks or country boundaries are imported into the model, aiming to ease the spatial orientation during the model building and output interpretation. Well locations are incorporated into the model together with the calibration data they contain (value vs depth). In this study, calibration data consisted on measured vitrinite reflectance (%Ro) and temperatures (borehole and DST temperatures).

Assignment of layer ages, hiatus and erosions. A depositional age was assigned to each of the formation layers implemented in each model. Moreover, the beginning and end age of hiatus periods were specified. In the case of erosions, maps indicating the magnitude of this event at different location were implemented.

Lithofacies definition. This consisted on the assignment of defined lithological (and therefore petrophysical) properties to each formation layer. Lateral lithological variations within a same layer were considered by the implementation of facies maps. In the case of the Western Canada Basin, available data allowed for the creation of mixed lithologies, which are shown in Appendix section.

Source rock definition. The amount and type of products generated by each source rock interval, as well the timing of generation, will not only depend on burial history and source rock thickness, but also on the total organic carbon (TOC), hydrogen Index (HI) and petroleum generation kinetics. Therefore, reasonable values of the last three parameters were assigned to each modeled source rock.

Establishment of boundary conditions. Boundary conditions define the basic energetic conditions for temperature and burial history of the source rock and, consequently, for the maturation of organic matter though time (Schlumberger, 2009). The three parameters in this group are the heat flow, paleo water depth and sediment-water interface temperature. They were incorporated in each model whether as single value or distribution maps depending on the geological setting and available data.

Simulations without petroleum migration. Calibration quality check. The first simulation of each model was performed without implementing petroleum migration in order to minimize the computing time. The main objective of this step was to test how well the model achieves to predict the measured temperature and vitrinite reflectance values. In general, the maximum accepted difference between predicted and measured values was of 10°C and 0.1 %Ro, respectively. In case the calibration

was not satisfactory, the model definition was reconsidered and reasonably adjusted until a good calibration was achieved.

Implementation of faults. In relevant cases and when data were available, fault geometries were incorporated in the model. At the same time, faults were assigned as open or closed to fluid migration during different stages of fault development. Details for each particular case are provided in chapters 2, 3 and 4.

Simulation including petroleum migration. Output analysis. In this last step, the model was run including the migration algorithms mentioned earlier in this manuscript. The mass and/or volumes of present-day accumulations were compared against known discoveries and output data were analyzed. Output data provided by these models include generated, migrated and accumulated petroleum mass, secondary cracking losses and gas outflow at the sediment surface during each model's time step.

1.4.2 Input data for 3-D model building definition

Western Canada Sedimentary Basin

In the case of the WCSB, a full-scale initial model of the basin containing 22 isopach maps and preliminary lithofacies assignment was provided by the U.S Geological Survey. Further refining of the model properties, definition of boundary conditions, and sensitivity study of source rock properties performed on this model were mostly based on published data. A summary of the model definition is shown in Table 1.3, and an extensive description is provided in Chapter 2.

Table 1.3 Input data for building the WCSB 3D petroleum system model.

Source rock properties					
Unit	**Kerogen Type**	**TOC** (wt. %)	**HI** (mgHC/gTOC)	**Average thickness** (m)	**Kinetic model**
Poker Chip Shale A	II	7.36	550	15.8	Higley et al. (2009)
Gordondale Member	I/II S	15.89	740	26	
Doig Formation	II	2.90	450	40	
Exshaw Formation	II	9.64	500	12	
Duvernay Formation	II	5.81	510	43.6	
Mannville Coal	Coal	60	200	10	Pepper and Corvi (1995)
Boundary conditions					
Heat Flow					
Map/single value	**Time (Ma)**		**Value (mW/m^2)**	**Source (s)**	
Map	380 - 119		48-65	Bachu and Burwash (1994); Blackwell and Richards (2004); Allen and Allen (1990); Deming (1994)	
Map	119-0		48-77		
Erosion					
Map/ value	**Time (Ma)**		**Value (m)**	**Source (s)**	
Map	150-119		<100	Magara (1976); Hacquebard (1977); Nurkowski (1984); Kumar and Magara (1979)	
Map	58-0		500-2500		
Sediment-water interface temperature					
Map/ value	**Time (Ma)**		**Value (°C)**	**Source (s)**	
Value	380-10		24-10	Wygrala (1986)	
Value	10-0		10-05		
Paleo-water depth					
Map/ value	**Time (Ma)**		**Value (°C)**	**Source (s)**	
Map	380-58		100-300	Fowler et al (2004); Stasiuk and Fowler (2004); Edwards et al (1994); Ross and Bustin (2006)	
Map	58-0		100-0		

Mackenzie Basin

Eleven Formation top depth maps were used as the starting point for the building of the Beaufort/Mackenzie Basin 3-D model. These maps were provided by Judith Sippel and the Basin Analysis department at the GeoForschungsZentrum (GFZ) Potsdam. Most of the input parameters for model definition were taken from Sippel et al. (2012), Kroeger et al. (2008, 2009) and different publications including Dixon (e.g., 1992). A summary is provided in Table 1.4 and a wider discussion in Chapter 3.

Table 1.4 Input data for building the BMB 3D petroleum system model

Source rock properties					
Unit	**Kerogen Type**	**TOC** (wt. %)	**HI** (mgHC/gTOC)	**Average thickness** (m)	**Kinetic model**
Taglu*		3	300	300	Bakken Shale (di Primio and Horsfield. 2006)
Aklak		3.5	150	250	Brown Coal (di Primio and Horsfield. 2006)
Smoking Hills		3	300	100	Bakken Shale (di Primio and Horsfield. 2006)
Boundary conditions					
Heat Flow					
Map/single value	**Time (Ma)**	**Value (mW/m^2)**	**Source (s)**		
Map	650-0	47-58	Sippel et al. (2014)		
Erosion					
Map/ value	**Time (Ma)**	**Value (m)**	**Source (s)**		
Map	6.5-8	40-960	Dixon (1992); Kroeger et al. (2008, 2009)		
Map	23.8-25	0-550			
Map	33.9-35	10-800			
Map	37.2-39	30-820			
Map	60.9-62	0-563			

Continued on next page

Table 1.4 - Continued

Sediment-water interface temperature			
Map/ value	**Time (Ma)**	**Value (°C)**	**Source (s)**
Map	0-0.5	0 to -15	Wygrala (1986); Kroeger et al. (2008); Chen et al. (2008); Issler (1990)
Map	0.5-1	-2 to -17	
Map	1-5	1	
Map	5-10	1.5	
Map	10-18	3	
Map	18-22	4	
Map	22-23	3	
Map	23-30	8	
Map	30-40	13	
Map	40-54	14	
Map	54-65	19	
Map	65-200	19	
Paleo-water depth			
Map/ value	**Time (Ma)**	**Value (°C)**	**Source (s)**
Map	0-8	0-86	Williams et al. (2006); Dixon et al. (2008)
Map	8-25	0-98	
Map	25-33	0-85	
Map	33-39	0-96	
Map	39-55	0-97	
Map	55-62	0-99	
Map	62-100	5-25	
Map	100-240	25	
Map	240-650	12	

Central Graben of the North Sea

The 3-D model of the Central Graben applied in this study was previously developed at GeoForschungsZentrum (GFZ) Potsdam, and is described by di Primio and Neumann (2008) and Neumann (2007). A summary of the main input parameters contained in this model is provided in Table 1.5.

Table 1.5 Input data for building the Central Graben petroleum system model.

Source rock properties					
Unit	**Kerogen Type**	**TOC** (wt. %)	**HI** (mgHC/gTOC)	**Average thickness** (m)	**Kinetic model**
KFC/Mandal	II	6	450	160	Vandenbroucke et al. (1999)
Heather/Farsund	II/III	5	400	500	
Pentland/Bryne	III	3	200	380	

Boundary conditions			
Heat Flow			
Map/single value	**Time (Ma)**	**Value (mW/m^2)**	**Source (s)**
Value	290-245	62	Neumann (2007); di Primio and Neumann (2008)
Value	245-210	62-70	
Value	210-155	62	
Value	155-50	62-90	
Value	50-00	62	
Erosion			
Map/ value	**Time (Ma)**	**Value (m)**	**Source (s)**
No erosion			
Sediment-water interface temperature			
Map/ value	**Time (Ma)**	**Value (°C)**	**Source (s)**
Value	290-170	16-12	Neumann (2007); di Primio and Neumann (2008)
Value	170-100	12-10	
Value	100-50	10-16	
Value	50-0	16-08	
Paleo-water depth			
Map/ value	**Time (Ma)**	**Value (°C)**	**Source (s)**
Value	290-150	0-10	Neumann (2007); di Primio and Neumann (2008)
Value	150-90	10-200	
Value	90-70	200-0	
Value	70-5	0-10	
Value	5-0	0-60	

1.4.3 Estimation of biodegradation rates and biogenic methane masses

For the estimation of the biogenic methane mass generated during the formation of the oil sands in the WCSB, a mass balance approach was followed. The mass balance focused only on the Athabasca accumulation because it is the main oil sand deposit, accounting for 70% of the total petroleum volume in the WSCB basin (Canada, 2010), and its mode and history of formation has been modelled in detail (Berbesi et al. 2012).

Total mass of biogenic methane generated

A simple biodegradation mass balance was performed following a similar methodology to the one applied by Milkov (2011). This is based on the net equation describing methanogenic alkane biodegradation by Zengler et al. (1999) and Jones et al. (2008), which are discussed in 1.2.6.

$$4\ C_{16}H_{34} + 30\ H_2O \rightarrow 49\ CH_4 + 15\ CO_2$$

Based on previous works (Head et al., 2003; Larter et al., 2006; Larter et al., 2005; Brooks et al., 1988; Adams et al., 2012) it was assumed that 30 % to 70 % of the originally accumulated oil mass at Athabasca has been lost during petroleum biodegradation (results and discussion in Chapter 4).

Methane generation rates

Firstly, the biodegradation process was sub-divided in time intervals of 10 Myr, and the equation 1 was applied for each of them:

$$M = I \times T \times R \qquad \text{(Eq 1)}$$

In Equation 1, (M) is the mass of oil consumed during a time interval, (I) is the initial (in subsequent steps to the remaining) oil mass, (T) represents the duration of the

time interval, and (R) the biodegradation flux or rate*, which is variable through time.

After the consumed oil mass (M) for each stage was calculated, the microbial methane mass was estimated using the stoichiometric model proposed by Zengler et al. (1999) and Jones et al. (2008). The rate of microbial methane generation for each time step was obtained dividing the mass of methane generated (in Teragram) by the duration of the time interval (in years).

***Estimation of the "R" factor, or biodegradation flux:**

R was estimated considering the most likely biodegradation scenarios proposed by published data (Larter et al., 2005, 2006; Higley et al., 2009; Berbesi et al., 2012). The 220 000 Tg of oil predicted by 3D modelling to have reached the Athabasca accumulation (Berbesi et al., 2012) were used as the total, potentially degradable oil mass. Most of the biodegradation was considered to take place during burial and shortly after the onset of uplift, coinciding with the main charging phase. This is consistent with the general idea that continuous oil charging, decrease in biodegradation rates by reservoir filling to the underseal and early reduction in the water leg, combined with very low reservoir temperatures are required to explain the non-complete destruction of Athabasca oils (Adams et al., 2012; Larter et al., 2006).

Two scenarios for the onset of oil charging were considered; these were 100 Myr ago and 80 Myr ago. The reason for these two scenarios is the existing discussion regarding the Athabasca oil charging time. Based on PSM, Higley et al. (2009) suggest that oil accumulations in the Lower Cretaceous Mannville Group should have been filled at about 75 Ma, although no details are given when it comes to the filling of individual accumulations. The 3D PS model by Berbesi et al. (2012) proposes that around 220 000 Tg of oil gradually reached the Athabasca from 70 to 50 Ma, and that more than 75 % of this mass entered the accumulation before the onset of the Laramide orogeny. On the other hand, biodegradation modeling by Adams et al. (2012) managed to reproduce the present-day API gravity in Athabasca

when the reservoir is gradually charged from 100 Ma until the time of maximum burial (60 Ma in this case). Some other attempts to constrain the timing of oil generation in the basin as well as charging of Athabasca oils include Creaney et al. (1994), Creaney and Allan (1990), Selby et al. (2011). An up- to- date discussion of the topic can be found in Adams et al. (2012) and Berbesi et al. (2012). In general, the literature proposes onset times for the Athabasca oil charging ranging from ca 110 to 70 Ma, and seems to agree on the conclusion that most of the original oil accumulated before the Eocene. The obtained R values ranged from $9x10^{-5}$ to $9x10^{-3}$ Kg of consumed oil per year.

Chapter 2

Source rock contributions to the Lower Cretaceous heavy oil accumulations in Alberta: a basin modelling study

This chapter has been published as: Berbesi, L. A., R. di. Primio, Z. Anka, B. Horsfield, and D. K. Higley, 2012, Source rock contributions to the Lower Cretaceous heavy oil accumulations in Alberta: a basin modeling study: AAPG Bulletin, v. 96, p. 1211-1234.

2.1 Abstract

The origin of the immense oil sand deposits in Lower Cretaceous reservoirs of the Western Canada Sedimentary Basin is still a matter of debate, specifically with respect to the original in-place volumes and contributing source rocks. In this study, the contributions from the main source rocks were addressed using a three-dimensional (3D) petroleum system model calibrated to well data. A sensitivity analysis of source rock definition was performed in the case of the two main contributors, which are the Lower Jurassic Gordondale Member of the Fernie Group and the Upper Devonian to Lower Mississippian Exshaw Formation. This sensitivity analysis included variations of assigned TOC and HI for both source intervals, and in the case of the Exshaw Formation, also variations of thickness in areas beneath the Rocky Mountains were considered. All of the modeled source rocks reached the early or main oil generation stages by 60 Ma, before the onset of the Laramide orogeny. Reconstructed oil accumulations were initially modest, due to limited trapping efficiency. This was improved by defining lateral stratigraphic seals within

the carrier system. An additional sealing effect by biodegraded oil may have hindered the migration of petroleum in the northern areas, but not to the east of Athabasca. In the later case, the main trapping controls are dominantly stratigraphic and structural. Based on available data, the 3D model identifies the Gordondale source rock as the contributor of more than 54% of the oil in the Athabasca and Peace River accumulations, followed by minor amounts from Exshaw (15%) and other Devonian to Lower Jurassic source rocks. The proposed strong contribution of petroleum from the Exshaw Formation source rock to the Athabasca oil sands is only reproduced by assuming 25 m (82 ft) of mature Exshaw in the kitchen areas, with original TOC of 9% or more.

2.2 Introduction

The huge petroleum deposits in the foreland basins of Venezuela and Canada are exploitable resources which have only recently become more attractive to the petroleum industry, as oil prices have risen. The heavy and extra-heavy crude oil deposits in Venezuela's Orinoco Belt are the biggest of their type (PDVSA, 2006), and have in-place estimates of 206 billion cubic meters (BCM), or 1300 billion barrels (BB). The oil sands in the Western Canada Sedimentary Basin (WCSB) are estimated to contain 260 BCM (1635 BB), which represents the largest known concentration of petroleum classified as crude bitumen (Canada, 2010). The main difference between these two types is that heavy oils are still mobile in reservoir conditions, while the crude bitumen found in oil sands is immobile and therefore cannot be produced by conventional techniques (Tissot and Welte, 1984).

The main oil sand deposits of the WCSB are in Alberta. These deposits are, from highest to lowest in-place estimates, Athabasca (189 BCM), Cold Lake (32 BCM) and Peace River (21 BCM). Seventy-three percent of the reserves are present within the Lower Cretaceous Mannville Group, where sandstones of the McMurray Formation are the main host rocks (Gingras and Rokosh, 2004). The possible ages of the source rocks contributing to these accumulations range from Devonian to early Cretaceous.

The oil sand accumulations are the product of microbial degradation of initially light oils, occurring after the onset of the Laramide orogeny (Head et al., 2003). The high level of biodegradation of these oils, ranging from four to eight on the Peters and Moldowan scale (Adams et al., 2006; Brooks et al., 1988), has made the use of chemical parameters and biomarkers for oil-oil and oil-source rock correlations difficult. This has limited the understanding of the relative proportions of petroleum contributed by different source rocks.

Some organic geochemical studies (Fowler et al., 2001; Leenheer, 1984; Riediger et al., 2001) propose the Upper Devonian to Lower Mississippian Exshaw Formation as the main source of petroleum in Alberta. However, an alternative interpretation proposes the Gordondale Member of the Fernie Group as the main contributor. A 3D model covering most of Alberta by Higley et al. (2009) indicated that long-distance migration of oils generated by the Gordondale Member is possible. This work also proposed the organic-rich strata of the Fernie Group as the main oil contributor to the oil sands in Alberta, but had problems reproducing the volumes of trapped oil. The main reasons were the coarse grid size required for the simulations, exclusion of parts of the kitchen areas from the model, migration of oil to zones outside of the modeled area, as well as software limitations, such as the inability to simulate the formation of biodegraded oil seals.

In this contribution, new understanding and results derived from an extended model of the WCSB, covering Alberta, Saskatchewan and a part of the Rocky Mountains in British Columbia (Figure 2.1) are presented. Most of the input data used for the construction of this model was previously applied in the model described by Higley et al. (2009). However, this contribution differs from the previously referred work in two main aspects. First, this work puts special attention to the trapping efficiency of Cretaceous strata as the main factor limiting the accurate assessment of accumulated volumes. Second, this study performs a sensitivity analysis of TOC and HI values, as well as source rock thickness for the two main proposed source rocks (Exshaw and Gordondale). The purpose of this assessment was to minimize the uncertainty related to source rock occurrence beneath the Rocky Mountains, and discuss the

implications of the source rock definition on results derived from 3D modelling of the petroleum systems in the region.

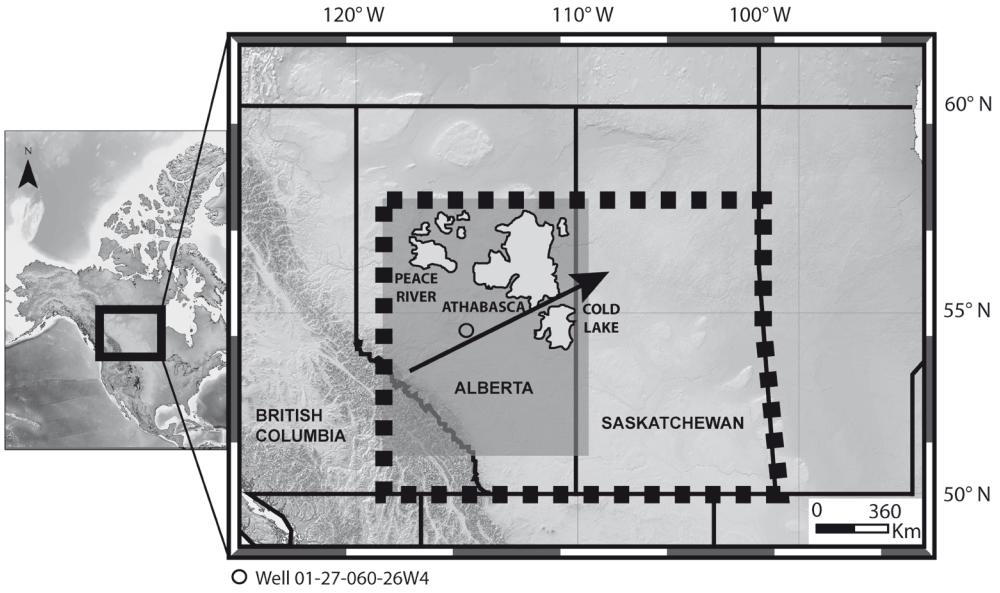

Figure 2.1 Location map of the Western Canada Sedimentary Basin. The square marked by thick dashed lines indicates the area modeled in this study. A dark-grey square indicates the area modeled by Higley et al. (2009). The arrow indicates an increase in the percentage of low-energy facies that is referred to in the discussion (from Berbesi et al., 2012). AAPG©[2015], reprinted by permission of the AAPG whose permission is required for further use.

2.3 Tectono-stratigraphic history of the Western Canada Basin

The sedimentary sequence in the Western Canada basin extends from the Early Paleozoic to the Early Tertiary (Figure 2.2), and reflects the deposition and erosion of sediments under two main tectonic phases: a Paleozoic to Jurassic platform and a Late-Jurassic to Paleocene foreland basin (Wright et al., 1994).

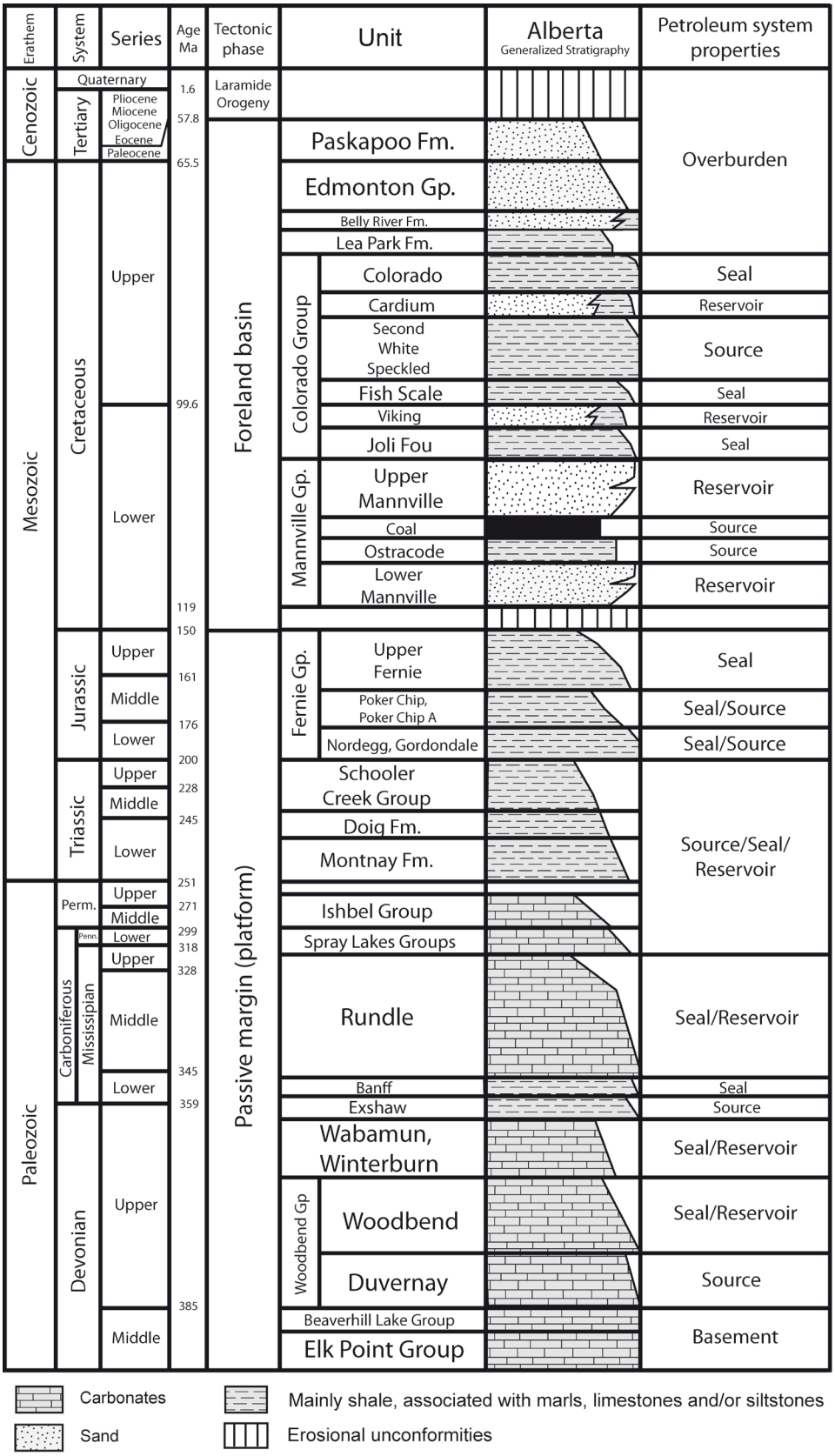

Figure 2.2 Generalized stratigraphy and petroleum system elements as introduced in the WCSB 3D model (from Berbesi et al., 2012). AAPG©[2015], reprinted by permission of the AAPG whose permission is required for further use.

The platform succession resembles a stable craton adjacent to the ancient, dominantly passive margin of North America. In the study area, the base of this interval is represented by the middle Devonian Elk Point Group carbonate rocks (Wright et al., 1994). The strata contain mainly carbonates, with some siliciclastic (mainly shales and marls) and evaporitic layers. Several series of transgressions and regressions occurred during deposition of this stratigraphic section, resulting in the prolific oil and gas reservoirs associated with the former Peace River Embayment (Podruski et al., 1988; Gibson, 1975).

The Lower Jurassic strata represent the pre-orogenic stage and consist of the limestones and phosphatic sequences of the Nordegg Member and the organic-rich Poker Chip Shale Member (Figure 2.2). Upper Jurassic strata were then deposited in the transitional phase from a stable continental shelf to a subsiding foredeep trough (Wright et al., 1994), as a consequence of the collision of allochthonous terranes in the eastern Pacific with the westerly drifting North American Continent (Poulton et al., 1990). A major drop of sea level was responsible for significant erosion across the foreland trough (pre-Mannville unconformity) during the Early Cretaceous. During the late Barremian, the western edge of the craton was loaded with thrust sheets associated with allochthonous terrane accretion, bringing a new period of subsidence, and the deposition of the Lower Cretaceous Mannville Group (Cant and Stockmal, 1989).

The oldest sediments of the Mannville Group consist of sandstones deposited mainly by alluvial fans and rivers. Continued basin subsidence and relative sea level rise resulted in the succession of shales, siltstones and lenticular sandstones of the Ostracode interval (Finger, 1983). Major sediment input associated with the Cordilleran evolution pushed the shoreline northward and converted most of Alberta and Saskatchewan into floodplains. Fluvial channel sandstones, siltstones, shale and coal are characteristic of this depositional period (Finger, 1983; Christopher, 1984). Deposition of the upper part of the Mannville Group was followed by Middle to Late Albian lowstand and erosion, giving origin to the post-Mannville unconformity. During Late Albian time, most of the basin was flooded due to a major rise in sea

level, with associated deposition of Joli Fou Shale (Smith, 2008), the main seal for the oil accumulations within the Lower Cretaceous reservoirs (Creaney and Allan, 1990). The Joli Fou Shale is also the main seal in our 3D model.

The stratigraphic section represented by the Lower to Upper Cretaceous Colorado Group corresponds to several periods of marine inundations and regressions, as well as lateral variation from offshore to shoreface facies. As indicated by Mack and Jerzykiewicz (1989), the Paleocene Paskapoo Formation in Alberta and the equivalent Ravenscrag Formation in Saskatchewan were deposited during the thrusting event in the Cordillera, containing mainly fluvial channel sandstones, siltstones, shales and in some locations, coal. The deposition of this interval was followed by major uplift and erosion associated with the Laramide Orogeny, thus terminating the phase of foreland basin deposition.

2.4 Petroleum system geometry and elements

The Western Canada Basin has typical asymmetrical foreland basin geometry, with a gently dipping eastern margin and a steeper thrust-bounded western margin. The kitchen areas are located in the deep western areas, where highest temperatures were reached. The tilted migration pathways promoted lateral migration of the generated petroleum to the shallower traps in the east (Higley et al., 2009). Once accumulated, low reservoir temperatures promoted subsequent biodegradation of the petroleum.

2.4.1 Source Rocks

Ages of the petroleum source rocks within the WCSB range from Devonian to Upper Cretaceous. Here we describe the source rocks that are proposed as the main contributors to Mannville petroleum accumulations. From oldest to youngest these are: Duvernay, Exshaw, Doig, Gordondale, Poker Chip, as well as the Ostracode and coal zones within the Mannville Group (Figure 2.2). The Second White Speckled Shale has been proposed as a source rock for oil in some Upper Cretaceous reservoirs (*e.g.,* Creaney and Allan, 1990; Creaney et al., 1994); however, because it

did not contribute oil to the Lower Cretaceous oil sands, the Second White Speckled Shale was not modelled. The Ostracode zone and coal within the Mannville Group have been indicated as important contributors of oil to the Cold Lake oil sands and the Provost field (Higley et al., 2009; Riediger et al., 1997). However these strata were not considered as source rocks, because efforts were focused on the Devonian to Jurassic intervals.

Duvernay Formation (Devonian Woodbend Group)

As widely described in the literature (Creaney and Allan, 1990; Creaney et al., 1994), the Duvernay Formation is characterized by extensive basinal deposits and consists of dark brown to black bituminous carbonates interbedded with gray-green calcareous shales. The Duvernay represents a period of great accumulation and preservation of organic carbon under marine deep water conditions. Evidence of euxinic water-column conditions and low sedimentation rates were reported by Stoakes (1980) among others. The organic matter in this interval can be classified as Type II (oil prone) kerogen, with TOC values ranging from 2 to 20 wt% and hydrogen indices between 500 and 600 mg HC/g TOC. The thickness of this formation is variable, with an average of 44 m (144 ft), although greater thickness (around 100 m or more) has been described in some areas (Switzer et al., 1994).

Exshaw Formation (Upper Devonian-Lower Mississippian)

The Bakken and Exshaw formations comprise fine-grained siliciclastics deposited in euxinic to shallow neritic environments during Late Famennian and earliest Tournaisian time (Richards et al., 1994), following a major drowning event that terminated the carbonate system of the Devonian (Creaney and Allan, 1990). The Exshaw Formation lies beneath the Alberta Plains and in outcrops in the Foothills and Front Ranges of the Rocky Mountains, thickening from east to west. This source rock can be divided into lower black shale and upper siltstone members. The TOC values of the black shale, which is the main generating interval, are up to 21 wt% (Caplan and Bustin, 1996; Creaney and Allan, 1990; Leenheer, 1984; Smith and Bustin, 2000a). The average HI is around 515 mg HC/g TOC, but values as high as

909 mg HC/g TOC have been reported for this Type II, marine source rock (Smith and Bustin, 2000a).

Doig Formation (Triassic)

The Triassic Doig Formation consists of an upper siltstone unit and a lower, highly radioactive, shale unit. The generating interval is the basal unit, which is also called the Phosphate Zone (Creaney and Allan, 1990; Riediger et al., 1990b). Published TOC and HI values for this interval are up to 11 wt% and 480 mg HC/g TOC, respectively (Riediger et al., 1990b). Oil in some Triassic reservoirs is proposed to originate from this source rock, which contains Type II, marine organic matter (Riediger et al., 1990a). Riediger et al. (1990b) reported a thickness of 78 m (256 ft) in the type section, of which 39 meters (128 ft) correspond to the basal Phosphate Zone.

Gordondale and Poker Chip Shale Members of the Fernie Group (Lower Jurassic)

The Gordondale Member (Figure 2.2) consists mainly of dark brown, finely-laminated calcitic mudstones, calcilutites and calcarenites with variably phosphatic content and high radioactivity due to the presence of uranium (Asgar-Deen et al., 2004). This stratigraphic interval corresponds to the "Nordegg Member" of the Fernie Group, mentioned in many publications (Riediger et al., 1990a; Riediger and Coniglio, 1992; Poulton et al., 1990). It covers a significant portion of west-central Alberta and northeastern British Columbia, and was deposited after a major marine transgression in the Early Jurassic. The thickness of this formation is variable, reaching maximum values of 67.7 m (222 ft), with approximately 25 m (82 ft) as an average (Mossop and Shetsen, 1994). The Gordondale Member contains sulfur-rich Type I/II-S marine kerogen, with TOC values reaching up to 28 wt% (Asgar-Deen et al., 2004; Riediger et al., 1990a). The HI ranges from 26 to 273 mg HC/g TOC for mature samples (Ibrahimbas and Riediger, 2004; Riediger et al., 1990a), and reaches up to 800 mg HC/g TOC for immature samples (Asgar-Deen et al., 2004; Creaney and Allan, 1990; Riediger et al., 1990a) .

The Early to Late Toarcian Poker Chip A shale is the rock interval with the best source rock potential within the Poker Chip Shale Member of the Fernie Group. It consists of black, calcareous shales and thin limestones deposited in marine environments, and is present in southern and western Alberta. It contains Type II organic matter, with TOC values reaching up to 18.5% and HI of up to 740 mg HC/g TOC for immature samples (Riediger, 2002).

Ostracode Zone and coals in the Mannville Group (Lower Cretaceous)

The lowest stratigraphic section of the foreland basin is rich in deltaic and coastal plain strata, as well as coals, which are described as mainly gas-prone source rocks (Creaney and Allan, 1990; Riediger et al., 1999). The Ostracode Zone comprises estuarine valley fill strata, deposited during a north to south transgression as limestone and calcareous fossiliferous shale. Riediger et al. (1997) described the section as consisting of a mixture of units containing Type III kerogen with beds containing Type I and II kerogen. Reported values of TOC and HI for thermally immature samples (Moshier and Waples, 1985; Riediger et al., 1997) are around 2.5 wt. % and 317 mg HC/g TOC, respectively.

Oil contribution from source rocks to accumulations in Lower Cretaceous strata

There is no agreement as to the main source rocks for reservoirs in the Lower Cretaceous Mannville strata. Brooks et al. (1988) used biomarkers to propose that the Cretaceous reservoirs were charged by oil that had experienced long-distance migration, and which was generated by the same or at least very similar source rocks. However, they did not identify specific source rock candidates.

Creaney and Allan (1990) estimated that at least 1.7 trillion barrels (270×10^9 m^3) of oil in Lower Cretaceous Mannville Group sands originated from source rocks in the following order of importance: Nordegg (Gordondale) Member, Exshaw Formation, Phosphate Zone of the Doig Formation, and Duvernay Formation (Figure 2.2). A 4D model of a portion of Alberta and Saskatchewan developed by Higley et al. (2009) proposed that source rocks in the Jurassic Fernie Group (Gordondale Member and

Poker Chip A shale) were the initial and major contributors of petroleum to Mannville Group reservoirs.

In contrast, the idea of the "Nordegg" (Gordondale) Member as the main source rock was not supported by Riediger (1994), who considered that oils generated by sulfur-rich kerogen in this interval should have very low API gravities, and would not be able to migrate long distances. This author also indicated that oil samples found in Athabasca showed some biomarker distributions such as pristane/phytane, diasterane/regular sterane, and abundance of C_{35} relative to C_{34} hopanes that were inconsistent with those found in Gordondale bitumens (Riediger et al., 1990a). Many biomarker correlations indicate that the Exshaw source rock was the primary contributor to the Lower Cretaceous oil sand deposits in Alberta (Fowler et al., 2001; Leenheer, 1984; Riediger et al., 2001). Adams et al. (2010) used biodegradation-resistant parameters to conclude that the Peace River reservoirs received an important contribution from the Gordondale Member, but that the Athabasca and Cold Lake deposits originated mainly from the Exshaw Formation.

2.4.2 Reservoir formations

The main oil sand deposits in the WCSB occur at Athabasca, Cold Lake and Peace River. More than 70% of the oil found in these deposits are within formations belonging to the Lower Cretaceous Mannville Group (Gingras and Rokosh, 2004). The Athabasca and Cold Lake oil sands occur mainly within the McMurray and Clearwater Formations and equivalent strata (Vigrass, 1968). The accumulations at Peace River are mainly in the Bluesky and Gething Formations (Gingras and Rokosh, 2004; Vigrass, 1968).

In general, the Mannville Group consists of interbedded sandstone and shale deposited on an erosional surface that truncates the Jurassic and older strata of the WCSB. Interested readers are referred to (Vigrass, 1968) for a more extended geological description of the oil sands area.

Accumulations at Peace River and Cold Lake correspond to pinchouts of the reservoirs against shales and structural highs (Vigrass, 1968). The trapping mechanism of the Athabasca oil sands is controversial (Ranger, 2006). Vigrass (1968) indicated that most of the Athabasca accumulation corresponds to a subtle domal structure, that began to form before deposition of the reservoir sands, with a later increase in amplitude around Early Cretaceous time. The same author indicated that another portion of the Athabasca accumulation occurs in the trough and northeastern limb of a syncline that resulted from salt dissolution of Devonian evaporites. Ranger (2006) proposed that the structural control exerted by salt dissolution was important in the southeastern part of Athabasca, but not to the northeast, where the timing of evaporite dissolution may have precluded the development of a structural trap before migration. For the later case, this author suggested a stratigraphic control where Upper Mannville shales overlapped and sealed the McMurray reservoir Formation against Paleozoic and Precambrian rocks. However, this hypotheses has not been confirmed by direct evidence, which might have been destroyed during Pleistocene erosion (Ranger, 2006).

2.4.3 Seals

Among the Paleozoic to Tertiary sedimentary sequences shown in Figure 2.2, there are many rock intervals that act as seals within the different petroleum systems in the WCSB. The main seal for petroleum within Mannville strata across the WCSB is represented by the Joli Fou Formation of the Middle Cretaceous Colorado Group. This formation is present across most of Alberta and extends eastwards, reaching the Manitoba Escarpment, where it is called the Skull Creek Member (Leckie et al., 2008). It consists of non-calcareous marine shale with a small proportion of interbedded fine-to medium-grained sandstone, which was deposited during a major sea level high (Leckie et al., 2008; Wickenden, 1949).

2.5 3D model definition and calibration

2.5.1 Input Data

The 3D model presented here includes parts of Alberta, Saskatchewan, and the Rocky Mountains of British Columbia (Figure 2.1), covering a total area of 1 412 400 Km^2 (545 330 mi^2). A full scale model of the basin containing 22 isopach maps and preliminary lithofacies assignment was kindly provided by the U.S. Geological Survey and Debra K. Higley. The modelling software used in this work was Schlumberger's PetroMod 3D version 11.3.

2.5.2 Lithologies and source rock definition

The stratigraphic sequences shown in Figure 2.2 were reproduced in the model by 22 layers that are regionally extended versions of those described by Higley et al. (2009). They extend south to the limits of Alberta and east to the border of Saskatchewan-Manitoba. The ages and initial lithofacies are described by Higley et al. (2009). The model includes lateral facies variation for each layer. Vertical rock heterogeneity within each stratigraphic unit was not represented in detail but was influenced by the use of mixed lithologies within assigned lithofacies. Conversion of the original 3D model to a newer version of the modelling software required a subtle change on the initial lithofacies definition. The new lithofacies are slightly more permeable than those described by Higley et al. (2009) for carrier beds and reservoirs.

For comparison purposes, the model of Higley et al. (2009) is here termed as "previous model", and the larger version described in this manuscript will be termed "extended model". The thickness of the source rock layers as well as the TOC and HI contents were initially assigned as in the previous model of Alberta, and are summarized in Table 2.1.

In order to reduce the uncertainty related to source rock heterogeneity, a sensitivity analysis with respect to TOC and HI was performed. This sensitivity analysis focused on the Gordondale Member of the Fernie Group and the Exshaw Formation, because they are described in the literature as the main likely contributors to the Mannville reservoirs. As it will be discussed later, the results based on initial assumptions were inconsistent with some interpretations from organic geochemistry, in relation to the origin of petroleum in the Lower Cretaceous strata of Alberta. Attending to this, also the impact of Exshaw Formation thickness variations was evaluated.

Table 2.1 Modeled source rocks and initial input parameters applied in the WCSB model. The values correspond to those applied in the previous 3D model of Alberta published by Higley et al. (2009) (from Berbesi et al., 2012). AAPG©[2015], reprinted by permission of the AAPG whose permission is required for further use.

Source rock layer	Kerogen Type	TOC (wt. %)	HI (mgHC/gTOC)	Average Thickness (m)	Ea* (Kcal/mol)	$LogA_0$** (1/m.y)
Poker Chip Shale A (Fernie Group)	II	7.36	550	15.8	37.6	21.9
Gordondale member (Fernie Group)	I/IIS	15.89	740	26	37.6	21.9
Doig Formation	II	2.90	450	40	52.5	26.8
Exshaw Formation	II	9.64	500	4.2	53.6	27.1
Duvernay Formation	II	5.81	510	43.6	58.5	28.7

*The values correspond to those applied in the previous three-dimensional model of Alberta published by Higley et al. (2009)
**Ea = activation energy; A_0 = frequency factor

2.5.3 Oil generation kinetics

The first kinetic parameters applied in the model were based on the relationship between the organic sulfur content of kerogen and the kinetic parameters determined by hydrous pyrolysis (Higley et al., 2009). This methodology is described by Lewan and Ruble (2002), and it basically consists of estimates of the activation energy derived from hydrous pyrolysis experiments using the organic sulfur mole fraction of kerogen (S_{org}/S_{org} + C). By means of this activation energy, the frequency factor can be determined from the compensation relationship between these two variables.

Table 2.1 shows the values used for these initial activation energies and frequency factors. Composite samples of immature Poker Chip A shale were not available when these kinetic parameters were obtained. For this reason, the kinetic parameters for this source rock are the same as those for Type IIS kerogen from the Gordondale Member, which is a reasonable assumption based on its lithology, consisting of organic-rich, black calcareous shale and thin limestone (Higley et al., 2009).

2.5.4 Boundary Conditions

For model calibration the main control lies in the correct reproduction of maximum burial temperature and timing. In a basin currently at maximum burial, the principal variable to achieve a good temperature calibration is the basal heat flow. In inverted (uplifted) basins maximum paleo-temperatures reached by the sediments depend on a combination of heat flow, erosion magnitude and timing.

For the WCSB model, the calibration started by addressing the heat flow distribution. Afterwards, the erosion magnitudes and the sediment water interface temperature (SWIT), as well as the paleo-bathymetry were addressed. During each step of the process, multiple 1D extractions across the basin were calibrated to vitrinite reflectance ($\%R_o$) and temperature measurements from wells.

- **Heat Flow**

The heat flow maps used in the model are shown in Figure 2.3a and 2.3b, and were developed by combining two published maps.

Bachu and Burwash (1994) analyzed the geothermal regime in the sedimentary rocks of the Western Canada Basin using corrected bottom-hole temperature (BHT) measurements. Based on 487 data points, they constructed a basement heat flow map that includes the foothills and northern parts of Alberta and the southern part of Saskatchewan. Their values, which range between 40 mW/m^2 in southern Alberta and Saskatchewan to more than 80 mW/m^2 in the northern parts of Alberta and

Northwestern Canadian Territories, correspond well with the geothermal gradient in the region.

The second data source for our heat flow maps was the geothermal map of North America (Blackwell and Richards, 2004), which integrates extensive industry thermal datasets and research on heat flow data. This map shows heat flow values around 80 mW/m^2 beneath the Rocky Mountains in southeastern British Columbia, and 50-60 mW/m^2 in Alberta and Saskatchewan, with a trend of increasing heat flow from south to north in Alberta.

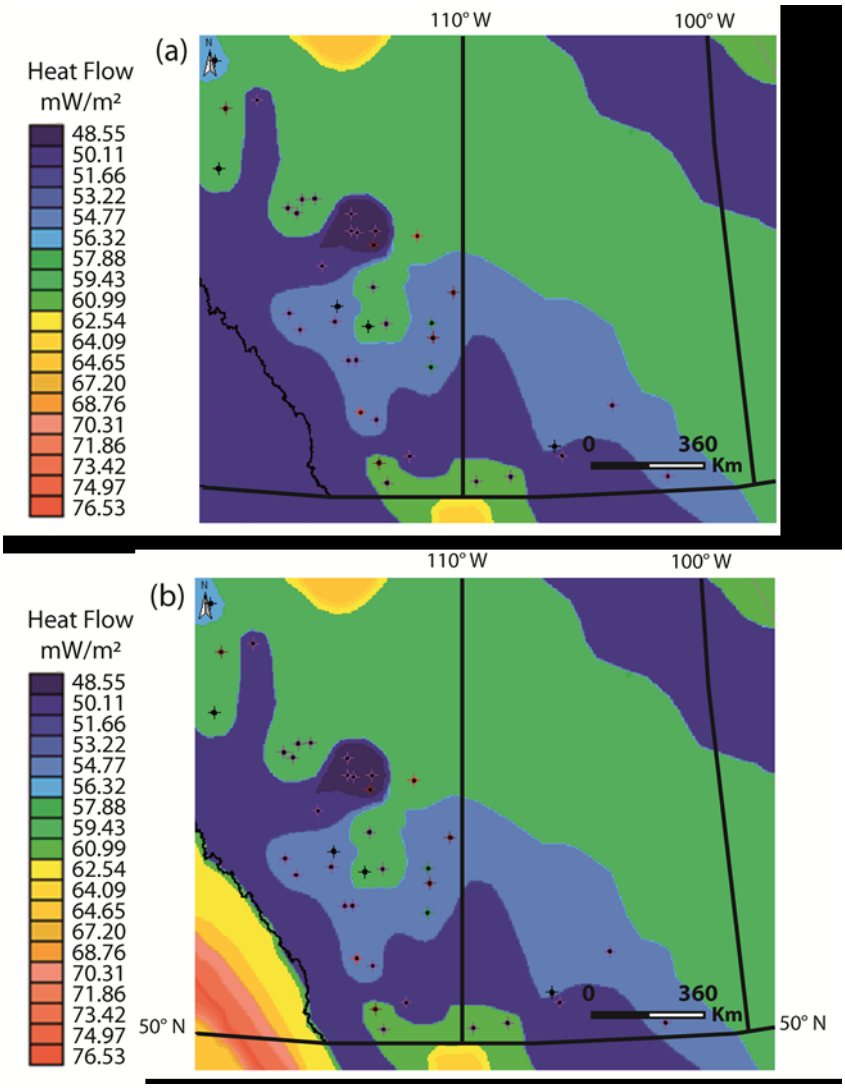

Figure 2.3 Basal heat flow maps developed for this study. (a) Pre-foreland phase (380-119 Ma). (b) Foreland phase (119 - 0 Ma). Plus symbols are locations of wells that have vitrinite reflectance data (from Berbesi et al., 2012). AAPG©[2015], reprinted by permission of the AAPG whose permission is required for further use.

In general, the heat flow values in Figure 2.3a and 2.3b are within the normal range for a foreland basin (Allen and Allen, 2005; Deming, 1994). Variation of heat flow through time was considered for the areas located beneath the Rocky Mountains, taking into account the transition from a platform in a passive margin to rapid accretion and subsidence associated with the Laramide Orogeny. For the areas corresponding to the plains in Alberta and Saskatchewan, the heat flow values were considered as constant, because these areas were not affected by any major thermal event.

Erosion

The next step in the calibration of the model was the estimation of erosion magnitudes. The two main erosional events that influenced thermal maturation and petroleum migration were introduced into the model based on reported data discussed below. The minor event was assigned between 150 and 119 Ma (pre-Mannville erosion), corresponding to early stages of development of the foreland basin. The main event began at 58 Ma and finishes at the present time, and corresponds to the onset of the Laramide Orogeny and subsequent basin uplift and erosion. In the case of pre-Mannville erosion, a relatively low value of 180 m (590 ft) was assigned. This value corresponds to an erosion rate of 0.006 mm/yr, which is comparable to estimates for geological settings under the influence of slow erosion (Flowers et al., 2006). Most attention was put into the Laramide erosion because it followed the period of maximum burial in Alberta, and thus had a major influence on the temperature and pressure evolution on the basin (Hitchon, 1984; Issler et al., 1999).

Magara (1976) used shale-transit time values recorded on sonic logs to estimate the magnitude of Laramide erosion in the southwestern part of the Western Canada Basin, obtaining values up to 1400 m (4600 ft). These magnitudes were later discussed by Kumar and Magara (1979), who indicated that the rate of velocity increase is a parameter that changes with depth and therefore, the estimates of erosion using Magara's technique are highly dependent on the method of

extrapolation in a curve of transit time versus depth. Hacquebard (1977) used the equilibrium moisture of coals published by Steiner et al. (1972), and compared these values with a graph derived from European data, which relates the equilibrium moisture of coal to its original depth of burial. He estimated maximum thickness of erosion of about 800 m (2600 ft) in the east of Alberta and 3000 m (9800 ft) in the west. These values are considerably higher than those estimated initially by Magara. Later, Nurkowski (1984) applied a similar methodology, but included the ranks of coal that are present in the Alberta plains in the curve that relates equilibrium moisture with depth of burial. He obtained similar trends, although around 500 m (1600 ft) less erosion for each area.

After integrating and combining the published data, the erosion magnitude map in Figure 2.4 was built. According to this map, the erosion magnitude has an average value of 500 m (1600 ft) in the Alberta plains and Saskatchewan, and reaches 2500 m (8200 ft) beneath the Rocky Mountains, coinciding mostly with the values proposed by Nurkowski (1984).

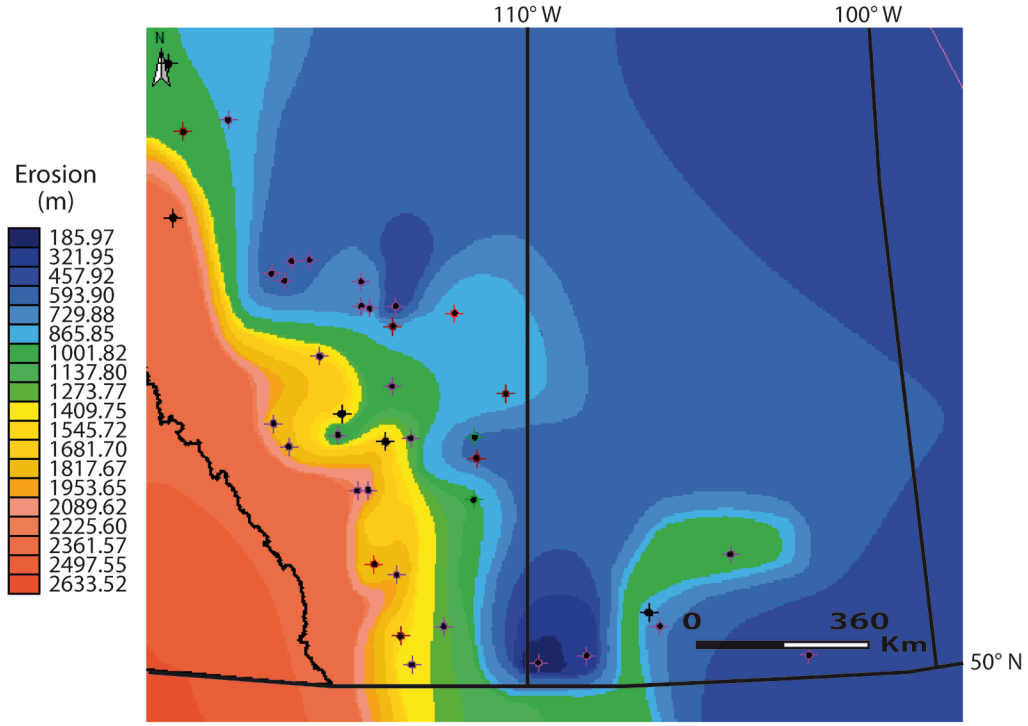

Figure 2.4 Erosion map assigned for the Laramide orogenic period (from Berbesi et al., 2012). AAPG©[2015], reprinted by permission of the AAPG whose permission is required for further use.

Sediment-Water Interface Temperature (SWIT) and Paleo-bathymetry

The temperature at the sediment-water interface was initially estimated using a tool of the modelling software, which generates a SWIT trend over geologic time for a given present-day latitude, longitude and paleo-water depth (Wygrala, 1986). The application of this tool resulted in SWIT values around 20°C for most of the modeled period of time, except since the onset of the last glaciation to the present, where the SWIT ranges between 5°C and 10 °C.

Given the large area covered by the model, paleo water depth distribution maps were constructed instead of assigning a single paleo-water depth trend. Ten (10) maps representing the paleo-bathymetry for the time from Devonian to Late Cretaceous were built. These maps are based on organic facies distribution for Devonian and Mississippian strata (Fowler et al., 2004; Stasiuk and Fowler, 2004), lithofacies described for Triassic and Jurassic rocks (Edwards et al., 1994; Ross and Bustin, 2006), and Early Turonian paleobathymetry reconstruction based on lithofacies and faunal data. Finally, zero meters of water depth was assigned from the Laramide orogeny to present.

2.5.5 Calibration data

Thermal data from 33 wells across Alberta and Saskatchewan were used for model calibration, and include drill stem test (DST) and corrected bottomhole temperatures, as well as measured vitrinite reflectance (%R_o). Figure 2.5 shows the calibration results and burial history curve for one well located in west-central Alberta (Figure 2.1).

In general, the model achieves a very good reproduction of the temperatures and maturity trends with depth. Nonetheless, the temperature calibration was problematic for a few wells in central Alberta, possibly reflecting local heat flow anomalies (Hitchon et al., 1990; Bachu and Burwash, 1994) related to basement radiogenic heat production or heat transfer by groundwater flow.

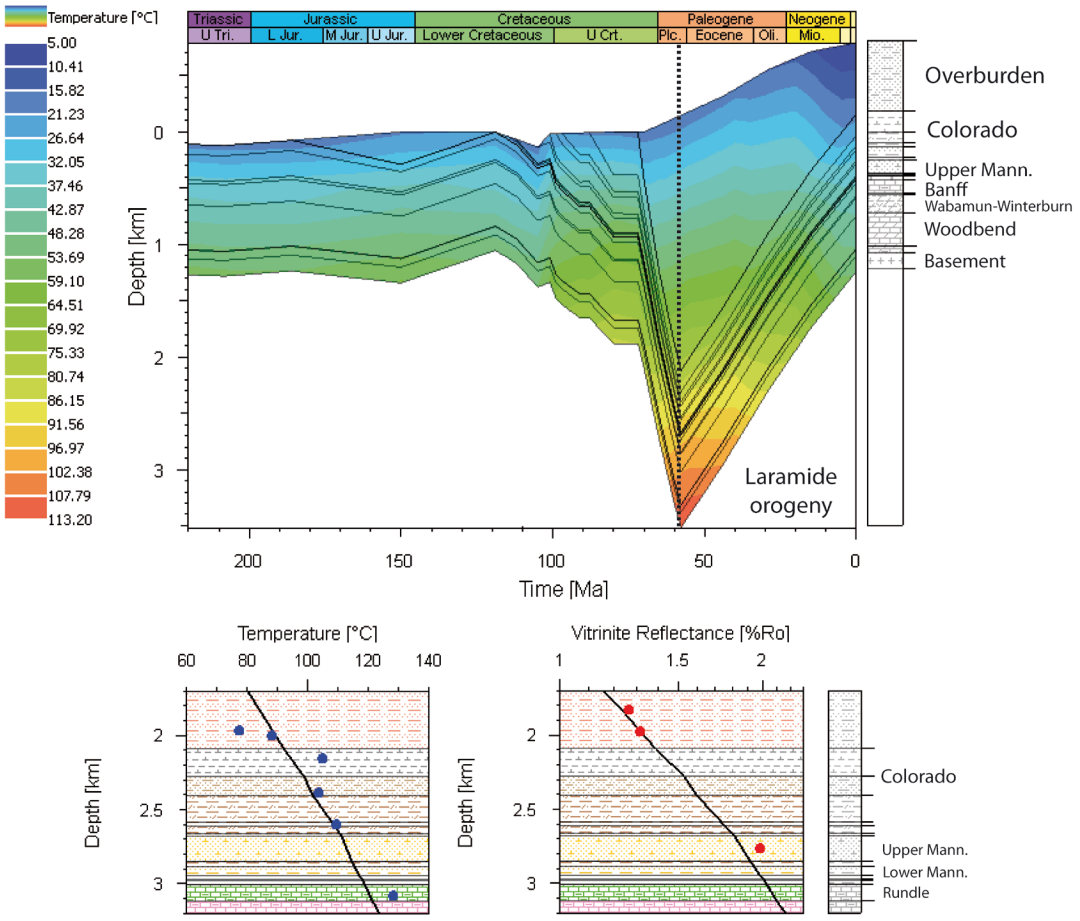

Figure 2.5 Burial history and calibration at well 01-27-060-26W4 (see location in Figure 2.1). The onset of the Laramide orogenic phase is indicated with the dashed line in the burial curve (from Berbesi et al., 2012). AAPG©[2015], reprinted by permission of the AAPG whose permission is required for further use.

2.5.6 Migration modelling

The hybrid calculation method was applied for petroleum migration simulation. This method combines Darcy flow and flow-path (ray tracing) techniques (Schlumberger, 2010). In the hybrid method, a threshold permeability value is set. When this permeability threshold is exceeded by the modeled lithofacies, the flow-path method is activated, otherwise migration is modeled by Darcy flow. In this manner migration through low permeability lithologies (e.g., shales and siltstones) is based on Darcy flow and in more permeable carrier lithologies (i.e., sandstones) flow-path modelling is implemented (Welte et al., 2000).

2.6 Results and discussion

2.6.1 Generation

The first petroleum generation results to be discussed are those obtained when applying the initial source rock input parameters as defined in Table 2.1. As shown in Figure 2.6, the kitchen areas are located in western and southwestern Alberta, corresponding to the foothills and sedimentary section below the Rocky Mountains.

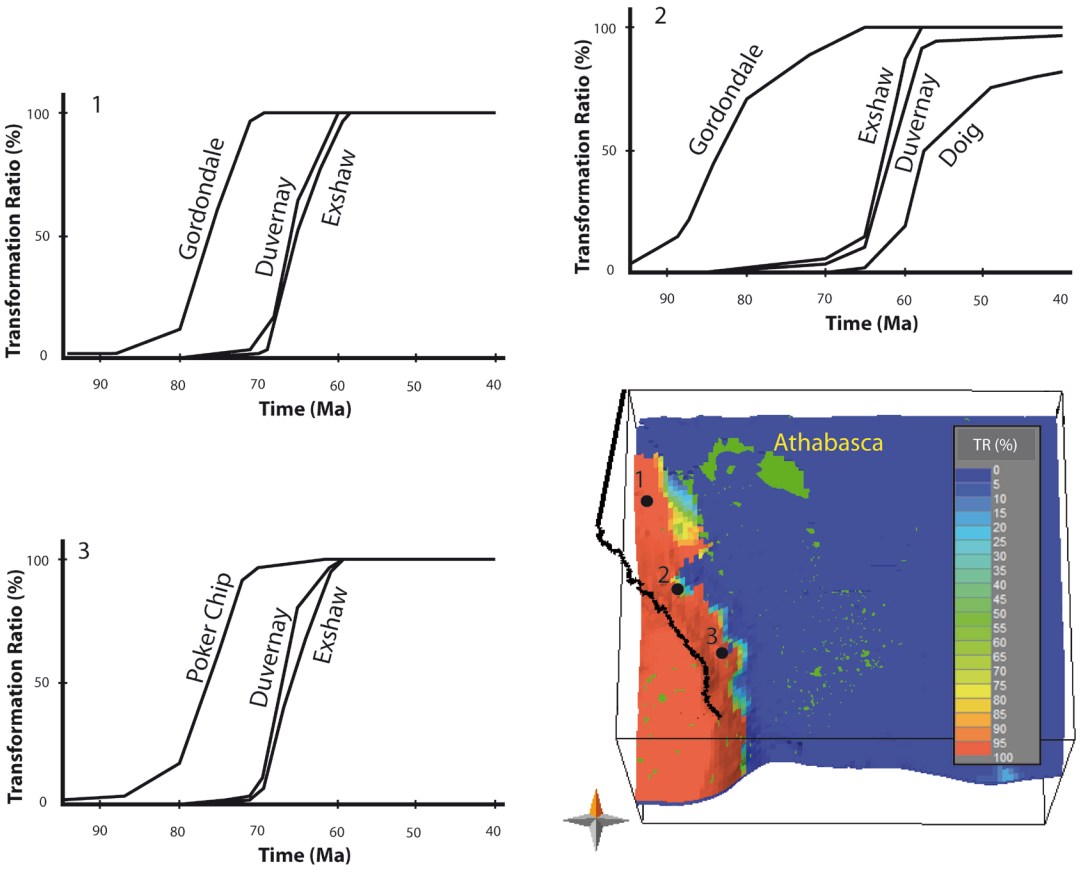

Figure 2.6 Present day transformation ratio distribution, showing the location of kitchen areas and time extractions for 3 selected points (from Berbesi et al., 2012). AAPG©[2015], reprinted by permission of the AAPG whose permission is required for further use.

Significant transformation ratios (50% or more) are reached by the Gordondale Member and Poker Chip A shale of the Fernie Group at 75 Ma. Such transformation ratios are also observed for the Duvernay and Exshaw formations at 65 Ma, and around 5 million years later for the Doig Formation. This sequence of generation

timing reflects the burial history of the sequences. Early generation from the Lower Jurassic Fernie Group source rocks is due to the "fast" kinetic parameters corresponding to labile Type II-S kerogen. At 60 Ma all of the source rocks considered in the model reached R_o values that correspond to early or main oil generation in western or southwestern Alberta and wet or dry gas generation beneath the accretion zone. This time represents the point of maximum burial before the onset of the Laramide orogeny (Issler et al., 1999). From this point on, the rate of kerogen transformation decreased and ultimately ceased, as a consequence of the continuous decrease in temperature.

Figure 2.7 shows the cumulative evolution of oil generation for the modeled source rocks. The results for the Gordondale Member and the Poker Chip A are closely similar to those published by Higley et al. (2009). According to this first scenario, the Gordondale Member of the Fernie Group is the main generator, producing a maximum yield of oil of almost 400 BCM (2515 BB), which is around four times more oil than the amount generated by any other source rock. Total generation values for the Duvernay, Doig and Exshaw Formations are higher than those of the previous 3D model of Alberta, due to the extension of the kitchen area to southern Alberta and software changes (Figure 2.1). In summary, the organic rich-intervals within the Lower to Middle Jurassic section generate more oil than the sum of all organic-rich strata located between the Devonian and Triassic sedimentary sections.

2.6.2 Migration and accumulation

a) Initial model's definition

Using the initial conditions described in Table 2.1, a total oil contribution from the modeled source rocks to the Mannville Formation (reservoir layer) of approximately 19 BCM (119 BB) was obtained, which coincides in general with that obtained from the previous model of Alberta. However, this volume is low compared with current estimates of 260 BCM (1635 BB) for the Lower Cretaceous oil sands (National Energy Board Canada, 2010). Two possible reasons for this result were addressed,

(1) Inadequate source rock definition and amount of generated oil, and (2) inadequate trap definition and that enough petroleum was generated but it was not efficiently trapped.

The total volume of oil generated by the five modeled source rocks shown in Figure 2.7 is 694 BCM (4365 BB), which is more than the amount of petroleum required to fill the oil sand accumulations in Alberta. This seems to indicate that the low accumulation volumes are not a direct consequence of the source rock definition or assigned generative potential. The model also shows an efficient expulsion of generated hydrocarbons from the source rock layers that exceeds 70% in all the cases.

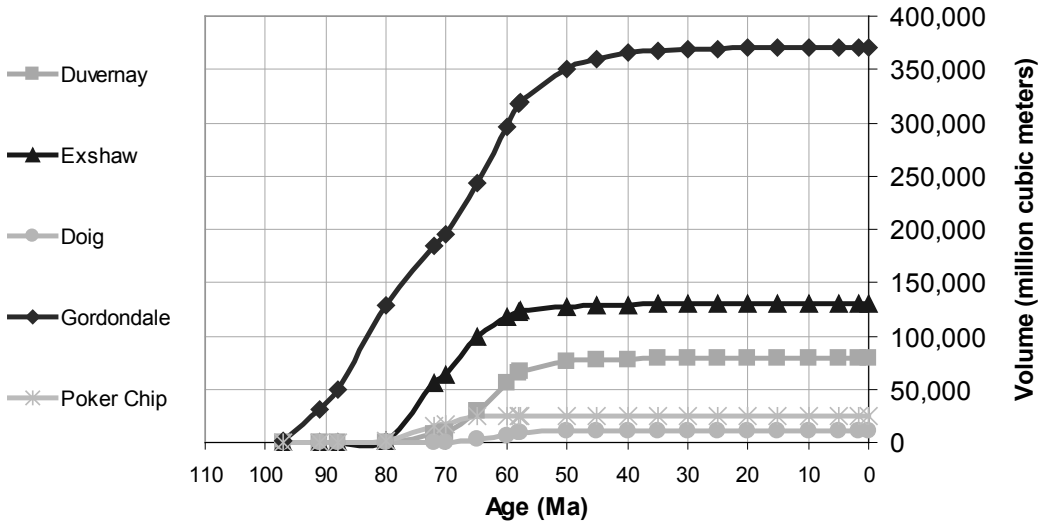

Figure 2.7 Cumulative oil generation using initial source rock parameters (from Berbesi et al., 2012). AAPG©[2015], reprinted by permission of the AAPG whose permission is required for further use.

Under this configuration of the model, the traps are filled to spill, and/or have experienced remigration during one or more periods of time. Most of the oil reaching the Lower Cretaceous strata continued migrating beyond Athabasca to the north and northeast, escaping from the modeled area, or migrated to the east to form large shallow oil accumulations along the Precambrian shield in Saskatchewan. In other words, the initial trap definition in the model was insufficient to account for present-day accumulations. Higley et al. (2009) listed the coarse grid size of the model relative to subtle stratigraphic traps as one of the main reasons why insufficient

amounts of petroleum were trapped. Another possible reason was the incapacity of the modelling software to simulate biodegradation. In the WCSB nonbiodegraded light oil reached shallow reservoirs and suffered water washing and biodegradation, resulting in a heavier, viscous oil that played a role in the trapping of the subsequently accumulated oil. Both possibilities were addressed in this contribution, starting with a revision of the initial facies distribution maps.

b) Evaluation of trapping efficiency

The Lower Cretaceous sequence of the WCSB consists of interbedded sandy, silty and shaly units whose lateral and vertical lithological variations could not be reproduced in detail. These lithological variations play a strong role in the trapping of petroleum. Vigrass (1968) indicated, for example, the importance of onlap traps as controls on oil accumulations at Peace River, and the poor lateral continuity of the sandstone beds in the Athabasca area. The dominance of shaly units in Lower Cretaceous strata to the north of the Peace River area has been reported (Mossop and Shetsen, 1994; Vigrass, 1968) and relates to the predominantly marine conditions in northern Alberta during this geologic interval (Leckie and Smith, 1992). The abundance of low energy facies has been also described for the northeastern limits of the Athabasca accumulation. Hayes et al. (1994) showed an increase in the percentage of low-energy facies following an orientation similar to that indicated by the arrow in Figure 2.1. In a detailed study by Ranger (2006), the author proposes that the main controls hindering the migration of petroleum to the northeast of Athabasca were stratigraphic, although evidence for this hypothesis might have been removed during erosion.

Accordingly, a stratigraphic barrier that covered the northern parts of Alberta and the northeastern edges of the Athabasca deposit was created, aiming to reproduce the lithological variations that could increase the trapping efficiency of the model. The total amount of accumulated oil in the Mannville Group strata using this configuration is about 230 BCM (1450 BB), which represents more than 1200% increase with respect to the first set of results. Another improvement achieved by implementing this impermeable barrier is related to the stability of the oil

accumulations. The initial configuration of the model (i.e., without this barrier) resulted in remigration of petroleum, with accumulations that changed continuously in volume and area through time after the onset of the Laramide erosion. This occurred as a consequence of the shallow nature of these reservoirs, which made them vulnerable to tilting produced by non uniform erosion across the basin. When this low-permeability lateral seal was applied, remigration of petroleum diminished, allowing the study of the compositional evolution of independent reservoirs through time. The contribution from the main sources to Lower Cretaceous strata as a function of time is shown in Figure 2.8. The reservoir filling curves are slightly susceptible to variations in the Laramide uplift pattern; however, the total contributions from individual source rocks as well as the general trends are constant.

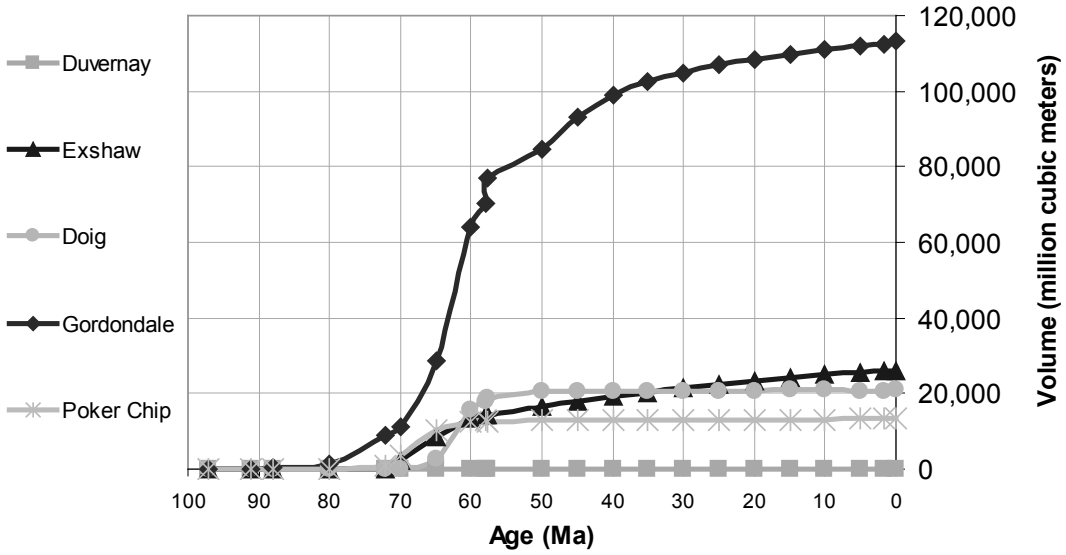

Figure 2.8 Cumulative oil contributions from the modeled source rocks to the Mannville Group reservoirs, using an impermeable barrier covering the northern limits of Alberta and the eastern edge of the Athabasca accumulation (from Berbesi et al., 2012). AAPG©[2015], reprinted by permission of the AAPG whose permission is required for further use.

A second approach implemented an impermeable barrier as discussed above, however, as a "piercing" lithology that simulates the time-dependent sealing effect of biodegraded oil. This piercing body appears in the north and eastern limits of the known trapping areas of Alberta at 55 Ma, extending progressively to the south and west until it occupies its final area at 30 Ma, as shown in Figure 2.9.

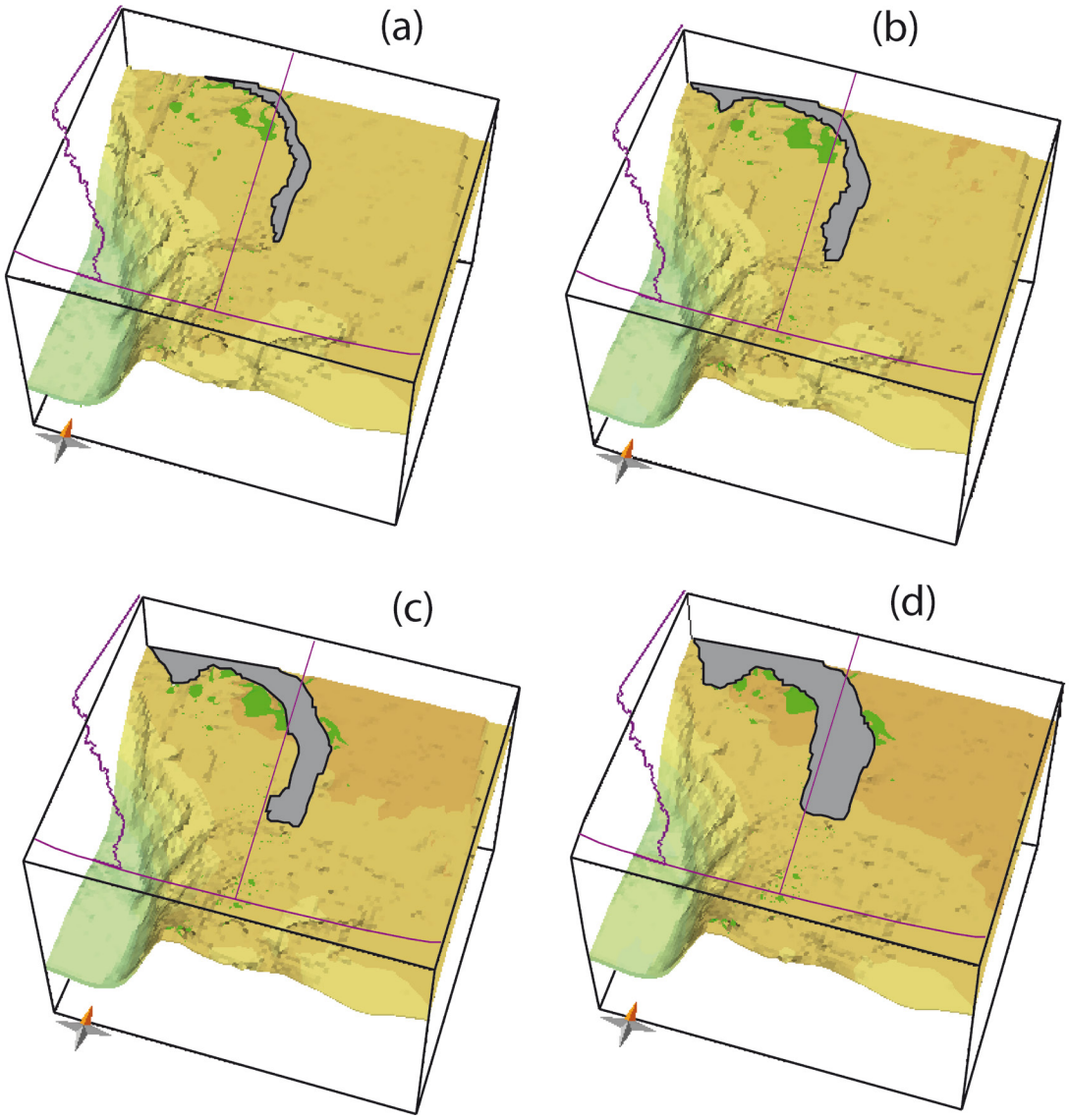

Figure 2.9 Implementation of an impermeable barrier in the Mannville Group reservoirs, in order to enhance the trapping efficiency of the 3D model. (a), (b), (c) and (d) correspond to the view at 55, 50, 40 and 30 Ma, respectively. Present-day oil accumulations are represented in green. The gray shape represents the evolution of the impermeable barrier though time (from Berbesi et al., 2012). AAPG©[2015], reprinted by permission of the AAPG whose permission is required for further use.

This time-configuration assumes that biodegraded seals did not occur before the onset of Laramide erosion and further introduction of fresh water to the reservoirs. This approach resulted in large accumulations in northwestern Saskatchewan and northeastern Alberta before the piercing lithology reached its maximum extension. After experimenting with the timing and areas for this piercing barrier, it appears that the sealing effect of biodegraded oil may have been important in hindering the

migration of petroleum in the northern areas, but the timing was not optimal for impeding the movement of fluids to the east of Athabasca.
One limitation of this progressive lateral seal is that it cannot model the volume decrease of petroleum through time as biodegradation occurs. However, since the main limitation of a biodegraded seal is the timing of its occurrence and not the masses involved, it can be said that the main trapping control was structural and stratigraphic, as previously proposed by Vigrass (1968) and Ranger (2006).

c) Oil composition and source rock contributions

Some authors propose the Exshaw Formation as the main contributor to Mannville Group oils (Fowler et al., 2001; Leenheer, 1984; Riediger et al., 2001) based on organic geochemical analysis and biomarker characterization. Heavy biodegradation complicates interpretations of biomarkers for the Athabasca oil sands. Nevertheless, new techniques for the analysis of this type of hydrocarbons have allowed addressing the sources of the oil within the accumulations of interest for this study. For the identification of hydrocarbon contributions from the Exshaw, Gordondale and Duvernay source rocks to the Alberta oil sands, Adams et al. (2010) used quantitative GCMS methods optimized for heavy oils, as well as highly biodegradation-resistant proxies like the metal S content, and analysis of source-dependent high molecular-weight multi-heteroatom compounds (HMWMH). In the case of the Peace River region, they indicated mixing of Gordondale and Exshaw sourced oils. In the case of southern Athabasca, they indicate an origin from the Exshaw Formation with minor contributions from Duvernay Formation.

In contrast, the importance of the Gordondale Member as a main contributor to the accumulations within the Mannville Group has been suggested by the previous 3D model of Alberta (Higley et al., 2009), which proposed that source rocks of the Fernie Group generated almost twice the combined volume of oil from all other Devonian through Lower Cretaceous source rocks. This 3D model also suggested that oils generated from the high-sulfur Gordondale Member were able to experience long-distance migration, which can be compared with some other known systems

were long-distance migration of oils generated from high-sulfur sources took place (Higley et al., 2009). Examples include migration of oils from the Phosphoria source rocks in Wyoming and Jurassic source rocks in Iraq (Claypool et al., 1978; Sheldon, 1967; Pitman et al., 2004). The importance of Gordondale as source rocks has been also suggested by other analysis of biomarkers, metals and stable sulfur isotopes (Lewan et al., 2008), and by a recently developed technique based on the comparison of ^{187}osmium/^{188}osmium at the time of generation (Os_g) and platinum/palladium (Pt/Pd) ratios in oils and their potential source units (Selby et al., 2011). Moreover, Orr (2001) listed oils and tars in reservoirs of the Mannville Group that were indicative of Type IIS kerogen and, as indicated by kerogen analysis (Asgar-Deen et al., 2004; Riediger et al., 1990a), the only important source interval containing IIS organic matter within the study area is the Fernie Group.

In Figure 2.8 the Gordondale Member contributes more than five times more petroleum to the Mannville layer than the Exshaw Formation. This same model also proposes that more than 54% of the oil volume in all present-day individual accumulations corresponds to Gordondale-sourced petroleum, while the contribution from Exshaw never exceeds 15%. This set of results is in agreement with the proposition that oils in the Western Canada Sedimentary Basin were mainly sourced by rocks of the Jurassic Fernie Group (Higley et al., 2009; Lewan et al., 2008; Selby et al., 2011).

d) Source rock sensitivity

The initial TOC and HI values applied in this study are reasonable based on available data. However, a significant portion of the kitchen areas of the modeled source rocks are located beneath the Rocky Mountains, where source rock occurrence and properties are uncertain. Therefore, taking into account these uncertainties as well as the known source rock heterogeneity, a sensitivity study of TOC and HI values for the Gordondale Member and Exshaw Formation was performed.

Increasing the TOC value for the Gordondale source rock results in generation and accumulation volumes that explain the amounts of petroleum in the Alberta deposits,

suggesting a strong predominance of Fernie oils with only minor contributions from other source rocks. Using a TOC of 15% and HI of 600 mg HC/g TOC for the Exshaw Formation results in 860 BCM total oil from Devonian to Lower Cretaceous sources, from which 250 BCM are produced only by the Exshaw Formation. Nevertheless, within the Lower Cretaceous reservoirs, Gordondale-sourced oil represents 75% for Athabasca-Cold Lake and 70% for Peace River, with Exshaw-sourced petroleum representing less than 5% of the oil volumes in these reservoirs.

The other revised source rock parameter was thickness of the Exshaw Formation. Initial thickness assigned to this source rock in Alberta is generally < 8 meters (Figure 2.10a), which is in accordance with the previous model of Alberta and data published by Caplan and Bustin (1996). However, some literature indicates increasing thickness of this formation from east to southwestern Alberta. For example, Savoy et al. (1999) and Smith and Bustin (2000b) indicate a thin Exshaw Formation for most of the study area but describe thickening in some areas in western Alberta, where the lower black shale member can have a thickness of 20 m (65.6 ft) or more. Since the kitchen areas are located in the western part of the model, the effects of variations in the thickness of the western areas of the Exshaw layer were analyzed.

This was achieved by creating a model that contained the same input data used for the first simulations of the expanded model (Table 2.1), but also included the stratigraphic barrier described in section b. Assigned thickness for the Exshaw Formation was from around 3 m (9.9 ft) in Athabasca to an average of 25 m (82 ft) in the kitchen areas beneath the Rocky Mountains (Figure 2.10b). This was achieved through uniform thickening of the entire Exshaw layer that, given its geometry, affected mostly the kitchen areas located on the west of Alberta. This modification did not influence the predicted timing of oil generation, which is controlled by the thermal history of the basin and the deposition history of the overburden rock (Deming, 1994). However, effects of this change are seen in the volumes of generated oil (Figure 2.11) and the composition of the modeled accumulations.

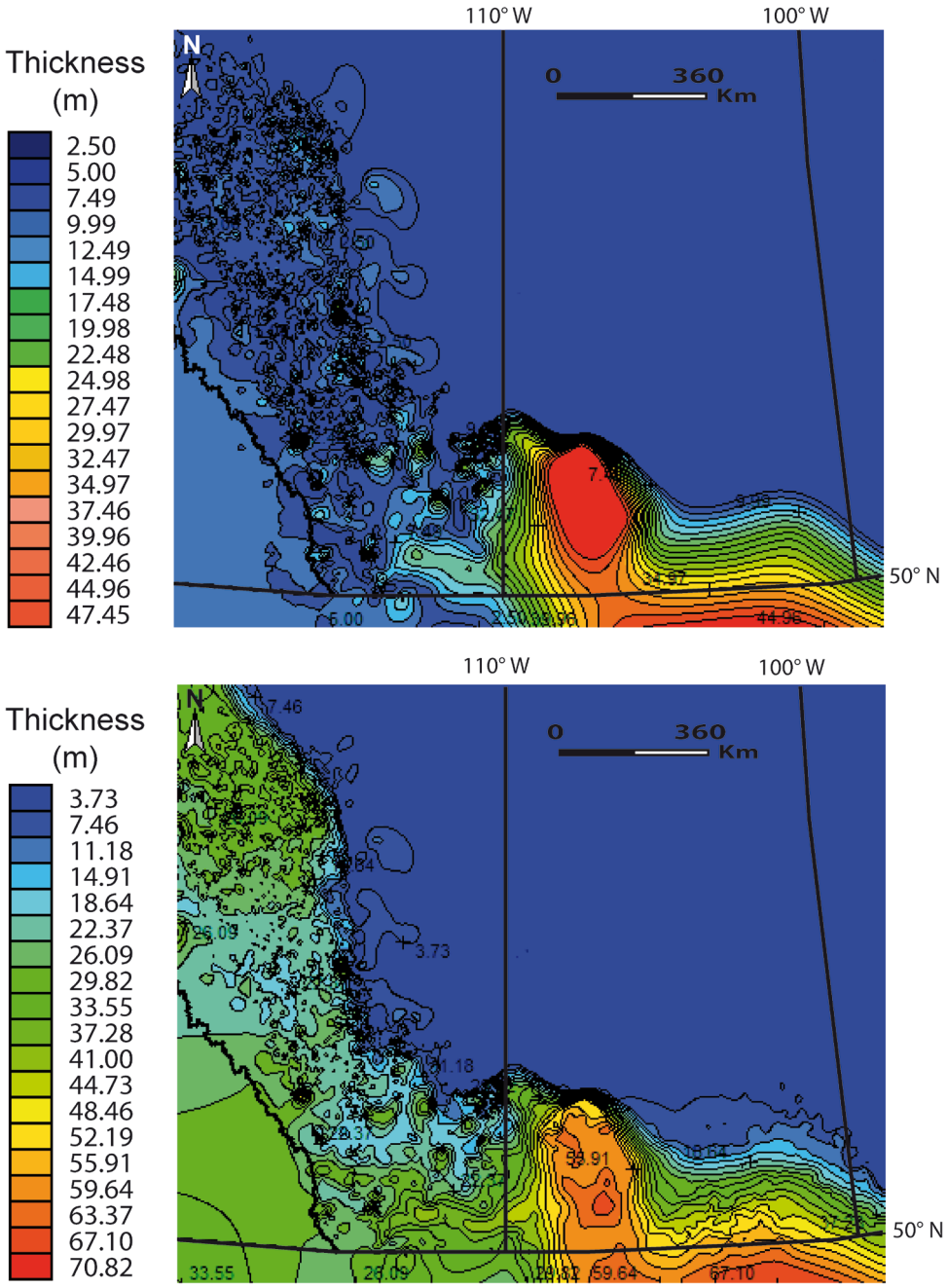

Figure 2.10 Thickness of the Exshaw layer: (a, upper) applied to the initial configuration of the 3D model. It corresponds to the thickness applied by Higley et al. (2009); (b, lower) applied in the revised version of the model that considers thickening of the Exshaw Formation from eastern to western Alberta. Subtle thickness increase in southern Saskatchewan was not intended, and resulted from the methodology described in the text. However, because this section was modeled as non-generative, it did not influence the observed differences in generated and accumulated masses with respect to the initial version of the model (from Berbesi et al., 2012). AAPG©[2015], reprinted by permission of the AAPG whose permission is required for further use.

This revised model resulted in > 700 BCM (4402 BB) of Exshaw-sourced oil (Figure 2.11), followed by, 400 BCM (2515 BB) of oil generated by the Gordondale Member and minor amounts from the other source rocks, giving a total of 1300 BCM (8173 BB) of generated petroleum.

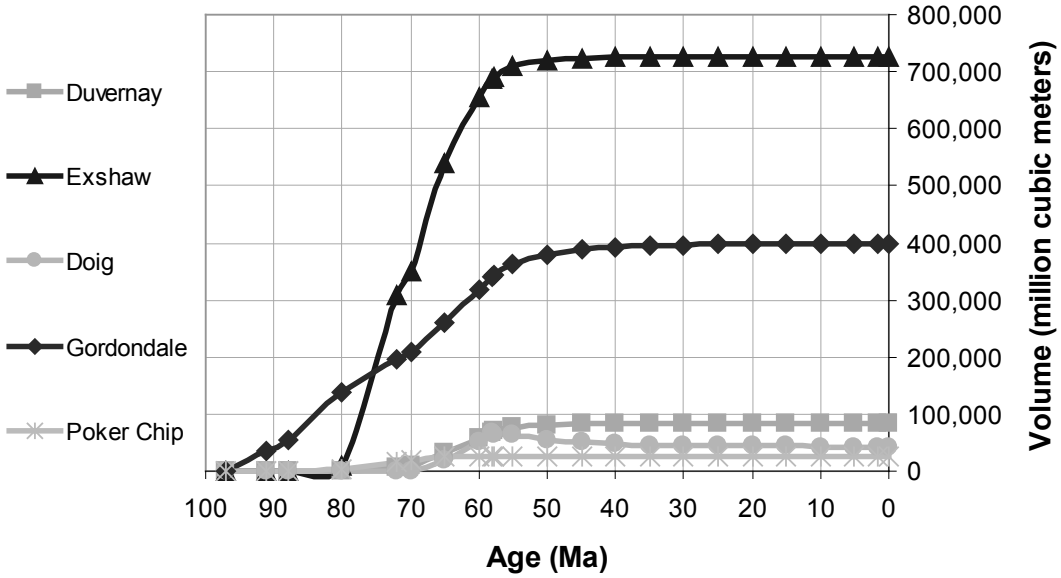

Figure 2.11 Cumulative oil generation from the main modeled source rocks when the thickness of the layer corresponding to the Exshaw source rock is increased (from Berbesi et al., 2012). AAPG©[2015], reprinted by permission of the AAPG whose permission is required for further use.

The volume of trapped oil within Mannville strata (Figure 2.12) is 303 BCM (1905 BB), from which approximately 280 BCM (1761 BB) is in the Athabasca and Cold Lake accumulations. This represents 28% more oil than the initial present day estimates for this area (National Energy Board Canada, 2010), even when the model does not include what are believed to be the main sources for the Cold Lake accumulations. For the Peace River accumulation, the model predicts 24 BCM of oil (151 BB) which is also higher than initial estimates of 20.5 BCM (126 BB) for this area. These results appear reasonable, especially since the applied modelling software does not consider petroleum mass loss due to biodegradation.

The revised model proposes that the Exshaw Formation provided 41% of the oil within the Athabasca and Cold Lake accumulation, followed by a 35% of contribution from the Gordondale Member and minor amounts from the other source rocks. From eastern to western Alberta, the importance of the contribution from the

Gordondale source rock increases. The same model predicts that 52% of the oil in the Peace River deposit originated from the Gordondale source rock. These results generally agree with those of Adams et al. (2010), although the model does not suggest an important contribution from the Duvernay Formation.

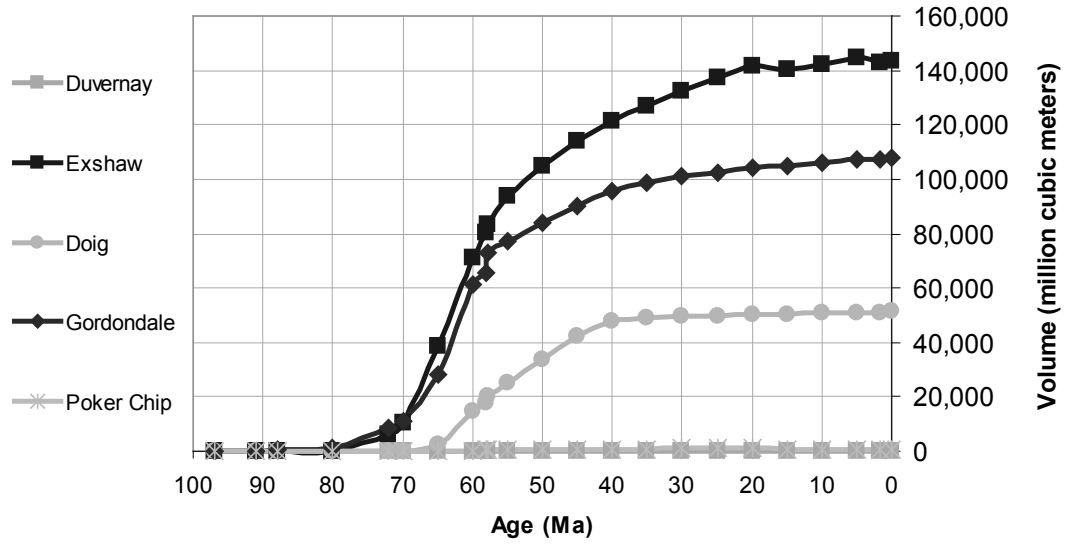

Figure 2.12 Cumulative oil contribution from the main source rocks to the Manville Group reservoirs as a function of time. Average thickness of the kitchen areas of the Exshaw Fm is 25 meters. An impermeable barrier is present in the areas shown in figure 9 (d) before the oil starts reaching the reservoir layer (from Berbesi et al., 2012). AAPG©[2015], reprinted by permission of the AAPG whose permission is required for further use.

This model manages to reproduce both the volumes and compositions of the main oil accumulations in the WCSB, favoring published results proposing the Exshaw Formation as the main source rock in the basin (Adams et al., 2010; Fowler et al., 2001; Riediger et al., 2001). However, there is one main limitation of this model that must be taken into account until new accurate data are available to support or contradict the assumed source rock properties. Even though some studies (Savoy et al., 1999; Smith and Bustin, 2000b) indicate thickening of the Exshaw Formation (including the lower black shale member) to the west of Alberta, no data is available to support the modelling assumption that the TOC content remains constant through all the generative section. Besides, many studies on Devonian-Mississippian source rocks in North America (Comer, 1991, 1992; Robl et al., 1983; Schmoker, 1980) show an inverse relation between TOC and thickness as a result of some degree of organic matter dilution by additional sedimentary contributions.

When this thicker Exshaw layer is assigned only a half of the initial TOC content, the Gordondale source rock is the dominant contributor at 43% of the oil in Athabasca, followed by Exshaw (26%), Doig (23%) and less than 1% from each of the other source rocks. Very similar trends are obtained when the 25 m average thick Exshaw is split into two equivalent layers with only the lower member modeled as generator, with initial TOC and HI contents as indicated in Table 2.1. Based on these results, unless new data demonstrate that the thicker western portions of the Exshaw Formation possess immature TOC levels of 9% or more across all of its extension, modelling results based on available data continue to support the Gordondale Member of the Fernie Group as the main contributor to the oil sand deposits in the Western Canada Basin.

2.7 Conclusions

A 3D model of the WCSB was constructed and calibrated to well data. Thermal calibration results propose heat flow values between 45 and 75 mW/m^2, and total erosion of up to 1400 m (4593 ft), coinciding well with previously reported values. All the modelled source rocks reached early or main oil generation before 60 Ma, when the onset of the Laramide orogeny took place. The model supports the possibility of long-distance migration of oil from the Gordondale source rock proposed by Higley et al. (2009), and does not consider this as a limitation for a contribution from Jurassic oils to the Lower Cretaceous accumulations. Without appropriate barriers, the model generates large and shallow oil accumulations along the Precambrian shield in Saskatchewan and most of the oil escapes through the northern limits of Athabasca. The coarse grid size needed for simulations does not allow reproduction of the subtle structures that improve the trapping efficiency in the natural system; however, the incorporation of stratigraphic seals within the reservoir layer trapped the accumulated volumes and hindered the remigration of oil, making the modeled accumulations stable through time. These results support the stratigraphic control to the northeast of Athabasca proposed by Ranger (2006). The effect of additional trapping due to seals formed by biodegradation of petroleum was

found to be minor, and its influence is proposed to be restricted only to the north of Athabasca.

Having improved the trapping efficiency of the model and using the initial source rock definition, the model predicts that about 230 BCM (1450 BB) of oil would reach the Mannville Group strata. At individual accumulations, the Gordondale source rock appears to contribute more than 54% of the oil, while the contribution from the Exshaw Formation never exceeds a 15%.

The proposed strong contribution of Exshaw products to the Athabasca oil sands can be only supported by the model when the initial thickness in the kitchen areas of the Exshaw layer is increased to an average of 25 m (82 ft). However, until new data can demonstrate that the Exshaw Formation possesses TOC levels of 9% or more across its entire extension beneath the Rocky Mountains, modeling results support the idea that the Gordondale Member of the Fernie Group was the main contributor to the oil sands in the Western Canada Sedimentary Basin.

Chapter 3

Inferences of gas hydrate deposits in the Beaufort/Mackenzie Basin based on petroleum system analysis

This chapter was submitted as: Berbesi L.A., R. di Primio, Z. Anka, J. Sippel, B. Horsfield., 2014, Inferences of gas hydrate deposits in the Beaufort/Mackenzie Basin based on petroleum system analysis.

3.1 Abstract

The main objective of this work was to contribute to the gas hydrate methane resource assessment on the Beaufort-Mackenzie Basin (BMB), through the quantification of thermogenic gas generation, migration and leakage. For this purpose, a 3D petroleum system model combining input and output data from previous contributions (Kroeger et al., 2008, 2009; Sippel et al., 2013) was built. The model considers not only the lateral and vertical lithological variations, but also the main structural elements influencing the petroleum system in the basin, as well uncertainties related to source rock properties. Modeled total generated gas masses are in the order of 10^4 to 10^5 Tg (10^{13}–10^{14} m^3), depending on the extent of source rock considered and the kinetic model applied. The predicted gas generation rate from Eocene to Miocene is of 10^{-4} to 10^{-3} Tg/yr, while it ranges from 10^{-5}-10^{-3} Tg/yr between Pliocene and present day. The predicted in-reservoir accumulated volumes range from 1.9-2.4 x10^{12} m^3, matching well with previous in-place conventional resource estimates. Different scenarios for gas hydrate formation were assumed

based on previous findings (Majorowicz et al., 2008). It is postulated that a maximum volume of 1-7x10^{12} m^3 of thermogenic methane could have been transferred from deep petroleum systems into the shallower gas hydrate zone of the BMB.

3.2 Introduction

The Beaufort-Mackenzie Basin (BMB), located in North-Western Canada (Figure 3.1), represents an important petroleum province whose geological history can be sub-divided into two main phases; a mid-Mesozoic period of rift faulting, and a latest Cretaceous to Tertiary period of regional folding and faulting (Lane, 2002).

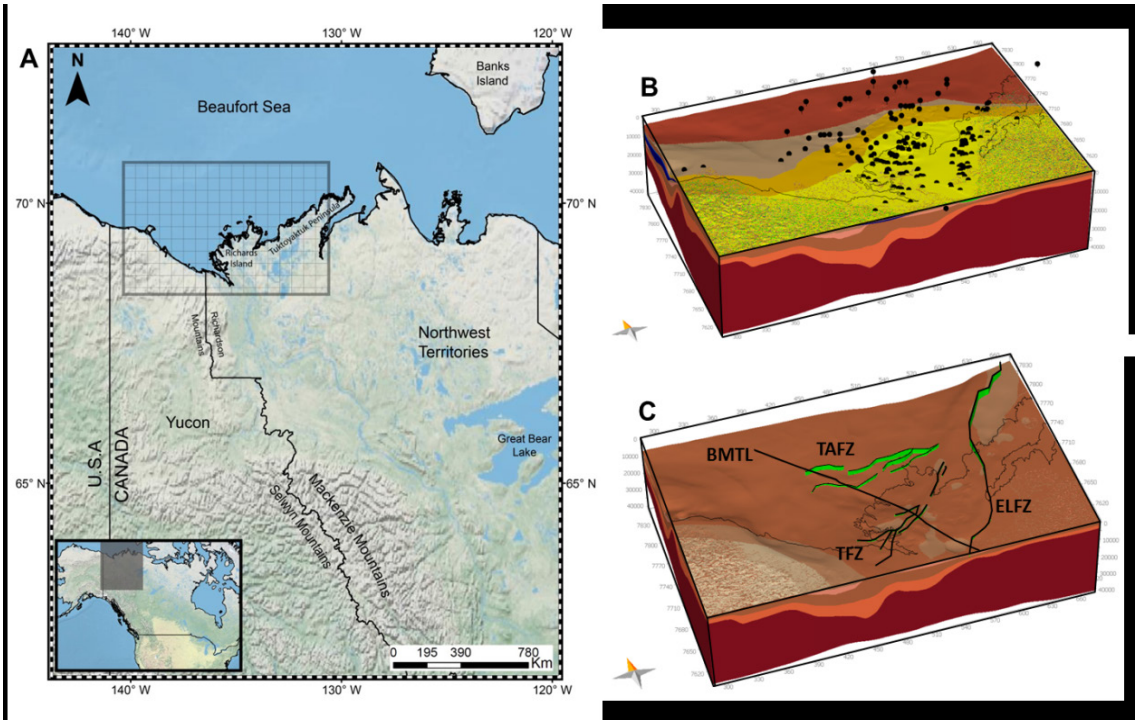

Figure 3.1 (A) Location of the study area. The meshed rectangle indicates the modelled portion of the BMB. (B) and (C) are 3D views of the model. B shows the location and distribution of the wells available for model calibration. C shows the main structural elements of the BMB that were modeled in this study. ELFZ = Eskimo Lakes fault zone, TFZ = Taglu fault zone, TAFZ = Tarsuit-Amauligak fault zone, BMTL = Beaufort-Mackenzie tectonic lineament.

Recoverable oil reserve estimates in the order of 1.5-2 billions of barrels, and around 12 trillion cubic feet of natural gas (Dixon, 1994), suggest the important contribution that the BMB could offer to fulfill North America's hydrocarbon supply in the near future (Chen et al., 2007; Lane, 2002). Besides the conventional oil and gas reserves, the BMB also possesses an immense natural gas potential in the form of gas hydrates (Chen et al., 2007; Osadetz and Chen, 2005).

Previous works have proposed that gas hydrates in the region may hold between $2.4x10^{12}$ and $87x10^{12}$ m^3 of natural gas (Chen et al., 2012; Davidson, 1978; Dixon, 1994; Majorowicz and Osadetz, 2001). These estimates are based on parameters such as the volume of the gas hydrate stability zone, reservoir porosity, hydrate saturation and gas volume expansion factor. In the BMB, gas hydrates occur associated with 75% of the conventional natural gas discoveries, 91% of the crude oil discoveries, and 72% of the oil and gas discoveries in deeper strata (Osadetz and Chen, 2005).

Moreover, the thermogenic signature of gas hydrates in the BMB suggest the strong role of the petroleum system on the presence of gas hydrates in the region (Lorenson et al., 1999). In order to better constrain the gas hydrate resources in the BMB, this work intends to quantify thermogenic gas generation and migration through petroleum system numerical modeling and analysis. The 3D petroleum system model we developed represents a further step on previous contributions by Kroeger and co-workers (Kroeger et al., 2009; Kroeger et al., 2008). The model considers not only the lateral and vertical lithological variations, but also the main structural elements influencing the petroleum system in the basin, as well uncertainties related to source rock properties. Additionally, an estimate of the total thermogenic gas generation and leakage during the evolution of petroleum systems in the region is provided.

3.3 Geologic background

3.3.1 Tectono-stratigraphic history

The evolution of petroleum systems in the BMB took place during two main tectonic phases (Figure 3.2): a Mesozoic extensional phase and a Maastrichtian to late Miocene orogenic phase (Lane, 2002). Jurassic to Aptian sedimentation was mostly characterized by shoreface to marine shelf deposits with some non-marine, deltaic beds and fan-delta deposits (Dixon, 1992a). Tectonically, this period was characterized by extensional faulting. During the Albian, the Cordilleran Orogen started influencing sedimentation in northern Canada, promoting a shift in the sedimentological regime (Dixon, 1996, 1992a).

The Upper Cretaceous to Tertiary sedimentation in the BMB was dominated by large delta systems which can be divided into three main tectono-stratigraphic phases, each of them marked by a major unconformity (Dixon, 1996, 1992a). Deposits corresponding to this time range from organic-rich shales deposited in anoxic to disaerobic environments, slope and basin shales, submarine fan deposits, shelf shales and sandstones, or interbedded sandstone, shale and coal related to deltaic successions (Dixon, 1992a).

The first tectono-stratigraphic phase started with the deposition of the Fish River sequence and ended with the development of an unconformity between the Taglu and Richards sequences (Figure 3.2). Deposition was initially concentrated in the southwest basin margin, but shifted to the east and slightly basin-ward with time. The second phase is represented by the deposition of the Richards, Kugmallit, Mackenzie Bay, and Akpak sequences (Figure 3.2). Sedimentation was initially focused in the south-central part of the basin, and shifted basin-ward during this time. This phase culminated by the end of the Miocene, as evidenced by a major erosional unconformity (Dixon, 1992a). Deformation in the BMB was minimal during the Pliocene tectono-stratigraphic phase, which is characterized by basin-ward deposition. The Iperk sequence represents this sedimentation period (Figure 3.2).

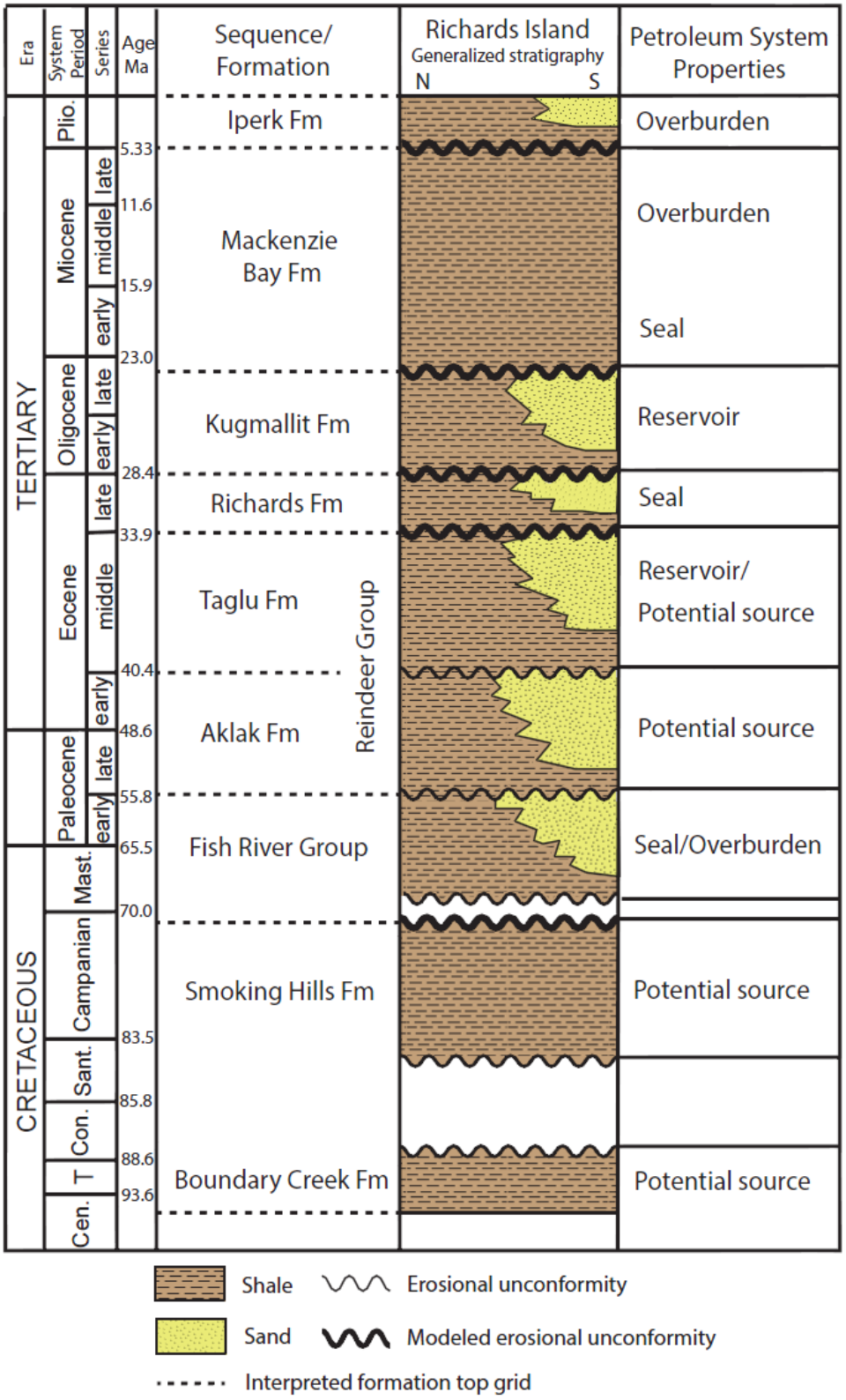

Figure 3.2 Generalized Cretaceous-Tertiary stratigraphy of the BMB as considered in the 3D model. Formation top depth maps available for model building are shown in segmented lines (Sippel et al. 2012). The model extends down to the Moho depth; however, only the main petroleum system elements are shown in this figure.

3.3.2 Glacial history and relevant considerations for gas hydrate resource assessment

Glacial processes in the Mackenzie Region are the main mechanism controlling permafrost distribution, the extent of the hydrate stability field in the subsurface and, hence, gas hydrate resources. The occurrence and duration of glaciations in this region and other places on Earth are interpreted based on the type and distribution of sedimentary deposits, fossil assemblages and their isotopic composition, and in some cases, on erosional features (Gornitz, 2009). Isotopic data ($\delta^{18}O$) from marine microfossils suggest that the earliest recorded significant global glaciation during the last 100 Ma was the continental glaciation of Antarctica, starting during the early Oligocene (Gornitz, 2009, and references therein). However, the onset of glaciations in the Northern Hemisphere did not take place until much later (Thiede et al., 1998). Traces of Miocene and Pliocene glaciations found in Alaska have been dated at 5-6 Ma using planktonic foraminifera, while correlation with neighboring deep sea drilling sites suggests an age for the initial tidewater glaciations between 5 and 6.7 Ma (Ehlers, 1996).

In the case of the Mackenzie region, geological records suggest the onset of significant glacial activity around the Late Pliocene (Rodkin and Lemmen, 2000). The detailed work by Rodkin and Lemmen (2000) clasifies glaciations as “montane” and “continental”., the former referring to valley glaciers that occupied the Mackenzie Mountains (Figure 3.1), while the second refers to continuous ice that occupied the Selwyn Mountains on the continental divide. The earliest montane glaciation of the region is recorded in the Mackenzie Mountains and is considered to be of Late Pliocene age (Rodkin and Lemmen, 2000). Continental ice is considered to have advanced at least five times over the Canadian northwest, according to records from the Banks Islands (Barendregt and Irving, 1998), although stratigraphic and geomorphic records seem to indicate that the Late Wisconsian (around 30 Ka BP) Laurentide Ice Sheet was the only glaciation that reached the Richardson and Mackenzie Mountains. Marine benthic $\delta^{18}O$ data suggests that the Quaternary has been a period of significant climatic change, characterized by a sequence of around

30 glacial-interglacial cycles in the Northern Hemisphere (Gornitz, 2009). Although the reason for the multiple periods of ice sheet growth and retreat are not completely understood, there is a strong link with cyclic variations (Milankovitch cycles) in the Earth's axis rotation and its orbit around the Sun (Gornitz, 2009). The Early Pleistocene glacial-interglacial episodes occurred at 40 Kyr scales, while the late Pleistocene cycle duration is around 100 Kyr (Gornitz, 2009). This switch must have been caused by changes in internal climate and ice sheet dynamics, since the periodicity and amplitude of orbital variations have not changed during the Quaternary (Gornitz, 2009).

Majorowicz et al. (2008) performed 1D numerical modeling of permafrost and gas hydrate formation in the Beaufort Mackenzie Basin and provided interesting discussions regarding the possible timing and depth of occurrence of these processes. The main concepts derived from Majorowicz et al. (2008) that are of relevance for this work are:

- In a scenario 1, which assumed gas hydrate formation in the area confined under geological seals, gas hydrates formed at depths of around 900 m some 0,9 Myr ago.
- In a scenario 2, in which gas hydrates formed from gas in all of the free pore space and simultaneouly with the formation of ice bearing permafrost, the gas hydrates formed at depths of around 290-300 m shortly after 6 Ma, when the ground surface temperatures were around -4.5 °C to -5.5 °C.

In the study area, the ground surface temperature is estimated to have dropped below the solidus temperature of ice bearing permafrost around 14 Ma. This means that a permafrost layer could have started forming at this time, possibly hindering methane surface leakage before the conditions were optimal for gas hydrate formation. For a ground surface temperature of -5 °C, the equilibrium ice bearing permafrost thickness is around 250 m.

3.3.3 Petroleum system

Potential source rocks in the Beaufort/Mackenzie Basin range in age from Upper Cretaceous to Late Eocene (Dixon, 1992b). They are, from older to younger, the Boundary Creek/Smoking Hills, Fish River shales within the Reindeer supersequence, as well as the Richards and Kugmallit Fomrations (Dixon, 1992b). Kerogen in Upper Cretaceous source rocks is marine-dominated, whereas Tertiary equivalents are mostly terrestrial (Dixon, 1992b). Previous 3D petroleum system modelling by Kroeger et al. (2008, 2009) proposed that organic matter in Upper Eocene and younger units in the Mackenzie Basin has not reached significant transformation. Accordingly, the Richards sequence is considered as a minor source to petroleum accumulations in the region, in spite of its source rock potential.

The main reservoirs are sandstones within the Eocene to Oligocene section, those belonging to the Kugmallit and Taglu sequences being of special relevance (Dixon, 1992b). Sandstones of the Kugmallit sequence have porosity values of 20-25 %, although values of even 30 % have been measured in some wells (Dixon, 1992b). Sandstones in the Taglu sequence tend to be (on average) less porous than those of the Kugmallit sequence (Dixon et al., 2008). The lateral distribution and vertical stacking of individual deltaic reservoirs is a result of basin configuration, syndepositional tectonics and deltaic processes (James and Baxter, 1988).

Important gas and oil accumulations are trapped in Mesozoic extensional structures, in particular the Eskimo Lakes Fault Zone, beneath the Tuktoyaktuk Peninsula (Lane, 2002) (Figure 3.1). Some other accumulations are related to the hinge areas of Tertiary anticlines (Lane, 2002).

3.4 Methods

3.4.1 3D Model building

The 3D petroleum systems model applied in this study (Figure 3.1) represents a further step adding to the modelling contributions of Kroeger et al. (2008, 2009) and Sippel et al. (2012). As the model by Sippel et al. (2012), the 3D model here presented covers a significant portion of the Beaufort/Mackenzie Basin and extends from the sediment surface to the Moho depth (Table 3.1). In addition, the model considers the lateral and vertical lithological heterogeneity of Tertiary strata with a comparable level of detail as in the model of the central Mackenzie area by Kroeger et al. (2009).

Layer building and lithological assignment

The starting point for the building of the model was a set of 11 depth maps extending from the top of the Iperk Fm. to the Moho depth (Table 3.1). As described in detail by Sippel et al. (2012), these maps were built by integrating a large set of data from different sources. Some of them are the present-day bathymetry and topography of the area (Amante and Eakins, 2009), data from more than 287 wells (National Energy Board Canada, 2009), a previous 3D petroleum systems model of the Central Mackenzie Basin (Kroeger et al., 2008) and the geological atlas of the Beaufort-Mackenzie area (Dixon, 1996). The original depth maps were imported into PetroMod 2011.1.1 software, in which 12 initial layers representing Cambrian to Quaternary strata were created. The initial layers were later divided into 32 sub-layers, attempting to consider variations in lithology related to sea level changes, especially during deposition of the Tertiary units. The number of Cenozoic sub-layers, as well as their thickness and lithology, corresponds to those in the model by Kroeger et al. (2009), who subdivided the Kugmallit and Taglu Formations by flooding cycles, following a sequence-stratigraphic approach. In the case of the Paleozoic to Mesozoic section, units were defined as by Sippel (2012), and lithologies were approximated using data from Dixon (1996).

Table 3.1 Model layers building and lithology assignment. The terms "Upper (or U)" and "Lower (or L)" applied for the sub-layer names are informal, and respond to modelling purposes.

Depth/Erosion map	To(Ma)	From(Ma)	Parental Layer (PL)	PL thickness (m)	Sub-layers*		Lithology
Top Iperk Fm.							
	0.00	6.50	Iperk Fm.	0 - 4500			Facies distribution map
	6.50	8.00	Erosion				
Top Mackenzie Bay Fm.							
	8.00	25.00	Mackenzie Bay Fm.	0 - 4000			Facies distribution map
Top Kugmallit Fm.							
	25.00	33.90	Kugmallit Fm.	10 - 1500	Kugmallit progradation 3		Facies distribution map
					Kugmallit retrogradation 3		Facies distribution map
					Kugmallit progradation 2		Facies distribution map
					Kugmallit retrogradation 2		Facies distribution map
					Kugmallit progradation 1		Facies distribution map
					Kugmallit retrogradation 1		Facies distribution map
	33.90	35.00	Erosion				
Top Richards Fm.							
	35.00	37.20	Richards Fm.	1 - 3200	Upper Richards		Facies distribution map
					Lower Richards		Facies distribution map
	37.20	39.00	Erosion				
Top Reindeer Gp.							
	39.00	57.00	Taglu Fm.	1 - 4200	Taglu progradation 3		Facies distribution map
					Taglu retrogradation 3		Facies distribution map
					Taglu progradation 2		Facies distribution map
					Tagluretrogradation 2		Facies distribution map
					Tagu progradation 1		Facies distribution map
					Taglu retrogradation 1		Facies distribution map
Top Aklak Fm.			Erosion				
	57.00	62.00	Aklak Fm.	20 - 4400	Upper Aklak	U_Aklak_U	Facies distribution map
						U_Aklak_M	Facies distribution map
						U_Aklak_L	Facies distribution map
					Lower Aklak		Shale (organic rich)
	62.00	63.40	Erosion				
Top Cenomanian to Lower Paleocene							
	63.40	65.70	Cenomanian to Lower Paleocene	Fish River Gp. 1 - 6000	Upper Fish River		Facies distribution map
					Middle Fish River	MFR_U	Facies distribution map
						MFR_L	Facies distribution map
					Lower Fish River		Facies distribution map
	65.70	65.92		Smoking Hills Fm. 1 - 700	Upper Smoking Hills		Facies distribution map
					Lower Smikong Hills		Shale (organic rich)
	65.92	100.00		Boundary Creek Fm. 1- 7000			Shale
Top Jurassic to Albian							
	100	240.00	Jurassic to Albian	3-7700	Upper_JA		80% Shale, 20% Sand
					Lower_JA		50% Shale, 50% Sand
Top Low-Density Pre-Mesozoic Continental Crust (LDPN)*							
	240.00	530.00	Low-Density Pre-Mesozoic Continental Crust (LDPN)*	100 - 21000	Upper LDPN		Limestone 70%, Sand 20%, Siltstone 10%
					Lower LDPN		Limestone 75%, Shale 25%
Top Crystalline Crust							
	530.00	650.00	Crystalline Crust	2300 - 37500			Basement
Top Moho							

Source rock properties

Total Organic Carbon (TOC) and Hydrogen Index (HI) of the modeled source rocks were assigned according to Rock-Eval data published by Snowdon (1990) and Snowdon et al. (2004), and Rock-Eval analysis by Saison (2010). Several scenarios with different source rock definitions were tested in order to consider the wide range of source rock facies (and therefore source rock properties) observed in the basin (Table 3.2). The range of TOC and HI applied was determined by the ranges observed in published data (Kroeger et al., 2008, 2009; Snowdon, 2004; Saison, 2010). Due to the lack of geological information that allows constraining the aerial extent and thickness of the Upper Cretaceous source rock, different scenarios were considered as explained in Table 3.2.

Table 3.2 Variability of input parameters and resulting modeled generated gas volumes in the BMB. See Figure 3.8 for more details about the variability of the predicted generated, accumulated and leakage volumes.

Source rock Interval	Variable	Applied range	Gas generation
Taglu Fm	TOC (wt. %)	3-8	10^4 - 10^5 Tg [b] 10^{13} – 10^{14} m^3 [b]
	HI (mgHC/gTOC)	100-300	
Aklak Fm	TOC (wt. %)	2-4	
	HI (mgHC/gTOC)	200-300	
Smoking Hills Fm	TOC (wt. %)	4-6	
	HI (mgHC/gTOC)	400-500	
	Source rock extent and thickness[a]	1) Present only where drilled as part of the Smoking Hills Fm (Dixon et al., 1992). Maximum thickness of 180 m	
		2) Present in the entire basin. Maximum thickness of 220 m	

[a] As modelled by Kroeger et al., 2009
[b] Minimum case: minTOC and minHI for all source rocks, condition 1 for Smoking Hills extent and thickness.
[b] Maximum case: maxTOC and maxHI for all source rocks, condition 2 for Smoking Hills extent and thickness.

The kinetic models assigned to these source rocks were obtained following the PhaseKinetic approach (di Primio and Horsfield, 2006). Compositional kinetic models from source rocks in the Mackenzie Delta have not yet been determined; however, an extended PhaseKinetic dataset from source rocks around the world was available for this study. From the latter set of kinetic models, those constituting similar organofacies as those found in the Mackenzie Basin were applied. The kinetic

models that resulted in the best reproduction of oil and gas accumulations across the basin were those from the Bakken Shale (marine Type II kerogen, applied to the Smoking Hills and Taglu sequences), and a liptinitic brown coal from the Moscow Basin (applied to the Aklak sequence).

Erosions

Five major erosion phases were implemented in the model (Figure 3.2). The first of them is related to a shift in sedimentation during the Maastrichtian, leading to the development of an unconformity at the top of the Smoking Hills sequence (Dixon, 1992b). The other four erosion events correspond to phases of significant deformation. These are Middle and Late Eocene, Late Oligocene and Late Miocene, which correspond to the top of the Taglu, Richards, Kugmallit and Mackenzie Bay sequences, respectively (Dixon, 1992b). Erosion at the top of the Smoking Hills Fm. was considered as minor, ranging from 0 to 50 m to the east of the Beaufort-Mackenzie Tectonic Lineament, and reaching a maximum of 500 m in the most south-western portion of the modelled area. Cenozoic erosion values and trends were assigned as in Kroeger et al. (2008, 2009).

Heat Flow

Sippel et al. (2014) present a crustal-scale 3D model of the present-day thermal field in the Beaufort-Mackenzie Basin. This thermal model is based on the 3D geological model of the area (Sippel et al., 2013) and on the assumption that heat is transported primarily by diffusion in the lithosphere. For solving the conductive heat equation, Sippel et al. (2013) assign values of radiogenic heat production and thermal conductivity to all geological units, thereby considering dominant lithologies (Dixon, 1996) and a public-domain data set of measured thermal conductivities (Issler and Jessop, 2011). The upper boundary condition for the calculations was given by the depth of the base of permafrost (i.e. the depth of the 0°C isotherm) known from numerous wells in the study area (Smith and Burgess, 2002). The temperatures predicted by the model are validated by a public-domain set of measured borehole temperatures from 227 wells and depths of up to 5 km below sea level (Hu et al., 2010). Sippel et al. (2014) show that modelled temperatures are very sensitive to the

assumed lower boundary condition, which is the heat flux density at the crust-mantle boundary (Moho). The model best fitting the measured temperatures is characterised by a Moho heat flux of q=15 mW/m². At a constant depth level, the main temperature trends observed and reproduced by the thermal model of Sippel et al. (2014) comprise (i) an increase of temperatures from the basin margin in the south to the basin centre in the north due to the thermal blanketing effect of the low-conductive sedimentary basin fill, and (ii) a decrease of temperatures from the western to the eastern basin due to higher thermal conductivities in the east. The heat flux predicted for the base of permafrost is highest along the basin margin, where the sub-sedimentary crystalline crust is thick enough to produce significant amounts of radiogenic heat and the sedimentary cover is thick enough to store much of this heat (Sippel et al., 2014).

Paleo-water depth and surface temperatures

Present-day water depth values in the modelled area do not exceed 100 m (Williams et al., 2006). Using the latter as a reference, and considering the maximum progradation of delta front deposits through time, as shown in the Figure 12 of Dixon et al. (2008), seven paleo-water depth (PWD) maps corresponding to the time from the Paleocene to the Holocene were built (Figure 3.3).

The surface temperature before the Pliocene was approximated through a Surface-Water-Interface Temperature (SWIT) tool available in the modelling software used which is based on the work by Wygrala (1986). This method estimates a SWIT trend over geologic time based on the present-day latitude, longitude and paleo-water depth of the study area. Surface temperatures exceed 10°C before the Eocene and reach 3°C before the Pliocene (Figure 4). Previous work (Issler, 1990; Kroeger et al., 2008) indicated the strong influence of low surface temperatures and permafrost on subsurface temperature in the region during the Pleistocene. Accordingly, the model considers a temperature decrease since the Pliocene (Figure 3.4), reaching a minimum of -15 °C in some areas at present day (Domain D-II in Chen et al., 2008). Minimum temperature values were taken from Kroeger et al. (2008), while the

surface temperature distribution followed a similar trend to that of the temperature contour maps at 1 Km depth by Chen et al. (2008).

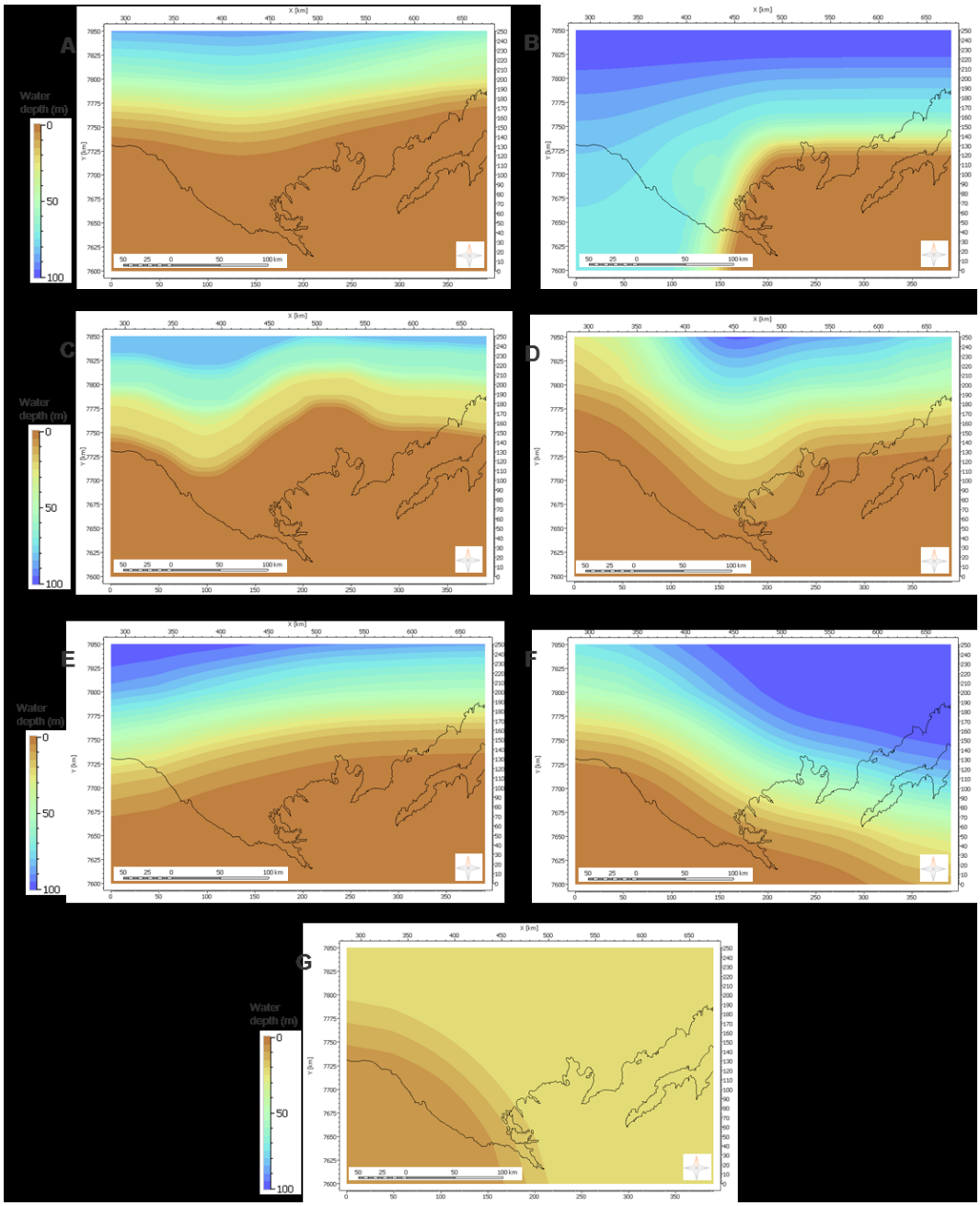

Figure 3.3 PWD maps applied to time intervals from Upper Cretaceous to Holocene. The present-day coast line is shown as a reference. Each map corresponds to the depositional time of a particular sequence, being (A) Iperk (B) Mackenzie, (C) Kugmallit (D) Richards (E) Taglu (F) Aklak (G) Fish River, Smoking Hills and Boundary Creek. Uniform waterdepth of 25 m was applied for the Upper Cretaceous, and 12 m were applied for older time intervals.

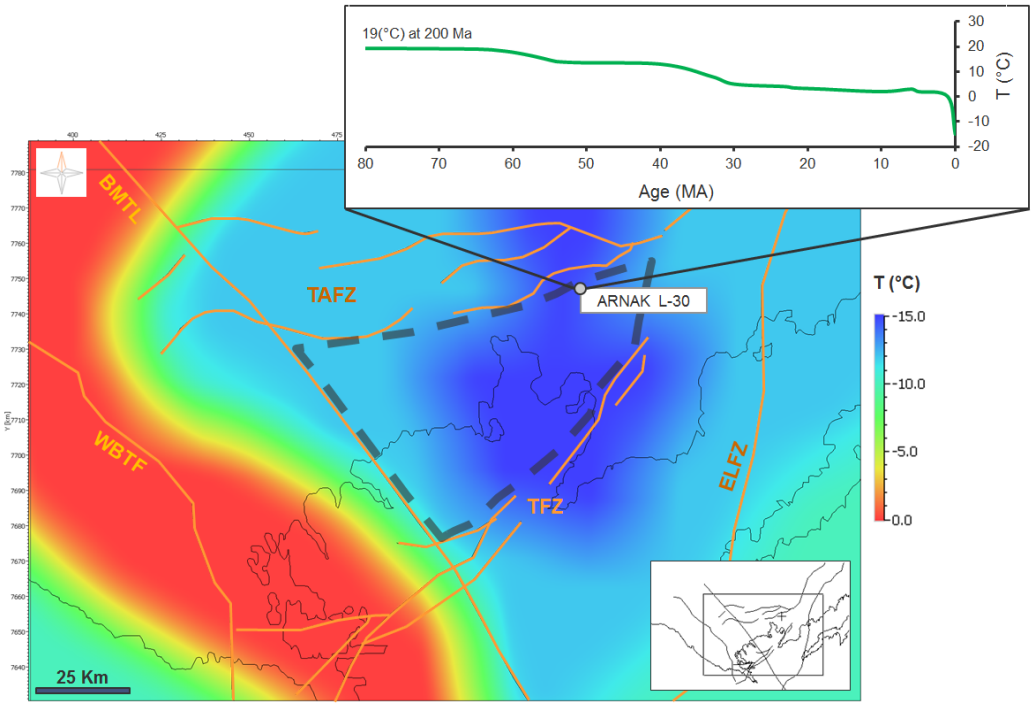

Figure 3.4 Present-day SWIT map as defined in the 3D model, and time extraction showing paleo-SWIT at the ARNAK L-30 well location. The area within the segmented lines corresponds to the Domain D-II in Chen et al (2008). ELFZ = Eskimo Lakes fault zone, TFZ = Taglu fault zone, TAFZ = Tarsuit-Amauligak fault zone, BMTL = Beaufort-Mackenzie tectonic lineament.

Definition of faults

The 3D model here presented includes the three most important fault systems in the Mackenzie Basin, which are the Eskimo Lakes fault zone, the Taglu fault zone, and the Tarsuit-Amauligak fault zone (Figure 3.1 and Figure 3.4). The location and depth of these faults were taken from Dixon (1996). Additionally, the model includes the Beaufort-Mackenzie tectonic lineament, which can be traced onshore by seismically mapped fault segments and folds (Chen et al., 2008). All the faults were modeled as closed to petroleum migration, following previous studies (Chen et al. 2008) indicating the limited migration of fluids across these fault planes. In the modeling software applied, faults have to follow cell boundaries and, as a consequence, the resulting fault geometry is generally not smooth but rather resembles staircases (Schlumberger, 2011). In order to avoid geometric complications related to gridding effects, all faults were modelled as vertical, even though many of them are listric in nature (Cook et al., 1987a; Cook et al., 1987b).

3.4.2 Model calibration

For calibration purposes, drill stem test (DST) temperatures from 197 wells (Hu et al., 2010) and vitrinite reflectance (% R0) data from 37 wells (Gunther, 1976) were available. As shown in Figure 3.5, the model achieves a good reproduction of both the measured temperature and maturity trends.

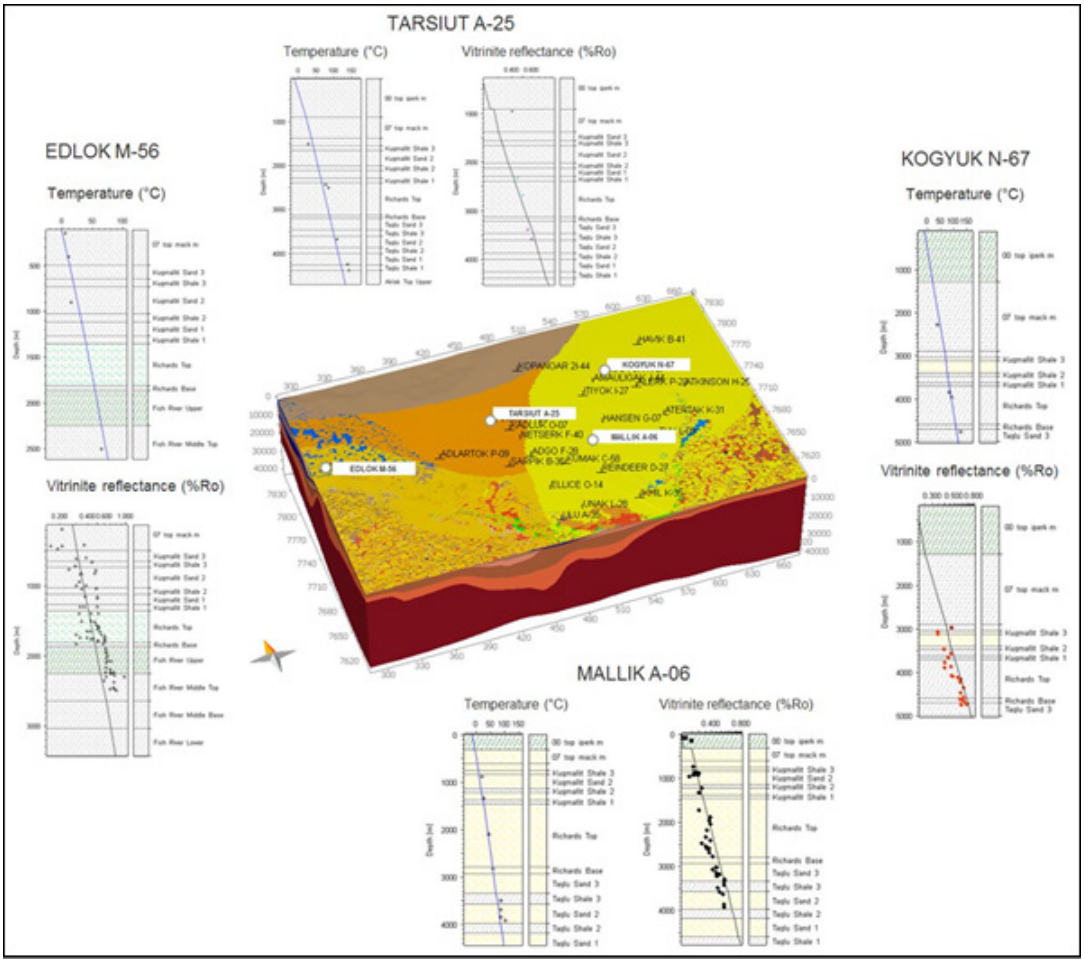

Figure 3.5 Depth extractions at different well locations across the 3-D model. Model calibration with respect to temperature and vitrinite reflectance is shown for each selected well.

The calibration is difficult at some particular well locations in the Central Mackenzie Basin where the vitrinite reflectance shows an almost vertical trend, or where temperatures are considerably higher than in surrounding wells. The possible reasons for these local anomalies have been discussed in detail by Kroeger et al. (2008) and Chen et al. (2008). Kroeger et al. (2008) suggested that almost vertical

trends in % R_0 could be a consequence of re-deposition of more mature material from areas subjected to uplift, such as the Richards Islands. The same work also suggested that anomalous % R_0 trends might be related to the effects of overpressure on vitrinite reflectance, which are explained by Carr (1999). Chen et al. (2008) suggest that many temperature anomalies observed in the region might be the result of the movement of warm fluids following a pattern determined by tectonic and stratigraphic controls.

3.5 Results and discussion

3.5.1 Oil and gas generation

Type III Kerogen, which is the most common in Tertiary source rocks in the Mackenzie basin, is characterised by a wide range of stability (Dieckmann, 2005). Therefore, the time of the onset of petroleum generation predicted by the model is susceptible to vary depending on the kinetic model applied. In addition, heterogeneous source rock properties within the same formation complicate the matter. Saison (2010) determined the bulk kinetic parameters of samples from Cretaceous to Tertiary strata and indicated that even differences in organic matter from different facies within a same deltaic sequence can lead to variations of up to 2500 m in the prediction of the oil window. Combining the results from the model here described (Figure 3.6) with those from the work of Kroeger et al. (2008) the onset of gas generation is placed between 60-50 Ma for the Smoking Hills sequence, between 40 and 30 Ma for the Aklak and between 20-10 Ma for the Taglu formation.
The Smoking Hills sequence is predicted to reach 50% transformation ratio at the Arnak L-30 well location (Figure 3.6) around 40 Ma. The Aklak Fm. reaches this level of transformation around 30 Ma. The kerogen in the Taglu Fm experiences much less thermal maturation, with TR reaching a maximum of 40% in the most offshore part of the model at 10 Ma. At the Arnak L-30 well location, this sequence reaches a maximum TR of less than 20%. The model supports previous studies indicating that intervals younger than Late Eocene are immature, independent of the location in the basin (Kroeger et al. 2008).

The mass of petroleum and gas generated in the model is variable depending on the source rock scenario considered, as well as variations of input parameters summarized in Table 3.2 and briefly explained earlier in the source rock properties section of this work. The model suggests a total thermogenic gas generation ranging from 10^4 to 10^5 Tg (10^{13}–10^{14} m^3), summing all generative intervals. From Eocene to Miocene, the model predicts maximum gas generation rates ranging from 10^{-4} to 10^{-3} Tg/yr. From the Pliocene to present-day, maximum predicted rates range from 10^{-5} to 10^{-3} Tg/yr.

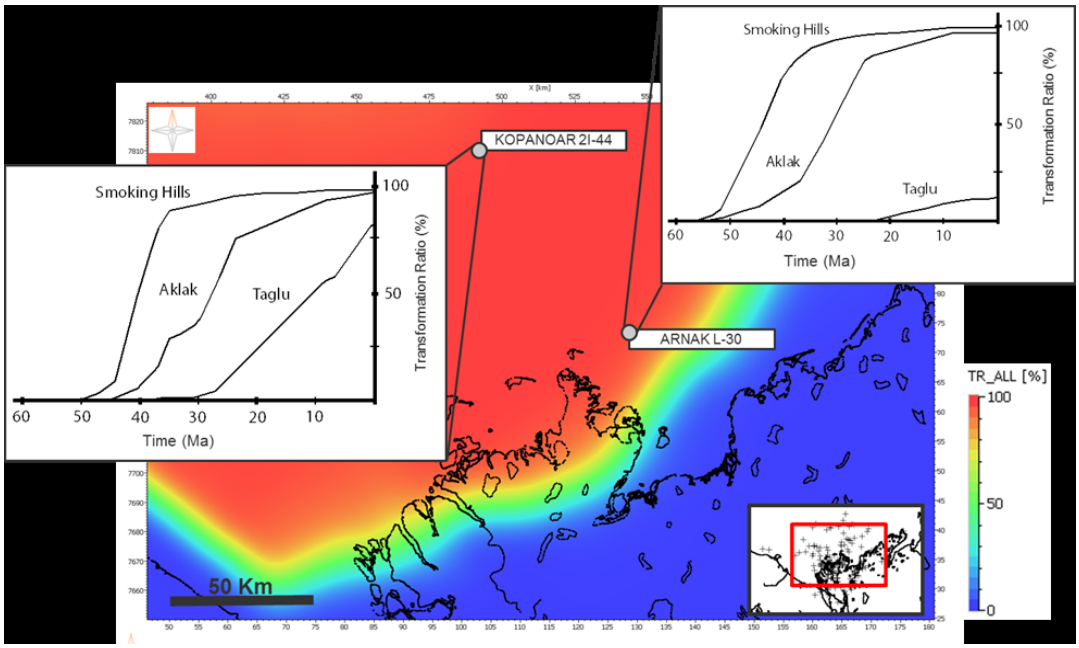

Figure 3.6 Present-day transformation ratio (TR, in %) of the Smoking Hills Fm. as predicted by 3D modeling. The TR value reached by the modeled source rocks through time is shown at Kopanoar 2I-44 and Arnak L-30 well locations.

3.5.2 Reproduction of petroleum accumulations

Individual accumulations in the basin have different filling histories. However, a general trend can be observed for reservoirs belonging to the same stratigraphic interval. Modeled reservoir intervals within the Aklak sequence start filling during the Eocene and continue receiving both oil and gas until the end of the Miocene (Figure 3.7). Reservoirs within the Taglu and Kugmallit sequences start receiving oil during the Oligocene and, in the case of the Kugmallit sequence, some intervals continue being charged up to present day.

The 3D model predicts that a major charge pulse of the Richards Fm. took place during the Oligocene, followed by only minor filling.

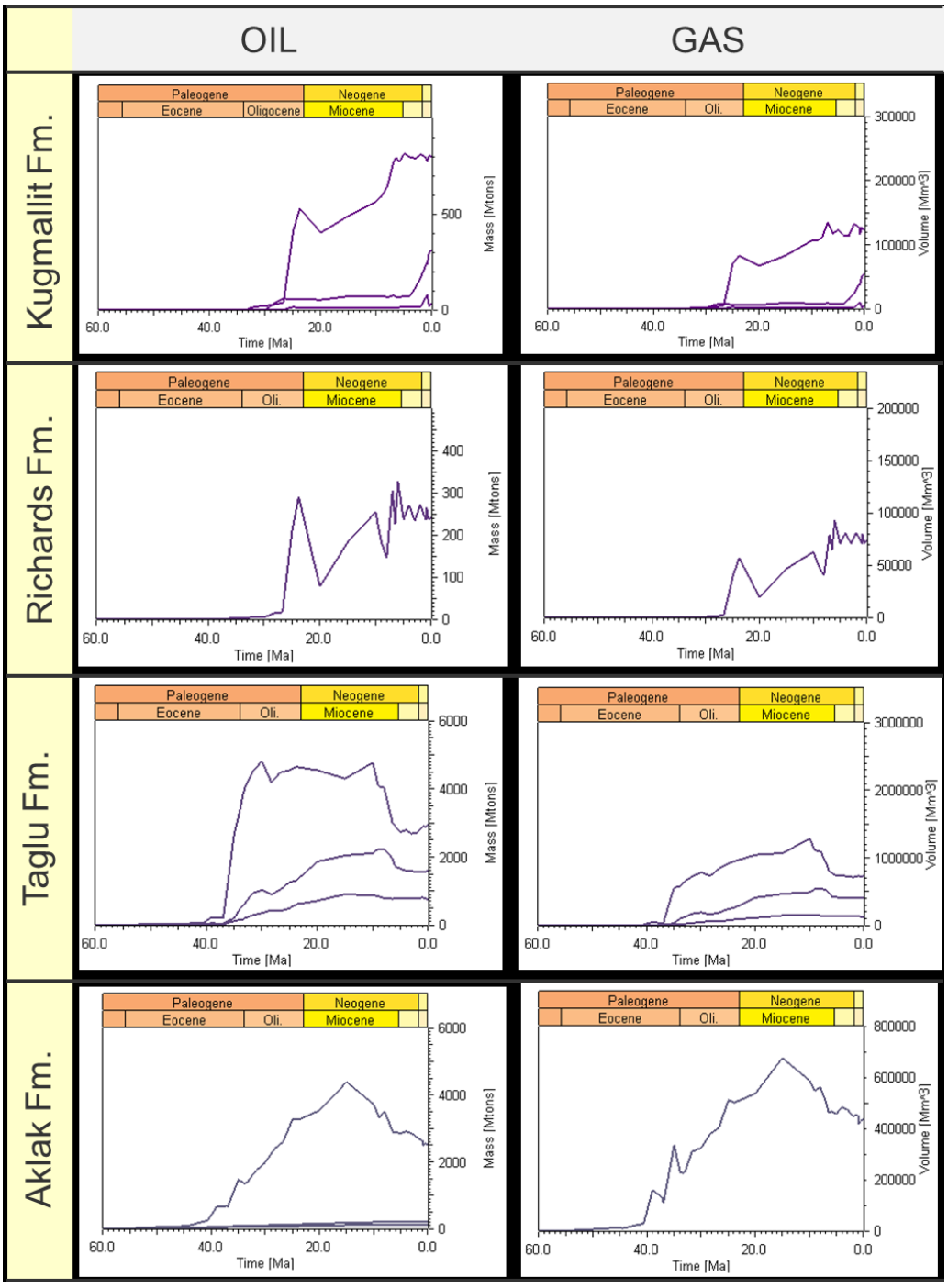

Figure 3.7 Filling time of the modelled reservoirs.

The model reproduces the general locations and compositional trend of the Beaufort-Mackenzie Basin accumulations, which have been described to be more oil-dominated basinwards (Osadetz and Chen, 2006, 2010). Summing all reservoir layers, the total accumulated gas volume in the model is around 1.9-2.4 $x10^{12}$ m^3, which is in the range of marketable conventional natural gas volumes (1.63-2.07 $x10^{12}$ m^3) proposed by Osadetz and Chen (2006).

3.5.3 Estimation of gas hydrate resources

One of the main challenges when attempting to quantify gas hydrate resources through petroleum systems modeling is related to time scales. Temperature fluctuations in the order of 10^4-10^5 years, as those taking place during ice ages, are difficult to incorporate in such models, in which time scales are usually in the order of 10^6 years. In addition, numerical descriptions of permafrost and gas hydrate formation and decay in petroleum system modelling software still represent an area of research, and should therefore be applied carefully. This is why gas hydrate formation or the sealing effect exerted by permafrost were not modelled in this work. Instead, the methane gas hydrate resource in the area was estimated based on the availability of the gas; this means, based on the modelled generated, accumulated and leaking gas volumes. From now on, the gas leaking from the sediment surface of the model will be termed as "SS leakage" (Figure 3.8).

Chen and Osadetz (2010) showed the strong link between the gas hydrate stability zone in the BMB and the thickness of terrestrial permafrost. As described by Rodkin and Lemmen (2000), the earliest montane glaciation of the region is recorded in the Mackenzie Mountains and is considered to be of Late Pliocene age (~2.6 Ma). On the other hand, one of the model scenarios by Majorowicz et al. (2008) suggested that an ice bearing permafrost lid could have started forming in the Beaufort Mackenzie from 14 Ma. This permafrost lid could have reached a thickness of around 250 m at 6 Ma, time when the ground surface temperatures were -4.5 °C to -5.5 °C, allowing the formation of gas hydrates. Another scenario in which gas hydrate formation was confined to areas beneath a geological seal (fine-grained

siltstones and claystone beds) suggested the onset of gas hydrate formation around 0.9 Ma, at depths of about 900 m. Based on the previous ideas it is possible to estimate the methane volume available for gas hydrate formation, by assuming three different scenarios (Table 3.3):

a) The modeled SS leakage is hindered by an ice bearing permafrost layer which has reached considerable thickness around 10 Ma. The gas trapped below permafrost is assumed to be available for later gas hydrate formation.

b) Only the modeled SS leakage taking place since 6 Ma (when the conditions for gas hydrate formation were met) is trapped within gas hydrates.

c) Gas hydrates start forming beneath geological seals at 0.9 Ma. Because most of the conventional hydrocarbon deposits in the BMB are at much larger depths than gas hydrates (Majorowicz and Osadetz, 2001), only the SS leakage component from the model would contribute to the gas hydrate methane volume during this time period (0.9- 0.0 Ma).

Table 3.3 Estimation of the methane volume available for gas hydrate formation in the BMB.

Scenario	Gas generation (m^3)	SS leakage (m^3)	Maximum trapped in GH (m^3)	
			50% of SS leakage	70% SS leakage
A (10-0) Ma	$(1\text{-}3)\times10^{13}$	4×10^{12} - 1×10^{13}	$2\text{-}5\times10^{12}$	$3\text{-}7\times10^{12}$
B (6-0) Ma	8×10^{12}-2×10^{13}	2×10^{12} - 1×10^{13}	$1\text{-}5\times10^{12}$	$1\text{-}5\times10^{12}$
C (0.9-0) Ma	$(2\text{-}5)\times10^{12}$	4×10^{11} - 3×10^{12}	2×10^{11} - 2×10^{12}	3×10^{11} - 2×10^{12}

It is important to note that the gas volume predicted to leak from the sediment surface of the model since the Eocene is 20 to 70 times larger than the volume accumulated in reservoirs (Figure 3.8). Regardless of the arguments used to justify the application of only the "SS leakage" component in the gas hydrate estimates, the "accumulated" component would add unimportant volumes such that it can be neglected.

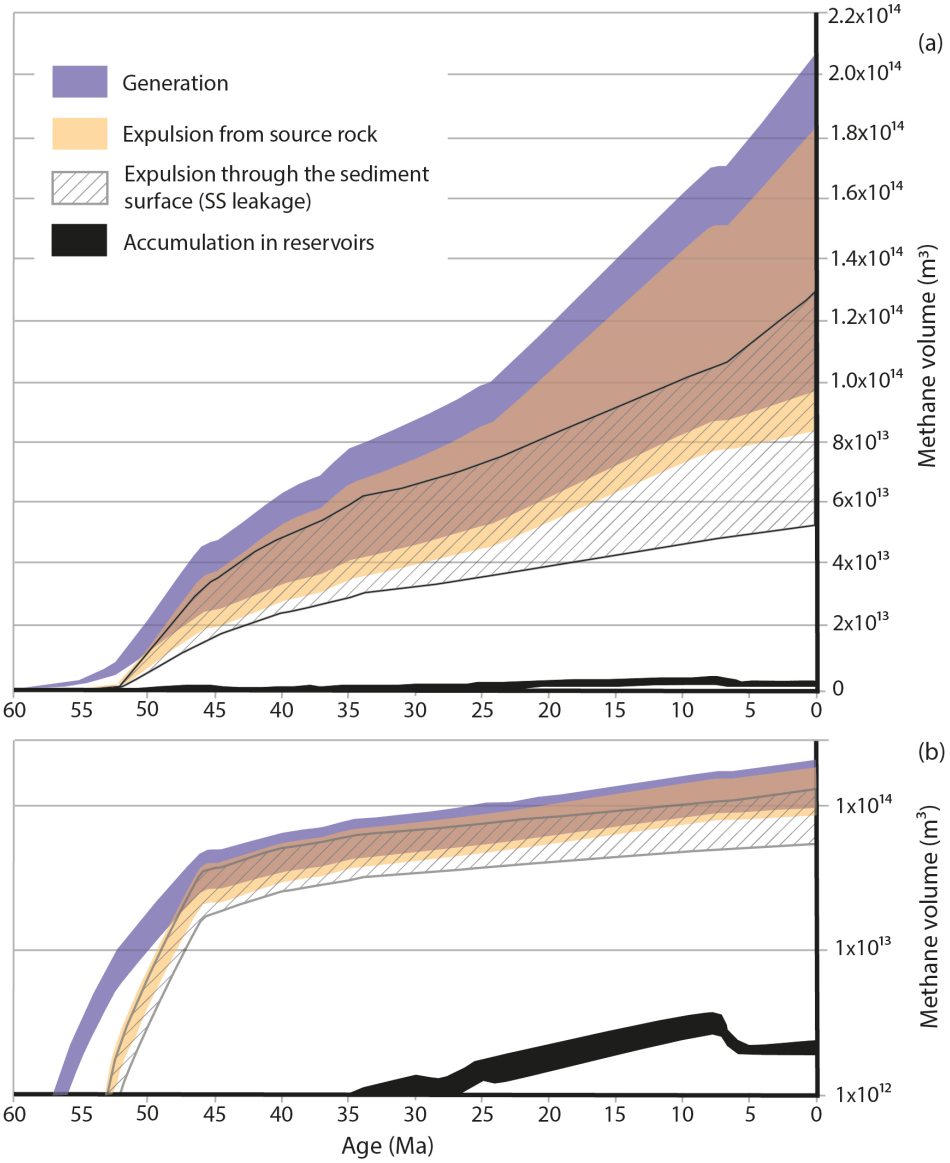

Figure 3.8 General balance of the BMB petroleum system. The total variability of each component derives from the scenarios considered in table 2.

As summarized in Table 3.3, the amount of gas predicted to cross the upper boundary of our model, or "SS leakage" from scenarios a, b. and c range from $3x10^{12}$-$1x10^{13}$ m^3. It would be unrealistic to consider that the entirety of this volume is trapped in gas hydrates, as it is well known that not all the methane passing through the gas hydrate stability zone remains there (Osadetz and Chen, 2005). Gas can be transported through sediments at pressure and temperatures optimal for hydrate formation without being incorporated into the hydrate system, in particular in faulted areas as the BMB (Taylor et al., 2000). One explanation could be that the upward migration of the fluid carries with it heat, developing a warm channel

through which gas can be transported (Taylor et al., 2000; Wood et al., 2002). Besides, gas hydrates do not occupy all the pore space in the sedimentary section with gas hydrate stability conditions; instead, they occupy a percentage of the pore space which is referred to as the gas hydrate saturation. Although most marine biogenic gas hydrates have low saturations of less than 10 % (Osadetz and Chen, 2005), higher gas hydrate concentrations are expected in fractured, thermogenic gas hydrate systems such as the BMB (Hovland et al., 1997; Milkov and Sassen, 2002). Calculated gas hydrate saturations within the gas-bearing units of the Mallik 2L-38 well have an average of 44 % (Collet et al., 2009). Majorowicz and Osadetz (2001) estimated the gas hydrate saturation for the BMB to range between 2 and 38 %. However, this parameter was assumed to be of 60 % in latter modeling work (Majorowicz et al., 2008). Considering that the presence of thick permafrost in some areas of the BMB should increase the methane trapping potential of the gas hydrate stability zone, it is proposed that a 50–70 % of the available methane volume ($3x10^{12}$-$1x10^{13}$ m^3) estimated in Table 3.3 could be retained within gas hydrates. This would place our upper limit for the gas hydrate resource in the BMB in the order of 1-7 $x10^{12}$ m^3.

Proposing a lower limit for the previous estimate would be more difficult due to uncertainty about the extent to which interglacial periods would have affected the gas hydrate stability zone, as well as the thickness and areal extent of permafrost. One possibility would be that interglacial periods resulted in thawing of gas hydrates and leakage of the gas trapped during the previous glacial period. Another possibility would be that the interglacials were not warm enough or long enough to result in gas hydrate decomposition. Numerical modeling in the BMB (Majorowicz et al., 2008) suggests that the gas hydrate thickness generally increases during glacial intervals and decreases during the interglacial episodes. In the more recent glacial history of the ~100 ka cycles these variations are around 200 m for the ice bearing permafrost and about 100 m for the gas hydrate layer (Majorowicz et al., 2008). In areas where the ice bearing permafrost layer is thick, it is considered unlikely that the gas hydrates beneath ice bearing permafrost disappeared entirely during previous interglacial intervals (Majorowicz et al., 2008). In the previously described a, b, and

c scenarios, it is assumed that gas hydrates did not disappear during interglacial periods. Considering this, our estimates should be considered as optimistic, or maximum, rather than conservative ones.

Predictions by the 3D modelling approach coincide reasonably well in terms of orders of magnitude with previous gas hydrate natural gas estimates. Based on the GH stability zone volume, reservoir porosity, hydrate saturation and gas volume expansion factor, Majorowicz and Osadetz (2001) estimated $2.4x10^{12}$-$87x10^{12}$ m^3. Results from this study suggest that the lower end of the estimate by Majorowicz and Osadetz (2001) would be more likely. The 8.8 $x10^{10}$ m^3 calculated by Davidson (1978) are two orders of magnitude lower than the maximum estimates here presented. However, as indicated before in this work, a minimum value which can be compared against Davidson (1978) is not provided. In contrast, the $1.6x10^{13}m^3$ proposed by Smith (1995) are close to the here modeled maximum total gas generation since the Pliocene. This last estimate is therefore considered as too optimistic.

3.5.4 Gas leakage through geologic time

The 3D model suggests that the gas leakage at the top of the sedimentary sequence before the onset of Cenozoic glaciations ranges from $5x10^{13}$ to $1x10^{14}$ m^3 (Figure 3.8), which is equivalent to around 60% of the total generated gas. Modeled gas leakage rates during this period of time range from 10^{-1} to 10^{6} m^3/yr (10^{-10}-10^{-3} Tg/yr) which is comparable to reported present-day leakage at Toney River, Canada (Cranston, 1994) or Rías Baixas, Spain (Garcia-Gil, 2003). The leakage here modeled is mainly controlled by the generation in deep mature source rocks and later migration of the gas through carrier beds and high permeability zones such as faults and fractures (Berbesi et al., 2014). Surface methane seepage after the onset of Cenozoic glaciations is more difficult to estimate because of the inability to model the dynamics of permafrost and gas hydrate formation.

Arctic systems have been previously proposed as an important channel for lithospheric carbon fluxes into the hydro- and atmosphere, due to the hydrocarbon accumulations-fast release mechanisms role exerted by gas hydrates and ice caps (Berbesi et al., 2014, and references therein). The reasoning behind is that methane and other gases can accumulate in gas hydrates/beneath ice layers over time and then be released within thousands of years when the gas hydrate/ice layer stability conditions are not present anymore (Rodrigues et al., 2013; Ostanin et al., 2013; MacDonald, 1990; Archer et al., 2009). However, modeling work has suggested that terrestrial, sub-ice bearing permafrost gas hydrates such as those in the BMB have higher thermal inertia, and therefore more probability to survive interglacial periods, than marine non-ice bearing permafrost gas hydrates (Majorowicz et al., 2008; Osadetz and Chen, 2010). Majorowicz et al. (2008) consider a total disappearance of BMB gas hydrates unlikely, both during previous glacial intervals and during the present "natural" interglacial. If this hypothesis is correct, the BMB might constitute a setting where methane has entered the gas hydrate system with minor associated leakage in a time scale of millions of years. If any future climate process results in total permafrost/gas hydrate retreat in the area, methane leakage rates are expected to be considerably higher than the pre- glaciation rates suggested in this work.

3.6 Conclusions

A three-dimensional petroleum systems model of the Beaufort-Mackenzie Basin has been developed and calibrated to well data. The model predicts the onset of gas generation to occur around 60-50 Ma in the case of the Cretaceous SR (Smoking Hills Fm.). The corresponding time is 40-30 Ma for the Upper Paleocene SR (Aklak Fm.) and 20-10 Ma in the case of the Eocene SR (Taglu). The model supports previous studies indicating that those intervals younger than Late Eocene are immature, independent of their location in the basin (Kroeger et al., 2008).

The model proposes a total generated gas mass in the order of 10^4 to 10^5 Tg (10^{13}–10^{14} m^3) of methane, depending on the extent of source rock considered and the kinetic model applied. The predicted gas generation rate on a basin scale is of 10^{-4} to

10^{-3} Tg/yr from Eocene to Miocene, and 10^{-5}-10^{-3} Tg/yr from Pliocene to present day.

The modelled accumulation volumes in conventional reservoirs fall in the range of 1.63-2.07x10^{12} m^3, which coincides with the volume of marketable natural gas proposed by previous studies. Assuming different gas hydrate formation scenarios with onset between the Late Miocene and Pleistocene, the maximum methane volume stored in this reservoir is placed around 1-7 x10^{12} m^3. This volume is of comparable order of magnitude to previous gas hydrate resources based on GH stability distribution and properties. Gas leakage from the upper boundary of the model (sediment surface) before of onset of Cenozoic glaciations is estimated to range between 5x10^{13} to 1x10^{14} m^3, which translates into 10^{-1} to 10^{6} m^3/yr (10^{-10}- 10^{-3} Tg/yr). If any future climate process results in total permafrost/gas hydrate retreat in the area, leakage rates are expected to be higher than before glaciations, due to the concentration/fast release effect exerted by gas hydrates and permafrost.

Chapter 4

Methane leakage from evolving petroleum systems: masses, rates and inferences for climate feedback

This chapter has been published as: Berbesi, L.A., R. di Primio., Z. Anka., B. Horsfield., H. Wilkes.,2014, Methane leakage from evolving petroleum systems: masses, rates and inferences for climate feedback. Earth and Planetary Science Letters. 2014. Volume 387, p 219–228.

4.1 Abstract

The immense mass of organic carbon contained in sedimentary systems, currently estimated at $1.56x10^{10}$ Tg (Des Marais et al., 1992), bears the potential of affecting global climate through the release of thermally or biologically generated methane to the atmosphere. This study investigates the potential of naturally-occurring gas leakage, controlled by petroleum generation and degradation as a forcing mechanism for climate at geologic time scales. The main goal is to analyze the potential methane contributions to the atmosphere during the evolution of petroleum systems in two different, petroliferous geological settings: the Western Canada Sedimentary Basin (WCSB) and the Central Graben area of the North Sea. Besides 3D numerical simulation, different types of mass balance and theoretical approaches were applied depending on the data available and the processes taking place in each basin. In the case of the WCSB, maximum thermogenic methane leakage rates in the order of

10^{-2}-10^{-3} Tg/yr are modelled, while the maximum calculated biogenic methane generation rates are of 10^{-2} Tg/yr. In the case of the Central Graben, maximum estimates for thermogenic methane leakage are in the order in 10^{-3} Tg/yr. Extrapolation of our results here obtained to a global scale suggests that, at least as a single process, thermal gas generation in hydrocarbon kitchen areas would not be able to influence climate, although it may contribute to a positive feedback. Conversely, only the sudden release of subsurface methane accumulations, formed over geologic timescales, can possibly allow for petroleum systems to exert an effect on climate.

4.2 Introduction

The chemistry of organic compounds is based on carbon. The ability of carbon to form an immense variety of naturally occurring compounds, primarily with hydrogen, oxygen, sulphur and nitrogen, with a wide range of physical and chemical properties is unparalleled by other elements. Coming from mainly biological systems, organic compounds can be incorporated into sedimentary rocks, and remain within the lithosphere for extended geological time periods, gradually undergoing exposure to elevated temperatures and pressures, and ultimately returning to the Earth's surface and atmosphere, either by tectonic movements, seepage or via human action, where they are oxidised back to CO_2 and made available one more to take part in biosynthetic reactions.

The cycle of organic carbon in nature consists of two parts. There is a primary small "biochemical" (BIO) sub-cycle with a pool of approximately 10^6 Tg (1 Tg = 10^{12} g) of organic carbon whose half life is measured in tens of years or even days and a secondary, much larger "geochemical" (GEO) cycle comprising approximately 10^{10} Tg with a half life of several million years (Berner, 1989; Des Marais et al., 1992). The two cycles are interconnected via incorporation interfaces, namely soils and sediments, and removal interfaces, namely via weathering and leakage phenomena. The leakage of carbon from the GEO into the BIO cycles is of great interest because, as Kroeger et al. (2011) suggested, if only 0.1 % of the sedimentary carbon mass

undergoes cycling in active surface pools, this might have had a considerable impact on Earth climate over geological time.

The largest fluxes of the carbon cycle are those related to CO_2, which is recognized as the main climate driver (Dickinson and Cicerone, 1986; Schimel et al., 1994). On the other hand, methane, which is the main component of natural gas, has an atmospheric burden around 600 times lower than CO_2 (Schlesinger, 1997) but holds a global warming potential (simplified index based upon radiative properties and the time it takes to remove that substance from the atmosphere) that is 23 times higher than that of CO_2 on a 100 year time horizon (Forster et al., 2007). Hence, methane is a crucial compound to investigate when studying the carbon exchange dynamics between deep sedimentary sources and the atmosphere.

Naturally occurring methane seepage from petroleum systems has been quantified using direct measurements at actively seeping locations and indirectly via gas leakage appraisals based on surface data (Dimitrov, 2002; Hornafius et al., 1999; Judd, 2004). This approach has allowed the relevance of geological sources of atmospheric methane with respect to the total annual atmospheric methane budget to be recognised (Etiope, 2004; Etiope, 2012; Etiope et al., 2008). Nonetheless, the approach is challenged by the non-uniform nature of the mechanism being addressed, which hinders the accurate (a) estimation of seepage rates in areas between and around sampling locations (Etiope et al., 2008) and (b) extrapolation of measured rates in time, which results in the incapacity to reconstruct paleo-seepage. The two previously mentioned limitations need to be addressed because gas fluxes within and from petroleum systems are not infinite, and are limited by the generated and accumulated gas mass during specific geologic time frames. In this sense, the use of petroleum systems modelling and analysis as a complementary technique is to be recommended.

Studies applying petroleum system modelling have been able to infer paleo-leakage from different types of geological settings (Cavanagh et al., 2006; Kuhlmann et al., 2011; Naeth et al., 2005; Paton et al., 2007), but, unfortunately, most of them have

suffered from the lack of present-day measured seepage to calibrate model predictions. Although it is obvious that direct surface measurements and petroleum system modelling both have limitations and provide different, albeit complementary, pieces of information, these two approaches have been carried out entirely independently in the said literature.

Regardless of the methodology applied, the task of investigating a link between methane seepage from world-wide petroleum systems and climate evolution faces a big challenge: the fact that there are 576 sedimentary basins on planet Earth. Each has the potential to contribute greenhouse gases, but what is their combined influence on Earth climate at any given geological age? Because the database for conducting an integrated evaluation does not exist, an alternative strategy is to systematically answer four selected questions: (1) what are the basic conditions or mechanisms present in basins where significant seepage is known to take place? (2) How relevant is the carbon inventory of a basin in terms of potential for climate feedback? (3) Do we really need to address all sedimentary basins in the world, or should we concentrate on basins where representative mechanisms are present? (4) How far can we extrapolate, in space and time, present-day measured seeping rates?

In order to address these questions, this study analysed two different geological settings that constitute representative prolific hydrocarbon provinces: the Western Canada Sedimentary Basin (WCSB) and the Central Graben area of the North Sea. The WCSB, holding the largest oil sand deposits in the entire world and covering an area more than 10 times larger than England, represents an ideal place to investigate the relevance of basin size and sedimentary organic mass in terms of potential for climate feedback. Here, the masses of leaked methane predicted by a recently published 3-D petroleum system model (Berbesi et al., 2012) were used. In order to analyze the climate feedback potential of thermal gas generation and migration in absence of focused leakage paths, this model simulates uplift but does not incorporate faults or fractures in the system. Additionally, this study includes a mass balance of the biodegradation process and an assessment of the total mass of biogenic methane generated in the basin. A potential for climate feedback is

addressed considering scenarios in which this mass is released during different, but geologically reasonable time spans.

On the other hand, the Central Graben represents an area where recent leakage has been documented (Hovland and Sommerville, 1985) and estimated by means of surface data and theoretical considerations (Judd et al., 1997). This area of the North Sea provides therefore a great opportunity to compare indirect appraisals based on surface data with results derived from numerical models of the subsurface petroleum system. Moreover, hydrocarbon migration and leakage in/from this area are known to be mostly controlled by pressure-induced fractures and graben margin faults. This gives a chance to compare leakage spread out over a large area; not concentrated or focused, and mainly derived from thermogenic generation in kitchen areas, as was the case of the WCSB, with focused leakage arising from fractured reservoirs (Central Graben). Seepage estimates from this study are compared against published data from other basins around the world. Finally, the study discusses the different mechanisms promoting significant methane seepage from petroleum systems, and provides a set of recommendations for future works in this challenging but interesting field.

4.3 Study areas

The WCSB is a foreland basin hosting the world's largest known oil sand deposits, which occupies more than 1 400 000 Km^2, and contains in-place natural gas reserves of around 6500 Tg (7200 billion m^3) (Drummond, 1995; Head et al., 2003). For Alberta alone, crude bitumen reserves have been estimated at 250 000 Tg (260 billion m^3) (Canada, 2010). The main source rocks for the hydrocarbon discoveries are of Devonian through Cretaceous age. During the late Barremian, the western edge of the basin was loaded with thrust sheets related to allochthonous terrain accretion, resulting in rapid subsidence and thermal maturation of the source rocks. Petroleum generation, migration and accumulation in this basin could have been accompanied by leakage of large masses of thermogenic gas. Moreover, low

reservoir temperatures in this basin promoted biodegradation of the oils, most probably during the burial and charging phase (Adams et al., 2012, and references therein). A significant portion of the biogenic methane generated during this process may have leaked to the atmosphere (Larter et al., 2008). Considering the enormous masses of organic matter transformed into thermogenic and biogenic CH_4 in this basin, the WCSB represents an ideal place to address the relevance of both processes in terms of potential climate feedback.

The North Sea Graben Province occupies territorial waters of Denmark, Germany, the Netherlands, Norway, and the United Kingdom and, according to the USGS, is ranked number 8 among the 76 world priority provinces in terms of volumes of discovered oil and gas. It is estimated that the North Sea contains up to 3200 Tg (4 billion m^3) of undiscovered oil and up to 1800 Tg (2000 billion m^3) of undiscovered associated and non-associated natural gas (Gautier, 2005). It can be divided into three sub-basins: the Viking Graben, the Central Graben and the Moray Firth/Witch Ground. The main source rocks were deposited from Late Jurassic to early Cretaceous time, during a period of extensional tectonics and rifting. By the end of the Jurassic, extension ceased and subsidence dominated in most of the region. Oil and gas generation began locally during the Cretaceous, and continued at several locations up to the present (Gautier, 2005). Oil and gas expelled from the source rocks experienced lateral and vertical migration through continuous porous carriers, fractures and faults respectively until reaching their accumulation sites, or leaking through the seafloor (Cornford, 1994). In the latter case, gas escaping into the water column has given origin to pockmark fields identified across the North Sea (Hovland and Sommerville, 1985). Previous estimates of methane seepage fluxes based on surface data and theoretical considerations from the UK Continental Shelf have been carried out (Judd et al., 1997). These emissions have been proposed to be related to, inter alia, the thermal maturation of Kimmeridgian Shales, the same sources providing petroleum to accumulations in the Central Graben. This portion of the North Sea provides therefore an excellent opportunity to compare indirect and extrapolated appraisals based on surface data with results derived from numerical models of the petroleum system in the subsurface.

4.4 Surface methane seepage from petroleum systems

By definition, a petroleum system includes the four basic elements, namely the active source rock, the reservoir interval, the seal and the trap, depicted as a function of time so that the key factors controlling accumulation are displayed (Magoon and Dow, 1995).

Petroleum is generated in subsiding sedimentary basins by the effect of temperature on kerogen (often of algal and bacterial origin) over millions of years. Concomitant with generation, the petroleum may be expelled from the source rock into adjacent permeable carrier beds. Various mechanisms have been proposed to explain this process, among them diffusion, flow controlled by capillary forces, and flow driven by petroleum potential gradients (England et al., 1987; Kuo, 1997; Stainforth and Reinders, 1990). Once expelled from the source rock, petroleum is subjected to secondary migration, which is basically the movement of a petroleum phase through the porous carrier bed, controlled by buoyancy, fluid potential gradients and to a subsidiary extent by capillary forces, in what can be described as non-turbulent Darcy flow (Hantschel and Kauerauf, 2009). Petroleum migration will continue until the generated hydrocarbons reach a trap (sealed reservoir), resulting in an oil and/or gas accumulation. At later stages, tectonic processes may affect these reservoirs resulting in leakage of the initially accumulated petroleum, or a portion of it. Some of the oil and gas expelled from the source rock may never find a suitable trap and continue migrating until it reaches the Earth surface. Depending on the case in question and the basin's geological history, gas seepage can take place as macro-seepage, which disturbs surface and near-surface morphology (Etiope et al., 2008; Etiope and Martinelli, 2002), or as micro-seepage, defined as an invisible but pervasive, diffuse exhalation of light hydrocarbons, that can be detected by standard analytical procedures (Brown, 2000; Etiope and Klusman, 2010).

Previous studies indicate that significant gas leakage from petroleum systems is usually related to reservoirs (Etiope, 2004; Etiope et al., 2008; Judd et al., 2002) particularly in presence of enhanced-permeability zones, such as faults and fracture

networks (Etiope and Martinelli, 2002; Ostanin et al., 2013). Unfortunately, a clear perspective of the magnitude of the measured seepage with respect to the time of generation in deep kitchen areas, migration and accumulation is lacking. Moreover, there is a knowledge gap regarding the relevance of the leakage mechanism compared to the organic carbon availability in the basin, and regarding how far measured seepage rates can be extrapolated in time and space. The combination of direct seepage measurements (at the surface) with numerically reconstructed seepage volumes from models of the petroleum system (in the subsurface) might be the key for filling some of the previously mentioned knowledge gaps.

4.5 Petroleum systems modelling

A petroleum systems model is, as its name suggests, a digital representation of a petroleum system in which all its elements and processes are simulated, in order to better understand and predict them (Hantschel and Kuerauf, 2009). The scale of these models ranges from tens to hundreds of kilometers, and the periods covered may reach hundreds of millions of years (Al-Hajeri et al., 2009). These models are dynamic regarding their geometry, which often changes during the simulation, and regarding the processes they simulate, including sediment deposition, faulting, burial, kerogen maturation kinetics and multiphase fluid flow (Al-Hajeri et al., 2009). In this way, petroleum system models can provide information regarding generation, migration, accumulation and loss of oil and gas in a sedimentary basin through geologic time (Hantschel and Kuerauf., 2009).

The modelling tool applied in this study was PetroMod 3-D version 11.3, from Schlumberger (2010). The reader is invited to consult the literature for extensive descriptions of the discipline (Hantschel and Kauerauf, 2009; Schlumberger, 2009, 2010; Waples, 1998; Welte et al., 2000; Higley et al., 2006). Although the input data and parameters applied during the building of each model depend on each basin's geological history, the general workflow is the same. In a first step, formation top depth maps and faults usually derived from seismic interpretation are imported into

the modelling software, and formation layers are created between consecutive formation tops. Wells are incorporated in the model by specifying their location, drilled depth and the calibration data they contain. In this study, calibration data consisted on measured vitrinite reflectance ($\%R_0$) and temperatures. Afterwards, ages are assigned to the deposition of each layer, to hiatus periods, faulting and to erosions. In the latter case, also the thickness of removed sediment is specified. Each layer in the model is characterized by lithological (and therefore petrophysical) properties, which should also reflect lateral facies variations in the depositional environment. The amount and type of petroleum generated, as well the timing of generation, will be a consequence of the burial history and source rock thickness, together with the total organic carbon (TOC), hydrogen Index (HI) and petroleum generation kinetics assigned to each generating interval. Finally, the boundary conditions (heat flow, paleo water depth and sediment-water interface temperature) define the basic energetic conditions for temperature and burial history of the source rock and, consequently, for the maturation of organic matter though time (Schlumberger, 2009).

Simulations applied in our work are deterministic, which means that one value is assigned to each variable, and each model output is also a single value. In this way, the variability of the model results can only be appreciated after performing several simulations applying different but reasonable input values. Usually, the first model simulation is run without petroleum migration algorithms, aiming to decrease the computing time. In case the model results do not match calibration data, the model definition is adjusted until a good calibration is achieved. At that point, a simulation including petroleum migration is performed.

In this work, three-dimensional numerical modelling is combined with mass balance and theoretical approaches depending on the available data and the processes taking place in each basin. A description about the main considerations behind the migration calculation in our models, as well as their most important output parameters, including petroleum system losses and leakage at the top model boundary, are provided in supplementary material A.

4.6 Methods and results

4.6.1 Western Canada Sedimentary Basin

Generation and leakage of thermogenic methane

The modelled area is depicted in Figure 4.1 (detailed description of the model is given by Berbesi et al. (2012)). The model not only estimated the generated and accumulated petroleum masses in the basin, but also provided understanding on the individual contributions of the main source rocks to Lower Cretaceous accumulations. It has been calibrated to measured vitrinite reflectance (% Ro) and corrected borehole temperatures (Figure 5 in Berbesi et al (2012)). The model discerns between petroleum properties in sub-surface and surface conditions (Hantschel and Kauerauf, 2009; Schlumberger, 2010) and takes into account the mass losses that have occurred during petroleum migration

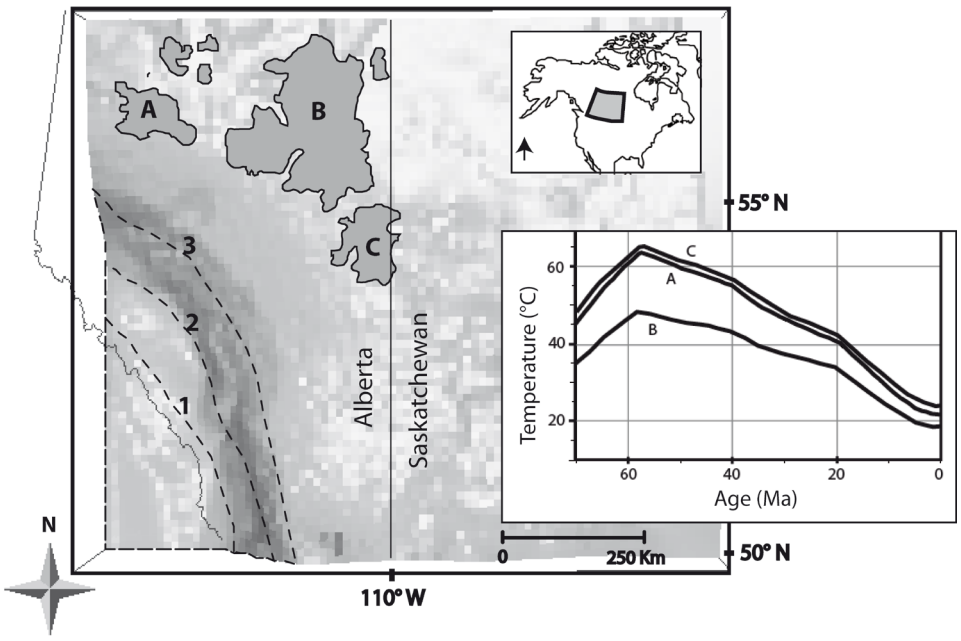

Figure 4.1WCSB projected over the main modelled reservoir layer. The figures in dark grey represent the three main oil sand reservoirs in the basin : A= Peace River, B = Athabasca, C= Cold Lake. The segmented lines identified as 1, 2 and 3 correspond to different areal extensions considered for the modelled coal strata. The chart on the right side shows the temperature evolution of the reservoir layer at the main oil sand locations.

The source rock properties used as input are shown in Table 4.1. One of the main limitations is the uncertainty related to the presence, distribution and size of coal bodies and Type III kerogen-rich intervals across the basin. This is a consequence of the depth of these strata, which is generally beyond current conventional mining capabilities (Smith, 2008). This was minimized by varying the aerial extent of gas-generative coal, as indicated in Figure 4.1.

Table 4.1 Average source rock parameters applied in the 3D petroleum system model of the Western Canada sedimentary basin. See Berbesi et al. (2012) and Higley et al. (2009) for more details.

Period	Source rock layer	Kerogen Type	TOC (wt. %)	HI (mgHC/gTOC)	Average Thickness (m)	Kinetic model
Cretaceous	**Mannville Coal**	Coal	60	200	10	Pepper and Corvi (1995a)
Devonian to Late Jurassic	**Poker Chip Shale A**	II	7.36	550	15.8	Higley et al. (2009)
	Gordondale	I/IIS	15.89	740	26	
	Doig Formation	II	2.90	450	40	
	Exshaw Formation	II	9.64	500	12	
	Duvernay Formation	II	5.81	510	43.6	

The modelled kitchen area is located beneath a portion of the Rocky Mountains in SE British Columbia and SW Alberta, as shown in Figure 6 of Berbesi et al. (2012). Here, significant petroleum generation started around 80 Ma and continued until the onset of the Laramide orogenic phase, at 58 Ma (Figure 4.2). After roughly 50 Ma, generation ceased. Summing all sources, gas generation occurs at rates in the order of 10^{-2} Tg per year for the entire kitchen area. The predicted total gas mass generated ranges from 200 000 to 300 000 Tg, mainly depending on source rock definition (supplementary material B).

Based on the applied kinetic model, up to 80% of this mass is assumed to be dry gas, which is dominantly composed of methane. Maximum leakage of thermogenic gas is estimated to have taken place between 80 Ma and 60 Ma, coinciding with the timing of maximum burial and consequent gas generation and migration. In the

quantification of generated gas masses we included both oil-associated as well as free thermogenic gas (gas and gas-condensate). Petroleum phase behaviour was taken into account using the Peng-Robinson equation of state as implemented in the modelling software (Peng and Robinson, 1976).

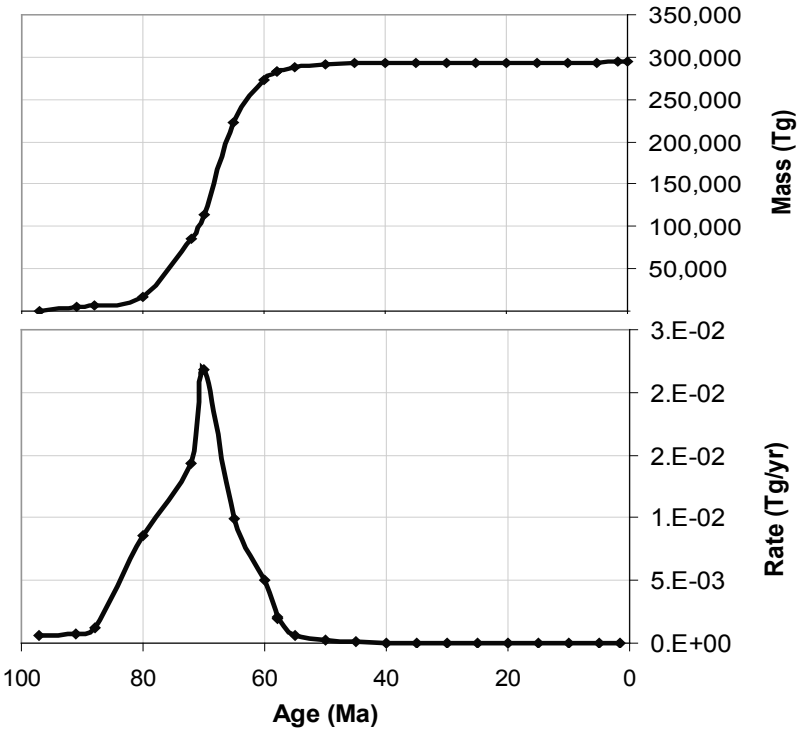

Figure 4.2 Thermogenic gas generation in the WCSB according to our 3D model. The upper chart illustrates cumulative gas generation summing all generative intervals. The lower chart shows the rate of gas generation per year.

The Laramide orogeny, leading to uplift and cooling of the basin, does not exert a major control on the thermogenic emissions in our model due to the slow temporal nature of the event. In the absence of methane consumption in soils, the potential gas emissions from the sediment surface are estimated to be in the order of 10^{-2}-10^{-3} Tg/yr during the period of maximum leakage (from 80 Ma to 60 Ma). The rest of the generated hydrocarbons remain underground, both within migration routes and trapped in reservoirs.

The variability (one order of magnitude) of our gas surface leakage estimates is consequence of the source rock definition (gas generation), and the permeability assigned to the main seal layer. Values assigned to different parameters during our

iterated deterministic simulations, as well as the total variability of the obtained results can be found in supplementary material B.

Biogenic methane generation

This section will focus only on the Athabasca accumulation because it is the main oil sand deposit accounting for 70% of the total petroleum volume in the WSCB basin (Canada, 2010), and its mode and history of formation has been modelled in detail (Berbesi et al., 2012).

Total mass of biogenic methane generated

The modelling software applied in this study does not simulate either oil mass loss due to biodegradation, nor methane generation during this process. However, 1D extractions at Peace River, Athabasca and Cold Lake (Figure 4.1) show that temperatures at those locations did not exceed 70°C during the time of maximum burial (58 Ma), which agrees with previous work proposing that none of these deposits have been subjected to natural pasteurisation (Adams et al., 2006; Wilhelms et al., 2001) and experienced therefore different levels of biodegradation.

A simple biodegradation mass balance can be performed following a similar methodology (Figure 4.3) to the one applied by Milkov (2011). This is based on a stoichiometric model of methanogenic alkane biodegradation that considers hexadecane ($C_{16}H_{34}$) as a representative compound of the alkane family (Zengler et al., 1999). Some other models (Jones et al., 2008) propose different intermediate steps for the methanogenic hydrocarbon degradation reaction, but using the same net equation proposed by Zengler et al. (1999).

Previous works estimate that 30 % to 70 % of the originally accumulated oil mass at Athabasca has been lost during petroleum biodegradation. (Head et al., 2003; Larter et al., 2006; Larter et al., 2005; Brooks et al., 1988., Adams et al., 2012; see discussion in supplementary material 3). Following the stoichiometric model of Zengler et al. (1999), it is estimated that $6x10^4$ to $1.3x10^5$ Tg of biogenic methane would have been generated during this process. The later mass represents around

10 % of all the methane generated during biodegradation of world-wide reservoirs throughout geologic history, as calculated by Milkov (2011).

Biodegradation and methane generation rates

The latter approach does not provide information about masses of consumed oil, nor about the mass of generated methane at different stages of alteration. A more detailed analysis required the subdivision of the biodegradation mass balance into time intervals. For each interval, the mass of consumed oil (M) will be given by the equation M = I x T x R; where (I) is the initial (in subsequent steps to the remaining) oil mass (I), the duration of the time interval (T), and the biodegradation flux or rate (R).

Previous biodegradation modelling (Larter et al., 2006; Larter et al., 2003) has shown that average degradation fluxes for fresh petroleum in clastic reservoirs are in the range of 10^{-4} Kg of petroleum destroyed per m^2 oil-water contact (OWC) per year, but diminish at very low reservoir temperatures and as the oil becomes degraded, as in the Athabasca case (Larter et al., 2006; Adams, 2008; Adams et al., 2012). Here, the rate of biogenic methane generation through time was estimated (Figure 4.3) (Tg yr^{-1}) considering the most likely biodegradation scenarios based on published data (supplementary material C). The 220 000 Tg of oil predicted by 3D modelling to have reached the Athabasca accumulation (Berbesi et al., 2012) were used as the total, potentially degradable oil mass. Most of the biodegradation was considered to take place during burial and shortly after the onset of uplift, coinciding with the main charging phase. This is consistent with the general idea that continuous oil charging, decrease in biodegradation rates by reservoir filling to the underseal and early reduction in the water leg, combined with very low reservoir temperatures are required to explain the non-complete destruction of Athabasca oils (Adams et al., 2012; Larter et al., 2006). The calculated biodegradation rates range from $9x10^{-5}$ to $9x10^{-3}$ Kg of consumed oil per year, depending on the combination of timing-percentage of oil mass loss assumed.

Finally, the equation M = I x T x R is applied for each biodegradation step (Figure 4.3). The remaining oil mass at the end of the first calculation step was considered as the initial mass for the next one and so on. The same procedure was repeated until the end of the temporal extent of biodegradation.

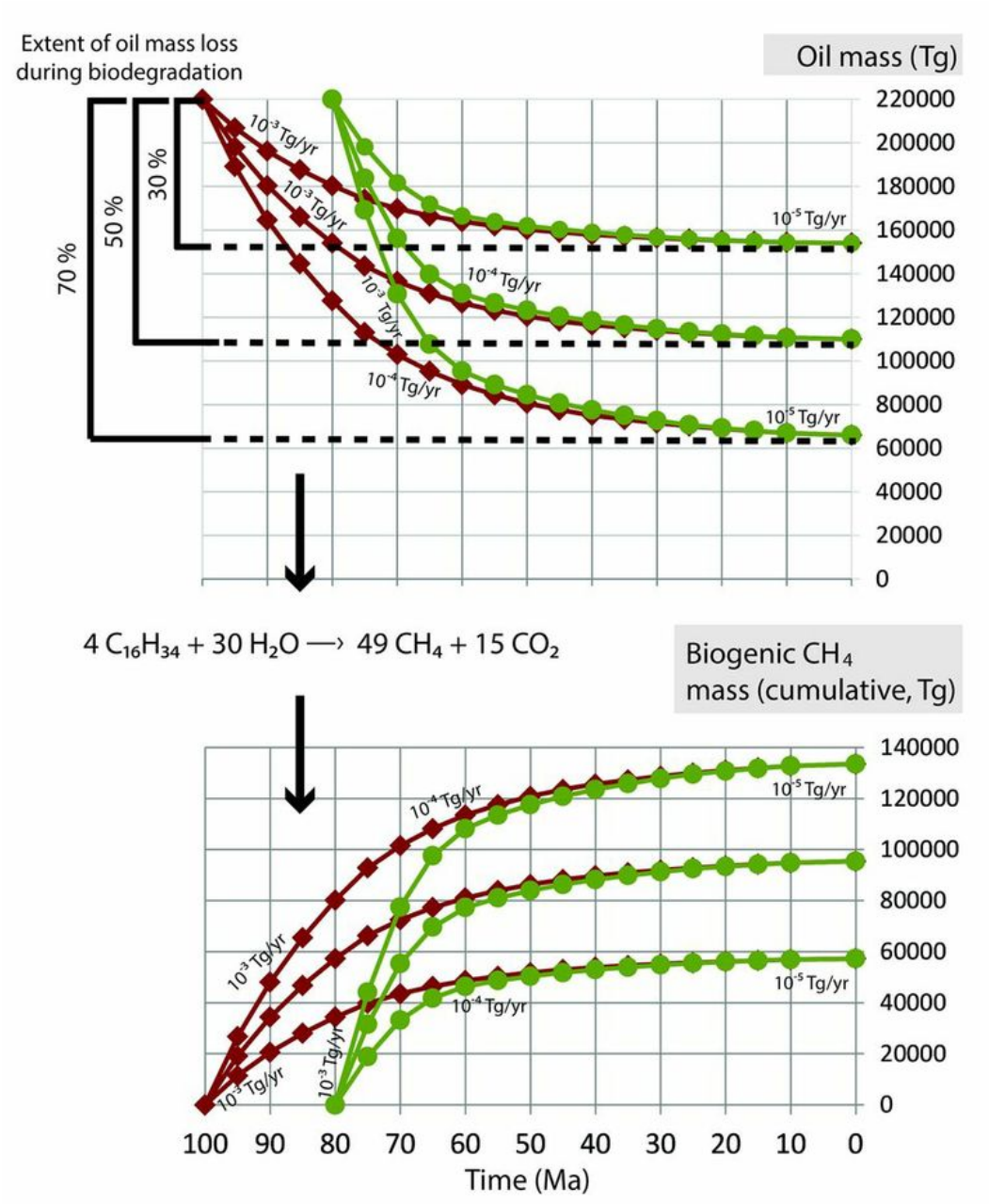

Figure 4.3 Scenarios proposed for the biodegradation of Athabasca oils. Most of the biodegradation took place during burial and shortly after uplift. Diamonds indicate the most likely charging time proposed by biodegradation modeling and geochemical techniques (Adams et al., 2012; Selby et al., 2011). Charging time proposed by PS modeling (Berbesi et al., 2012; Higley et al., 2009) is indicated by circles. The stoichiometric model applied is discussed by Jones et al. (2008) and Zengler et al. (1999).

The potentially degradable oil mass of 220 000 Tg leads to rates of biogenic methane generation no higher than $9x10^{-3}$ Tg yr^{-1}. These rates are sensitive to considerations of initial oil masses, but their order of magnitude, which is the main information of interest for this study, does not range considerably. For example, the National Energy Board Canada (2010) states the present in-place reserves in Athabasca to be around 180 000 Tg. If this represents the remaining mass after a 30% of the original charge has been degraded (Adams et al., 2012), then the original charge should have been around 250 000 Tg, which is very close to the petroleum system modelling results and calculated biodegradation rates here presented.

However, if oil charging was 2 to 3 times higher than predicted by the 3-D model (Brooks et al., 1988; Larter et al., 2006), the maximum estimated rate of biogenic methane generation would be $2x10^{-2}$ Tg yr^{-1}. This indicates that the rates offered in this contribution are susceptible to vary only by one order of magnitude. The fact that the reservoirs are full, largely without gas caps, but that biodegradation produces large methane and CO_2 volumes at reservoir conditions, might be explained by continuous leakage of gas during charging and degradation (Steve Larter, personal communication).

4.6.2 Central Graben

Thermal gas generation

Thermogenic methane generation was addressed through a 3-D petroleum system model (Figure 4.4) previously described by di Primio and Neumann (2008) and Neumann (2007) covering a portion of the Central Graben, and further extrapolation of the results to other areas of the basin.

The model covers both UK and Norwegian portions of Quadrant 30 of the UK and Blocks 1 and 2 in Norway. The exact location is, however, confidential due to proprietary reasons.

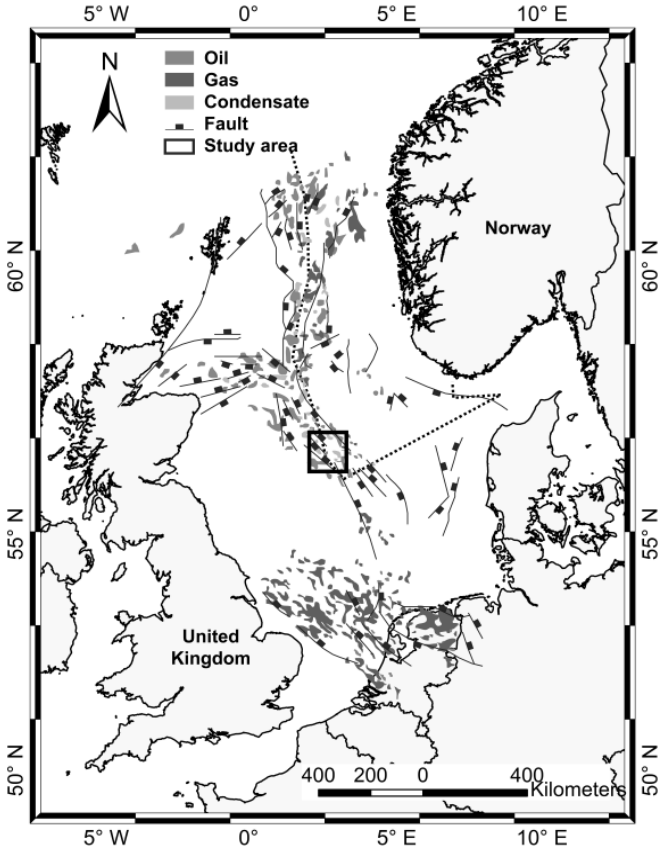

Figure 4.4 Location map of the North Sea Graben Province. The total area where gas and oil accumulations are present is of more than 150000 Km2. The Central Graben portion occupies around 15000 Km^2 (Cornford, 1994). The 3D model applied in this study corresponds to an area of around 555 Km^2 located in the Norwegian side of the zoomed square (Modified from di Primio and Neumann, 2008, and Neumann 2007).

The 3D model consists of 14 surfaces that correspond to strata deposited from Eocene to Permian time, and is calibrated to well temperatures and vitrinite reflectance data. The properties of the source rock intervals are shown in Table 4.2.

Table 4.2 Source rock properties applied in the 3D petroleum system model of the Central Graben (di Primio and Neumann, 2007 and Neumann 2007). KFC stands for Kimmeridge Clay Formation.

Source rock layer	**Kerogen Type**	**TOC** (wt. %)	**HI** (mgHC/gTOC)	**Average Thickness** (m)	**Kinetic model**
KFC/Mandal	II	6	450	160	Vandenbroucke et al. (1999)
Heather/Farsund	II/III	5	400	500	
Pentland/Bryne	III	3	200	380	

As compared to the WCSB model, the Central Graben model covers an area in which only thermogenic gas was generated, neither biodegraded oilfields occur here, nor is any biogenic gas accumulation present.

The onset of petroleum generation occurs around 50 Ma for the Middle Jurassic sources and around 30-20 Ma for the Upper Jurassic sources (Figure 4.5). Both the time of the petroleum generation onset and the present-day maturity level vary locally due to differences in burial histories. Petroleum expulsion from the source rocks does not occur until the early Tertiary. At present-day, all modelled generating intervals are in the main oil- to wet gas generation window. The depth of the strata is higher to the south, where some intervals are predicted to be generating dry gas. Summing all the source intervals, gas is generated at rates with an order of magnitude of 10^{-4} to 10^{-3} Tg yr^{-1} (10^{-8} Tg Km^2 yr^{-1}) during the phase of maximum generation (~25 Ma-present). The total gas mass generated in the modelled portion of the Central Graben ranges from 870 to 1300 Tg, depending on source rock definition. If source rock properties and maturity levels in this area are taken as representative of the entire Central Graben area described by Cornford (1994), then a range of 20 000-30 000 Tg of gas are estimated to have been generated during the geologic evolution of the Central Graben.

Similarly to the WCSB, the applied kinetic models assume that most of the gas phase corresponds to dry gas, which can therefore be considered to consist dominantly of methane. Modelled generation rates are considered as average or high as compared to those expected in other portions of the Central Graben because: (1) The source rock thickness in the modelled area falls in the upper part of the thickness interval reported for the Kimmeridgian Shales and its equivalent units. (2) Applied TOC and HI are in the average range proposed in previous publications (3) The heat flow values of 62 to 72 mW/m^2 (Neumann, 2007) are in the medium to upper limit of the ranges proposed in the literature for the entire Graben (Burley, 1993; Cornford, 1994; Jensen and Doré, 1993; Swarbrick et al., 2000).

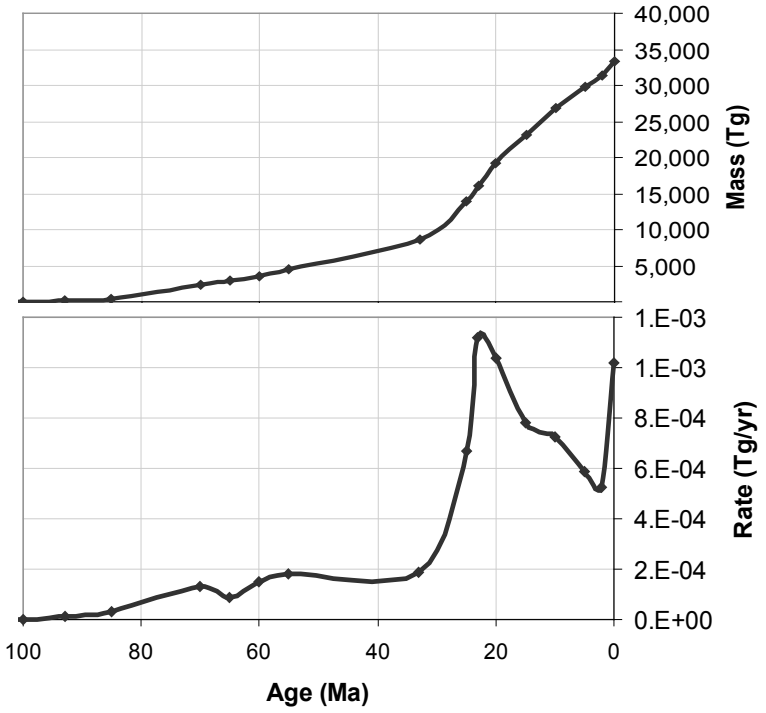

Figure 4.5 Thermogenic gas generation in the Central Graben, extrapolating results derived from the 3D model. The upper chart illustrates cumulative gas generation summing all generative intervals. The lower chart shows the rate of gas generation per year.

Leakage of thermogenic gas

Petroleum system modelling is restricted for addressing gas leakage in the Central Graben because of the difficulty of simulating pressure-induced fractures and migration along graben margin faults (Cornford, 1994). Therefore, a simplified, yet representative, more general approach was used to address the mass of methane that would have been available for leakage (Figure 4.6). Three differently obtained masses of generated oil and gas in the entire Central Graben area (Figure 4.6) were used as starting points from which the methane available for leakage was constrained, using the average mass distributions in petroleum systems indicated by Hunt (1996). According to this approach, the maximum gas available for leakage during the geological evolution of the Central Graben area should be in the order of 10^4 Tg. Hence, uniform and continuous leakage during the phase of petroleum generation (which lasted at least 30 million years) would have resulted in thermogenic methane emissions in the order of 10^{-4}-10^{-3} Tg yr^{-1}.

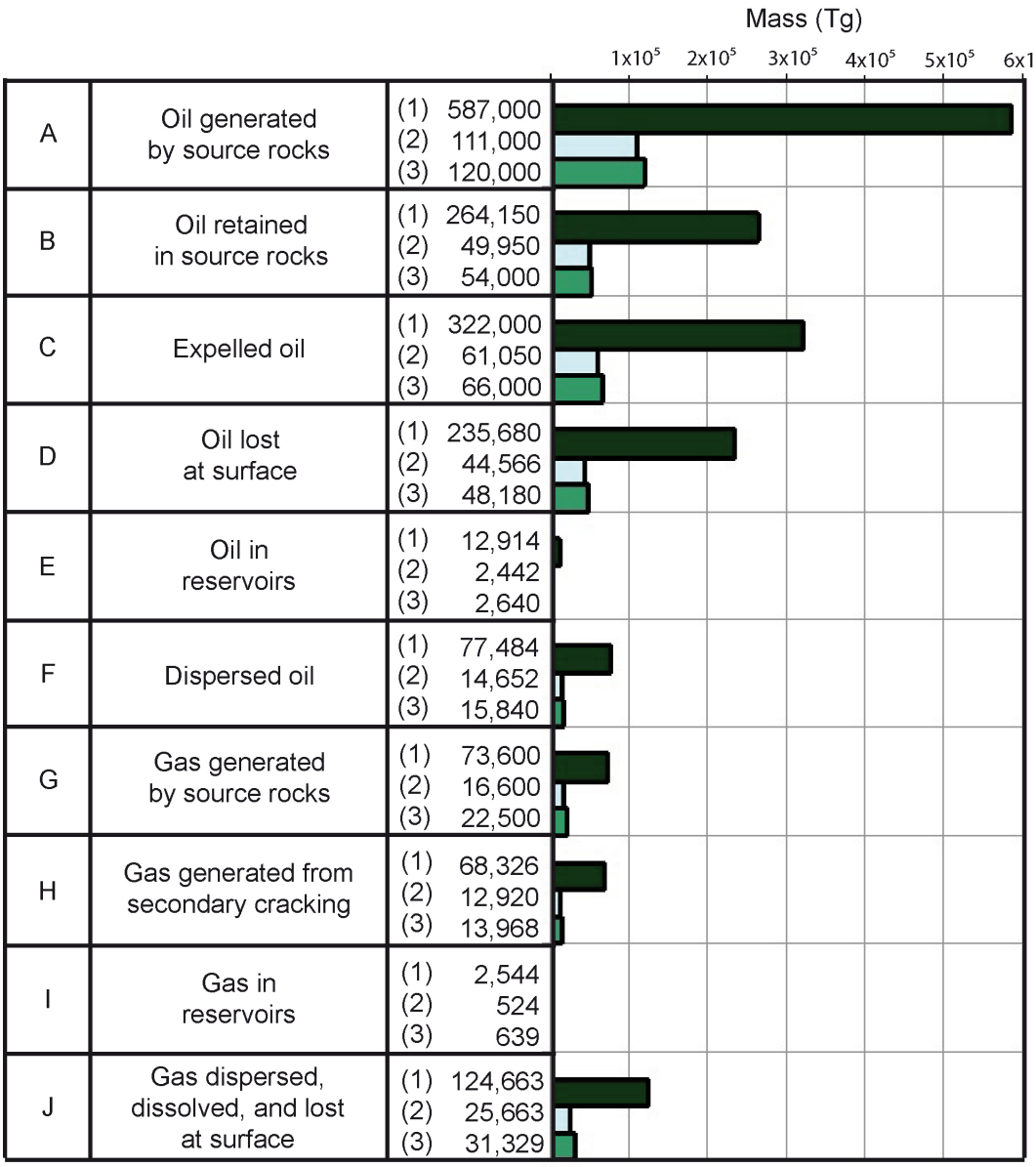

Figure 4.6 Mass balance of the petroleum system in the Central Graben of the North Sea (same area studied by Cornford, 1994). All the values are shown in Teragrams (10^{12} g). Differently-calculated masses in A and G were used as starting points for the estimation of the values in the other boxes. These estimates are susceptible to variation depending on the efficiency of the of oil and gas transfer from one petroleum system element to another; however, the order of magnitude of the masses is not expected to vary considerably. (1) Based on masses from Cornford (1994) using the methodology of Schmoker (1994). (2) Calculated using the method of Schmoker (1994), based on input data for the 3D modeled area (Figure 4.1 and Table 4.2) and then extrapolating results to the Central Graben. (3) Extrapolating results from 3D petroleum system modelling to a Central Graben scale. The proportions among the masses in the boxes are similar to those by Hunt (1995). B = A-C; C= A x 0.55; D = C x 0.73; E= C x 0.04; F= C x 0.24; H = ((B+F) x 0.5) x 0.4; I = (Gx0.8 + H) x 0.02; J = (Gx0.8 + H) x 0.98. The value J1 is considered unrealistic. The estimated in-place oil mass (Box E) coincides with the 3384 Tg reported for the area (Cornfod, 1994).

If the seepage is considered uniformly distributed across the 15 000 Km^2 of the study area, the resulting flux per area would be in the order of 10^{-8}-10^{-7} Tg Km^{-2} yr^{-1}. The later value falls within the minimum range of the present-day seepage proposed by previous indirect appraisals at the UK Continental Shelf (Judd et al., 1997). However, uniformly distributed gas seepage across the entire area is not likely, as it is known that marine seepage in the Central Graben is a localized process controlled by fracture systems (Cornford, 1994). If the potential total seepage is focused in 10% of the study area, maximum fluxes in the order of 10^{-7}-10^{-6} Tg $Km^{-2}yr^{-1}$ are obtained. The latter fluxes are similar to the range proposed by Judd et al. (1997).

4.7 Discussion

4.7.1 Thermal gas generation, oil biodegradation and possible influence on climate evolution

Based on the methane flux estimations offered so far, it is possible to formulate answers to the main scientific questions presented in the introduction to this study. The first aspect to discuss is the relevance of the size and sedimentary organic C inventory of a petroleum basin in terms of its potential for climate feedback.

This work lacks of a climate model that allows the effects of estimated fluxes to be evaluated regarding climate evolution. However, this can be assessed by examining the increase of the atmospheric methane mass during known hyperthermal events in Earth's climate history. The present-day warming trend and the Paleocene-Eocene Thermal Maximum (PETM) represent very good comparison points. The present-day warming trend has been attributed to an annual increase in the atmospheric methane concentration, together with CO_2 increase, that ranged from 40 to 46 Tg/yr in the 1980s (Cicerone and Oremland, 1988), although it has decreased during the 1900s (Bousquet et al., 2006) and 2000s (Denman et al., 2007).

The PETM, in turn, represents a period around 55 Ma when the temperatures at high-latitude locations and in the deep oceans increased more than 4 °C over less than 10^4

yr (Kennett and Stott, 1991; Zachos et al., 1993). Climate models within the framework of the present-day carbon cycle indicate that a sustained methane release of 112 Tg/yr over that entire period of 10^4 yr could drive this climatic event (Dickens et al., 1997). Based on these two cases it can be stated that methane emissions in the range of tens to hundreds of Tg/yr are required to have an effect on Earth's climate.

As indicated in the results section, the mass of thermogenic gas generated in the giant Western Canada Sedimentary Basin amounts to rates in the order of 10^{-2} Tg/yr, summing up all modelled sources. This is three orders of magnitude lower than the current annual increase in CH_4 concentration reported during the 80s (46 Tg/yr) and four orders of magnitude lower than the annual CH_4 release needed to explain the PETM (i.e., 10^2 Tg/yr over 10^4 yr). In the case of the Central Graben, the rate of thermogenic gas generation is around ten times smaller than in the WCSB. Before considering the detail on migration and leakage, the implications of these results can be discussed in terms of the single annual availability of the leaking gas, without considering accumulation mechanisms. For global petroleum kitchen areas to be able to annually feed CH_4 masses similar to those promoting alterations in the carbon cycle during the 1980s or those driving the PETM, three conditions should be met: (1) A mass of organic carbon in sedimentary basins of the Earth at least 1800 times larger than the one considered in the WCSB model, or 13 000 times larger than the one considered in the Central Graben, (2) all the sedimentary organic matter considered in the previous calculations generate gas at the same time, and (3) 100% of the gas generated reaches the atmosphere. None of these conditions is likely to occur. The thermal generation of only 5 Tg/yr of methane requires, as estimated in this work, 250 equivalents of the WCSB. Moreover, less than 20% of this generated mass would survive methanotrophic consumption in soils or methane oxidation through water columns, according to Etiope and Klusman (2002). With this in mind, it is suggested that the thermal maturation of organic matter as a single mechanism has a very limited influence on Earth's climate evolution. Hence, a large basin, or more precisely, large organic carbon inventory of a basin does not necessarily make it a good possible culprit for causing climate change.

The same applies in the case of biodegradation. Mass balance calculations as presented in this and previous works (Adams, 2008; Larter et al., 2008) indicate that continuous leakage of the biogenic gas generated during the formation of the largest known oil sand deposit would have resulted in leakage rates which are of 5 orders of magnitude lower that those expected to exert significant climate feedback. The significance of biogenic methane generation on a global scale is beyond the scope of this work.

4.7.2 Methane leakage from reservoirs

As mentioned before, the transformation of organic matter in petroleum systems leads not only to hydrocarbon generation, but also to the formation of petroleum deposits. These deposits contain enormous masses of hydrocarbon that, if released to the atmosphere in a relatively short time span, might have an impact on climate.

For example, a system like the WCSB (or equivalent sum of smaller sedimentary basins simultaneously generating petroleum) would generate around 300 000 Tg of thermogenic methane in 10 Million years. If only one third of this mass is stored in reservoirs of any kind (e.g., conventional and unconventional reservoirs, gas hydrates, beneath permafrost) and later released to the atmosphere in a 10^3-10^4 years time span, the effect would be large enough to possibly promote hyperthermals such as the PETM. The same effect would be expected if the methane generated from biodegradation of a pre-existent accumulation or equivalent sum of accumulations of the size of Athabasca is released to the atmosphere in a 10^3-10^4 time span.

A clear picture of the need for a focusing mechanism can be gained by comparing the continuous and uniformly distributed leakage that the model of the giant WCSB predicts, against seepage measured in several smaller basins in Europe and the United States. Even if absence of methanothrophic degradation in soils is assumed, the WCSB model predicts leakage rates (in Tg/yr) that are ten to hundreds of times smaller than seepage documented in e.g. the Bulgarian Black Sea, the Black Sea

Continental Shelf, or Coal Oil Point California (Dimitrov, 2002; Hornafius et al., 1999; Judd, 2004). At these locations, the high methane fluxes have been attributed to leaking gas reservoirs (Clarke and Cleverly, 1991; Dimitrov, 2002; Hornafius et al., 1999) where faults provide not only a focused migration route, but also conduits where methane can migrate fast enough to survive microbial consumption during upward migration (Etiope and Klusman., 2002; Etiope and Martinelli; 2002; Brown, 2000). To illustrate the point even better, the modelled kitchen area in the model of the WCSB is more than 20 times larger than the Central Graben's. Likewise, the modelled thermogenic gas generation rates and the predicted total gas generation are 10^{-2} Tg/yr and 300 000 Tg, respectively. This is orders of magnitude higher than those in the Central Graben. Yet, leakage rates from the WCSB are predicted to never have been as high as present-day estimates from the Central Graben, because leakage in the latter case derives from faulted reservoirs.

4.8 Recommendations for future work

Based on the results derived from this contribution, there is no need to address all sedimentary basins in the world in order to study and quantify the role of sedimentary organic matter in climate evolution. Instead, efforts should concentrate on those sedimentary basins where two basic elements are present. These elements are hydrocarbon accumulation and fast release mechanism (temporarily and aerially focused flow).

Besides fractured conventional reservoirs, Arctic basins represent appropriate study areas because they contain the two basic conditions above mentioned. Here large amounts of methane can accumulate over time and be released again when hydrate stability conditions no longer occur. This process can take place on a scale of thousands of years (Archer et al., 2009; Krey et al., 2009; Macdonald, 1990). A similar effect can be exerted by ice caps during glacial maxima. In this case, the ice cap represents a seal for upward migration of hydrocarbons until the end of the

glaciation when the ice cap disappears, allowing the gas accumulated below to reach the atmosphere.

Because only the reservoir (accumulations) part of the petroleum system will be able to interact with the atmosphere at significant speed, care should be taken when extrapolating measured seepage. Aerial extrapolations should consider the area above accumulations (Etiope and Klusman, 2010) and fractures controlling leakage, and not the entire extension of the sedimentary basin, nor the area of mature source rock. Likewise, the total leakage resulting from this extrapolation should be weighed against the gas mass accumulated in the sub-surface reservoir. Moreover, the timing of reservoir formation and filling must be understood before paleo-seepage can be inferred. At this point, it is clear that the accurate extrapolation of measured surface seepage, particularly over geological time-scales, requires the application of petroleum system modelling and analysis. Once the area above leaking reservoirs has been assessed and leakage has been measured, large scale extrapolations can be performed following the “emission factor" approach, widely used in literature addressing global emissions of greenhouse gas from natural sources (e.g., Etiope et al. 2007).

4.9 Conclusions

The mass of thermogenic and biogenic methane generated during the geological evolution of the WCSB is comparable to the total amount of world's known and risked undiscovered gas resources. However, 3-D petroleum system modelling and mass balance considerations indicate that the rate of methane generation was lower than the annual atmospheric carbon input required to induce major hyperthermal events. Moreover, the estimated gas leakage rates turned out to be lower than those reported for smaller basins at present day.

Global scale extrapolation of the estimated rates of thermogenic gas generation for the WCSB and the Central Graben indicates that, regardless of the size of the kitchen area, thermal generation of methane, as a single process, would not be able to drive

climate changes at geologic time scales. A mechanism promoting focused flow and sudden gas release from the reservoirs is required as condition for petroleum systems to exert a significant effect on Earth's climate. Therefore, further studies should concentrate on specific areas where a suitable combination of large accumulations and focused release mechanism is present, rather than on the single organic carbon abundance of hydrocarbon-bearing basins. Moreover, because the mass available for leakage is limited and to some extent defined by the generated masses, the combination of direct surface measurements with subsurface petroleum system analysis is crucial for the understanding of geologic emissions of methane, both at present-day and during the Earth's geologic history.

4.10 Supplementary materials

A. Main aspects behind petroleum migration modeling in this study

There are several fluid-flow approaches to model the secondary migration of petroleum. The most comprehensive formulation of fluid flow in porous media is given by Darcy flow, which is based on a balance of all the forces acting on the fluid. These include capillary pressures rising due to interfacial tensions in rock pores and throats, friction which is described by petroleum viscosity and rock permeability, buoyancy of the petroleum in water, and additional external forces such as aquifer flow (Hantschel and Kauerauf, 2009). In models constituting this work, Darcy flow describes multicomponent three-phase flow based the relative-permeability and capillary-pressure concept (Al-Hajeri et al., 2009). The main advantage of this migration method is that it takes into account most of the physical relationships within the petroleum system; however, it requires enormous computer processing times (Hantschel et al., 2000). Alternatively, the flowpath migration method assumes that migration mainly occurs in a carrier layer which is located beneath a seal, and is controlled by buoyancy. In this way, the buoyant flow displaces laterally along the seal until reaching a trap, where it accumulates (Hantschel et al., 2000). Another method, which is the hybrid Darcy/flowpath, enables fast calculations of flow processes in efficient carriers to be performed without losing any of the dynamic framework provided by the full physics calculations (Welte et al., 2000). This method alternates between Darcy and flowpath modeling depending on the permeability of the layer though which the fluid migrates. In this way, it applies Darcy flow for migration trough low permeability lithologies such as shales and siltstones, and flowpath for migration though more permeable carrier lithologies

(Hantschel et al., 2000; Welte et al., 2000). In this work, the hybrid Darcy/flowpath method was applied. Focus was first put on reproducing the known fields and discoveries in the study areas. Afterwards, the rest of the output data were analyzed, including gas leakage at the sediment surface. Output from the models includes the most relevant elements of a petroleum system mass balance. Here, a summary of the petroleum system mass balance considerations from Hantschel and Kauerauf (2009) is presented. In basin modeling, expulsion masses (M_E) of a source are defined by the generated mass (M_G), the amount of secondary cracking product coke (M_C) and hydrocarbons that left the source rock (M_{HC})

$$M_E = M_G - M_C - M_{HC} = \Delta M_{FLOW} \qquad \text{Eq A.1}$$

Hydrocarbon losses of the petroleum system ($M_{LOSS,\ PS}$) are defined by the expelled masses from all sources ($\Sigma ME,s$) minus the amount found in the reservoirs ($\Sigma MHC,r$)

$$M_{LOSS,\ PS} = \Sigma ME,s - \Sigma MHC,r \qquad \text{Eq A.2}$$

At the same time, hydrocarbon losses are constituted by three main groups which are:

$$M_{LOSS,\ PS} = \Sigma_{MO} + \Sigma_{MC} + \Sigma M_{HC} \qquad \text{Eq A.3}$$

Σ_{MO} represents the total flow out of the basins including all the layers in the model. Σ_{MC} corresponds to the amount of losses by cracking, and ΣM_{HC} describes the amount of petroleum which is neither located within the source rock nor accumulated in a reservoir.

For each time-step in the simulation, the models sub-divide $\Sigma_{MO,}$ in two portions which are “outflow top” and “outflow side” (Schlumberger, 2010). The first term refers to the amount of petroleum (oil and gas) leaving the uppermost layer of the model (sediment surface). The second term expresses the petroleum mass escaping from the lateral boundaries of the model. The model’s output include the outflow masses for each petroleum component corresponding to the kinetic model applied. In this way, two-component kinetics can provide the separate oil and gas outflows, whereas multi-component kinetic models can provide information regarding each of the modeled compound types (e.g., C+10 hydrocarbons, methane, ethane, etc).

B. 3D Model definition and variability of results

Table B.1 WCSB model boundary conditions.

Heat Flow			
Map/single value	**Time (Ma)**	**Value (mW/m^2)**	**Source (s)**
Map	380 - 119	48-65	Bachu and Burwash (1994); Blackwell and Richards (2004); Allen and Allen (1990); Deming (1994)
Map	119-0	48-77	
Erosion			
Map/ value	**Time (Ma)**	**Value (m)**	**Source (s)**
Map	150-119	<100	Magara (1976); Hacquebard (1977); Nurkowski (1984); Kumar and Magara (1979)
Map	58-0	500-2500	
Sediment-water interface temperature			
Map/value	**Time (Ma)**	**Value (°C)**	**Source (s)**
Value	380-10	24-10	Wygrala (1986)
Value	10-0	10-05	
Paleo-water depth			
Map/value	**Time (Ma)**	**Value (°C)**	**Source (s)**
Map	380-58	100-300	Fowler et al. (2004); Stasiuk and Fowler (2004); Edwards et al. (1994); Ross and Bustin (2006)
Map	58-0	100-0	

Table B.2 Variability of input parameters and predicted range of surface gas leakage from the WCSB

Variable	**Applied range**			**Gas generation (Tg)[b]**	**Surface gas leakage (Tg)[c]**
Exshaw Fm. thickness[a]	(4.2-2.5) m			200 000-300 000	60 000-225 000
Exshaw Fm. source rock[a] quality	TOC = (9.6-15) wt. % HI = (500-600) mgHC/gTOC				
Mannville Group coal area	60 000-120 000 Km^2				
Seal (Joli Fou Fm.) efficiency	Lithology	Porosity (%)	Permeability [log(mD)]		
	Shale (typical)	1	-8.52		
		25	-3.00		
		70	-1.00		
	Shale (organic lean, silty)	1	-8.47		
		25	-2.50		
		67	0.50		

In Table B.2:

a Applied ad discussed in Berbesi et al. (2012).

b During the time of maximum generation (80-60 Ma), as indicated in main text.

c For a 1 million year time-step in the model, predicted values range from 3000-11 200 Tg. Uniform leakage during this time would mean rates of $3x10^{-3}$ to $1x10^{-2}$ Tg/yr ($3000/1x10^{6}=3x10^{-3}$; $11\ 200/1x10^{6}=1x10^{-2}$). In the main text, focus is put on the order of magnitude of the estimates, rather than on their absolute value. However, variability is considered to be of one order of magnitude.

Table B.3 Central Graben model boundary conditions

Heat Flow			
Map/single value	**Time (Ma)**	**Value (mW/m^2)**	**Source (s)**
Value	290-245	62	Neumann (2007); di Primio and Neumann (2008)
Value	245-210	62-70	
Value	210-155	62	
Value	155-50	62-90	
Value	50-00	62	
Erosion			
Map/ value	**Time (Ma)**	**Value (m)**	**Source (s)**
No erosion			
Sediment-water interface temperature			
Map/ value	**Time (Ma)**	**Value (°C)**	**Source (s)**
Value	290-170	16-12	Neumann (2007); di Primio and Neumann (2008)
Value	170-100	12-10	
Value	100-50	10-16	
Value	50-0	16-08	
Paleo-water depth			
Map/ value	**Time (Ma)**	**Value (°C)**	**Source (s)**
Value	290-150	0-10	Neumann (2007); di Primio and Neumann (2008)
Value	150-90	10-200	
Value	90-70	200-0	
Value	70-5	0-10	
Value	5-0	0-60	

C. Input for timing of Athabasca biodegradation and extent of oil mass loss during this process

The time when the Athabasca oil sands were charged with originally lighter oil remains controversial. Based on PSM, Higley et al. (2009) suggest that oil accumulations in the Lower Cretaceous Mannville Group should have been filled at about 75 Ma, although no details are given when it comes to the filling of individual accumulations. The 3D PS model by Berbesi et al. (2012) proposes that around 220 000 Tg of oil gradually reached the Athabasca from 70 to 50 Ma, and that more than 75 % of this mass entered the accumulation before the onset of the Laramide orogeny. On the other hand, biodegradation modeling by Adams et al. (2012) managed to reproduce the present-day API gravity in Athabasca when the reservoir is gradually charged from 100 Ma until the time of maximum burial (60 Ma in this case). Some other attempts to constrain the timing of oil generation in the basin as well as charging of Athabasca oils include Creaney et al. (1994), Creaney and Allan (1990), and Selby et al. (2011). An up- to- date discussion of the topic can be found in Adams et al. (2012) and Berbesi et al. (2012). In general, the literature proposes onset times for the Athabasca oil charging ranging from ca 110 to 70 Ma, and seems to agree on the conclusion that most of the original oil accumulated before the Eocene.

In the case of Athabasca, the Peters and Moldowan (PM) biodegradation level of the oils reaches up to 8, which would suggest that more than 50 % of the initially accumulated oil was lost due to microbial degradation (Head et al., 2003; Larter et al., 2006; Larter et al., 2005). Even a larger extent of mass consumption (40 to 70%) was proposed by Brooks et al. (1988), which would imply that the original oil in place (OOIP) would have been more than the double of the present in-place resources. However, recent biodegradation modelling (Adams et al., 2012) in the Peace River oil sands suggest that, indeed, only about 30 % of mass reduction is

needed to reproduce the SARA composition. The previous work also shows the importance of appropriate considerations regarding the nature of the precursor oil and variations of the relative biodegradation rate of the SARA fractions as long as the PM biodegradation level increases, in order to predict and understand present-day oil compositions. The original low API gravity (and high content of polar compounds) of the oils charging Athabasca (Adams, 2008) may be the key to explain why these oils did not reach a higher PM level despite their long residence times and temperature history (Larter et al., 2006).

Chapter 5

Synthesis and integration

5.1 Western Canada Sedimentary Basin

5.1.1 Petroleum generation and migration

According to the 3-D model, significant kerogen transformation ratios (≥ 50%) are reached around 80 Ma. The sequence of generation from different source rocks corresponds to the sequence of deposition; except from the Fernie Group source rocks (Gordondale Member and Poker Chip A shale), which generate earlier than expected due to "fast" kinetic parameters corresponding to labile Type II-S kerogen. The rate of petroleum generation is predicted to start decreasing the by onset of the Laramide orogenic phase (58 Ma), and ultimately to stop around 50 Ma. Modelled present-day maturities fall in the range of oil-to dry gas generation for Cretaceous to Jurassic source rocks and oil window to over-mature for Mississippian and Devonian.

As explained in Chapter 2, the initially applied source rock definition resulted in predicted oil generation from the Gordondale Member of almost 400 BCM (2515 BB), which is around four times more oil than the amount generated by any other source rock. In a revised version of the model in which the thickness of the Exshaw Formation was increased attending to suggestions in the literature, for example Savoy et al. (1999) and Smith and Bustin (2000), the Exshaw source rock generates 700 BCM of oil. In total, all sources generate 600 000-750 000 Tg of oil and 200 000-300 000 Tg of gas over 80 million of years, with maximum generation rates between 80-60 Ma (Figure 5.1). In the gas case, these numbers translate in 10^{-8} Tg/yr

per area of kitchen (Tg yr^{-1} Km^{-2}) during the phase of maximum generation, which means 10^{-2} Tg per year for the entire kitchen area. The main parameter influencing the predicted generated gas mass is the areal extent of generative coal (Steiner et al., 1972). Based on the applied kinetic model, up to 80% of this mass is assumed to be dry gas, which is dominantly composed of methane.

The initial model definition did not allow reproducing the expected petroleum volumes in Cretaceous reservoirs. A considerable portion of the oil did not accumulate in Athabasca but instead continued migrating towards Saskatchewan and towards the north of Athabasca. When stratigraphic barriers were implemented into the model, the trapping efficiency increased by 1200% with respect to previous simulations, supporting the stratigraphic control to the northeast of Athabasca proposed by Ranger (2006). Conversely, different scenarios described in paper 1 do not support the role of heavy biodegraded oil on improving the trapping potential at Athabasca, as proposed by Highley et al. (2009). The main limitation of the latter hypothesis lies on the timing of events. The WCSB model predicts that by the time the heavy oil barrier is formed, a considerable portion of the oil had already migrated towards the east and north of Athabasca. Once the trapping efficiency of the model was improved, the initial source rock definition resulted in around 230 billion cubic meters (~200 000 Tg) of oil reaching the Mannville Group strata. From this mass, more than 54% was generated by the Gordondale source rock, and less than 15% was generated by the Exshaw Formation.

The Exshaw Formation is the main contributing source rock in the model only when average thickness of 25 m (in kitchen areas), and TOC values of 9% are assigned to it. The thickening of the Exshaw Formation to the west of Alberta is supported by the literature (Savoy et al., 1999; Smith and Bustin, 2000). However, no data is available to support the modeling assumption that the TOC content remains constant through all the generative section. Therefore, the Gordondale Member of the Fernie Group is suggested as the main source of the petroleum filling the oil sands in the WCSB.

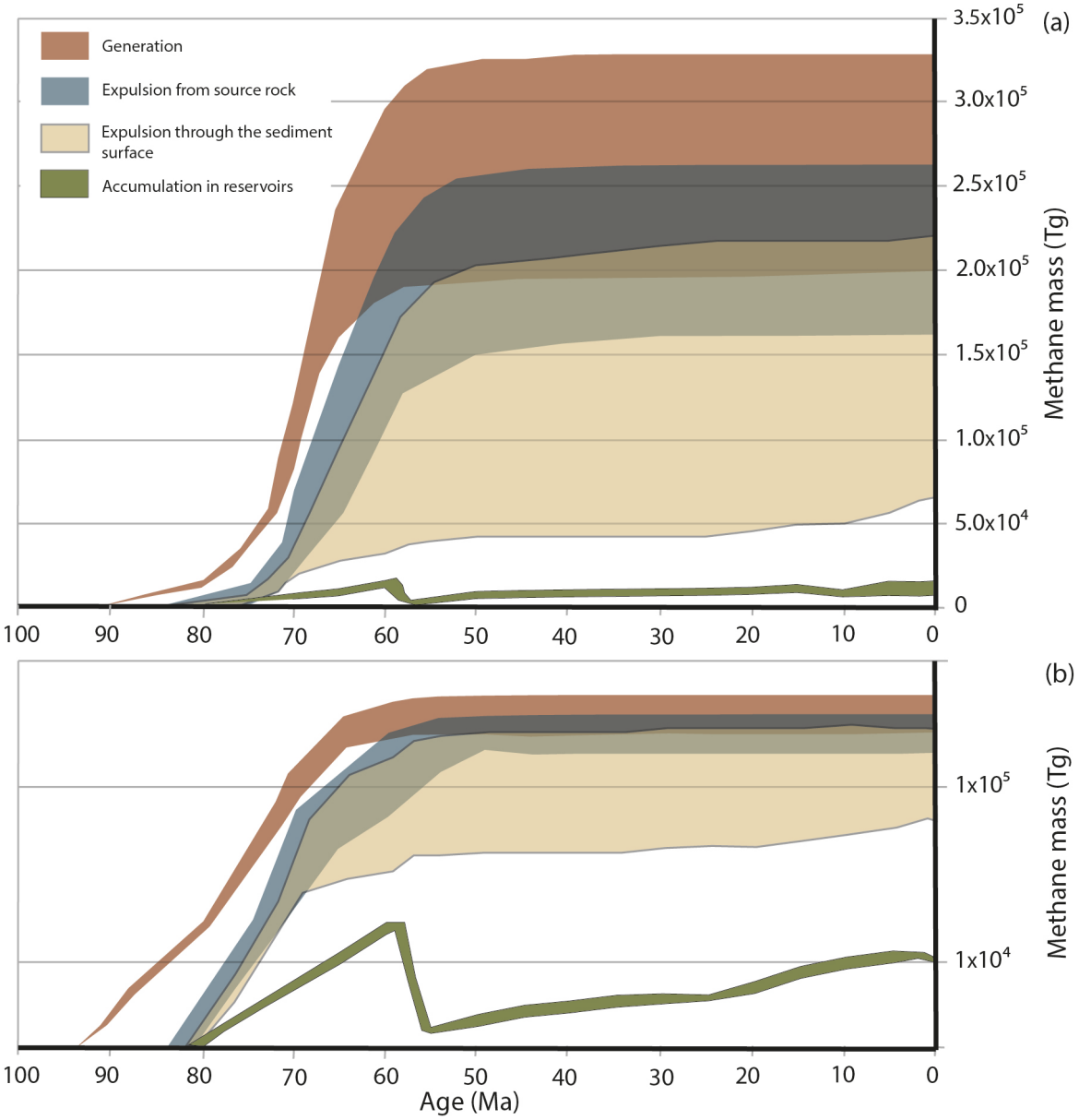

Figure 5.1 General mass balance of the Devonian-Lower Cretaceous WCSB petroleum system. The variability of the results derives from the scenarios presented in table B.2 of chapter 4 (Berbesi et al., 2014).

5.1.2 Oil biodegradation and biogenic methane generation

The ideas presented in this section are derived from chapter 4, which offers a wide discussion on biodegradation affecting oil sand accumulations in Alberta (in particular Athabasca), biodegradation rates, and methane masses generated during this process. 1D extractions at Peace River, Athabasca and Cold Lake show that the temperatures at the Lower Cretaceous Mannville Group reservoirs never exceeded

70°C, which means they were not subjected to burial sterilization, and therefore suffered different levels of biodegradation (Adams et al., 2004, 2006; Wilhelms et al., 2001).

Some previous publications have attributed the PM level of up to 8 found in Athabasca to an oil mass loss of more than 50 % (Head et al., 2003; Larter et al., 2006; Larter et al., 2005), even reaching 70% (Brooks et al., 1988). If these considerations are correct, then the original oil in place (OOIP) should have been more than the double of the present in-place resources. However, recent biodegradation modeling (Adams et al., 2012) in the Peace River oil sands suggest that, indeed, only about 30 % of mass reduction is needed to reproduce the present-day oil SARA composition. If the 220 000 Tg of oil predicted by 3D modeling to have reached the Athabasca accumulation (Berbesi et al., 2012) are considered as the total degradable oil mass, an oil mass loss of 30% to 70 % would have resulted in $6x10^4$ to $1.3x10^5$ Tg of biogenic methane.

This first approximation gives a general idea about the scale of the microbial methane generation in the study area, but it does not provide information regarding the masses involved in each stage of the process. A more detailed analysis required the application of the methodology explained in section 4.6.1 of this manuscript.

Basin modelling performed in Chapter 2 (Berbesi et al., 2012) suggests that 220 000 Tg of oil could have reached the Athabasca trap. This mass was considered as the initial, potentially degradable oil mass. Most of the biodegradation was assumed to take place during burial and shortly after the onset of uplift (Figure 5.2), corresponding to the main charging phase (Higley et al., 2009; Berbesi et al., 2012; Adams et al., 2012). In this way, the obtained methane generation rates had maximum magnitude of 10^{-3} $Tgyr^{-1}$. In order to test the variability of this result, scenarios with a 2 to 3 times higher initial (degradable) oil mass were considered (Brooks et al., 1988; Larter et al., 2006). Maximum biogenic generation rates were in the range of 10^{-2} $Tgyr^{-1}$, showing that the range of variability of the estimate is of 1 order of magnitude.

The fact that the reservoirs are full, largely without gas caps, and that biodegradation produces large methane and CO_2 volumes at reservoir conditions, suggests that the generated gas should have leaked (Steve Larter, personal communication, 2013).

5.1.3 Thermogenic and biogenic methane seepage

In the quantification of generated gas masses both oil-associated as well as free thermogenic gas (gas and gas-condensate) were considered. Petroleum phase behavior was taken into account using the Peng-Robinson equation of state as implemented in the modeling software.

The Laramide orogeny, leading to uplift and cooling of the basin, did not exert a major control on the thermogenic emissions in our model due to the slow temporal nature of the event. In the absence of methane consumption in soils, the potential gas emissions from the sediment surface are estimated to be in the order of 10^{-2}-10^{-3} Tg/yr during the period of maximum leakage (from 80 Ma to 60 Ma), depending on the assigned permeability of the seal layer and the aerial extent of gas-generative coal (Figure 5.1). The rest of the generated hydrocarbons remain underground, both within migration routes and trapped in reservoirs. Variations in the source rock properties of Devonian to Upper Jurassic units, as those implemented in Chapter 2 (Berbesi et al., 2012), had only a minor effect on the predicted amount of gas leakage. In the case of biogenic methane, continuous release would have resulted in leakage of maximum $9x10^{-3}$ Tg yr^{-1}, which is of a similar magnitude to the thermogenic emissions.

5.2 5.2 Mackenzie Basin

5.2.1 Petroleum generation and migration

Combining the results from this work with those from Kroeger et al. (2008) the onset of gas generation is placed between 60-50 Ma, with the Smoking Hills sequence being the only source interval generating during this time. The Aklak Formation

generates between 40 and 30 Ma and the Taglu Formation between 20-10 Ma. The total amount of petroleum and gas generation predicted by the model varied depending on the source rock quality (TOC and HI) and aerial extent considered in different scenarios as described in Table 3.2 of Chapter 3. Total gas generation ranged from 10^4 to 10^5 Tg (Figure 5.2) summing all source intervals. The maximum modeled gas generation rates ranged from 10^{-4} to 10^{-3} Tg/yr from Eocene to Miocene, and from 10^{-5} to 10^{-3} Tg/yr from Pliocene to present-day.

Although different filling histories are observed for individual accumulations, they can be grouped according to the stratigraphic interval they belong to. Reservoir intervals within the Aklak sequence start filling during the Eocene and continue receiving both oil and gas until the end of the Miocene. Reservoirs within the Taglu and Kugmallit sequences start filling during the Oligocene and, in the case of Kugmallit, some intervals continue being charged up to the present day. The 3D model predicts that a major charge pulse of the Richards Fm. took place during the Oligocene, followed by only minor filling. When the gas volume contained in all reservoirs is summed up, a total of 1.5-2.4 $x10^{12}$ m^3 is obtained. This coincides with the 1.63-2.07 $x10^{12}$ m^3 of marketable conventional natural gas proposed by Osadetz and Chen (2006). The accumulations in the BMB have been reported as becoming more oil-prone basinwards (Osadetz and Chen, 2006, 2010). That trend has been successfully reproduced in the model here described.

5.2.2 Estimation of gas hydrate reserves

The applied modeling software does not simulate gas hydrate formation or the sealing effect exerted by permafrost. Therefore, the gas hydrate resources in the BMB were estimated combining the modeled generated, migrated and leaked volumes with previous interpretations of the permafrost and gas hydrate formation process in the region.

Chen and Osadetz (2010) indicate a strong link between the gas hydrate stability zone in the BMB and the thickness of terrestrial permafrost. Among different

interpretations about the Cenozoic glacial history of the BMB presented in Chapter 3, those from Majorowicz et al. (2008) served as base for the following scenarios for gas hydrate methane resource assessment:

a) The modeled gas leakage from the sediment surface of the model (SS leakage) in retained below an ice bearing permafrost layer that has considerably developed around 10 Ma. All the gas trapped below permafrost is considered to be available for later gas hydrate formation.
b) Conditions for gas hydrate formation are met at 6 Ma. The modeled methane SS leakage from 6-0 Ma is considered in the resource assessment.
c) Similar to scenario b, but with gas hydrate formation conditions met at 0.9 Ma.

As explained in Chapter 3, only the gas volume predicted to leak from the model sediment surface is considered in the gas hydrate methane resource assessment because:

- The modeled SS component since the Eocene is 20 to 70 times larger than the volume accumulated in reservoirs.
- Most of the known gas hydrate occurrences in the BMB are considerably shallower than conventional hydrocarbon deposits (Majorowicz and Osadetz, 2001).

Although the SS leakage values derived from this analysis range from $3x10^{12}$-$1x10^{13}$ m^3, it is not realistic to assume that all these volumes will remain trapped within the gas hydrate stability zone. It has been suggested that the heat accompanying the migrating fluid can create a warm channel allowing gas to pass through the gas hydrate stability zone without being retained there (Taylor et al., 2000; Wood et al., 2002). Besides, gas hydrates do not occupy all the pore space within the gas hydrate zone, and typical gas hydrate saturations in the BMB are around 40% on average (Collet et al., 1999; Majorowicz and Osadetz, 2001). Considering the trapping improvement associated to the thick permafrost presence, Chapter 3 suggested a gas

hydrate stability zone trapping potential of 50-70%, resulting in a maximum of 1-7 $x10^{12}$ m^3 (700-5000 Tg) of methane available for gas hydrate formation. No lower limit was assigned to this estimate due to the uncertainties on the extent to which gas hydrates were affected during interglacial periods. However, Majorowicz et al. (2008) considered their entire disappearance unlikely due to the higher thermal inertia of terrestrial sub-ice bearing permafrost with respect to marine hydrates.

5.2.3 Methane seepage

The 3D model predicts leakage at the top of the sedimentary sequence ranging from $5x10^{13}$ to $1x10^{14}$ m^3 from Upper Cretaceous to Pliocene (Figure 5.2). This corresponds to around 60% of the total generated gas. Modeled gas leakage rates during this period of time range from 10^{-1} to 10^{6} m^3/yr (10^{-10}- 10^{-3} Tg/yr) which is comparable to reported present-day leakage at Toney River, Canada (Cranston, 1994) or Rías Baixas, Spain (Garcia-Gil, 2003). The modeled pre-glaciations leakage is mainly controlled by the generation in deep mature source rocks and later migration of the gas through carrier beds and high permeability zones such as faults and fractures (Berbesi et al., 2014).

Leakage during and between glaciations is more difficult to estimate because permafrost and gas hydrate evolution were not modeled. Majorowicz et al. (2008) consider the total disappearance of permafrost and gas hydrates in the BMB during previous and present interglacials unlikely. This would mean that most of the gas reaching the gas hydrate stability zone in the BMB has been accumulated during a minimum of 0.9 Ma. If any future climatic process resulted in total destabilization of gas hydrates in the area within thousands of years, methane leakage rates could be about ten times higher than the pre-Pliocene rates reported in this work.

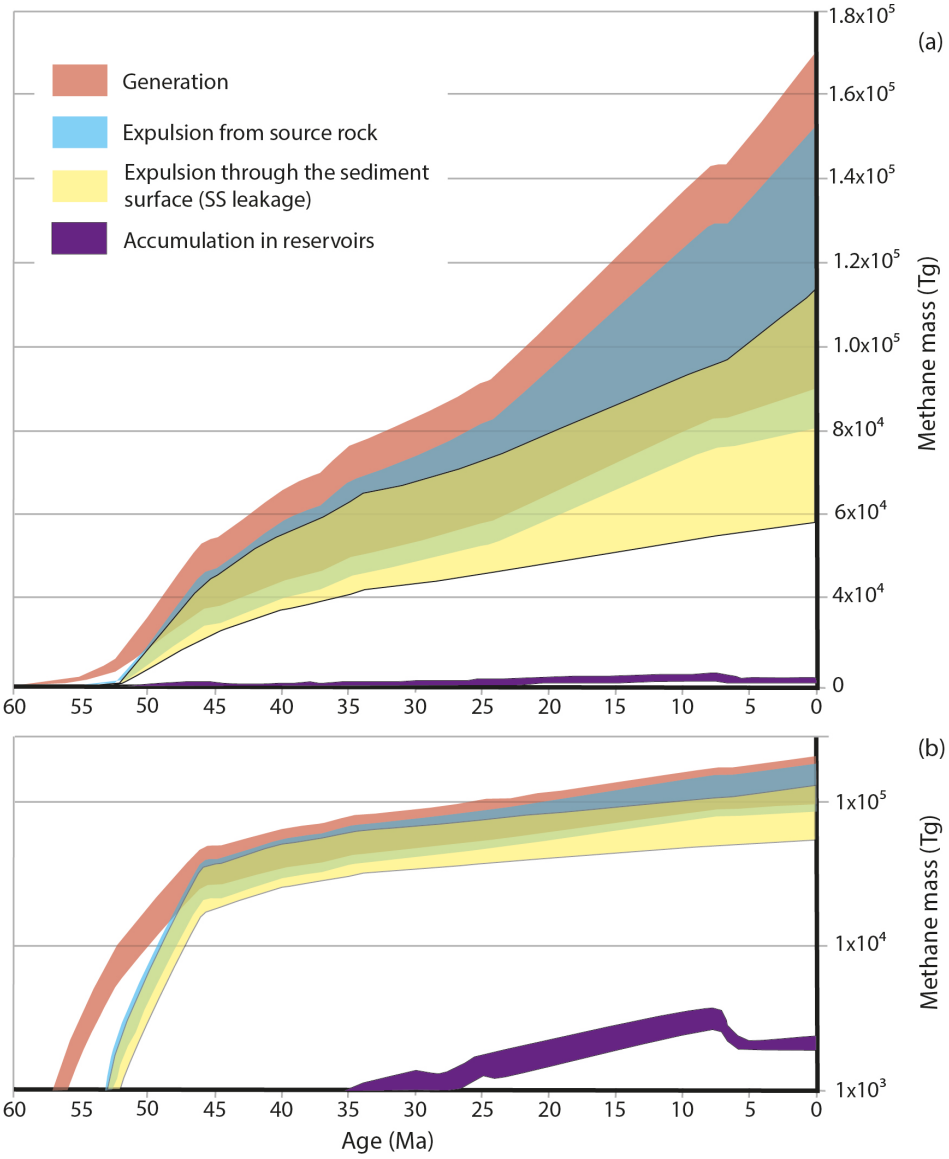

Figure 5.2 General mass balance of the BMB petroleum system. The variability of the results derives from the scenarios presented in table 2 of paper 2 (Berbesi et al., 2014, submitted).

5.3 Central Graben of the North Sea Petroleum province

5.3.1 Petroleum generation and migration

As compared to the WCSB model, the Central Graben model covers an area in which only thermogenic gas was generated, neither biodegraded oilfields occur here, nor is any biogenic gas accumulation present. The onset of petroleum generation is around 115 Ma in the deeper kitchen areas and around 50 Ma for the shallower kitchen areas

(di Primio and Neumann, 2008). Both the time of the petroleum generation onset and the present-day maturity level vary locally due to differences in burial histories. All the modeled source rock intervals are within the main oil-to wet gas generation window at present day.

The different source rock definition scenarios tested result in total gas mass generation of 870 to 1300 Tg, at rates of 10^{-4} to 10^{-3} Tg yr^{-1} (10^{-8} Tg Km^2 yr^{-1}) during the phase of maximum generation (from around 25 Ma to present). Assuming that the rest of the Central Graben area described by Cornford (1994) generates similar amounts to the area modeled here, results in around 20 000-30 000 Tg of gas generation in the Central Graben. The reasoning behind this assumption are offered in Chapter 4 (Berbesi et al., 2014).

5.3.2 Methane seepage

Petroleum systems modeling is somewhat a limited tool when it comes to reproducing mechanisms such as pressure-induced fracturing and migration along graben margin faults, which are known to exert a significant role on gas leakage from the area (Cornford, 1994). Hence, leakage was estimated using averaged mass distributions within petroleum system elements, as in Hunt (1995). For this approach, the mass of generated oil and gas are the starting points from which the masses within the other petroleum system elements (e.g. retained in source rocks, expelled, migrated, expelled from sediment surface) can be appraised. Considering the uncertainties of the method, discussions were based on orders of magnitude rather than absolute values. As explained in detail in chapter 4 (Berbesi et al., 2014), three differently estimates of generated masses were applied (Figure 4.6):

- Estimates from Cornford (1994).
- Calculated by means of the Schmoker (1980) method, using input data related to the petroleum systems model by di Primio and Neumann (2008) and Neumann (2007).

- Extrapolating results from the applied petroleum systems model to the entire Central Graben

The maximum gas mass available for leakage was estimated at 10^4 Tg. Uniform and continuous leakage during the ~ 30 Myr phase of maximum generation would have resulted in thermogenic emissions of orders of 10^{-4} to 10^{-3} Tg/yr. A focalized leakage occurring from 10% of the 15 000 Km^2 of the study area derive in 10^{-7}-10^{-6} $TgKm^{-2}yr^{-1}$, which is of a similar magnitude to the ranges suggested by Judd et al. (1997).

5.4 Geological methane emissions from petroleum systems and their potential for climate feedback

As suggested in the introductory part of this manuscript, a few questions need to be answered before the goal of assessing worldwide petroleum system-related emissions of methane and a link to the Earth's climate evolution can be achieved. These are:

- What are the main mechanisms acting in sedimentary basins where significant methane seepage in known to occur?
- What has higher impact on the methane emission potential from a sedimentary basin, its carbon inventory (organic matter pool), or the mechanism(s) driving leakage?
- Should all sedimentary basins be investigated, or only a particular group of them? In the second case, which ones?

This section discusses the three above mentioned issues, mostly taking ideas from Chapter 4 (Berbesi et al., 2014), but this time also including results from Chapter 3, which were not integrated to the discussions before.

Out of the three questions, the first one is probably the easiest. Its answer already lies in the literature regarding methane seepage measurements (and indirect estimates) in petroleum-bearing sedimentary basins. Besides the United Kingdom

continental shelf (Judd et al., 1997), some of the most relevant settings where significant submarine methane seeps have been documented are Coal Oil Point California (Hornafius et al., 1999) the Bulgarian Black Sea (Dimitrov, 2002), and the Black Sea Continental shelf (Dimitrov, 2002), whose annual individual CH_4 emissions are estimated to range from 0.033 to 3.5 Tg. When carefully reading the relevant publications, some common characteristics among these cases stand out: a) the gas seepage is not uniformly distributed across the sedimentary basin, but rather focalized in particular areas (Etiope et al., 2008; Etiope and Martinelli, 2002; Judd et al., 1997), b) The basin geology is known to be influenced by an active tectonic regime; and therefore high density of faults and fractures are observed (Etiope and Martinelli, 2002; Leifer et al., 2010, Dimitrov, 2002), and c) There is a positive correlation between the high seepage locations and the presence of petroleum accumulations, in some cases famous oil and gas fields (Leifer et al., 2010; Etiope, 2004; Dimitrov, 2002; Judd et al., 1997).

Conditions (a) and (b) have not only been known and reported in the past, but they have also been studied in detail. Fault systems or fissures act as preferential pathways and facilitate the fast escape of the oil and gas, this way reducing the probability of microbial hydrocarbon consumption during its upwards migration (Etiope and Klusman, 2002; Etiope and Martinelli, 2002; Brown, 2000). Besides, the focused seepage leads to formation of methane bubbles that can rise through the water column quickly enough to avoid total oxidation (Albert et al., 1998; Boone, 2000). Of particular relevance for this manuscript is the condition c, i.e., the positive correlation between significant seeps and underlying leaking petroleum reservoirs. This fact has been generally acknowledged (Clarke and Cleverly, 1991; Dimitrov, 2002; Hornafius et al., 1999) but it has seldom inspired comparisons of the seepage magnitude against the magnitude of the petroleum system from where the gas derives, and the mass fluxes within/from it. This leads to addressing the second question raised at the beginning of this chapter.

In order to illustrate the relevance of carbon pool vs leakage mechanism, it is appropriate to bring the WCSB into discussion. The reason for it is simple: this basin

holds the largest oil sand deposits in the entire world and covers an area more than ten times larger than England. In the WCSB petroleum system model described in Chapter 2 and 4, leakage is spread out over a large area, not concentrated or focused, and it basically derives from thermogenic gas generation in kitchen areas (not from leaking reservoirs). Even when methanotrophic gas degradation in soils is not considered, the lack of the mechanisms mentioned in a-c results in maximum predicted leakage of 10^{-2} to 10^{-3} Tg/yr, which is ten to hundreds of times smaller than present-day seepage from the UK continental shelf, the Black Sea or Coal Oil Point California (Clarke and Cleverly, 1991; Dimitrov, 2002; Hornafius et al., 1999). This suggests that that thermal methane generation alone cannot result in seepage rates as those reported in the literature, regardless of the sedimentary basin size and carbon pool. This can be supported by looking at the maximum gas generation rates from the models in this manuscript, which are 10^{-2} Tg/yr in the WCSB, 10^{-3} Tg/yr in the BMB and 10^{-3} Tg/yr in the modeled portion of the Central Graben. If all the gas generated in the three models was directly injected into the atmosphere, the methane contribution would still be of less than a tenth of Teragram per year.

Kroeger et al. (2011) analized the influence of surface temperature increase on oil and gas generation through 1D geochemical modeling. In their study, results from two versions of the same model (same source rock, subsidence history/rates, and heat flow) differing only on Eocene temperature definition were compared. Both models considered sedimentation rates of 20 m/Myr until the Tertiary, were higher subsidence rates of 50 m/Myr were applied (Kroeger et al., 2011). While one of the models considered an Eocene increase in surface temperatures by 15 °C, the other model considered constant surface temperatures through the entire Paleocene. Results showed that the source rock in the former model generated significant amounts of hydrocarbons within a time interval of 5 Myr, while the generation of same amount took the entire Paleocene interval if Paleocene temperatures were modeled as constant (Kroeger et al., 2011). These observations lead Kroeger et al. (2011) to propose that initial Late Paleocene warming combined with increased subsidence rates along major orogenic belts could have resulted in a four times increase of natural gas generation rates. In the case of the gas generation rates

obtained in the models from the WCSB, BMB and Central Graben discussed in this manuscript (10^{-3} - 10^{-2} Tg/yr) a similar combination of factors resulting in four time increase of generation rates would still not be enough to account to 1 Tg/yr.

A picture of the limited potential of thermal gas generation on climate evolution can be gained comparing generation rates predicted by our models against increases in the atmospheric methane burden related to known relevant climate events. The present-day warming trend and the Paleocene-Eocene Thermal Maximum are good illustrations of the latter. The present-day warming trend has been attributed to an annual increase in the atmospheric methane concentration, together with CO_2 increase, that ranged from 40 to 46 Tg/yr in the 1980s (Cicerone and Oremland, 1988), although it has decreased during the 1900s (Bousquet et al., 2006) and 2000s (Denman et al., 2007). The PETM, in turn, represents a period around 55 Ma when the temperatures at high-latitude locations and in the deep oceans increased more than 4 °C over less than 10^4 yr (Kennett and Stott, 1991; Zachos et al., 1993). Climate models within the framework of the present-day carbon cycle indicate that a sustained methane release of 112 Tg/yr over that entire period of 10^4 yr could drive this climatic event (Dickens et al., 1997). Based on these two cases it can be stated that "significant" methane emissions are those with orders of magnitude of tens to hundreds of Tg/yr. As partly mentioned in Chapter 4 (Berbesi et al., 2014), for global petroleum kitchen areas to annually feed methane masses as those alterations reported during the 1980s of those driving the PETM, some conditions should be met:

- Sedimentary Basins on Earth should hold an organic carbon mass at least 1800 times larger than that considered in the WCSB model, or more than 13 000 times larger than those considered in the Beaufort-Mackenzie Basin or Central Graben Studies.
- All the sedimentary organic matter in the previous scenario should generate gas at the same time.
- 100 % of the generated gas should be able to reach the atmosphere.

None of these conditions is likely to occur, and actually, only less than 20% of the generated mass would survive metanotrophic consumption in soils or methane oxidation through water columns (Etiope and Klusman, 2002).

The same type of conclusion applies in the case of biodegradation. Mass balance calculations as presented in Berbesi et al. (2014) and previous works (Adams, 2008; Larter et al., 2008) indicate that continuous leakage of the biogenic gas generated during the formation of the largest known oil sand deposit would have resulted in leakage rates of maximum 10^{-2} Tg/yr, which is a negligible mass when it comes to inducing climate feedback. At this point, the second question can be considered as answered. The mechanisms driving leakage are, by far, more relevant than the carbon inventory of sedimentary basins.

Most of the numbers discussed here point towards the idea that not all sedimentary basins, but only a particular group of them, would be enough to investigate any role on climate evolution. This group would be constituted by basins where both hydrocarbon accumulations and fast release mechanisms are present; this means, basins where temporarily and aerially focused flow is expected (Berbesi et al., 2014). Up to now, only fractured conventional reservoirs have been mentioned, but this not the only type of setting where accumulation/fast release mechanisms are expected to coexist. Arctic basins might represent another important primordial target. Here large amounts of methane can be accumulated over time and be released again in a scale of thousands of years when climate conditions are not optimal for gas hydrate stability (Archer et al., 2009). Ice caps developed during glacial maxima can exert a similar effect, as they constitute a seal for upward gas migration until the end of the glaciation when the ice cap disappears, allowing the gas accumulated below to reach the atmosphere (Rodrigues et al., 2013; Ostanin et al., 2013). The presence of thick permafrost above terrestrial gas hydrates provides them of a higher thermal inertia (and therefore higher chance to survive interglacial phases) than that of marine gas hydrates (Majorowicz et al., 2008; Osadetz and Chen, 2010). Because of this, they could be able to accumulate gas with minor associated leakage during longer time intervals (possibly millions of years) until the "natural" end of the ice age, or until an

interglacial of significant dimensions takes place. Then, they might release significant methane masses and exert a positive feedback on the already ongoing warming process. As suggested in section 3.5.4, up to 700 – 5000 Tg of methane might have entered the gas hydrate system in the BMB since the Pliocene. If any process results in disappearance of the gas hydrate stability conditions and permafrost retreat within a 10^3 -10^4 time span, methane leakage could reach values of 0.07 to 5 Tg per year, which is a very significant emission rate for a single sedimentary basin.

As presented in the introductory chapter, the immense mass of carbon contained in sedimentary systems ($1.56x10^{22}$ g, Des Marais et al., 1992) would suggest that the remobilization of insignificant portions from this carbon pool could be enough to exert an impact on Earth Surface processes, including climate (Kroeger et al., 2011). However, this work has shown that thermal gas generation from source rocks in deep kithen areas takes places at too low speeds compared to those needed to induce climate change, and that only the reservoir (i.e., accumulations) part of petroleum systems would be able to interact with the atmosphere at significant speeds. Therefore, additional mechanisms for a "fast" remobilization of dispersed sedimentary carbon should be considered if any link with climate evolution is to be addressed. An interesting alternative is the emplacement of large sill bodies into carbon-rich sedimentary successions, resulting in rapid conversion of the organic matter into methane due to elevated temperatures in the range of the gas window (Dickens, 2004; Svensen et al., 2004). For example, studies in the Vøring and Møre basins in the Norwegian Sea suggest that intrusion of voluminous mantle-derived melts in organic-rich strata could have resulted in generation of 0.3 to 3 $x10^{18}$ g (0.3 to 3 million Tg) of methane close to the Paleocene/Eocene boundary (Svensen et al., 2004; Skogseid et al., 1992; Berndt et al., 2000). It is also estimated that the mass of methane generated in the entire sill complex in the North Atlantic Volcanic Province (NAPV) was possibly five times higher than in the Vøring and Møre basins (Svensen et al., 2004). Because the time needed to produce the observed 100-300 m thickness of the sills (Smallwood, 2002; Berndt et al., 2000) ranges from only 1000 to 60 000 yr (Eldholm, 1995) methane leakage rates associated with the development of the

NAPV could be significantly higher than those discussed in this manuscript. Methane emissions large enough to have impact on climate could also have taken place during the evolution of large igneous provinces (LIPs) in Siberia (~250 Myr ago; Permo-Triassic boundary) and the Karoo Igneous Province (~183 Myr ago; Early- Middle Jurassic boundary) (Wignall, 2001).

Chapter 6

Conclusions and outlook

6.1 Conclusions

Petroleum systems modeling suggests that source rocks in the Western Canada Sedimentary Basin reached significant transformation ratios during the Upper Cretaceous, and are mature enough to generate oil-to dry gas at present day. In the model, the total gas generation is the order of 10^5 Tg, most of it taking place between 80-60 Ma. Maximum predicted gas generation rates are in the order of 10^{-2} Tg/yr, deriving in associated surface methane seepage of 10^{-3} to 10^{-2} Tg/yr. Mass balance calculations suggest that 60 000 to 130 000 Tg of microbial methane might have resulted from biodegradation in Athabasca. Biogenic methane could have been produced at rates of up to 10^{-3} – 10^{-2} Tg/yr, depending on assumption regarding the degradable oil mass.

In the case of the Beaufort-Mackenzie Basin, the onset of significant gas generation from Cretaceous source rocks is suggested to take place between 60-50 Ma, and considerably later in the case of Cenozoic sources. Total gas generation ranged from 10^4 to 10^5 Tg, summing all source intervals. The maximum modeled gas generation rates ranged from 10^{-4} to 10^{-3} Tg/yr from Eocene to Miocene, and from 10^{-5} to 10^{-3} Tg/yr from Pliocene to present-day. The gas mass available for gas hydrate formation in the region is proposed to be of maximum 700-5000 Tg (mostly methane), which is in the order of magnitude of previous methane gas hydrates assessments for this study area. Seepage of thermogenic gas from this basin into the atmosphere could have taken place at rates of 10^{-10} to 10^{-3} Tg/yr before the onset of glaciations (before the Pliocene). If any future climate process resulted in disappearance of the gas

hydrate stability conditions and permafrost retreat within a 10^3-10^4 time span, methane leakage could reach values of 0.07 to 5 Tg per year, which would be a considerably elevated seepage rate for a single sedimentary basin.

A petroleum system model of the Central Graben developed in previous studies and applied in this work places the onset of significant petroleum generation around 115 Ma for the deeper kitchen areas and around 50 Ma for the shallower kitchen areas, being all the modeled source rock intervals within the main oil-to wet gas generation window at present day. Total gas generation within the model area takes places at rates of 10^{-4} to 10^{-3} Tg yr^{-1}, and extrapolation of modeling results suggests that gas masses in the order 10^4 Tg could have been generated in the entire Central Graben. Theoretical estimates based on averaged mass distributions within petroleum system elements are consistent with modeling results, suggesting thermogenic emissions of orders of 10^{-4} to 10^{-3} Tg/yr. Focalized leakage occurring from 10% of the study area translates into 10^{-7}-10^{-6} $TgKm^{-2}yr^{-1}$, which is of a similar magnitude to rates suggested by previous indirect appraisals based on surface data.

A comparison of the outcome from this work against published data indicates that the coexistence of gas accumulations (reservoirs) and mechanisms promoting fast release of the gas is a basic condition for petroleum systems to significantly contribute to the atmospheric methane budget. The mass of thermogenic and biogenic methane generated during the geological evolution of the WCSB is comparable to the world's known and risked undiscovered gas resources. However, seepage rates from this basin are expected to be just similar or even lower than measurements at smaller areas due to the lack of the above mentioned basic conditions.

Global extrapolation of modeling results indicates that regardless of the kitchen area, thermal generation of methane, as a single process, would not be able to induce climate events. The mechanisms driving leakage are, by far, more relevant than the carbon inventory of sedimentary basin. In this sense, both conventional gas reservoirs in highly faulted and fractured settings and arctic petroleum systems represent a good target for studies addressing similar topics as those presented in this

manuscript. The fact that only the reservoir part of the petroleum systems is able to interact with the atmosphere at significant speed also means that the mass available for leakage is finite. Therefore, the combination of surface measurements with petroleum systems modeling and analysis would be the key in order to provide reasonable aerial extrapolations of measurements, and in order to address paleo-seepage.

6.2 Outlook

This study has been able to model, analyze and/or discuss the evolution of petroleum systems in the three selected study areas, quantify their potential individual methane contributions to the atmosphere, and place the obtained results in a global context. By doing so, relevant information for the understanding of methane fluxes within these systems and towards the atmosphere have been provided. This information allows providing some recommendations for future studies addressing a connection between petroleum systems (or even more generally speaking, sedimentary basins) and the Earth's climate evolution:

- There is no need to address all sedimentary basins in the world in order to study and quantify the role of sedimentary organic matter in climate evolution. Instead, efforts should concentrate on those sedimentary basins where two basic elements are present. These elements are hydrocarbon accumulation and fast release mechanism (temporarily and aerially focused flow). Besides fractured conventional reservoirs, Arctic basins represent appropriate study areas because they contain the two basic conditions above mentioned.
- The fact that only the reservoir part of the petroleum systems is able to interact with the atmosphere at significant speed also means that the mass available for leakage is finite. This provides a reference point for time and area extrapolations performed on measurements derived from seepage surveys. Aerial extrapolations should consider the area above accumulations and fractures controlling leakage, and not the entire extension of the

sedimentary basin, nor the area of mature source rock. Basin-scale seepage resulting from such extrapolations should be clearly compared against the size of the sub-surface gas accumulations feeding the gas. Moreover, the timing of reservoir formation, filling, and in some cases alteration should be understood before paleo-seepage can be reasonably inferred (e.g., Hartwig et al., 2012). With this in mind, the parallel application of direct measurements (surface, present-day) with petroleum systems modeling and analysis (sub-surface, geologic time scale) is proposed as the basic workflow to follow by future studies in this field. Several works have shown the strengths and weaknesses of surface (e.g., Dimitrov, 2002; Hornafius et al., 1999; Judd, 2004; Etiope et al., 2008) and sub-surface (e.g., Cavanagh et al., 2006; Kuhlmann et al., 2011; Naeth et al., 2005; Paton et al., 2007) approaches to the topic. It is time to close the gap and perform integrated studies.

A limitation of this and similar contributions (e.g., Hartwig et al., 2012; Ostanin et al., 2013; Rodrigues et al., 2013; Paton et al., 2007; Kuhlman et al., 2011) is the fact that they have focused on known plays. Therefore, modeling efforts have been directed towards source rocks which have been correlated with known oil/gas fields, whose quality is known from outcrops, well cores and drill cuttings, and which are also thick and continuous enough to be reliably mapped on seismic data. This means that:

- Several organic rich intervals which are not considered as source of major petroleum accumulations or which are at sub-seismic scale might have been ignored so far. This could have important implications because, as discussed in this manuscript, the mass of carbon estimated to be contained in fuel accumulations is negligible compared to the total carbon mass dispersed in sedimentary systems.
- The presence/extent of predominantly gas-generative type III kerogen and coals (which generate mostly gas) might have been overlooked and underestimated when focusing on calibrating the models to the known petroleum accumulations.

Although this work suggests that the rates of methane generation during thermal transformation of kerogen and oil biodegradation might be too slow compared with the leakage rates needed to explain hyperthermals, considering the presence of sub-seismic source rock intervals and paying particular attention to coals and type III kerogen-bearing claystones is recommended for future studies.

Abbreviations

‰	Parts per mille (1/1000 = 0.001)
1-D	One-dimensional
2-D	Two-dimensional
3-D	Three-dimensional
A	Pre-exponential factor of the Arrhenius equation (s^{-1})
API	American Petroleum Institute
API°	American Petroleum Institute gravity API° = (141.5/oil density) – 131.5
ASA	*Allmennaksjeselskap* (Norwegian term, equivalent to "public stock company")
Bbbl	Billion barrel
bbl	Barrel (1 bbl ~ 0.159 m^3)
bcm	Billion cubic meters
BHT	Bottom-hole temperature
BIO	Biochemical (cycle)
BMB	Beaufort-Mackenzie Basin
BMTL	Beaufort-Mackenzie tectonic lineament
BPSM	Basin and petroleum system modeling
CH_4	Methane
CO_2	Carbon dioxide
DST	Drill stem test
Ea	Activation energy (J/mol or Kcal/mol)
ELFZ	Eskimo Lakes fault zone
FID	Flame ionization detector
g	Gram
GC	Gas chromatography
GC-MS	Gas chromatography-mass spectrometry

GEM	Geologic Emissions of Methane
GEO	Geochemical (cycle)
GFZ	*GeoForschungsZentrum* (Helmholtz Centre Potsdam-GFZ German Research Centre for Geosciences)
GH	Gas hydrate
GOR	Gas to oil ratio
HC	Hydrocarbon
HF	Heat-flow
HI	Hydrogen index
HMWMH	High molecular-weight multi-heteroatom compounds
IPCC	Intergovernmental Panel on Climate Change
Ka BP	Thousand years before present
Km	Kilometer (1 Km = 1000 meters)
Kyr	Thousand years
LCAA	Long chain alkyl aromatics
LIPs	Large igneous provinces
Ma	Million years ago
md	MilliDarcy (1 md = 9.86923×10^{-16} m^2)
MMbbl	Million barrel
MOM	Methane on the Move (Research program at Helmholtz Centre Potsdam-GFZ German Research Centre for Geosciences)
MSSV	Micro Scaled Sealed Vessel (Horsfield et al., 1989)
Myr	Million years
NAVP	North Atlantic Volcanic Province
NSO	Nitrogen, sulfur, oxygen
OI	Oxygen index
OOIP	Original oil in place
OWC	Oil-water contact
PDVSA	*Petróleos de Venezuela, S.A* (Venezuelan state-owned oil and natural gas company)
PETM	Paleocene-Eocene Thermal Maximum

PI	Production index
PM	Biodegradation extent in the Peters and Moldovan (1983) scale
ppb	Parts per billion
ppm	parts per million
PS	Petroleum system
PSE	Petroleum system-related emissions of methane
PSM	Petroleum system modelling
PWD	Paleo-water depth
Py-GC	Pyrolysis gas chromatography
R_0	Vitrinite reflectance [%]
SARA	Saturate, Aromatic, Resin and Asphaltene
Sm^3	Standard cubic meter (1 m^3 at 15.6°C and 101.325 kPa)
SR	Source rock
SS leakage	Gas leakage from the sediment surface of the models in this study
SWIT	Sediment water interface temperature
T	Temperature
TAFZ	Tarsuit-Amauligak fault zone
TAN	Total Acid Number
TFZ	Taglu fault zone
Tg	Teragram (1 Tg=10^{12} g)
T_{max}	Temperature of maximum pyrolysis yield (°C) based on Rock-Eval pyrolysis
TOC	Total organic carbon wt.-%
TR	transformation ratio
UK	United Kingdom
UKCS	United Kingdom Continental Shelf
US	United States
USGS	United States Geological Survey
USSR	Union of Soviet Socialist Republics
WCSB	Western Canada Sedimentary Basin

	Deviation of the $^{13}C/^{12}C$ from the standard PDB limestone (belemnite carbonate from the Cretaceous Peedee Fm., South Carolina)
$\delta^{13}C$	$\delta^{13}C_{\text{Sample}} = \left(\frac{^{13}C/^{12}C_{\text{Sample}}}{^{13}C/^{12}C_{\text{PDB}}} - 1 \right) \cdot 1000$
	Deviation of the $^{18}O/^{16}O$ from the Vienna Standard Mean Ocean Water (VSMOW)
$\delta^{18}O$	$\delta^{18}O = \left(\frac{\left(\frac{^{18}O}{^{16}O}\right)_{sample}}{\left(\frac{^{18}O}{^{16}O}\right)_{standard}} - 1 \right) * 1000\ ‰$
µm	Micrometre, or micrometer (1 µm = 10^{-6} m)

References

Adams, J., Larter, S., Bennett, B., Huang, H., Westrich, J., and Kruisdijk, C. v., 2012, The dynamic interplay of oil mixing, charge timing, and biodegradation in forming the Alberta oil sands: Insights from geologic modeling and biogeochemistry, in: Hein, F.J., Leckie, D., Larter, S., Suter, J. (Eds.), Heavy-oil and oil-sand petroleum systems in Alberta and beyond: AAPG Studies in Geology 64, p. 1 – 80.

Adams, J., Larter, S., Bennett, B., Marcano, N., and Oldenburg, T., 2010, Alberta Oil Sands Charge Allocation: Mapping Source Rock Contributions, AAPG International Convention and Exhibition: Calgary, Alberta, Canada.

Adams, J., Riediger, C., Fowler, M., and Larter, S., 2006, Thermal controls on biodegradation around the Peace River tar sands: Paleo-pasteurization to the west: Journal of Geochemical Exploration, v. 89, no. 1-3, p. 1-4.

Adams, J. J., 2008, The Impact of Geological and Microbiological Processes on Oil Composition and Fluid Property Variations in Heavy Oil and Bitumen Reservoirs. PhD Thesis. University of Calgary, p. 738.

Adams, J. J., Rostron, B. J., and Mendoza, C. A., 2004, Coupled fluid flow, heat and mass transport, and erosion in the Alberta basin: implications for the origin of the Athabasca oil sands: Canadian Journal of Earth Sciences, v. 41, no. 9, p. 1077-1095.

Albert, D. B., Martens, C. S., and Alperin, M. J., 1998, Biogeochemical processes controlling methane in gassy coastal sediments—Part 2: groundwater flow control of acoustic turbidity in Eckernförde Bay Sediments: Continental Shelf Research, v. 18, no. 14–15, p. 1771-1793.

Al-Hajeri, M. M., M.A. Saeed, M. A., Derks, J., Fuchs, T., Hantschel, T., Kauerauf, A., Neumaier, M., Schenk, O., Swientek, O., Tessen, N., Welte, D., Wygrala, B., Kornpihl, D., and Peters, K., 2009, Basin and Petroleum System Modeling. Oilfield Review. Schlumberber.

Allen, P. A., and Allen, J., Richard, 1990, Basin analysis: principles and applications, Cambridge, Blackwell Scientific Publications, 451 p.

Allen, P. A., and Allen, J. R., 2005, Basin Analysis. Principles and Applications. Blackwell Scientific Publications. London. 451 p.

Amante, C., and Eakins, B. W., 2009, ETOPO1 1 Arc-Minute Global Relief Model: Procedures, Data Sources and Analysis NOAA Technical Memorandum NESDIS NGDC 24, 19.Athy, L.F., 1930. Density, porosity and compaction of sedimentary rocks. AAPG Bulletin 14, p. 1-24.

Archer, D., 2009, Methane hydrate stability and anthropogenic climate change. Biogeosciences Discuss., 4, p. 993–1057.

Asgar-Deen, M., Riediger, C., and Hall, R., 2004, The Gordondale Member: designation of a new member in the Fernie Formation to replace the informal "Nordegg Member" nomenclature of the subsurface of west-central Alberta: Bulletin of Canadian Petroleum Geology, v. 52, no. 3, p. 201-214.

Bachu, S., and Burwash, R. A., 1994, Geothermal Regime in the Western Canada Sedimentary Basin, *in* Mossop, G., and Shetsen, I., eds., Geological Atlas of the Western Canada Sedimentary Basin: Calgary, Alberta, Canadian Society of Petroleum Geologist and Alberta Research Council, p. 455-468.

Bailey, N. J. L., Jobson, A. M., and Rogers, M. A., 1973, Bacterial degradation of crude oil: comparison of field and experimental data. Chemical Geology 11, p. 203–221.

Bally, A. W., 1975, A geodynamic scenario for hydrocarbon occurrences: 9th World Petroleum Congress Proceedings, v. 2, p. 33-44.

Bally, A. W., and Snelson, S., 1980, Realms of subsidence, in A. D. Miall, ed.,Facts and principles of world petroleum occurrence: Canadian Society of Petroleum Geologists Memoir 6, p. 9-75.

Barendregt, R. W., and Irving, E., 1998, Changes in the extent of North American ice sheets during the Late Cenozoic: Can. J. Earth Sci. , v. 35, p. 504-509.

Baskin, D. K., and Peters, K. E., 1992, Early generation characteristics of a sulfur-rich Monterey kerogen. In: American Association of Petroleum Geologists Bulletin vol. 76, p. 1-13.

Bédard, C., and Knowles, R., 1989, Physiology, biogeochemistry, and specific inhibitors of CH4, NH4+, an CO oxidation by methanothrophs and nitrifiers. Microbiological Reviews 53, p. 68-84.

Beglinger, S. E., Doust, H., and Cloetingh, S., 2012, Relating petroleum system and play development to basin evolution: West African South Atlantic basins: Marine and Petroleum Geology, v. 30, no. 1, p. 1-25.

Behar, F., and Vandenbroucke, M., 1987, Chemical modelling of kerogens. Organic Geochemistry, 11, p. 15-24.

Berbesi L.A., di Primio, R., Anka, Z., Sippel, J., Horsfield, B., 2014, Inferences of gas hydrate deposits in the Beaufort/Mackenzie Basin based on petroleum system analysis. Submitted to Marine and Petroleum Geology, October 2014.

Berbesi, L. A., di Primio, R., Anka, Z., Horsfield, B., and Wilkes, H., 2014, Methane leakage from evolving petroleum systems: Masses, rates and inferences for climate feedback: Earth and Planetary Science Letters, v. 387, p. 219-228.

Berbesi, L. A., di Primio, R., Anka, Z., Horsfield, B., and Higley, D. K., 2012, Source rock contributions to the Lower Cretaceous heavy oil accumulations in Alberta: a basin modelling study: AAPG Bulletin, v. 96, p. 1211-1234.

Berndt, C., Skogly, O. P., Planke, S., and Eldholm, O., 2000, High-velocity breakup-related sills in the Vøring Basin, off Norway. J. Geophys. Res. 105, p. 28443–28454.

Berner, R. A., 1989, Biogeochemical cycles of carbon and sulfur and their effect on atmospheric oxygen over phanerozoic time: Global and Planetary Change, v. 1, p. 97-122.

Biddle, K. T., and Wielchowsky, C. C., 1994, Hydrocarbon Traps. AAPG Memoir, 60, p. 219-235.

Blackwell, D. D., and Richards, M., 2004, Geothermal map of North America, Am. Assoc. Petroleum Geologist (AAPG), 1 sheet, scale 1:6,500,000, Product code 423.

Blanc, P., and Connan, J., 1994, Preservation, degradation, and destruction of trapped oil. In: Magoon, L., Dow, W. (Eds.), The Petroleum System – From Source to Trap. The American Association of Petroleum Geologists, p. 237–251.

Bois, C., Bouche, P., and Pelet, R., 1982, Global geologic history and distribution of hydrocarbon reserves: AAPG Bulletin, v. 66, p. 1248-1270.

Boone, D. R., 2000, Biological formation and consumption of methane. In: Atmospheric Methane: Its Role in the Global Environment (ed. Khalil MAK), p. 42–62. Springer, Berlin.

Booth, J. S., Rowe, M. M., and Fisher, K. M., 1996, Offshore gas hydrate sample database: U.S. Geological Survey Open-File Report 96-272, 17 p.

Bousquet, P., Ciais, P., Miller, J. B., Dlugokencky, E. J., Hauglustaine, D. A., Prigent, C., Werf, G. R. V. d., Peylin, P., Brunke, E. G., Carouge, C., Langenfelds, R. L., Lathiere, J., Papa, F., Ramonet, M., Schmidt, M., Steele, L. P., Tyler, S. C., and White, J., 2006, Contribution of anthropogenic and natural sources to atmospheric methane variability: Nature, v. 443, p. 439-443.

Brennand, T. P., Hoorn, B. V., James, K. H., and Glennie, K. W., 1998, Historical review of North Sea exploration, in Glennie, K.W., ed., Petroleum geology of the North Sea (4th ed.): London, Blackwell Science, Ltd., p. 1–41.

Brooks, J., 1990, Classic petroleum provinces: Geological Society, London, Special Publications, v. 50, no. 1, p. 1-8.

Brooks, J., and Glennie, K. W., 1987, Petroleum geology of North-West Europe, in two volumes: London, Graham & Trotman, 1219 p.

Brooks, P. W., Fowler, M. G., and Macqueen, R. W., 1988, Biological marker and conventional organic geochemistry of oil sands/heavy oils, Western Canada basin: Organic Geochemistry, v. 12, no. 6, p. 519-538.

Brown, A., 2000, Evaluation of Possible Gas Microseepage Mechanisms. AAPG Bulletin 84, p. 1775-1789.

Burley, S. D., 1993, Models of burial diagenesis for deep exploration plays in Jurassic fault traps of the Central and Northern North Sea: Geological Society, London, Petroleum Geology Conference series, v. 4, p. 1353-1375.

Canada, N. E. B., 2010, Canada's oil sands: A supply and market outlook to 2015.

Cant, D. J., and Stockmal, G. S., 1989, The Alberta foreland basin: relationship between stratigraphy and Cordilleran terrane-accretion events: Canadian Journal of Earth Sciences, v. 26, no. 10, p. 1964-1975.

Caplan, M. L., and Bustin, R. M., 1996, Factors governing organic matter accumulation and preservation in a marine petroleum source rock from the Upper Devonian to Lower Carboniferous Exshaw Formation, Alberta: Bulletin of Canadian Petroleum Geology, v. 44, p. 474–494.

Carmalt, S. W., and St John, B., 1986, Giant Oil and Gas Fields' In: Halbouty, M. T. (ed.) Future Petroleum Provinces of the World AAPG, Tulsa, OK, p. 11-53.

Carr, A. D., Snape, C. E., Meredith, W., Uguna, C., Scotchman, I. C., and Davis, R. C., 2009, The effect of water pressure on hydrocarbon generation reactions: Some inferences from laboratory experiments. Petroleum Geoscience, 15(1), p. 17–26.

Carruthers, D., 1998, Transport modeling of secondary oil migration using gradient-driven invasion percolation techniques: Ph.D. dissertation, Heriot-Watt University, Edinburgh, United Kingdom, 288 p.

Carruthers, D., and Wijngaarden, M., 2000, Modeling viscous-dominated fluid transport using modified invasion percolation techniques: Journal of Geochemical Exploration, v. 69–70, p. 669–672, doi:10.1016/S0375-6742(00)00138-2.

Cavanagh, A. J., R. Di Primio, M., Scheck-Wenderoth, and Horsfield, B., 2006, Severity and timing of Cenozoic exhumation in the southwestern Barents Sea: Journal of the Geological Society, v. 163, p. 761-774.

Chen, Z., Dietrich, J. R., and Osadetz, K. G., 2012, Petroleum Resource Potential of the Canada (Amerasian) Basin rift margin of the Beaufort-Mackenzie Basin, Arctic Canada: GeoConvention 2012.

Chen, Z., and Osadetz, K. G., 2010, Geological Controls of Regional Petroleum Gas Hydrate Occurrence, Beaufort-Mackenzie Basin, Canada: Search and Discovery Article http://www.searchanddiscovery.com/documents/2010/80076chen/poster.pdf.

Chen, Z., Osadetz, K. G., Dixon, J., and Dietrich, J. R., 2007, Oil Resource Potential of the Beaufort-Mackenzie Basin: CSPG CSEG Convention.

Chen, Z., Osadetz, K. G., Issler, D. R., and Grasby, S. E., 2008, Hydrocarbon migration detected by regional temperature field variations, Beaufort-Mackenzie Basin, Canada: AAPG Bulletin, v. 92, no. 12, p. 1639-1653.

Christopher, J. E., 1984, The Lower Cretaceous Mannville Group, northern Williston Basin region, Canada, in D. F. Stott and D. J. Glass, eds., The Mesozoic of middle North America: Canadian Society of Petroleum Geologists Memoir 9, p. 109–126.

Cicerone, R. J., and Oremland, R. S., 1988, Biogeochemical aspects of atmospheric methane: Global Biogeochem. Cycles, v. 2, p. 299-327.

Clarke, R. H., and Cleverly, R. W., 1991, Petroleum seepage and post-accumulation migration: Geological Society, London, Special Publications, v. 59, p. 265-271.

Claypool, G. E., Love, A. H., and Maughan, E. K., 1978, Organic geochemistry, incipient metamorphism, and oil generation in black shale members of Phosphoria Formation, Western Interior, United States: AAPG Bulletin, v. 62, p. 98–120.

Collett, T. S., Johnson, A. H., Knapp, C. C., and Boswell, R., 2009, Natural Gas Hydrates: A Review, in T. Collett, A. Johnson, C. Knapp, and R. Boswell, eds., Natural gas hydrates—Energy resource potential and associated geologic hazards: AAPG Memoir 89, p. 146–219. DOI:10.1306/13201101M891602.

Collett, T. S., Lee, M. W., Dallimore, S., and Agena, W. F., 1999, Seismic and well-log inferred gas hydrate accumulations on Richards Island in the Mackenzie Delta,

N.W.T., Canada. In Dallimore et al. (eds.), Scientific Result from JPEX/JNOC/GSC Mallik 2L-38 Gas Hydrate Research Well, Mackenzie Delta, northwest Territories, Canada, Geological Survey of Canada Bulletin 544, p. 357–376.

Comer, J. B., 1991, Stratigraphic analysis of the Upper Devonian Woodford Formation, Permian Basin, west Texas and southeast New Mexico: Texas Bureau of Economic Geology, Report of Investigation 201, p. 63.

Comer, J. B., 1992, Organic geochemistry and paleogeography of Upper Devonian formations in Oklahoma and northwesternArkansas, in K. S. Johnson and B. J. Cardott, eds., Source Rocks in the Southern Mid-Continent: 1990 Symposium: Oklahoma Geological Survey Circular 93, p. 70–93.

Connan, J., 1984, Biodegradation of crude oils in reservoirs. In: J. Brooks, D.H. Welte (Eds.), Advances in Petroleum Geochemistry. Academic Press, London, p. 299-330.

Conrad, R., 2009, The global methane cycle: recent advances in understanding the microbial processes involved: Environmental Microbiology Reports, v. 1, no. 5, p. 285-292.

Cook, F. A., Coflin, K. C., Lane, L. S., Dietrich, J. R., and Dixon, J., 1987b, Structure of the southeast margin of the Beaufort-Mackenzie basin, Arctic Canada, from crustal seismicreflection data Geology 15, p. 931-935.

Cornford, C., 1994, Source rocks and hydrocarbons of the North Sea, *in* Glennie, K. W., ed., Petroleum Geology of the North Sea: Oxford, Blackwell Science, p. 376-462.

Cornford, C., and Brooks, J., 1989, Tectonic controls on oil and gas occurrences in the North Sea area. In: Balkwill, A.J.T.a.H.R. (Ed.), Extensional Tectonics and Stratigraphy of the North Atlantic Margins. AAPG, Tulsa, OK, USA, pp. 523–540.

Cranston, R. E., 1994, Marine sediments as a source of atmospheric methane: Bull. Geol. Soc. Denmark, v. 41, p. 101-109.

Creaney, S., and Allan, J., 1990, Hydrocarbon generation and migration in the Western Canada sedimentary basin: Geological Society, London, Special Publications, v. 50, no. 1, p. 189-202.

Creaney, S., Allan, J., Cole, K. S., Fowler, M. G., Brooks, P. W., Osadetz, K. G., Macqueen, R. W., Snowdon, L. R., and Riediger, C., 1994, Petroleum Generation and Migration in the Western Canada Sedimentary Basin, *in* Mossop, G., and Shetsen, I., eds., Geological atlas of the Western Canada Sedimentary Basin: Calgary, Alberta, Canadian Society of Petroleum Geologists and Alberta Research Council, p. 455-468.

Crutzen, P. J., 1991, Methane's sinks and sources. Nature 350, 380 - 381; doi:10.1038/350380a0.

Dallimore, S. R., Uchida, T., and Collett, T. S., 1999, Scientific Results from the JAPEX/JNOC/GSC Mallik 2L-38 Gas Hydrate Research Well, Mackenzie Delta, Northwest Territories, Canada, Geological Survey of Canada Bulletin 544.

Davidson, D. W., El-Defrawy, M. K., Feuglem, M. O., and Judge, A. S, 1978, Natural gas hydrates in northern Canada: Proceedings of the 3rd International Conference on Permafrost, Edmonton, National Research Council of Canada, Ottawa, v. 1, p. 937-943.

Demaison, G. J., 1984, The Generative Basin Concept. In: Demaison, G. & Murris, R. J. (eds), Petroleum Geochemistry and Basin Evaluation, AAPG Memoir 35, p. 1-14

Demaison, G. J., and Moore, G. T., 1980, Anoxic environments and oil source bed genesis, «American Association of Petroleum Geologists. Bulletin», 64, 1179-1209.

Deming, D., 1994, Overburden rock, temperature and heat flow, *in* Magoon, L. B., and Dow, W. G., eds., The Petroleum System—from Source to Trap, American Association of Petroleum Geologists, Memoir, 60, p. 165-186.

Denman, K. L., Brasseur, G., A. Chidthaisong, Ciais, P., Cox, P. M., Dickinson, R. E., Hauglustaine, D., Heinze, C., Holland, E., Jacob, D., Lohmann, U., Ramachandran, S., Dias, P. L., Wofsy, S. C., and Zhang, X., 2007, Coupling between changes in the climatic system and biogeochemistry, *in* Solomon, S. D., Qin, M., Manning, Z., Chen, M., Marquis, K. B., Averyt, M., and Miller, eds., Climate Change 2007: the Physical Science Basis. Contribution of working group I to the fourth assessment report of the Intergovernmental Panel on Climate Change: Cambridge, U.K., Cambridge Univ. Press, p. 499-587.

Des Marais, D. J., Strauss, H., Summons, R. E., and Hayes, J. M., 1992, Carbon isotope evidence for the stepwise oxidation of the Proterozoic environment: Nature, v. 359, p. 605-609.

di Primio, R., and Horsfield, B., 2006, From petroleum-type organofacies to hydrocarbon phase prediction: AAPG Bulletin, v. 90, no. 7, p. 1031-1058.

di Primio, R., and Neumann, V., 2008, HPHT reservoir evolution: a case study from Jade and Judy fields, Central Graben, UK North Sea: International Journal of Earth Sciences, v. 97, p. 1101-1114.

Dickens, G. R., 2004, Hydrocarbon-driven warming. Nature 429, p. 513–515.

Dickens, G. R., Castillo, M. M., and Walker, J. C. G., 1997, A blast of gas in the latest Paleocene: Simulating first-order effects of massive dissociation of oceanic methane hydrate: Geology, v. 25, p. 259-262.

Dickinson, R. E., and Cicerone, R. J., 1986, Future global warming from atmospheric trace gases. Nature 319, p. 109-115.

Dickinson, W. R., 1974, Plate tectonics and sedimentation, in Tectonics and sedimentation: SEPM Special Publication 22, p. 1-27.

Dieckmann, V., 2005, Modelling petroleum formation from heterogeneous source rocks: the influence of frequency factors on activation energy distribution and geological prediction: Marine and Petroleum Geology, v. 22, no. 3, p. 375-390.

Dimitrov, L., 2002, Contribution to atmospheric methane by natural seepages on the Bulgarian continental shelf: Continental Shelf Research, v. 22, p. 2429-2442.

Dixon, J., J. R. Dietrich, and D. H. McNeil, 1992a, Upper Cretaceous to Pleistocene sequence stratigraphy of the Beaufort-Mackenzie and Banks Islands areas, northwest Canada: Geological Survey of Canada Bulletin, v. 407.

Dixon, J., ed, 1996, Geological atlas of the Beaufort-Mackenzie area, Geological Survey of Canada Miscellaneous Report 59, 173 p.

Dixon, J., Dietrich, J., Lane, L. S., and McNeil, D. H., 2008, Geology of the Late Cretaceous to Cenozoic Beaufort-Mackenzie Basin, Canada, Sedimentary Basins of the world, v. 5.

Dixon, J., Dietrich, J. R., Snowdon, L. R., Morrell, G., and McNeil, D. H., 1992b, Geology and petroleum potential of Upper Cretaceous and Tertiary strata, Beaufort-Mackenzie area, northwest Canada: AAPG Bulletin, v. 76, p. 927-947.

Dixon, J., Morrell, G. R., Dietrich, J. R., Procter, R. M., Taylor, G. C., Conn, R. F., Dallaire, S. M., and Christie, J. A., 1994, Petroleum resources of the Mackenzie delta and Beaufort Sea: Geological Survey of Canada Bulletin, v. 474, p. 52.

Dlugokencky, E. J., Steele, L. P., Lang, P. M., and Masarie, K. A., 1994, The growth rate and distribution of atmospheric methane. Journal of Geophysical Research, v. 99, p. 17021-17043.

Doust, H., 2003, Placing petroleum systems and plays in their basin history context: a means to assist in the identification of newopportunities. First Break 21, p. 73-83.

Doust, H., and Summer, H. S., 2007, Petroleum systems in rift basins - a collective approach in Southeast Asian basins. Petroleum Geoscience 13, p. 127-144.

Dow, W. G., 1974, Application of oil correlation and source rock data to exploration in Williston basin. AAPG Bulletin, 58. p. 1253-1262.

Drummond, K. J., 1995, Gas reserves growth in the Western Canada Sedimentary Basin, CSPG-CWLS Symposium, Calgary, Alberta, National Energy Board Canada.

Durand, B., 1980, Sedimentary organic matter and kerogen. Definition and quantitative importance of kerogen, Paris-France, Éditions Technip, Kerogen: Insoluble Organic Matter from Sedimentary Rocks, 525 p.

Durand, B., and Espitalié, J., 1976, Geochemical studies on the organic matter from the Douala Basin (Cameroon) -- II. Evolution of kerogen. Geochimica et Cosmochimica Acta, 40, p 801-808.

Edwards, D. E., Barclay, J. E., Gibson, D. W., Kvill, G. E., and Halton, E., 1994, Triassic Strata of the Western Canada Sedimentary Basin, *in* Mossop, G., and Shetsen, I., eds., Geological atlas of the Western Canada Sedimentary Basin:

Calgary, Alberta, Canadian Society of Petroleum Geologists and Alberta Research Council, p. 259-275.

Ehlers, J., 1996, Quaternary and glacial geology, J. Wiley & Sons, New York, 549 p.
Eldholm, O., and Grue, K., 1995, North Atlantic volcanic margins: dimensions and production rates. J. Geophys. Res. 99, p. 2955–2968.

England, W. A., Mackenzie, A. S., Mann, D. M., and Quigley, T. M., 1987, The movement and entrapment of petroleum fluids in the subsurface. Journal of the Geological Society 144, p. 327-347.

ENI, 2005, Encyclopaedia of Hydrocarbons. Ente nazionale idrocarburi (ENI). Istituto della Enciclopedia italiana.

Environmental Literacy Council (2008). Sources and Sinks: http://www.enviroliteracy.org/article.php/439.html (Accessed July 04, 2011).
PDVSA (Petróleos de Venezuela, S.A.), 2006, Contact with the new PDVSA: A newsletter about Venezuela's national oil industry, v. 8, p. 10: http://www.pdvsa.com./interface.en/database/fichero/publicacion/2621/195.PDF (accessed November, 2010).

(EPA), U. S. E. P. A., 2011, Oil and Natural Gas Air Pollution Standards. Regulatory Actions.

Etiope, G., 2004, New Directions: GEM—Geologic Emissions of Methane, the missing source in the atmospheric methane budget. Atmospheric Environment 38, 3099-3100.

-, 2012, Methane uncovered. Nature Geoscience 5, p. 373-374.

Etiope, G., Fridriksson, T., Italiano, F., Winiwarter, W., and Theloke, J., 2007, Natural emissions of methane from geothermal and volcanic sources in Europe: Journal of Volcanology and Geothermal Research, v. 165, no. 1–2, p. 76-86.

Etiope, G., and Klusman, R. M., 2010, Microseepage in drylands: Flux and implications in the global atmospheric source/sink budget of methane. Glob. Planet. Change 72, p. 265–274.

Etiope, G., and Klusman, R. W., 2002, Geologic emissions of methane to the atmosphere: Chemosphere, v. 49, p. 777-789.

Etiope, G., Lassey, K. R., Klusman, R. W., and Boschi, E., 2008, Reappraisal of the fossil methane budget and related emission from geologic sources. Geoph. Res. Lett. 35.

Etiope, G., and Martinelli, G., 2002, Migration of carrier and trace gases in the geosphere: an overview. Physics of the Earth and Planetary Interiors 129, 185-204.
Ferry, J. G., 1993, Methanogenesis. Chapman & Hall, New York

Finger, K. L., 1983, Observations on the Lower Cretaceous Ostracode zone of Alberta: Bulletin of Canadian Petroleum Geology, v. 31, p. 326–337.

Fischer, A. G., 1975, Origin and growth of basins. In: Petroleum and global tectonics (Ed. by A.G. Fischer and S. Judson), Princetown University Press, 322 p.

Flowers, R. M., Bowring, S. A., and Reiners, P. W., 2006, Low long-term erosion rates and extreme continental stability documented by ancient (U-Th)/He dates: Geology, v. 34, no. 11, p. 925-928.

Forster, P., Ramaswamy, V., Artaxo, P., Berntsen, T., Betts, R., Fahey, D. W., Haywood, J., Lean, J., Lowe, D. C., Myhre, G., Nganga, J., Prinn, R., Raga, G., Schulz, M., and Dorland, V., 2007, Changes in Atmospheric Constituents and in

Radiative Forcing, in: Solomon, S., Qin, D., Manning, M., Chen, Z., Marquis, M., Averyt, K.B., M.Tignor, Miller, H.L. (Eds.), Climate Change 2007: The Physical Science Basis. Contribution of Working Group I to the Fourth Assessment Report of the Intergovernmental Panel on Climate Change. Cambridge University Press, Cambridge, United Kingdom and New York, NY, USA.

Fowler, M. G., Stasiuk, L. D., Hearn, M., and Obermajer, M., 2001, Devonian hydrocarbon source rocks and their derived oils in the Western Canada Sedimentary Basin: Bulletin of Canadian Petroleum Geology, v. 49, no. 1, p. 117-148.

-, 2004, Evidence for Gloeocapsomorpha prisca in Late Devonian source rocks from Southern Alberta, Canada: Organic Geochemistry, v. 35, no. 4, p. 425-441.

Frankenberg, C., Aben, L., Bergamaschi, P., Dlugokencky, E. J., Hees, R. v., Houwelling, S., Meer, P. v. d., Snel, R., and Tol, P., 2011, Global column-averaged methane mixing ratios from 2003 to 2009 as derived from SCIAMACHY: Trends and variability, Journal of Geophysical Research, v. 116, 12 p.

Garcia-Gil, S., 2003, A natural laboratory for shallow gas: the Rías Baixas (NW Spain): Geo-Marine Letters, v. 23, no. 3-4, p. 215-229.

Garven, G., 1989, A hydrogeologic model for the formation of the giant oil sands deposits of the Western Canada sedimentary basin: Am J Sci, v. 289, no. 2, p. 105-166.

Gautier, D. L., 2005, Kimmeridgian Shales Total Petroleum System of the North Sea Graben Province, U.S. Geological Survey, p. 24.

Gibson, D. W., 1975, Triassic rocks of the Rocky Mountain Foothills and Front Ranges of northeastern British Columbia and west-central Alberta: Geological Survey of Canada Bulletin, v. 247, 61 p.

Gingras, M., and Rokosh, D., A brief overview of the geology of heavy oil, bitumen and oil sand deposits, *in* Proceedings CSEG National Convention (abs.)2004.
Gornitz, V., 2009, Encyclopedia of Paleoclimatology and Ancient Environments, Springer, 2009, XXVIII, 1049 p.

Grasby, S. E., Chen, Z., Issler, D., and Stasiuk, L., 2009, Evidence for deep anaerobic biodegradation associated with rapid sedimentation and burial in the Beaufort-Mackenzie basin, Canada. Applied Geochemistry 24, p. 536-542.

Gunther, P. R., 1976, Palynomorph colour and dispersed coal particle reflectance from three Mackenzie delta boreholes: Geoscience and Man: 1976, v. 15, p. 35-39.

Hacquebard, P. A., 1977, Rank of coal as an index of organic metamorphism for oil and gas in Alberta, *in* Deroo, G., Powell, T. G., Tissot, B., and McCrossan, R. G., eds., The origin and migration of petroleum in the Western Canada Sedimentary Basin, Alberta. A geochemical and thermal maturation study, Volume 262, Geological Survey of Canada Bulletin, p. 11-22.

Halbouty, M. T., Meyerhoff, A. A., King, R. E., Dott, R. H., Sr., H. D. K., and Shabad, T., 1970, World's giant oil and gas fields, geologic factors affecting their formation, and basin classification, part I, giant oil and gas fields, in Geology of giant petroleum fields: AAPG Memoir 14, p. 502-528.

Hantschel, T., and Kauerauf, A. I., 2009, Fundamentals of Basin and Petroleum Systems Modeling. Springer. 476 p.

Hantschel, T., Kauerauf, A. I., and Wygrala, B., 2000, Finite element analysis and ray tracing modeling of petroleum migration: Marine and Petroleum Geology, v. 17, no. 7, p. 815-820.

Hayes, B. J. R., Christopher, J. E., Rosenthal, L., Los, G., McKercher, B., Minken, D., Tremblay, Y. M., and Fennell, J., 1994, Cretaceous Mannville Group of the

Western Canada Sedimentary Basin, *in* Mossop, G., and Shetsen, I., eds., Geological atlas of the Western Canada Sedimentary Basin: Calgary, Alberta, Canadian Society of Petroleum Geologists and Alberta Research Council, p. 317-334.

Head, I. M., Jones, D. M., and Larter, S. R., 2003, Biological activity in the deep subsurface and the origin of heavy oil: Nature, v. 426, no. 6964, p. 344-352.

Hedges, J. I., and Keil, R. G., 1995, Sedimentary organic matter preservation: an assessment and speculative synthesis. Marine Chemistry 49, p. 81–115.

Hein, F., and Cotterill, D., 2006, The Athabasca Oil Sands — A Regional Geological Perspective, Fort McMurray Area, Alberta, Canada: Natural Resources Research, v. 15, no. 2, p. 85-102.

Higley, D. K., Lewan, M., Roberts, L. N. R., and Henry, M. E., 2006, Petroleum System Modeling Capabilities for Use in Oil and Gas Resource Assessments: U.S. Geological Survey Open-File Report 2006-1024, 18 p.

Higley, D. K., Lewan, M. D., Roberts, L. N. R., and Henry, M., 2009, Timing and petroleum sources for the Lower Cretaceous Mannville Group oil sands of northern Alberta based on 4-D modeling: AAPG Bulletin, v. 93, no. 2, p. 203-230.

Hill, R. J., Tang, Y., Kaplan, I. R., and Jenden, P. D., 1996, The influence of pressure on the thermal cracking of oil. Energy & Fuels, 10(4), p. 873–882.

Hitchon, B., 1984, Geothermal gradients, hydrodynamics, and hydrocarbon occurrences, Alberta, Canada: AAPG Bulletin, v. 68, p. 713–743.

Hitchon, B., Bachu, S., and Underschultz, J. R., 1990, Regional subsurface hydrogeology, Peace River arch area, Alberta and British Columbia: Bulletin of Canadian Petroleum Geology, v. 38, no. A, p. 196–217.

Holba, A. G., Dzou, L. I. P., Hickey, J. J., Franks, S. G., May, S. J., and Lenney, T., 1996, Reservoir geochemistry of South Pass 61 Field, Gulf of Mexico: compositional heterogeneities reflecting filling history and biodegradation. Organic Geochemistry 24, p. 1179-1198.

Holba, A. G., Wright, L., Levinson, R., Huizinga, B., and Scheihing, M., 2004, Effects and impact of early-stage anaerobic biodegradation on Kuparuk River Field, Alaska. In: J.M. Cubitt, W.A. England, S.R. Larter (Eds.), Understanding Petroleum Reservoirs: Towards an Integrated Reservoir Engineering and Geochemical Approach, 237, Special Publications. Geological Society, London, p. 53-88.

Hornafius, J. S., Quigley, D., and Luyendyk, B. P., 1999, The world's most spectacular marine hydrocarbon seeps (Coal Oil Point, Santa Barbara Channel, California): Quantification of emissions: J. Geophys. Res., v. 104, p. 20703-20711.

Horsfield, B., 1989, Practical criteria for classifying kerogens: Some observations from pyrolysis-gas chromatography. Geochimica et Cosmochimica Acta, 53(4), p. 891–901.

Horstad, I., Larter, S. R., and Mills, N., 1992, A quantitative model of biological petroleum degradation within the Brent Group reservoir in the Gullfaks field, Norwegian North Sea. Organic Geochemistry 19 (1-3), p. 107–117.

Hovland, M., Gallagher, J. W., and Clennell, M. B., 1997, Gas hydrate and free gas volumes in marine sediments: Example from the Niger Delta front, Mar. Petrol. Geol., 14(3), p. 245–255.

Hovland, M., and Judd, A. G., 1988, Seabed Pockmarks and Seepages. Graham and Trotman, London. 293 p.

Hovland, M., and Sommerville, J. H., 1985, Characteristics of two natural gas seepages in the North Sea: Marine and Petroleum Geology, v. 2, p. 319-326.

Hu, K., Issler, D. R., and Jessop, A. M., 2010, Well temperature data compilation, correction and quality assessment for the Beaufort-Mackenzie Basin. Geological Survey of Canada Open File 6057.

Hubbard, S. M., Pemberton, S. G., and Howard, E. A., 1999, Regional geology and sedimentology of the basal Cretaceous Peace River Oil Sands deposit, north-central Alberta: Bulletin of Canadian Petroleum Geology, v. 47, no. 3, p. 270-297.

Hubbard, S. M., Smith, D. G., Nielsen, H., Leckie, D. A., Fustic, M., Spencer, R. J., and Bloom, L., 2011, Seismic geomorphology and sedimentology of a tidally influenced river deposit, Lower Cretaceous Athabasca oil sands, Alberta, Canada: AAPG Bulletin, v. 95, no. 7, p. 1123-1145.

Huff, K. F., 1978, Frontiers of world oil exploration: Oil and Gas Journal, v. 76, n. 40, p. 214-220.

Hunt, J. M., 1979, Petroleum Geochemistry and Geology. Freeman and Company, 617 p.

-, 1995, Petroleum Geochemsitry and Geology: New York, W. H. Freeman and Company, 743 p.

Hyndman, R. D., and Dallimore, S. R., 2001, Natural Gas Hydrate Studies in Canada, Canadian Society of Exploration Geophysicists, Recorder, 26, 11-20, 2001_.
Ibrahimbas, A., and Riediger, C., 2004, Hydrocarbon source rock potential as determined by Rock-Eval 6/TOC pyrolysis, NEBC and NW Alberta: Resource Development and Geoscience Branch Report, p. 7–17: http://www.em.gov.bc.ca/dl/Oilgas/COG/2004/ibrahimbas_riediger.pdf (accessed September 2010).

Ingersoll, R. V., 1988, Tectonics of sedimentary basins. Geological Society of America Bulletin, 100, p. 1704–1719.

Ingersoll, R. V., 2012, Tectonics of Sedimentary Basins, with Revised Nomenclature, Tectonics of Sedimentary Basins, John Wiley & Sons, Ltd, p. 1-43.

Ingersoll, R. V., and Busby, C. J., 1995, Tectonics of sedimentary basins, in Busby, C.J., and Ingersoll, R.V., eds., Tectonics of sedimentary basins. Oxford, Blackwell Science, p. 1–51.

Issler, D., Willett, S., Beaumont, C., Donelick, R., and Grist, A., 1999, Paleotemperature history of two transects across the Western Canadian Sedimentary Basin: Constraints from apatite fission track analysis: Bulletin of Canadian Petroleum Geology, v. 47, no. 4, p. 475-486.

Issler, D. R., and Jessop, A. M., 2011, Thermal conductivity analysis of Cenozoic, Mesozoic and Paleozoic core samples, Beaufort-Mackenzie Basin, northern Canada. Geological Survey of Canada Open File 6734, 128 p.

Issler, D. R., and Snowdon, L. R., 1990, Hydrocarbon generation kinetics and thermal modeling, Beaufort-Mackenzie Basin: Bulletin of Canadian Petroleum Geology, v. 38, p. 1-16.

James, D. P., and Baxter, A. J., 1988, Stratigraphy and sedimentology of the Kugmallit Formation, Nipterk structure: Beaufort-Mackenzie Basin, Canada, *in* James, D. P., and Leckie, D. A., eds., Sequences, stratigraphy, sedimentology: Surface and subsurface: Canadian Society of Petroleum Geologists Memoir 15, p. 117– 136.

Jensen, R. P., and Doré, A. G., 1993, A recent Norwegian Shelf heating event - fact or fantasy? Basin modelling; advances and applications: Proceedings of the Norwegian Petroleum Society conference, p. 85-106.

Jobson, A. M., Cook, F. D., and Westlake, D. W. S., 1979, Interaction of aerobic and anaerobic bacteria in petroleum biodegradation. Chemical Geology 24, p. 355–365.

Johnson, H. D., and Fisher, M. J., 2009, North Sea Plays: Geological Controls on Hydrocarbon Distribution, Petroleum Geology of the North Sea, Blackwell Science Ltd, p. 463-547.

Jones, D. M., Head, I. M., Gray, N. D., Adams, J. J., Rowan, A. K., Aitken, C. M., Bennett, B., Huang, H., Brown, A., Bowler, B. F. J., Oldenburg, T., Erdmann, M., and Larter, S. R., 2008, Crude-oil biodegradation via methanogenesis in subsurface petroleum reservoirs. Nature 451, 176-181.

Judd, A., Davies, G., Wilson, J., Holmes, R., Baron, G., and Bryden, I., 1997, Contributions to atmospheric methane by natural seepages on the U.K. continental shelf: Marine Geology, v. 140, p. 427-455.

Judd, A. G., 2004, Natural seabed gas seeps as sources of atmospheric methane: Environmental Geology, v. 46, p. 988-996.

Judd, A. G., Hovland, M., Dimitrov, L. I., García Gil, S., and Jukes, V., 2002, The geological methane budget at Continental Margins and its influence on climate change. Geofluids 2, p. 109-126.

Kennett, J. P., and Stott, L. D., 1991, Abrupt deep-sea warming, palaeoceanographic changes and benthic extinctions at the end of the Palaeocene: Nature, v. 353, p. 225-229.

Killops, S. D., and Killops, V. J., 1993, An introduction to organic geochemistry, New York, John Wiley.

Kim, S., Stanford, L. A., Rodgers, R. P., Marshall, A. G., Walters, C. C., Qian, K., Wenger, L. M., and Mankiewicz, P., 2005, Microbial alteration of the acidic and neutral polar NSO compounds revealed by Fourier transform ion cyclotron resonance mass spectrometry. Organic Geochemistry 36, p. 1117-1134.

King, G. M., and Adamsen, A. P. S., 1992, Effects of temperature on methane consumption in a forest soil and pure cultures of the methanotroph Methylomonas rubra, Applied and Environmental Microbiology, v. 58, p. 2758-2763.

Kingston, D. R., Dishroon, C. P., and Williams, P. A., 1983, Global basin classification system. AAPG Bulletin 67, p. 2175-2193.

Klemme, H. D., 1971, What giants and their basins have in common: Oil and Gas Journal, v. 69, n. 9, p. 85-90.

-, 1975, Giant oil fields related to their geologic setting—a possible guide to exploration: Bulletin of Canadian Petroleum Geology, v. 23, p. 30-66.

-, 1980, Petroleum basins - classification and characteristics. J. petrol. Geol., V. 3, p. 187-207.

Klemme, H. D., and Ulmishek, G. F., 1991, Effective petroleum source rocks of the world; stratigraphic distribution and controlling depositional factors: AAPG Bulletin, v. 75, no. 12, p. 1809-1851.

Knebel, G. M., and Rodriguez-Eraso, G., 1956, Habitat of some oil: AAPG Bulletin, v. 40, p. 547-561.

Kohlruss, D., Pedersen, P., and Chi, G., 2010, Preliminary facies characterization of the bitumen-bearing Lower Cretaceous Dina Member (Mannville Group) of northwestern Saskatchewan, Saskatchewan Geological Survey and Saskatchewan Ministry of Energy and Resources, Summary of Investigations 2010, 9 p.

Kroeger, K. F., di Primio, R., and Horsfield, B., 2009, Hydrocarbon flow modeling in complex structures (Mackenzie Basin, Canada): AAPG Bulletin, v. 93, no. 9, p. 1209-1234.

Kroeger, K. F., Ondrak, R., di Primio, R., and Horsfield, B., 2008, A three-dimensional insight into the Mackenzie Basin (Canada): Implications for the thermal history and hydrocarbon generation potential of Tertiary deltaic sequences: AAPG Bulletin, 92, 2, p. 225-247.

Kroeger, K. F., Primio, R. d., and Horsfield, B., 2011, Atmospheric methane from organic carbon mobilization in sedimentary basins — The sleeping giant?: Earth-Science Reviews, v. 107, p. 423-442.

Kuhlmann, G., Adams, S., Anka, Z., Campher, C., Primio, R. d., and Horsfield, B., 2011, 3D petroleum systems modelling within a passive margin setting, generation, Orange Basin, blocks 3/4, offshore South Africa — Implications for gas generation, migration and leakage: South African Journal of Geology, v. 114, p. 387-414.

Kumar, N., and Magara, K., 1979, Thickness of removed sedimentary rocks, paleopore pressure, and paleotemperature, southwestern part of Western Canada Basin; discussion and reply: AAPG Bulletin, v. 63, no. 5, p. 812-815.

Kuo, L. C., 1997, Gas exsolution during fluid migration and its relation to overpressure and petroleum accumulation. Marine and Petroleum Geology 14, p. 221-229.

Kvenvolden, K., 1995, A review of the geochemistry of methane in natural gas hydrate. Org. Geochem. 23, 997–1008. (doi:10.1016/0146-6380(96)00002-2).

Kvenvolden, K. A., 1993, A primer on gas hydrates. In: Howel, D.G. (Ed.), The Future of Energy Gases. Professional Paper-Geological Survey (U.S.), vol. 1570, p. 279 – 291.

Kvenvolden, K. A., and Rogers, B. W., 2005, Gaia's breath–global methane exhalations. Marine Petroleum Geol. 22, p. 579–90.

Lane, L., 2002, Tectonic evolution of the Canadian Beaufort Sea-Mackenzie Delta Region: A brief review: GSEG Recoder, v. 49, p. 49-55.

Larter, S., Adams, J., Gates, I. D., Bennett, B., and Huang, H., 2008, The Origin, Prediction and Impact of Oil Viscosity Heterogeneity on the Production Characteristics of Tar Sand and Heavy Oil Reservoirs, v. 47, no. 1.

Larter, S., Huang, H., Adams, J., Bennett, B., Jokanola, O., Oldenburg, T., Jones, M., Head, I., Riediger, C., and Fowler, M., 2006, The controls on the composition of biodegraded oils in the deep subsurface: Part II—Geological controls on subsurface biodegradation fluxes and constraints on reservoir-fluid property prediction: AAPG Bulletin, v. 90, p. 921-938.

Larter, S., Huang, H., Adams, J., Bennett, B., and Snowdon, L. R., 2012, A practical biodegradation scale for use in reservoir geochemical studies of biodegraded oils: Organic Geochemistry, v. 45, no. 0, p. 66-76.

Larter, S., Wilhelms, A., Head, I., Koopmans, M., Aplin, A., Primio, R. D., Zwach, C., Erdmann, M., and Telnaes, N., 2003, The controls on the composition of biodegraded oils in the deep subsurface—part 1: biodegradation rates in petroleum reservoirs: Organic Geochemistry, v. 34, p. 601-613.

Larter, S. R., Adams, J., Gates, I. D., Bennett, B., and Huang, H., 2006, The Origin, Prediction and Impact of Oil Viscosity Heterogeneity on the Production Characteristics of Tar Sand and Heavy Oil Reservoirs, Canadian International Petroleum Conference: Calgary, Alberta.

Larter, S. R., Head, I. M., Huang, H., Bennett, B., Jones, M., Aplin, A. C., Murray, A., Erdmann, M., Wilhelms, A., and Di Primio, R., 2005, Biodegradation, gas destruction and methane generation in deep subsurface petroleum reservoirs: an overview, p. 633-639.

Leckie, D. A., Bhattacharya, J. P., Bloch, J., Gilboy, C. F., and Norris, B., 2008, Cretaceous Colorado/Alberta Group of the Western Canada Sedimentary Basin, *in* Mossop, G., and Shetson, I., eds., Geological atlas of the Western Canada Sedimentary Basin: Calgary,Alberta, Canadian Society of Petroleum Geologists and Alberta Research Council, p. 455-468.

Leckie, D. A., and Smith, D., 1992, Regional setting, evolution, and depositional cycles of the Western Canada Basin, in R. Macqueen and D. A. Leckie, eds., Foreland basins and fold belts: AAPG Memoir 55, p. 9–46.

Leenheer, M. J., 1984, Mississippian Bakken and equivalent formations as source rocks in the Western Canadian Basin: Organic Geochemistry, v. 6, p. 521-532.

Leifer, I., Kamerling, M., Luyendyk, B., and Wilson, D., 2010, Geologic control of natural marine hydrocarbon seep emissions, Coal Oil Point seep field, California: Geo-Marine Letters, v. 30, no. 3-4, p. 331-338.

Lewan, M. D., and E., R. T., 2002, Comparison of petroleum generation kinetics by isothermal hydrous and nonisothermal open-system pyrolysis: Organic Geochemistry, v. 33, p. 1457–1475, doi:10.1016/S0146-6380(02)00182-1.

Lewan, M. D., Higley, D. K., Roberts, L. N. R., and Henry, M. E., 2008, Source of heavy oils and tars in the Athabasca oil sands based on geochemistry and 4-D basin modeling: Goldschmidt Conference, Vancouver, Canada, p. A538.

Lewan, M. D., and Ruble, T. E., 2002, Comparison of petroleum generation kinetics by isothermal hydrous and nonisothermal open-system pyrolysis: Organic Geochemistry, v. 33, no. 12, p. 1457-1475.

Li, Y. H., 1972, Geochemical mass balance among lithosphere, hydrosphere, and atmosphere. American Journal of Science, v. 272, p. 119-137.

Lüning, S., Craig, J., Loydell, D. K., Storch, P., and Fitches, B., 2000, Lower Silurian [`]hot shales' in North Africa and Arabia: regional distribution and depositional model: Earth-Science Reviews, v. 49, no. 1-4, p. 121-200.

Lüning, S., Kolonic, S., Belhadj, E. M., Belhadj, Z., Cota, L., Baric, G., and Wagner, T., 2004, Integrated depositional model for the Cenomanian-Turonian organic-rich strata in North Africa: Earth-Science Reviews, v. 64, no. 1-2, p. 51-117.

MacDonald, G., 1990, Role of methane clathrates in past and future climates, Clim. Change, 16, p. 247–281.

Macgregor, D. S., 1996, The hydrocarbon systems of North Africa: Marine and Petroleum Geology, v. 13, no. 3, p. 329-340.

Mack, G. H., and Jerzykiewicz, T., 1989, Provenance of post-Wapiabi sandstones and its implications for Campanian to Paleocene tectonic history of the southern Canadian Cordillera: Canadian Journal of Earth Sciences, v. 26, no. 4, p. 665-676.

Magara, K., 1976, Thickness of removed sedimentary rocks, paleopore pressure, and paleotemperature, southwestern part of Western Canada Basin: AAPG Bulletin, v. 60, no. 4, p. 554-565.

Magoon, L. B., 1987, The petroleum system – a classification scheme for research, exploration, and resource assessment. U.S. Geological Survey Bulletin, 1870, p. 2-15.

Magoon, L. B., and Dow, W. G., 1994, The Petroleum System-from source to trap: AAPG Memoir 60.

Majorowicz, J. A., and Osadetz, K. G., 2001, Gas Hydrate Distribution and Volume in Canada: AAPG Bulletin, v. 85, no. 7, p. 1211-1230.

Majorowicz, J. A., Osadetz, K. G., and Safanda, J., 2008, Onset and stability of gas hydrates under permafrost in an environment of surface climatic change — past and future. In: Proceedings of the 6th International Conference on Gas Hydrates (ICGH VI, 2008), Vancouver, British Columbia, Canada, July 6–10, 2008. CD-ROM Proceedings Paper 5585.pdf, 14 p.

McCarthy, K., Rojas, K., Niemann, M., Palmowski, D., Peters, K., and Stankiewicz, A., 2011, Basin petroleum geochemistry for source rock evaluation. Oilfield Review, 23, p. 32-43.

McKenzie, A. S., 1987, The expulsion of petroleum from Kimmeridge Clay source-rocks in the area of the Brae oilfield, UK continental shelf, in: Petroleum geology of North West Europe. Proceedings of the 3rd conference on petroleum geology of North West Europe, London, 26-29 October, p. 865-877.

McLean, J. R., 1977, The Cadomin Formation; stratigraphy, sedimentology, and tectonic implications: Bulletin of Canadian Petroleum Geology, v. 25, no. 4, p. 792-827.

Meakin, P., Wagner, G., Vedvik, A., Amundsen, H., Feder, J., and Jossang, T., 2000, Invasion percolation and secondary migration: Experiments and simulations: Marine and Petroleum Geology, v. 17, no. 7, p. 777–795, doi:10.1016/S0264-8172(99)00069-0.

Milkov, A. V., 2000, Worldwide distribution of submarine mud volcanoes and associated gas hydrates. Marine Geology 167, p. 29–42.

-, 2004, Global estimates of hydrate-bound gas in marine sediments: how much is really out there? Earth Sci. Rev. 66, 183–197. (doi:10.1016/j.earscirev.2003.11.002).

Milkov, A. V., 2011, Worldwide distribution and significance of secondary microbial methane formed during petroleum biodegradation in conventional reservoirs: Organic Geochemistry, v. 42, p. 184-207.

Milkov, A. V., and Sassen, R., 2002, Economic geology of offshore gas hydrate accumulations and provinces, Mar. Petrol. Geol., 19(1), p. 1–11.

Miller, B. M., 1987, The muPETROL expert system for classifying world sedimentary basins. USGS Publication. 87 p.

Milner, C. W. D., Rogers, M. A., and Evans, C. R., 1977, Petroleum transformations in reservoirs, J. Geochem. Explor. 7, No. 2, p. 101.

Moshier, S. O., and Waples, D. W., 1985, Quantitative evaluation of Lower Cretaceous Mannville Group as source rock for Alberta's oil sands: AAPG Bulletin, v. 69, no. 2, p. 161-172.

Mossop, G., and Shetsen, I., 1994, Geological atlas of the Western Canada Sedimentary Basin, Calgary, Alberta, Canadian Society of Petroleum Geologists and Alberta Research Council.

Naeth, J., Primio, R. d., Horsfield, B., Schaefer, R. G., Shannon, P. M., Bailey, W. R., and Henriet, J. P., 2005, Hydrocarbon seepage and carbonate mound formation: a basin modelling study from the Porcupine Basin (offshore Ireland): Journal of Petroleum Geology, v. 28, p. 147-166.

Nehring, R., 1978, Giant Oil Fields and World Oil Resources. Rand Corporation Report R-2284, CIA. .

Neumann, V., 2007, Numerical modeling and phase prediction in deep overpressured basinal settings of the Central Graben, North Sea, TU Berlin, Berlin, 192 p.

Nurkowski, J. R., 1984, Coal quality, coal rank variation and its relation to reconstructed overburden, Upper Cretaceous and Tertiary plains coals, Alberta, Canada: AAPG Bulletin, v. 68, no. 3, p. 285-295.

Orr, W. L., 2001, Evaluating kerogen sulfur content from crude oil properties: cooperative Monterey organic geochemistry study, *in* Isaacs, C., and Rullkötter, J., eds., The Monterey Formation; from rocks to molecules: New York, Columbia University Press, p. 348-367.

Osadetz, K. G., and Chen, Z., 2005, A re-examination of Beaufort Sea-Mackenzie delta basin gas hydrate resource potential using a petroleum play approach, Proceedings of the 5th International Conference on Gas Hydrate: June 13-16, 2005, Trondheim, Norway, vol. 2.

Osadetz, K. G., and Chen, Z., 2010, A re-evaluation of Beaufort Sea-Mackenzie Delta basin gas hydrate resource potential: petroleum system approaches to non-conventional gas resource appraisal and geologically-sourced methane flux: Bulletin of Canadian Petroleum Geology, v. 58, no. 1, p. 56-71.

Osadetz, K. G., Dixon, J., Dietrich, J. R., Snowdon, L. R., Dallimore, S. R., and Majorowicz, J. A., 2003, A Review of Mackenzie Delta-Beaufort Sea Petroleum Province Conventional and Non-conventional (gas hydrate) Petroleum Reserves and Undiscovered Resources: a contribution to the resource assessment of the proposed Mackenzie Delta-Beaufort Sea Marine Protected Areas: http://www.dfo-mpo.gc.ca/Library/281345.pdf.

Ostanin, I., Anka, Z., Primio, R. d., and Bernal, A., 2013, Hydrocarbon plumbing systems above the Snøhvit gas field: structural control and implications for thermogenic methane leakage in the Hammerfest Basin, SW Barents Sea. Marine &. Pet. Geol. v. 43, p. 127-146. Doi: http://dx.doi.org/10.1016/j.marpetgeo.2013.02.012.

Paton, D. A., Primio, R. d., Kuhlmann, G., Spuy, D. v. d., and Horsfield, B., 2007, Insights into the Petroleum System Evolution of the southern Orange Basin, South Africa: South African Journal of Geology, v. 110, p. 261-274.

PDVSA, 2006, Contact with the new PDVSA. A newsletter about Venezuela's National Oil Industry, Volume 8, p. 10.

Pegaz-Fiornet, S., Carpentier, B., Michel, A., and Wolf, S., 2012, Comparison between the different approaches of secondary and tertiary hydrocarbon migration modeling in basin simulators, in K. E. Peters, D. J. Curry, and M. Kacewicz, eds., Basin Modeling: New Horizons in Research and Applications: AAPG Hedberg Series, no. 4, p. 221–236.

Peng, D. Y., and Robinson, D. B., 1976, A New Two-Constant Equation of State, Ind. Eng. Chem. Fundam., 15, 59-64.

Pepper, A. S., and Corvi, P. J., 1995, Simple kinetic models of petroleum formation. Part I: oil and gas generation from kerogen: Marine and Petroleum Geology, v. 12, p. 291-319.

Perrodon, A., 1971, Essai de classification des bassins sedementaires: Nancy, France, Sciences de la Terre, V. 16, p. 195-227.

Perrodon, A., 1978, Coup d'oeil sur les provinces geantes d'hydrocarbures. Revue del'Institut Francois du Petrole, 33, p. 493-513.

Perrodon, A., 1992, Petroleum systems: Models and applications. Journal of Petroleum Geology, 15. p. 319-326.

Peters, K., Walters, C., and Moldowan, J., 2005, The Biomarker Guide II. Biomarkers and Isotopes in Petroleum Systems and Earth History. Cambridge University Press, Cambridge, UK.

Peters, K. E., and Moldowan, J. M., 1993, The biomarker guide: Interpreting molecular fossils in petroleum and ancient sediments, Englewood Cliffs, New Jersey, Prentice Hall, 363 p.

Peters, K. E., Schenk, O., and Wygrala, B., 2009, Exploration Paradigm Shift: The Dynamic Petroleum System Concept. Swiss Bulletin fuer Angewandte Geologie. Vol. 14/1+2, p. 65-71.

Pitman, J. K., Steinshouer, D., and Lewan, M. D., 2004, Petroleum generation and migration in the Mesopotamian Basin and Zagros fold belt of Iraq: Results from a basin-modeling study: GeoArabia, v. 9, p. 41-72.

Podruski, J. A., Barclay, J. E., Hamblin, A. P., Lee, A. P., Osadetz, K. G., Procter, R. M., and Taylor, G. C., 1988, Conventional oil resources of Western Canada: light and medium, Geological Survey Canada, p. 87-126.

Poulton, T. P., Tittemore, J., and Dolby, G., 1990, Jurassic strata of northwestern (and west-central) Alberta and northeastern British Columbia: Bulletin of Canadian Petroleum Geology, v. 38A, p. 159-175.

Prabhakara, C., and Dalu, G., 1976, Journal of Geophysical Research, v. 81, p. 3719-3724.

Rabus, R., Wilkes, H., Behrends, A., Armstroff, A., Fischer, T., and Widdel, F., 2001, Anaerobic initial reaction of n-alkanes in a denitrifying bacterium: Evidence for (1-methylpentyl)succinate as initial product and for involvement of an organic radical in n-hexane metabolism. Journal of Bacteriology 183, p. 1707-1715.

Ranger, M. J., 2006, The northeastern sector of the Lower Cretaceous Athabasca oil-sands basin: Facies and fluids, *in* Gilboy, C. F., and Whittaker, S. G., eds., Saskatchewan and Northern Plains Oil & Gas Symposium 2006: Saskatchewan Geological Society Special Publication 19, p. 249-256.

Reading, H. G., 1982, Sedimentary Basins and global tectonics. Proc. geol. Assoc. 93, p. 321-350.

Reynolds, T., 1994, Quantitative analysis of submarine fans in the Tertiary of the North Sea Basin: Marine and Petroleum Geology, v. 11, no. 2, p. 202-207.

Richards, B. C., Barclay, J. E., Bryan, D., Hartling, A., Henderson, C. M., and Hinds, R. C., 1994, Carboniferous strata of the Western Canada sedimentary basin, in G. Mossop and I. Shetsen, eds., Geological atlas of the Western Canada sedimentary basin: Calgary, Alberta, Canadian Society of Petroleum Geologists and Alberta Research Council.

Riediger, C. L., 1994, Migration of ‘‘Nordegg’’ oil in the Western Canada Basin. How much and how far?: Bulletin of Canadian Petroleum Geology, v. 42, no. 1, p. 63-73.

-, 2002, Hydrocarbon source rock potential and comments on correlation of the Lower Jurassic Poker Chip Shale, west-central Alberta: Bulletin of Canadian Petroleum Geology, v. 50, p. 263–276, doi:10.2113/50.2.263.

Riediger, C. L., Brooks, P. W., Fowler, M. G., and Snowdon, L. R., 1990b, Lower and Middle Triassic source rocks, thermal maturation, and oil-source rock correlations in the Peace River embayment area, Alberta and British Columbia: Bulletin of Canadian Petroleum Geology, v. 38A, p. 218–235.

Riediger, C. L., Brooks, P. W., Fowler, M. G., and Snowdon, L. R., 1990b, Lower and Middle Triassic source rocks, thermal maturation, and oil-source rock correlations in the Peace River embayment area, Alberta and British Columbia: Bulletin of Canadian Petroleum Geology, v. 38A, p. 218-235.

Riediger, C. L., and Coniglio, M., 1992, Early diagenetic calcites and associated bitumens in the “Nordegg Member”: Implications for Jurassic paleogeography of the Western Canada sedimentary basin: Bulletin of Canadian Petroleum Geology, v. 40, p. 381–394.

Riediger, C. L., Fowler, M. G., and Snowdon, L. R., 1997, Organic geochemistry of the Lower Cretaceous Ostracode zone, a brackish/nonmarine source for some lower Mannville oils in southeastern Alberta: Canadian Society of Petroleum Geology Memoir 18, p. 93–102.

Riediger, C. L., Fowler, M. G., Snowdon, L. R., Goodarzi, F., and Brooks, P. W., 1990a, Source rock analysis of the Lower Jurassic ‘‘Nordegg Member’’ and oil-source correlations, northwestern Alberta and northeastern British Columbia: Bulletin of Canadian Petroleum Geology, v. 38A, p. 236-249.

Riediger, C. L., Fowler, M. G., Snowdon, L. R., R.Mac-Donald, and Sherwin, M. D., 1999, Origin and alteration of Lower Cretaceous Mannville Group oils from the Provost oil field, east-central Alberta, Canada: Bulletin of Canadian Petroleum Geology, v. 47, p. 43–62.

Riediger, C. L., Ness, S., Fowler, M., and Akpulat, N. T., 2001, Timing of oil generation and migration, northeastern British Columbia and southern Alberta—Significance for understanding the development of the eastern Alberta tar sands deposits (abs.): AAPG Annual Convention Official Program, v. 10, p. A168.

Roberts, L. N. R., Higley, D. K., and Henry, M. E., 2005, Input data used to generate one-dimensional burial history models, central Alberta, Canada: U.S. Geological Survey Open-File Report Series 2005-1412, p. 4-5.

Robl, T. L., Barron, L. S., Koppenaal, D. W., and Bland, A. E., The geology and geochemistry of Devonian shales in south and west-central Kentucky, *in* Proceedings Proceedings of the 1983 Eastern Oil Shale Symposium, Lexington, KY, 1983, p. 59-71.

Rodkin, A. D., and Lemmen, D. S., 2000, Glacial history of the Mackenzie region, *in* Dyke, L. D., and Brooks, G. R., eds., The physical environment of the Mackenzie

Valley, Northwest Territories: a base line for the assessment of environmental change, Volume 542, Geological Survey of Canada, Bulletin, p. 11-20.

Rodrigues, E., Primio, R. d., Anka, Z., Stoddart, D., and Horsfield, B., 2013, 3D-Basin modelling of the Hammerfest Basin (southwestern Barents Sea): A quantitative assessment of petroleum generation, migration and leakage. Marine & Petroleum Geology. v. 45, p. 281-303.

Ross, D. J. K., and Bustin, R. M., 2006, Sediment geochemistry of the Lower Jurassic Gordondale Member, northeastern British Columbia: Bulletin of Canadian Petroleum Geology, v. 54, no. 4, p. 337-365.

Rueter, P., Rabus, R., Wilkes, H., Aeckersberg, F., Rainey, F. A., Jannasch, H. W., and Widdel, F., 1994, Anaerobic oxidation of hydrocarbons in crude oil by new types of sulphate-reducing bacteria. Nature 372, p. 455-458.

Röling, W. F. M., Head, I. M., and Larter, S. R., 2003, The microbiology of hydrocarbon degradation in subsurface petroleum reservoirs: perspectives and prospects. Res .Microbiol. 154, p. 321-328.

Saison, A., 2010, Petroleum Potential of Cretaceous and Tertiary sediments of the Mackenzie Delta (Canada): Influence of organic facies variations and gas system: TU Berlin.

Salisbury, R. S. K., 1990, Shallow gas reservoirs and migration paths over a Central North Sea diapir, in D. A. Ardus and C. D. Green, eds., Safety in offshore drilling: the role of shallow gas surveys: Underwater Technology, Ocean Science and Offshore Engineering, v. 25, p. 167-180.

Savoy, L. E., Harris, A. G., and Mountjoy, E. W., 1999, Extension of lithofacies and conodont biofacies models of Late Devonian to Early Carboniferous carbonate ramp

and black shale systems, southern Canadian Rocky Mountains: Canadian Journal of Earth Sciences, v. 36, no. 8, p. 1281-1298.

Schenk, H. J., di Primio, R., and Horsfield, B., 1997, The conversion of oil into gas in petroleum reservoirs. Part 1, comparative kinetic investigation of gas generation from crude oils of lacustrine, marine and fluviodeltaic origin by programmed-temperature closed-system pyrolysis. Organic Geochemistry, 26. p. 467–481.

Schimel, D. S., 1995, Terrestrial ecosystems and the carbon cycle. Global Change Biology, v. 1, p. 77-91.

Schink, B., 1997, Energetics of syntrophic cooperation in methanogenic degradation. Microbiol. Mol. Biol. Rev. 61, p. 262-280.

Schlesinger, W. H., 1997, Biogeochemistry. An Analysis of Global Change. Second Edition. Academic Press. San Diego, USA, p. 358 - 382.

Schlumberger, 2009, PetroMod 3D Basic Tutorial: Ritterstrasse, Aachen, Germany.

-, 2010, PetroMod 3D Advanced Tutorial: Ritterstrasse, Aachen, Germany.

-, 2011, PetroMod 2011.1.1 user guide: Aachen, Germany, Ritterstrasse.

Schmoker, J. W., 1980, Organic content of Devonian shale in western Appalachian Basin: AAPG Bulletin, v. 64, p. 2156-2165.

Selby, D., Finlay, A. J., and Osborne, M. J., 2011, Identifying the when and where of oil generation using platinum, palladium, osmium and rhenium geochemistry, Goldschmidt Conference: Prague, p. 1834.

Sheldon, R. P., 1967, Long-distance migration of oil in Wyoming: Mountain Geologist, v. 4, p. 53–65.

Shmonova, N. I., and Shaks, I. A., 1971, Alteration of the asphalt-tar fractions of petroleum under the effect of micro-organisms under aerobic and anaerobic conditions. Geologorazved Institute Translation 294, p. 4–19.

Sippel, J., Scheck-Wenderoth, M., Lewerenz, B., and Klitzke, P., 2014, Deep versus shallow controlling factors of the crustal thermal field – insights from 3D modelling of the Beaufort-Mackenzie Basin (Arctic Canada), Basin Research (*in press*). DOI: 10.1111/bre.12075.

Sippel, J., Scheck-Wenderoth, M., Lewerenz, B., and Kroeger, K. F., 2012, A crust-scale 3D structural model of the Beaufort-Mackenzie Basin (Arctic Canada): Tectonophysics. Available online 12 November 2012, no. 0.

Skaare, B., Wilkes, H., Vieth, A., Rein, E., and Barth, T., 2007, Alteration of crude oils from the Troll area by biodegradation: Analysis of oil and water samples. Organic Geochemistry 38, p. 1865-1883.

Skogseid, J., Pedersen, T., Eldholm, and Larsen, B. T., 1992, Tectonism and magmatism during NE Atlantic continental break-up: the Vøring Margin. Geol. Soc. Spec. Publ. 68, p. 305–320.

Sloan, E. D., 1998, Clathrate hydrates of natural gas, Marcel Dekker, New York.

Smallwood, J. R., and Maresh, J., 2002, The properties, morphology and distribution of igneous sills: modelling, borehole data and 3D seismic from the Faroe-Shetland area. Geol. Soc. Spec. Publ. 197, p. 271–306.

Smith, D. G., 2008, Paleogeographic evolution of the Western Canada Basin, in G. Mossop, and I. Shetsen, eds., Geological atlas of the Western Canada Sedimentary Basin: Calgary, Alberta, Canadian Society of Petroleum Geologists and Alberta Research Council, p. 455-468.

Smith, M. G., and Bustin, R. M., 2000, Late Devonian and Early Mississippian Bakken and Exshaw Black Shale Source Rocks, Western Canada Sedimentary Basin: A Sequence Stratigraphic Interpretation: AAPG Bulletin, v. 84, no. 7, p. 940-960.

Smith, S. L., and Burgess, M. M., 2002, A digital database of permafrost thickness in Canada. Geological Survey of Canada, Open File 4173, p. 38.

Smith, S. L., and Judge, A. S., 1995, Estimate of methane hydrate volumes in the Beaufort-Mackenzie region, Northwest Territories, Current Research 1995, Part B, Geological Survey of Canada, p. 81-88.

Snowdon, L. R., 1990, Rock-Eval/TOC results from 29 Beaufort-Mackenzie wells: Geological Survey of Canada Open File Report 2192, p. 209.

Stainforth, J. G., and Reinders, J. E. A., 1990, Primary migration of hydrocarbons by diffusion through organic matter networks, and its effect on oil and gas generation. Organic Geochemistry, v. 1-3, p. 61-75.

Stasiuk, L. D., and Fowler, M. G., 2004, Organic facies in Devonian and Mississippian strata of Western Canada Sedimentary Basin: relation to kerogen type, paleoenvironment, and paleogeography: Bulletin of Canadian Petroleum Geology, v. 52, no. 3, p. 345-410.

Steele, L. P., Dlugokencky, E. J., Lang, P. M., Tans, P. P., Martin, R. C., and Masarie, K. A., 1992, Slowing down of the global accumulation of atmospheric methane during the 1980s. Nature, v. 358, p. 313-316.

Steiner, J., Williams, G., and Dickie, G., Coal deposits of the Alberta plains, *in* Proceedings Proceedings of the 1st Geological Conference on Western Canadian Coal1972, Volume 60, Alberta Research Council Information Series, p. 85-96.

Stetter, K. O., Huber, R., Blochl, E., Kurr, M., Eden, R. D., Fielder, M., Cash, H., and Vance, I., 1993, Hyperthermophilic archaea are thriving in deep North Sea and Alaskan oil reservoirs: Nature, v. 365, no. 6448, p. 743-745.

Stoakes, F. A., 1980, Nature and control of shale basin fill and its effect on reef growth and termination: Upper Devonian Duvernay and Ireton formations of Alberta, Canada: Bulletin of Canadian Petroleum Geology, v. 28, p. 345–410.

Svensen, H., Planke, S., Malthe-Sorenssen, A., Jamtveit, B., Myklebust, R., Rasmussen Eidem, T., and Rey, S. S., 2004, Release of methane from a volcanic basin as a mechanism for initial Eocene global warming: Nature, v. 429, no. 6991, p. 542-545.

Swarbrick, R. E., Osborne, M. J., Grunberger, D., Yardley, G. S., Macleod, G., Aplin, A. C., Larter, S. R., Knight, I., and Auld, H. A., 2000, Integrated study of the Judy Field (Block 30/7a) — an overpressured Central North Sea oil/gas field: Marine and Petroleum Geology, v. 17, p. 993-1010.

Switzer, S. B., Holland, W. G., Christie, D. S., Graf, G. C., Hedinger, A. S., McAuley, R. J., Wierzbicki, R. A., and Packard, J. J., 1994, Devonian Woodbend–Winterburn strata of the Western Canada sedimentary basin, *in* Mossop, G., and Shetson, I., eds., Geological atlas of the Western Canada Sedimentary Basin: Calgary, Alberta, Canadian Society of Petroleum Geologists and Alberta Research Council, p. 163-202.

Taylor, C. E., Lekse, J., and English, N., 2004, NETL'S Methane Hydrate Research. Proceedings Of AAPG Hedberg Conference Gas Hydrates: Energy Resource Potential and Associated Geologic Hazards. September 12–16, 2004. Vancouver, BC, Canada.

Taylor, M. H., Dillon, W. P., and Pecher, I. A., 2000, Trapping and migration of methane associated with the gas hydrate stability zone at the Blake Ridge Diapir: new insights from seismic data: Marine Geology, v. 164, no. 1–2, p. 79-89.

Thiede, J., Winkler, A., Wolf-Welling, T., Eldholm, O., Myhre, A. M., Baumann, K. H., Henrich, R., and Stein, R., 1998, Late Cenozoic history of the polar North

Atlantic: results from ocean drilling. Quat. Sci. Rev., 17:185–208. doi:10.1016/S0277-3791(97)00076-0.

Tissot, B. P., Pelet, R., and Ungerer, P., 1987, Thermal history of sedimentary basins, maturation indices and kinetics of oil and gas generation. In: American Association of Petroleum Geologists Bulletin vol. 71, p. 1445-1466.

Tissot, B. P., and Welte, D. H., 1984, Petroleum formation and occurrence, Berlin-New York, Springer-Verlag, 699 p.

Trenberth, K. E., and Guillermot, C. J., 1994, The total mass of the atmosphere. Journal of Geophysical Research, v. 99, p. 23079-23088.

Uspenskaya, N. Y., 1967, Principles of oil and gas territories, subdivisions, and the classification of oil and gas accumulations: Amsterdam, Elsevier Publishing Co., 7th World Petroleum Congress, Proceedings, v. 2, p. 961-969.

Vandenbroucke, M., Behar, F., and Rudkiewicz, J. L., 1999, Kinetic modelling of petroleum formation and cracking: implications from the high pressure/high temperature Elgin Field (UK, North Sea). Organic Geochemistry 30 (9 SU), p. 1105-1125.

Vandenbroucke, M., and Largeau, C., 2007, Kerogen origin, evolution and structure. Organic Geochemistry, 38, p. 719-833.

Vassoyevich, N. B., Korchagina, Y. I., Lopatin, N. V., and Chernyshev, V. V., 1970, Principal phase of oil formation. International Geology Review, 12(11), p. 1276–1296.

Vigrass, L. W., 1968, Geology of Canadian heavy oil sands: AAPG Bulletin, v. 52, no. 10, p. 1984-1999.

W, G. K., and R, U. J., 1998, Origin, development and evolution of structural styles, in Glennie K.W. ed., Petroleum Geology of the North Sea: Oxford, U.K., Blackwell Science Ltd., p. 42–84.

Weeks, L. G., 1952, Factors of sedimentary basin development that control oil occurrence: AAPG Bulletin, v. 36, p. 2071-2124.

Welte, D. H., Hantschel, T., Wygrala, B. P., Weissenburger, K. S., and Carruthers, D., 2000, Aspects of petroleum migration modelling: Journal of Geochemical Exploration, v. 69-70, p. 711-714.

Welte, D. H., Horsfield, B., and Baker, D. R., 1996, Petroleum and basin evolution: Springer-Verlag, 536 p.

Wenger, L. M., Davis, C. L., and Isaksen, G. H., 2001, Multiple controls on petroleum biodegradation and impact on oil quality. Society of Petroleum Engineers Paper 71450.

Wenger, L. M., and Isaksen, G. H., 2002, Control of hydrocarbon seepage intensity on level of biodegradation in sea bottom sediments. Organic Geochemistry 33, p. 1277-1292.

Wickenden, R. T. D., 1949, Some Cretaceous sections along the Athabasca River from the mouth of Calling River to below Grand Rapids, Alberta: Geological Survey of Canada Paper, p. 15-49.

Widdel, F., Boetius, A., and Rabus, R., 2006, Anaerobic biodegradation of hydrocarbons including methane. In: Dworkin, M., Falkow, S., Rosenberg, E., Schleifer, K.H., Stackebrandt, E. (Eds.), The Prokaryotes, Ecophysiology and Biochemistry, vol. 2. Springer, New York, p. 1028–1049.

Widdel, F., Knittel, K., and Galushko, A., 2010, Anaerobic hydrocarbon-degrading microorganisms: an overview. In: K.N. Timmis (Ed.), Handbook of Hydrocarbon and Lipid Microbiology (Ed. by K.N. Timmis). Springer-Verlag, Berlin, p. 1997-2021.

Wignall, P. B., 2001, Large igneous provinces and mass extinctions. Earth Sci. Rev. 53, p. 1–33.

Wilhelms, A., Larter, S. R., Head, I., Farrimond, P., Primio, R. d., and Zwach, C., 2001, Biodegradation of oil in uplifted basins prevented by deep-burial sterilization: Nature, v. 411, p. 1034-1037.

Wilkes, H., Boreham, C., Harms, G., Zengler, K., and Rabus, R., 2000, Anaerobic degradation and carbon isotopic fractionation of alkylbenzenes in crude oil by sulphate-reducing bacteria. Organic Geochemistry 31, p. 101-115.

Wilkes, H., Rabus, R., Fischer, T., Armstroff, A., Behrends, A., and Widdel, F., 2002, Anaerobic degradation of n-hexane in a denitrifying bacterium: Further degradation of the initial intermediate (1-methylpentyl)succinate via C-skeleton rearrangement. Archives of Microbiology 177, p. 235-243.

Williams, W. J., Carmack, E. C., Shimada, K., Melling, H., Aagaard, K., Macdonald, R. W., and Grant Ingram, R., 2006, Joint effects of wind and ice motion in forcing upwelling in Mackenzie Trough, Beaufort Sea: Continental Shelf Research, v. 26, no. 19, p. 2352-2366.

Winters, J. C., and Williams, J. A., 1969, Microbiological alteration of crude oil in the reservoir, paper PETR86, E22 presented at the 1969 American Chemical Soc. Symposium on Petroleum Transform. in Geol. Envir., New York City, p. 7–12 September.

Wood, W. T., Gettrust, J. F., Chapman, N. R., Spence, G. D., and Hyndman, R. D., 2002, Decreased stability of methane hydrates in marine sediments owing to phase-boundary roughness. Nature, vol. 420, no. 6916, pp. 656-660. DOI: 10.1038/nature01263.

Wright, G. N., McMechan, M. E., and Potter, D., 1994, Structure and Architecture of the Western Canada Sedimentary Basin, *in* Mossop, G., and Shetsen, I., eds., Geological atlas of the Western Canada Sedimentary Basin: Calgary, Alberta, Canadian Society of Petroleum Geologists and Alberta Research Council, p. 455-468.

Wygrala, B., 1986, Integrated study of an oil field in the Southern Po Basin, Northern Italy: University of Cologne, 332 p.

Zachos, J. C., Lohmann, K. C., Walker, J. C., and W. S. W., 1993, Abrupt climate change and transient climates during the Paleogene: a marine perspective: Journal of Geology, v. 101, p. 191-213.

Zengler, K., Richnow, H. H., Rossello-Mora, R., Michaelis, W., and Widdel, F., 1999, Methane formation from long-chain alkanes by anaerobic microorganisms: Nature, v. 401, p. 266-269.

Appendix

Additional input for WCSB 3-D model definition

Layer name	Facies name	Content (%)										
		Sst	Sh	CarbSh	Slt	Lm	Dolo	Marl	Sand50 Cong50	Anhydrite	CementSilica	Coal
Overburden (Top)	90ss10sh18_2	90	10									
	Bearpaw_Co	25	75									
	90sh10slt16_1	10	90									
Bearpaw_Co	Bearpaw_Co	25	75									
Colorado	Colorado Group		100									
Cardium	40ss60sh	40	60									
	60ss40slt	60	40									
	75ss25slt	75	25									
	90sh10slt	90	10									
Second White Specks	Second White Specks		95		5							
Westgate	Westgate		95		5							
Viking	Viking_40ss13_3	10	80		10							
	Viking25ss13_2	15	60		25							
	Viking10ss13_1	10	80		10							
Joli Fou	Joli Fou		100									
Upper Mannville	Sandstone	100										
	Claystone		100									
Manville Coal	Coal											100
	67ss21sh09lst	67	21		7	5						
	Joli Fou		100									

Continued in next page

Additional input for WCSB 3-D model definition - continued

Layer name	Facies name	Content (%)										
		Sst	Sh	CarbSh	Slt	Lm	Dolo	Marl	Sand50 Cong50	Anhydrite	CementSilica	Coal
Ostracode	Ostracode09	24	49		17	5			5			
	67ss21sh09lm	67	21		7	5						
	50ss29sh09_2	47	28		15	5			5			
	67ss21sh09_1	67	21		7	5						
	Joli Fou		100									
Lower Mannville	67ss21sh09lm	67	21		7	5						
	Man30ss11_4	27	38		30	5						
	Ostracode094lm	29	35		25	5			6			
Fernie Upper	Joli Fou		100									
	67ss21sh09Lm	67	21		7	5						
	JurPoker08_5	11	21			68						
Poker Chip	Poker69sh31calc	6	69		20	5						
	Poker90sh10slt		90		10							
	Jur27lm08_2	13	21			21	12				33	
	Jur52sh08_4	12	50		5	12	5			16		
	Jur42sh08_3	5	42		9	26	11	7				
	Nordegg08_01		78			12	5	5				
Nordegg	Nordegg21sh_59ls	19	22			59						
	Jur27lm08_2	13	21			21	12				33	
	Jur52sh08_4	12	50		5	12	5			16		
	Nordegg21sh68ls	11	21			68						
	Nordegg08_1		78			12	5	5				
Permo-Triassic	67ss21sh09lm	67	21			09						
	Tri24ss07_1	25	17		37	7	14					
	Tri32sh07_2	23	32		30	5	10					
	Doig07_3	30	30		30	10						

Additional input for WCSB 3-D model definition - continued

Layer name	Facies name	Content (%)										
		Sst	Sh	CarbSh	Slt	Lm	Dolo	Marl	Sand50 Cong50	Anhydrite	CementSilica	Coal
Rundle/Charles	Run63do06_4		10			21	64				5	
	Run40lm06_3		17			39	39			5		
	Run73lm06_5		5		12	73	10					
	Run50anh06_1					50				50		
	Run60lm06_2		21			58	12				9	
Banff Top	Banf58lm05_3		20		7	58	9	6				
	Banf39lm05_4	9	31		10	39	5	6				
	Exshaw_Bakken		75		25							
	Banf38lm05_2	5	31		9	38	7	10				
	Banf58sh05_1	5	31		9	38	7	10				
Exshaw_Bakken	Exshaw_Bakken		75		25							
Wabamum/ Winterburn	Wab35anh03_1		11			5	49			35		
	Wab45sh03_3		45		19		22	5		9		
	Wab85lm03_02		5				11					
Woodbend	Wb50lmDo02_3					50	50					
	Wo100sh02_2			100								
	Wb100Lm02_6					100						
Duvernay	Dv50lmDo02_4					50	50					
	DvLeDuc05_5					100						
	Dv100sh02_2		100									
	Dv100lm02_6					100						
Underburden	Underburden											
Basement	Basement											